WARWICK
THE UNIVERSITY OF WARWICK

Elucidating the role of Bub1 in human checkpoint signalling

by

Cerys E. Currie

Supervisors:

Prof. Andrew D. McAinsh

Prof. Jonathan B.A. Millar

Thesis

Submitted to The University of Warwick for the degree of

Doctor of Philosophy

School of Life Sciences - September 2019

MIBTP
Midlands Integrative Biosciences Training Partnership

Table of Contents

List of figures

List of tables

Acknowledgments

I would like to thank my supervisor Prof. Andrew McAinsh for the opportunity to undertake this PhD project in his lab. I feel lucky to be able to say that I have truly enjoyed my PhD, despite the tough times, and this is owed to Andrew's unwavering positive attitude. I would also like to thank my joint supervisor Prof. Jonathan Millar for excellent guidance and support over the last three and a half years. I am incredibly grateful for all the opportunities I have been given during my PhD.

I would also like to thank past and present members of the McAinsh and Millar labs for being incredibly supportive and approachable at all times. This was invaluable to me during the first year of my PhD when I really had no idea what I was doing! For this I would especially like to thank Dr Virginia Silió for teaching me everything when I first started, Dr Mar Mora-Santos for helping me with all the biochemistry, Dr Paula Esquivias for help with later experiments and Dr Muriel Erent for general support and advice. Dr Chris Smith wrote the MATLAB code that enabled me to streamline my analysis and saved me many months of work! Dr Emanuele Roscioli has also been a great help, especially with the completion of my thesis.

I would like to thank Dr Ellis Ryan and Dr Clare Garcin for their incredible friendship and support, which has played a pivotal role in my positive experience at Warwick. It really would not have been the same without them. Also my amazing friend and sister-in-law to be Tammy Roe, for always being there for me, and my parents for believing in me and encouraging me to aim high from a young age. I also need to acknowledge my share horse Tommy, as there is no problem that cannot be fixed with a good gallop!

Last but not least, my incredible partner, fiancée and best friend of 7 years Dr Charlie Roe, I could never have made it to the end in one piece without you. Your unwavering support and belief in me gives me confidence every day and I am so excited for our future, especially now this chapter of our lives is almost over!

Declaration

This thesis is submitted to the University of Warwick in support of my application for the degree of Doctor of Philosophy. It has been composed by myself and has not been submitted in any previous application for any degree.

The work presented (including data generated and data analysis) was carried out by the author except in the cases outlined below that were carried out by Mar Mora-Santos and Paula Esquivias.

- Western blots for Bub1
- Immunoprecipitation experiment
- RT-PCR

Data presented in Chapter 3 has been published by the author, and can be found here:

Currie, C.E., Mora-Santos, M.D., Smith, C., McAinsh, A.D., and Millar, J.B. (2018) 'Bub1 Is Not Essential for the Checkpoint Response to Unattached Kinetochores in Diploid Human Cells'. *Current Biology* 28 (17), R929 – R930

Inclusion of published work

In the appendix I have included a paper to which I have contributed, 'Bub1 is not essential for the checkpoint response to unattached kinetochores in diploid human cells' (Currie *et al*, 2018). Here, I conducted all experiments with the exception of biochemistry, and prepared the manuscript with Prof. Andrew D. McAinsh and Prof. Jonathan B.A. Millar.

Abstract

The spindle assembly checkpoint (SAC) establishes a delay before anaphase, until all chromosomes are equally and stably attached to spindle microtubules via kinetochores. This acts as a surveillance mechanism to prevent chromosome segregation defects and safeguard genomic stability. The exact mechanisms regulating checkpoint activation and mitotic progression remain unclear. Previous work has shown that SAC activation requires Mps1-dependant phosphorylation of KNL1 MELT motifs. This allows recruitment of Bub1-Bub3, and subsequent localisation of BubR1-Bub3 and Mad1/Mad2 complexes onto Bub1. Localisation of Mad1/Mad2 to the kinetochore allows production of the mitotic checkpoint complex (MCC), which inhibits the APC/C to prevent initiation of anaphase. This was thought to represent a single, linear pathway for SAC activation. However, recent work in human cells has provided evidence that the Rod-Zwilch-ZW10 (RZZ) complex can offer a second receptor for Mad1/Mad2 complexes, thus allowing two separable pathways for SAC activation and maintenance in human cells. We have tested this dual-pathway model by knocking out *BUB1* in human hTERT-RPE1 cells using CRISPR-Cas9 technology. These Bub1$^{1-23}$ cells are able to generate a functional checkpoint in the presence of unattached kinetochores, however, Bub1$^{1-23}$ cells were later found to express residual amounts of Bub1 protein, referred to as 'zombie' Bub1. We have therefore repeated all key experiments using Bub1$^{1-23}$ cells in the presence of Bub1 siRNA to deplete 'zombie' Bub1, and again shown that these cells are able to generate a functional checkpoint in the presence of unattached kinetochores, although maintenance is perturbed. Furthermore, we have found that Bub1 plays an important role in the regulation of unperturbed mitosis which is at least partially mediated through an uncharacterised premitotic function. Together, these data provide further evidence for a Bub1-independent mechanism of checkpoint activation at unattached kinetochores, and uncover a novel role for Bub1 during interphase.

Abbreviations

APC/C – anaphase promoting complex/cyclosome

CCAN – constitutive centromere-associated network

CENP – centromere protein

CIN – chromosomal instability

CPC – chromosomal passenger complex

CRISPR - clustered regularly interspaced short palindromic repeats

GTP – guanosine triphosphate

hTERT- RPE1 – human telomerase reverse transcriptase retinal pigment epithelial 1 cells

K-fibre – kinetochore fibre

KBB – KNL1-Bub1-Bub3

KMN – KNL1-Mis12-Ndc80 network

KT – kinetochore

MCC – mitotic checkpoint complex

MT – microtubule

NE – nuclear envelope

NAS – nonsense associated splicing

NEB/NEBD – nuclear envelope breakdown

ORF – open reading frame

PSC – premature stop codon

RZZ – Rod-Zwilch-ZW10

SAC- spindle assembly checkpoint

siRNA – small interfering RNA

1. Introduction

1.1 The Cell Cycle

All cells possess the remarkable ability to create exact copies of themselves through the process of the cell cycle. This process supports growth and proliferation, and allows organisms to recover from damage. The cycle of growth and division can be divided into two basic steps, 'interphase' and 'M-phase', where interphase constitutes growth and M-phase division. Interphase is further divided into three stages; gap 1 (G1), synthesis (S) and gap 2 (G2). During G1, the cell either exits the cell cycle into the resting state of G0 (quiescence), or continues through the cell cycle by synthesising proteins required for entry into S phase and subsequently increases in size. The cell then enters S-phase, during which DNA is replicated along with the microtubule organising centre, or centrosome. The centrosome supports the cytoskeleton in interphase but forms the two poles of the mitotic spindle during mitosis. During G2 other cellular constituents are duplicated to cover the needs of two cells following division, and the cell prepares to enter M-phase. M-phase consists of two broad stages; mitosis which defines nuclear division and cytokinesis which defines the final cellular division. All cellular components are rearranged during M-phase so that following cell abscission two new daughter cells are capable of independent survival.

The accurate segregation of duplicated DNA one of the most complex tasks faced by a dividing cell. The DNA of any complete genome is considerably larger than the cell diameter, for example human DNA sums to around 2 metres, whereas our cells are less then 1/100,000th of that size (Mcintosh, 2016). To tackle this issue, DNA becomes tightly compacted to form discrete chromosomes during mitosis (Figure 1) . Briefly, during interphase DNA is tightly wrapped around histones to form nucleosomes. The nucleosomes are then packaged with histones to form chromatosomes, which combine to form chromatin. This is the state in which DNA exists during interphase. Upon entry into mitosis, chromatin becomes condensed to form the characteristic mitotic chromosomes, which are easier for

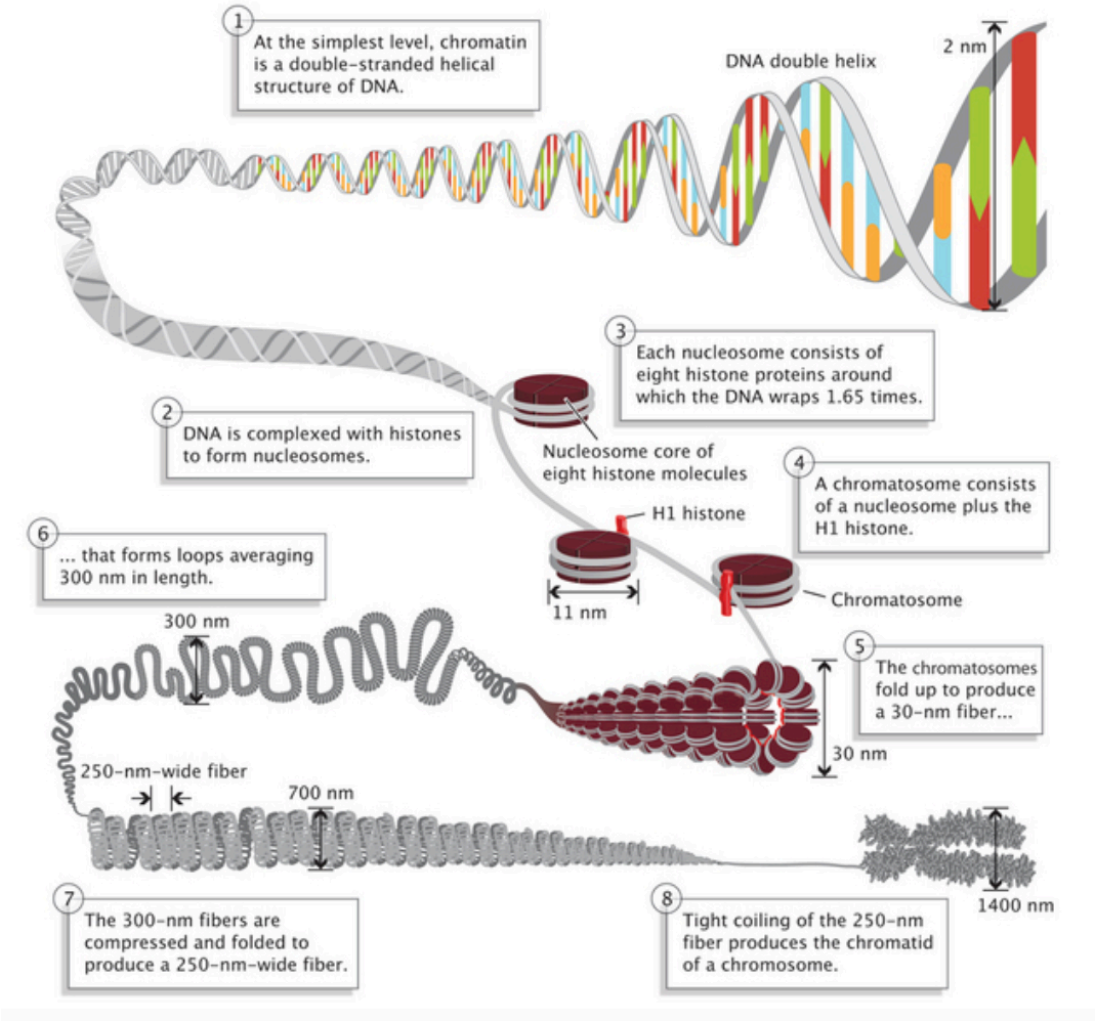

Figure 1: DNA structure and condensation. The double helix is wound around histones to form nucleosomes during interphase. This then complexes with a H1 histone to form a chromatosome, which is folded to become chromatin. Chromatid is then further compressed and coiled to form the mitotic chromosomes. Figure adapted from Pierce, Benjamin. *Genetics: A conceptual approach,* 2nd ed.

the cell to organise and segregate. Successful segregation of the genetic material is essential for maximum fitness of any organism.

All mitotic chromosomes possess the same basic structure (Figure 2). Each is formed of two sister chromatids, which are identical copies of the same chromosome replicated during S-phase. Sister chromatids consist of a short 'p' arm and a long 'q' arm and are joined together at a specialised region of DNA called the centromere, upon which a structure named the kinetochore is formed. The kinetochore will be further discussed in section 1.3.

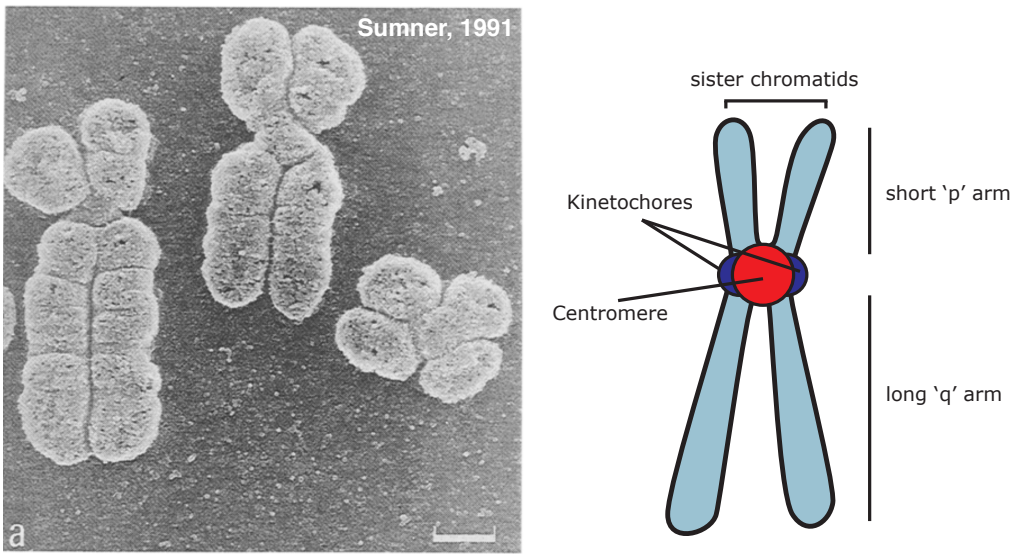

Figure 2: Mitotic chromosome structure. Left) electron micrograph of mitotic chromosomes from Sumner, 1991. Right) Schematic of a mitotic chromosome showing two sister chromatids tethered together at the centromere, on which the kinetochores are formed. Mitotic chromosomes possess a short 'p' arm and a longer 'q' arm.

1.1.1 Mitosis

Accurate segregation of sister chromatids to two new daughter cells is achieved through the process of mitosis, which is facilitated by the mitotic spindle. The mitotic spindle is a dynamic macromolecular machine formed from the microtubules of the cytoskeleton. Microtubules consist of polymers of α and β tubulin subunits that form protofilaments, which assemble together to form a hollow cylinder (Downing and Nogales, 1998). They are dynamic structures that undergo continuous assembly and disassembly within the cell. The microtubules of the cytoskeleton undergo a deep reorganisation upon mitotic entry to form the mitotic spindle. The mitotic spindle is comprised of microtubules and microtubule-associated proteins (MAPs). These MAPs stabilise the mitotic spindle and assist the dynamic lengthening and shortening of microtubules that is necessary to move sister chromatids precisely around the cell. This property of microtubules is termed 'dynamic instability', and is essential for the cell to progress through mitosis efficiently (Mitchison and Kirschner, 1984).

In order for a cell to divide successfully, the microtubules of the mitotic spindle must interact with the mitotic chromosomes. They do so at a specific site called the kinetochore - from the English 'kineto-' (of movement) and the Greek 'khōros' (place) (Figure 2). The kinetochore is a conserved macromolecular structure composed of ~100 proteins that is assembled at each centromere. Each mitotic chromosome possesses two sister kinetochore pairs; one for each sister chromatid. The kinetochore is recognised and bound by microtubules of the mitotic spindle, and this interaction generates the force needed to move individual chromosomes. Early scanning electron microscopy studies show that the kinetochore extends out from the centromere and has a trilaminar structure (Comings and Okada, 1971; Rattner, 1987). Kinetochore structure will be described in greater detail in section 1.3.

During interphase, the microtubules of the cytoskeleton originate from a single organelle named the centrosome. The centrosome becomes duplicated during S-phase, and the two duplicated centrosomes are tethered near the nuclear envelope during prophase (Bolhy *et al.*, 2011) (Figure 3A). At this point, the chromatin condenses to form the mitotic chromosomes and the outer kinetochore rapidly assembles on the centromeric region before nuclear envelope breakdown (NEBD). Following NEBD, the mitotic spindle starts to assemble and dynamic microtubules can be seen growing out of the duplicated centrosomes (Figure 3B). During this stage, named 'prometaphase', kinetochores on each chromatid pair start to interact with the spindle microtubules. These interactions allow chromosomes to move through the cell, facilitated by the dynamic instability of spindle microtubules. This movement is aided by motor proteins that pull chromosomes along the microtubule tracks to their destination: the equator of the spindle (Wood *et al.*, 1997). Once all chromosomes arrive at the equator, the cell is described as being in 'metaphase' (Figure 3C). Here chromatid pairs become 'bioriented', with each sister kinetochore attached only to the corresponding spindle pole, and oscillate back and forth along the spindle pole axis as the correct kinetochore-microtubule attachments are stabilised (Hughes and Swann, 1947).

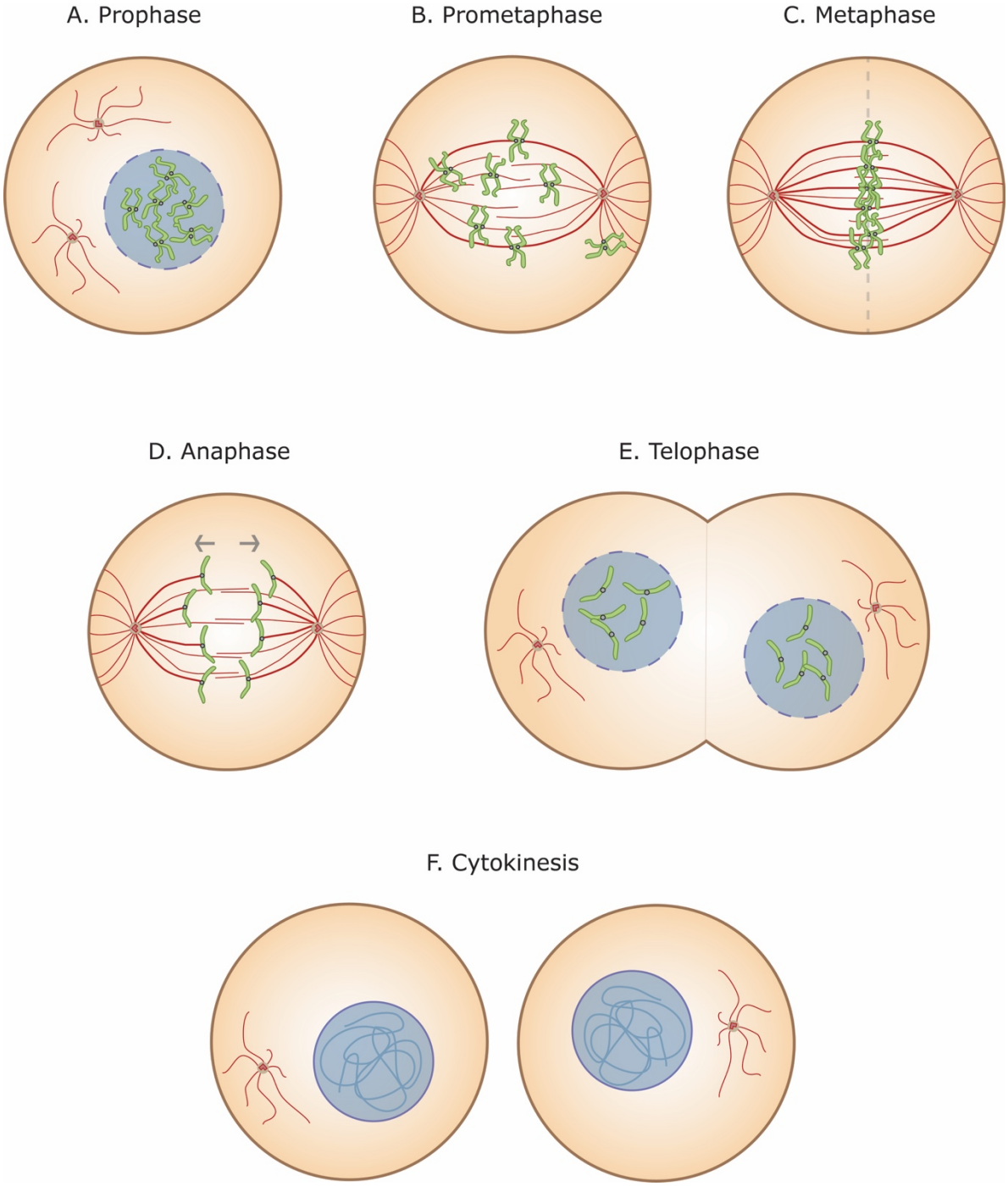

Figure 3: Stages of mitosis. (A) In prophase, sister chromatids condense and kinetochores assemble onto centromeres. Nuclear envelope breakdown (NEBD) signals the end of prophase. (B) Following NEBD, the mitotic spindle gains access to the chromosomes and attach to kinetochores in prometaphase. Chromosomes start moving through the cell. (C) By metaphase, chromosomes have aligned on the midline of the cell. (D) During anaphase, sister chromatids are segregated to opposite sides of the cell towards spindle poles. (E) In telophase the nuclear envelope reforms in each new daughter cell. (F) Cytokinesis divides the shared cytoplasm and results in two completely separated daughter cells.

Kinetochore-microtubule attachment stabilisation is a function of a kinase-phosphatase equilibrium that is discussed in section 1.6.

The end of metaphase is arguably the most dramatic stage of mitosis, as the sister chromatids begin to separate during anaphase (Figure 3D). This represents the point of no return for the cell as the centromeric links between sister chromatids are irreversibly cleaved, causing the sister chromatids to be released as two single chromosomes. Chromosomes are moved towards opposite spindle poles via microtubule depolymerisation-coupled pulling at the kinetochore (Koshland, Mitchison and Kirschner, 1988). Anaphase chromosome segregation occurs in two stages, a decrease in the distance of each chromosome from its pole (anaphase A) and an increase in the separation between spindle poles (anaphase B) (Makino and Nakanishi, 1955). This usually occurs in the sequence A then B.

While chromosomes are segregating, the cell prepares to exit mitosis. The activity of mitotic kinases drops and proteins of the nuclear envelope start to associate with still condensed chromosomes during 'telophase' (Figure 3E) (Güttinger, Laurell and Kutay, 2009). These proteins fuse to one another to rebuild the nuclear compartment, and chromosomes start to decondense. Mitosis is followed by the process of cytokinesis (Figure 3F). Here, an equatorial contractile ring is formed which constricts the shared cytoplasm of the two daughter cells. The central region of the anaphase spindle is remodelled to form a midbody, which directs the distinct membrane cleavage event of abscission (Green, Paluch and Oegema, 2012). The two daughter cells are now discrete and each possess a full set of the genetic material.

1.2 Cancer and aneuploidy

Cancer is defined as a disease in which abnormal cells divide without control and invade nearby tissues. During mitosis, the correct segregation of chromosomes ensures that the genetic content of the mother cell is equally distributed into the

two daughter cells. However chromosome segregation can occasionally go wrong, resulting 'lagging' chromosomes during anaphase that do not segregate with the mass. These can form micronuclei, where the nuclear envelope forms around the lagging chromosome and separates it from the main nucleus (Fenech, 2000). These errors in chromosome segregation have been long recognised as a hallmark of cancer, resulting in the hypothesis that mitotic defects drive genetic instability and tumourigenesis (Weaver and Cleveland, 2006; Sansregret and Swanton, 2017). Consistent with this, many of the genes controlling mitosis are differentially expressed in human tumours, including components of the spindle assembly checkpoint: the focus of this thesis that will be discussed later (Kops, Weaver and Cleveland, 2005; Schvartzman, Sotillo and Benezra, 2010).

The hypothesis that chromosome segregation errors drive cancer progression is supported by the observation that ~90% of solid human tumours have an abnormal chromosome number (Weaver and Cleveland, 2006). This phenomenon is termed aneuploidy, and describes the state of a cell bearing an abnormal chromosome number that is not a multiple of the haploid set that is characteristic of the species. This condition results in an improper set of chromosomes and subsequent changes in cell behaviour that have been shown to be a cause of malignant transformation, rather than a consequence (Li *et al.*, 1997). During malignant transformation, cells acquire mutations that override the mechanisms controlling cell proliferation and become cancerous due to abnormal cell division (Hahn *et al.*, 1999).

Two types of aneuploidy can occur in tumour cells. Numerical aneuploidy is a change in the number of whole chromosomes, either by gain or loss, and is the consequence of chromosome missegregation during mitosis in a process called chromosomal instability (CIN). Structural aneuploidy refers to gain or loss of large portions of individual chromosomes, often seen as chromosomal rearrangements. Both can be stably maintained over multiple generations of cell division (Funk, Zasadil and Weaver, 2016). For the purpose of this thesis, we will adhere to the definition of aneuploidy in its numerical form.

Aneuploidy often co-exists with a high ongoing rate of karyotypic change, through a phenomenon referred to as CIN. CIN is defined as a persistent high frequency in gain or loss of whole chromosomes and arises from mistakes in chromosome segregating during mitosis, usually in the form of lagging chromosomes at anaphase. A single chromosome missegregation event can cause a change in chromosome number (aneuploidy), while CIN describes persistent problems with chromosome segregation occurring over multiple divisions. In this way, CIN can drive cumulative changes in chromosome number resulting in severe aneuploidy. CIN is therefore positively correlated with poor patient prognosis (Thompson, Bakhoum and Compton, 2010). Furthermore, CIN has been shown to be a direct driver of metastasis due to activation of inflammatory pathways in response to the presence of DNA in the cell cytosol (Bakhoum *et al.*, 2018). The presence of cytosolic DNA resulting from micronuclei or chromothripsis (chromosome shattering and rearrangement) activates the NF-κB pathway, which has reported roles in EMT, cellular invasion and metastasis (Wang *et al.*, 2016). This can increase cancer progression.

Mounting evidence now suggests that a low level of CIN is weakly tumour promoting, while high CIN causes cell death and tumour suppression resulting from intolerance to severe aneuploidy (Weaver and Cleveland, 2008; Williams *et al.*, 2008; Sheltzer and Amon, 2011). Future chemotherapeutic strategy aims to exploit this phenomenon by increasing the rate of CIN within a tumour and therefore promoting severe aneuploidy and cell death. However before this is possible, we must first define the mechanisms controlling mitosis at the main site of signalling: the kinetochore.

1.3 Kinetochore structure

The centromere of a mitotic chromosome is the region of DNA that links two sister chromatids, sometimes referred to as the primary constriction (Figure 2). The centromere is defined epigenetically by the histone H3 variant Centromere

Protein (CENP) A that forms specialised nucleosomes found only in this location (Palmer *et al.*, 1987). This allows the protein complex cohesin to be maintained at this specialised centromeric region while it is removed from chromosome arms during prophase (Dej and Orr-Weaver, 2000). Centromeric cohesin allows sister chromatids to remain linked during mitosis until anaphase onset, the mechanisms of which will be discussed further in section 1.5.

The centromere is also the location for kinetochore assembly. The kinetochore can be divided into three distinct regions: the inner kinetochore that forms the chromatin interface, the outer kinetochore that interacts with spindle microtubules, and the fibrous corona (Figure 4). The kinetochore is linked to the centromeric region of the chromosome via proteins of the constitutive centromere-associated network (CCAN). These reside at the centromere throughout the cell cycle, and make up the inner kinetochore (Cheeseman and Desai, 2008). As the cell enters mitosis, outer kinetochore components assemble onto the CCAN.

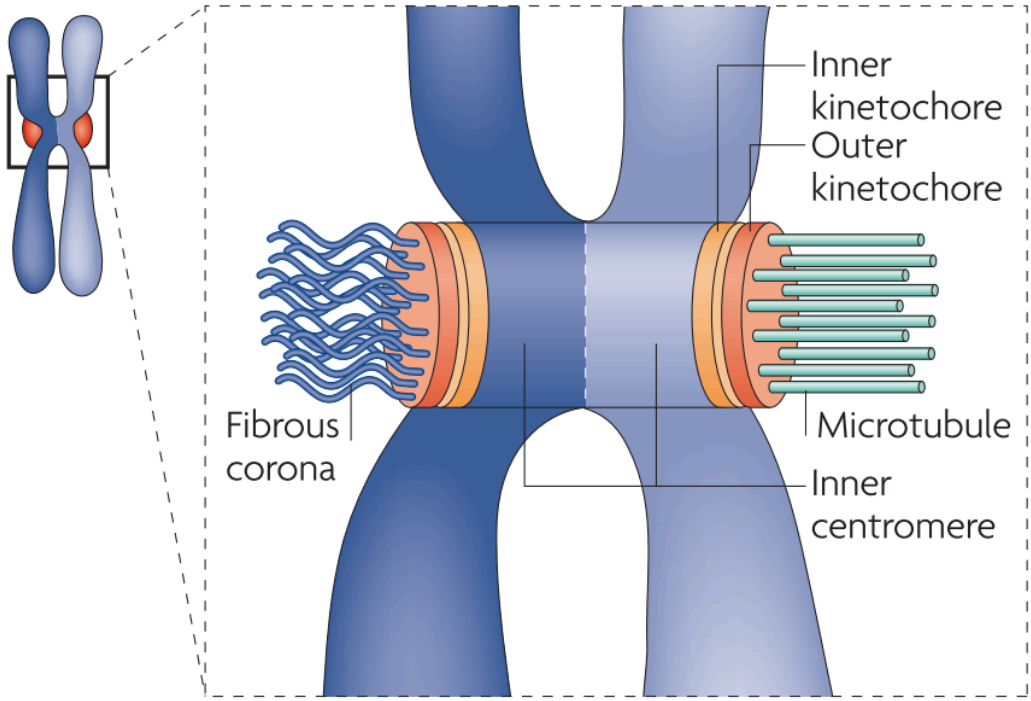

Figure 4: Basic kinetochore structure. A schematic of a paired sister chromatids. The chromatid on the left is attached to microtubules which bind the outer kinetochore. The chromatid on the left is unattached, allowing the fibrous corona to be extended away from the outer kinetochore. The inner kinetochore assembles upon the inner centromere. Figure adapted from Cheeseman and Desai, 2008.

The outer kinetochore is made up of the KMN network, which is highly conserved throughout evolution (Cheeseman *et al.*, 2006). Briefly, the CCAN component CENP-C interacts with the Mis12 complex containing Mis12, Nnf1, Nsl1 and Dsn1 subunits (Petrovic *et al.*, 2016). The Mis12 complex, in turn, recruits KNL1 and the Ndc80 complex. Overall, KNL1-Mis12-Ndc80 is referred to as the KMN network and constitutes a major microtubule-binding region of the kinetochore, with the calponin homology (CH) domains located at the N-terminal regions of Ndc80 and Nuf2 being the primary binding site (Alushin *et al.*, 2012; Varma and Salmon, 2012).

In the absence of microtubules, a fibrous structure named the corona forms to expand the kinetochore into a crescent-like shape (Ris and Witt, 1981; Sacristan *et al.*, 2018) (Figure 4). The corona is formed of kinetochore proteins CENP-E (Cooke *et al.*, 1997), CENP-F (Rattner *et al.*, 1993; Auckland and McAinsh, 2019, bioRXiv), the Rod-Zwilch-ZW10 (RZZ):Spindly complex (Buffin *et al.*, 2005; Karess, 2005; Mosalaganti *et al.*, 2017) and the dynein/dynactin minus-end directed motor complex (Rieder and Salmon, 1998). Corona expansion was recently reported to be driven by the RZZ complex and Spindly in a Mps1-dependant manner, where Spindly autoinhibition is released and RZZ:Spindly complexes oligomerise to form the filamentous network (Sacristan *et al.*, 2018). Upon binding a spindle microtubule the fibrous corona disappears and the kinetochore becomes compacted. (Magidson *et al.*, 2015). This is reported to be mediated through the Spindly-dependant recruitment of dynein (Gassmann *et al.*, 2010; Sacristan *et al.*, 2018). The kinetochore is a therefore a dynamic, multi-protein complex that responds to changes in microtubule attachment, although the mechanisms of this regulation remain unclear.

1.4 Mechanisms of kinetochore biorientation

A cell progressing through mitosis faces many challenges including the number and size of chromosomes, their initial locations, the locations of the spindle poles

and the stochastic behaviour of spindle microtubules. Each kinetochore binds 20 spindle microtubules on average (McEwen *et al.*, 1997), and the aim is ensure these originate from a single pole, while the sister kinetochore is attached to the opposite pole in a state termed biorientation (Lampson and Grishchuk, 2017). This is a complex task and takes time.

Microtubules originating from the spindle pole can be captured by the kinetochore at various angles. The initial interactions of kinetochores and microtubules are described in the simple yet fundamental model of 'search and capture' (Kirschner and Mitchison, 1986). Spindle microtubules grow from the centrosomes through the cell at random. These microtubules are rapidly turned over, but any that unwittingly contact a kinetochore are capped and stabilised. In addition to this, kinetochores also generate short microtubules that can interact with spindle microtubules to improve the chance of capture (Khodjakov *et al.*, 2003). This phase is not totally stochastic, and is at least partly aided by a Ran-GTP gradient around chromosomes which 'guides' polymerising spindle microtubules towards them (Clarke and Zhang, 2008). Due to the irregular nature of the initial search and capture phase, kinetochore-microtubule (KT-MT) attachment states can vary.

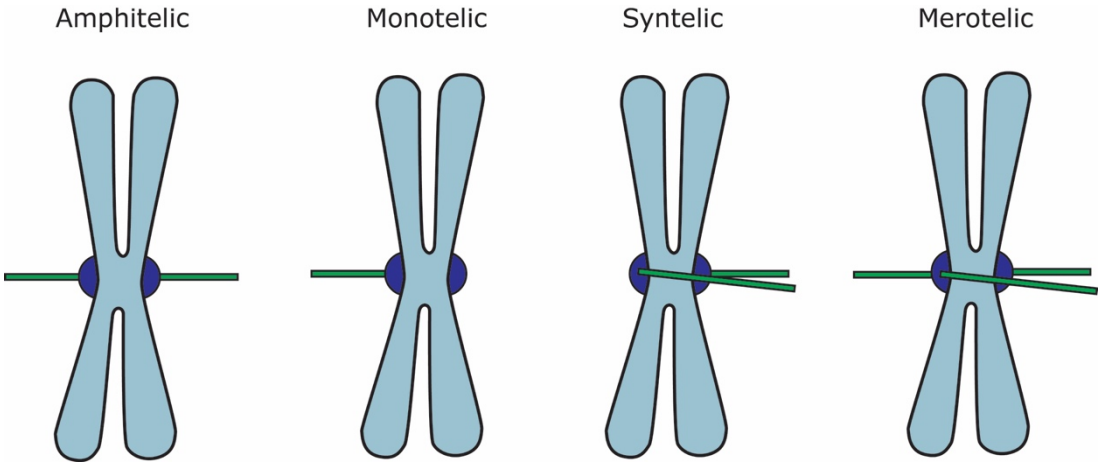

Figure 5: Kinetochore orientation states. Amphitelic chromosomes have spindle microtubules originating from opposite poles and are bi-oriented. Monotelic chromosomes have only one kinetochore attached to the correct pole and the other is unattached. Syntelic chromosomes have both kinetochores attached to the same spindle pole and require error correction. Merotelic attachments have one kinetochore attached to both poles, while the other is correctly attached. Merotelic attachments do not activate the SAC.

There are 4 possible attachment states; amphitelic (bi-oriented), monotelic (single KT attached), syntelic (both KTs attached to the same pole) and merotelic (one KT attached to both poles) (Figure 5) (Maiato *et al.*, 2004; Musacchio and Salmon, 2007). The latter two states must be actively corrected to allow all chromosomes to become bioriented. If a kinetochore is captured in the incorrect orientation, it becomes bioriented through the process of error correction. This process relies on the serine/threonine kinase Aurora B (Tanaka *et al.*, 2002; Hauf *et al.*, 2003). Aurora B forms part of the chromosomal passenger complex (CPC), and is recruited to centromeres in early mitosis along with INCENP, Survivin and Borealin (Adams, Carmena and Earnshaw, 2001). Aurora B destabilises microtubule attachments by phosphorylating multiple kinetochore substrates, including the Ndc80 complex (Akiyoshi *et al.*, 2009). Localisation to the centromere is essential for the current model of error correction: kinetochore-microtubule attachments that are not bi-oriented and therefore not under tension remain closer to the inner centromere and are destabilised by Aurora B phosphorylation. Bi-oriented kinetochores under tension are pulled away from the inner centromere and substrates are moved out of Aurora B's reach, allowing the k-fibres to be stabilised (Liu *et al.*, 2009). In this way, any incorrectly orientated kinetochores will become unattached and rebind microtubules through a process of trial and error to finally become bi-oriented. However, recent evidence shows that localisation of the CPC to the inner centromere is not required for proper error correction and chromosome segregation, at least in budding yeast (Campbell and Desai, 2013). Authors suggested that clustering of Aurora B on either microtubules or centromeric chromatin is sufficient to discriminate between correct and incorrect attachments. Therefore the mechanisms of error correction at mis-aligned kinetochores remain unclear. However, the process of error correction and biorientation is crucial to ensure the faithful segregation of chromosomes to daughter cells and prevent chromosomal instability and aneuploidy. To enable successful completion of this process, the cell needs to delay in mitosis for enough time to allow all chromosomes to complete error correction and become successfully biorientated. This is achieved through inhibition of the anaphase promoting complex (APC/C).

1.5 The anaphase promoting complex/cyclosome (APC/C)

The regulation of cell division relies on an intricately co-ordinated array of signalling pathways. In order for a cell to complete mitosis, the regulatory proteins that prevent its premature exit must be destroyed at exactly the right moment to ensure daughter cells receive an equal and identical set of chromosomes. A single multi-protein complex is responsible for the destruction of these proteins; the anaphase promoting complex or cyclosome (APC/C). The APC/C is an E3 ubiquitin ligase which targets proteins for proteolytic degradation (Pines, 2011).

Human APC/C is composed of 15 APC subunits, which are highly conserved throughout evolution (Pines, 2011). There are two co-activators of APC/C; Cdc20 and Cdh1 (Dawson, Roth and Artavanis-Tsakonas, 1995; Kramer *et al.*, 2000). While APC/C^{Cdc20} controls the metaphase to anaphase transition, APC/C^{Cdh1} becomes active from late mitosis to G1, and is required for mitotic exit. Phosphorylation of APC/C subunits is necessary to allow Cdc20 to activate the APC/C during mitosis, whereas Cdh1 can interact with both the interphase and mitotic forms of APC/C and binding depends on Cdh1 phosphorylation status (S. Zhang *et al.*, 2016). Cdc20 is negatively regulated by the activity of the spindle assembly checkpoint (SAC) through its sequestration into mitotic checkpoint complex (MCC) (Sudakin, Chan and Yen, 2001), which will be discussed in section 1.6. Conversely, APC/C^{Cdh1} is inhibited by the Rae1-Nup98 complex during mitosis rather than the MCC complex (Jeganathan, Malureanu and Van Deursen, 2005; Jeganathan, Baker and Van Deursen, 2006).

Once all mitotic chromosomes become biorientated during metaphase, Cdc20 is released from the SAC-dependant negative regulation that inhibits its binding to APC/C. APC/C^{Cdc20} degrades multiple substrates required to hold the cell in metaphase. These include cyclin B1 and securin. APC/C^{Cdh1} has also been shown to degrade securin independently of APC/C^{Cdc20} (Jeganathan, Baker and Van Deursen, 2006). Securin is the inhibitor of separase; the protease responsible for cleaving centromeric cohesin. Once the inhibition on separase is released, it is able

to cleave the cohesin links between sister chromatids allowing them to be segregated during anaphase (Uhlmann *et al.*, 2000). Cyclin B1 degradation inactivates Cdk1, the master mitotic kinase, to allow cells to exit mitosis and proceed to G1 (Hershko, 1999). Preventing APC/C activation is the strategy cells have evolved to generate a 'wait-anaphase' signal to allow the establishment of correct kinetochore-microtubule attachments and ensure accurate segregation of the genomic material. This regulation of the APC/C during mitosis is a function of the spindle assembly checkpoint (SAC).

1.6 Spindle assembly checkpoint

The spindle assembly checkpoint facilitates a delay in anaphase onset until all chromosomes are successfully bioriented and aligned at the metaphase plate. Components of the spindle assembly checkpoint (SAC) were first identified by two independent screens in *Saccharomyces cerevisiae* for mutants that failed to delay mitotic exit upon treatment with the microtubule depolymerising drug benomyl (Hoyt, Totis and Roberts, 1991; Li and Murray, 1991). These screens identified proteins of the Bub family (Budding Uninhibited by Benzimidazoles); Bub1 and Bub3 (Hoyt, Totis and Roberts, 1991), and the Mad (Mitotic Arrest Deficient) proteins; Mad1, Mad2 and Mad3 (BubR1 in human cells) (Li and Murray, 1991). Mutation of any gene in these two families caused defects in the ability of cells to arrest in response to the unattached kinetochores generated by spindle poisons. These genes are conserved in all eukaryotes, and are involved in a pathway that prevents the untimely separation of sister chromatids (Li and Benezra, 1996; Taylor and McKeon, 1997; Taylor, Ha and McKeon, 1998). This pathway is referred to as the spindle assembly checkpoint (SAC).

The target of the SAC is Cdc20, which is required to bind and activate APC/C to facilitate mitotic exit (Dawson, Roth and Artavanis-Tsakonas, 1995; Kramer *et al.*, 2000). Cdc20 was first identified as important for SAC signalling in yeast, where the fission yeast homolog Slp1 was shown to form a complex with Mad2 and SAC

failure resulted from interrupting these interactions (Kim *et al.*, 1998). Cdc20 was then formally identified as the target of the SAC in budding yeast, where it remained bound to Mad2 and Mad3 (BubR1) at all stages of the cell cycle (Hwang *et al.*, 1998). Cdc20 mutants that caused SAC failure were shown to abrogate Mad protein binding, suggesting it was the target of the SAC, as these interactions were essential for SAC function.

The SAC negatively regulates the activity of the APC/C by sequestering Cdc20 within the mitotic checkpoint complex (MCC). This mechanism ensures the precise and timely activation of APC/C only once all kinetochores become biorientated (Sudakin, Chan and Yen, 2001). MCC is produced at unattached kinetochores and amplified to inhibit all APC/C complexes (Figure 6). Mechanisms of this amplification will be discussed in section 1.6.2.

1.6.1 Human mitotic checkpoint complex (MCC)

MCC is a heterotetramer complex generated through activation of the spindle assembly checkpoint and is produced at kinetochores not yet attached to microtubules of the mitotic spindle. The onset of anaphase can be blocked by a single unattached kinetochore, therefore MCC is thought to be a diffusible signal which can inhibit all APC/C molecules in the cell (Rieder *et al.*, 1994). This ensures the cell can delay anaphase onset until all kinetochores have been correctly attached to the mitotic spindle, ensuring the genetic material is accurately segregated between two daughter cells.

Human MCC is comprised of BubR1, Bub3, Mad2 and the APC/C coactivator Cdc20 (Sudakin, Chan and Yen, 2001). Recruitment of Mad1:Mad2 complexes to unattached kinetochores is required for MCC formation, which revolves around the 'Mad2 template model' (De Antoni *et al.*, 2005). Mad2 adopts two distinct conformations, the inactive 'open' Mad2 (O-Mad2) and the active 'closed' Mad2 (C-Mad2), with the latter able to bind Cdc20. Kinetochore-bound Mad1 binds to

O-Mad2 and catalyses its conversion to C-Mad2. This stabilises the kinetochore-bound heterodimer and confers it with prion-like activity to induce the same conversion of cytoplasmic O-Mad2 to C-Mad2. C-Mad2 then engages with the N-terminus of Cdc20 (Luo *et al.*, 2002) and subsequently binds BubR1:Bub3 to form a heterotetramer of MCC (Sudakin, Chan and Yen, 2001; Fang, 2002; Davenport, Harris and Goorha, 2006). MCC is a potent APC/C inhibitor, whose target is $APC/C^{Cdc20.}$ APC/C^{MCC} comprises of two Cdc20 subunits, one within MCC and one bound to APC/C (S. Zhang *et al.*, 2016). BubR1 mediates contacts between the two Cdc20 molecules and obstructs any degron dependant binding to them. The MCC-bound molecule of Cdc20 is then auto-ubiquitinated by APC/C^{Cdc20} leading to disassembly of APC/C^{MCC} to allow a constant supply of 'free' APC/C. Efficient release of MCC at anaphase onset requires further ubiquitination of MCC subunits, such as BubR1 (Alfieri, Zhang and Barford, 2017).

1.6.2 Kinetochores as a scaffold for MCC production

The kinetochore provides the physical connection between chromosomes and spindle microtubules, and is therefore a platform for SAC signalling and MCC production. Mps1 acts as the master kinase for SAC activation at unattached kinetochores and localises through binding Ndc80 and Nuf2, components of the outer kinetochore (Stucke, Baumann and Nigg, 2004). The interaction is mediated by Aurora B activity, which is required to establish the SAC independently of its role in error correction (Santaguida *et al.*, 2011; Saurin *et al.*, 2011). Mps1 is then phosphorylated by Cdk1, which is required for its full kinase activity and activation of the SAC (in *Xenopus* egg extracts) (Morin *et al.*, 2012).

From here, Mps1 phosphorylates key substrates in the KMN network (Kang *et al.*, 2007; Combes *et al.*, 2018). These include the repeated 'MELT' motifs (Met-Glu-Leu-Thr) found on KNL1 that, once activated, allow recruitment of a Bub3:Bub1 heterodimer, followed by BubR1:Bub3 (London *et al.*, 2012; Shepperd *et al.*, 2012). Bub1 is then phosphorylated by Cdk1 and Mps1 to allow recruitment of

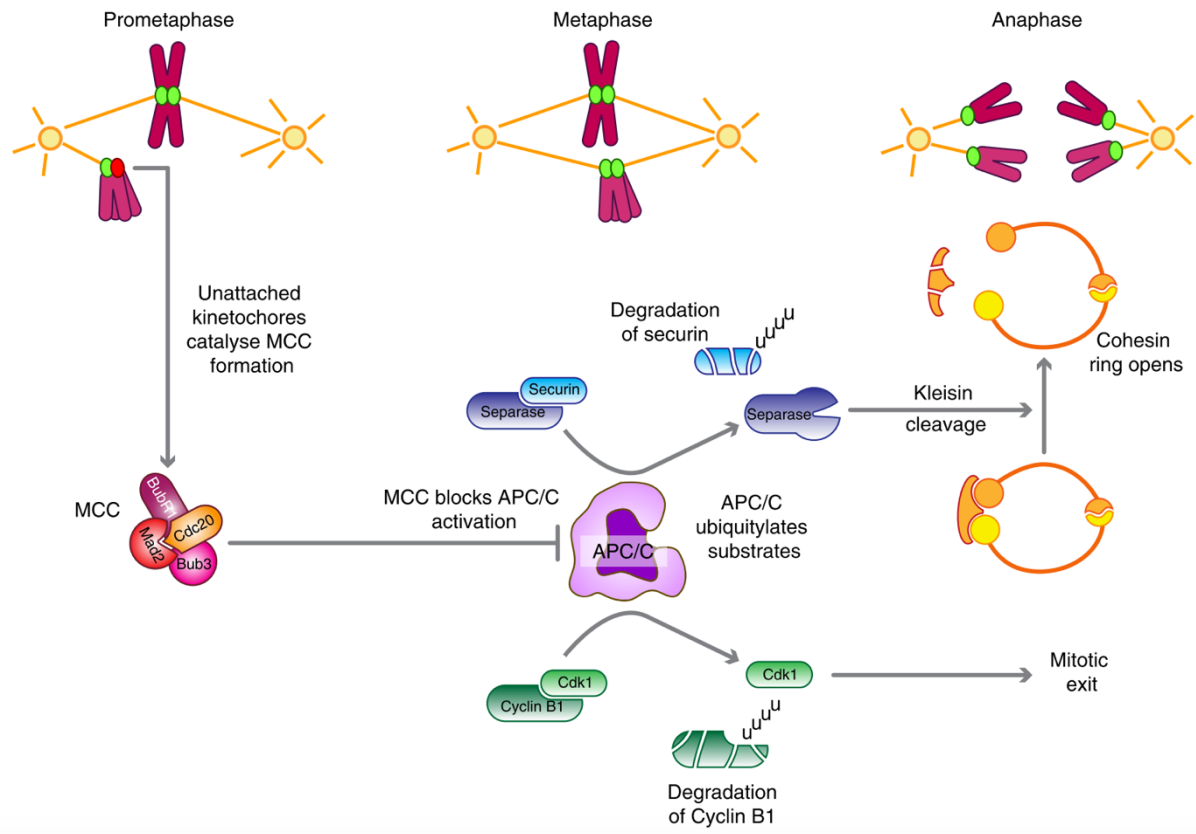

Figure 6: Molecular basis of the SAC. During prometaphase, unattached kinetochores catalyse formation of the mitotic checkpoint complex (MCC). This sequesters the APC/C co-activator Cdc20 and inhibits APC/C activation. Once all kinetochores are attached in metaphase MCC production is stopped and Cdc20 is released from MCC to activate APC/C. This leads to ubiquitination and degradation of securin and cyclin B1. Degradation of securin activates separase, which cleaves the kleisin subunit of the cohesin ring at centromeres. This opens the ring and allows sister chromatids to separate at anaphase. Degradation of cyclin B1 inactivates Cdk1 leading to mitotic exit. Figure adapted from Lara-Gonzalez, Westhorpe and Taylor, 2012.

Mad1:Mad2 complexes to the kinetochore (London and Biggins, 2014; Mora-Santos *et al.*, 2016; Ji *et al.*, 2017). Mps1 further phosphorylates Mad1 in order to stimulate Cdc20 binding and MCC formation (Ji *et al.*, 2017). These steps allow recruitment of individual MCC components to the kinetochore to promote the rapid formation of MCC, and is referred to as the KNL1-Bub1-Bub3 pathway (KBB).

Bub1 also recruits another mitotic kinase, Plk1, to the kinetochore where it is required for full activation of Mps1 (Ikeda and Tanaka, 2017). The same study also

found that Bub1-Plk1 promotes retainment of Mps1-phosphorylated KNL1 MELT repeats by counteracting phosphatase activity. This contributes to the maintenance of SAC activity following initial activation through a positive feedback loop promoting kinetochore retainment of Bub1.

A second pathway has also been proposed to recruit Mad1:Mad2 complexes to kinetochores and activate the SAC in metazoans. This involves the corona proteins Rod-Zwilch-ZW10 (RZZ) and Spindly, and is therefore referred to as the RZZ pathway. Importantly, these proteins are not conserved in yeast suggesting that SAC regulation in higher organisms has evolved with more complexity. Rod and Mad2 were shown to have very similar dynamics in *Drosophila* larval neuroblasts when labelled using fluorescent tags (Buffin *et al.*, 2005). Both appear at kinetochores during NEBD and are transported poleward along spindle microtubules following kinetochore capture. A separate study in HeLa cells found Mad1 was unable to bind unattached kinetochores following ZW10 knockdown (Kops *et al.*, 2005). Spindly, a dynein adaptor protein that binds to the RZZ complex (Mosalaganti *et al.*, 2017), is thought to mediate checkpoint silencing of the RZZ pathway through promoting dynein-mediated stripping along spindle microtubules from the kinetochore (Howell *et al.*, 2001; Griffis, Stuurman and Vale, 2007; Gassmann *et al.*, 2010; Gama *et al.*, 2017). Furthermore, Spindly has been shown to bind to Mad1 in *C.elegans* (Yamamoto *et al.*, 2008). It has recently been proposed that the KBB and RZZ pathways can provide two separable pathways for SAC activation at human kinetochores (Silió, McAinsh and Millar, 2015). This question forms the basis of this thesis and will be discussed in further detail in section 1.8.

1.6.3 Nuclear pores as a scaffold for MCC production

Mad1:Mad2 complexes have also been shown to localise to the nuclear envelope during interphase, in both yeast and human cells (Campbell, Chan and Yen, 2001; Iouk *et al.*, 2002). It is important here to note that yeast cells perform a closed

mitosis, where the nuclear envelope remains intact, while human cells undergo open mitosis following nuclear envelope breakdown. It has been shown that budding yeast the bulk of Mad1p and Mad2p remains associated with nuclear pore complexes (NPC) throughout the cell cycle, including mitosis, however Mad2p relocalises to kinetochores when the SAC is fully activated with nocodazole (Iouk *et al.*, 2002). These data suggest that Mad2p is somehow 'activated' at the NPC via the interaction with Mad1p, before it is recruited to unattached kinetochores.

In human cells NPC localisation of Mad1:Mad2 occurs via an interaction with the nucleoporin Tpr (translocated promoter region protein) located on the nucleoplasmic side of the membrane (Campbell, Chan and Yen, 2001; Lee *et al.*, 2008). Nuclear pore localisation of Mad1:Mad2 has been proposed to mediate assembly of MCC during interphase to inhibit interphase APC/C and stabilise Cyclin B1 before the cell enters mitosis (Rodriguez-Bravo *et al.*, 2014). The production of interphase MCC decreases the threshold of kinetochore-scaffolded MCC production needed to establish a functional SAC during early mitosis. It also ensures correction of merotelic attachments that do not trigger the SAC by defining the minimum length of time a cell will spend in mitosis.

There could also be another (unknown) function of this localisation of Mad1:Mad2 at the nuclear envelope. It has been suggested that Mad1p plays a role in regulating nuclear import in budding yeast (Cairo, Ptak and Wozniak, 2013). Mad1p is proposed to cycle between unattached kinetochores and the NPC during mitosis, causing nuclear import to be temporarily shut down when the SAC is activated. This subsequently excludes SAC antagonists from the nucleus, although this mechanism is not thought to be conserved in human cells as mitosis is open. It could, however, be possible for Mad1 and Mad2 to regulate nuclear transport during interphase in human cells.

1.6.4 MCC turnover for SAC responsiveness

The SAC must proficiently inhibit all APC/C in the presence of unattached kinetochores, while also allowing rapid activation when the last kinetochore attaches to the mitotic spindle. Exit from mitotic arrest requires the APC subunit APC15 (Mansfeld *et al.*, 2011). APC15 is required for the release of MCC from APC/C^{MCC} complexes during SAC signalling. This allows continual generation of 'free' APC/C, devoid of MCC and Cdc20, which is available for rapid activation once the SAC is satisfied. This enables the SAC to respond quickly to changes in kinetochore attachment state and allows the cell to complete mitosis efficiently.

Kinetochore-produced MCC complexes are then disassembled by TRIP13-mediated removal of Mad2. TRIP13 acts in combination with $P31^{comet}$ to partially unfold the N-terminus of C-Mad2 causing it to convert back to O-Mad2 and be released from MCC (Alfieri *et al.*, 2016). The combined activity of both APC15 and TRIP13 is required for cells to exit mitosis by first releasing MCC from APC/C, then disassembling the MCC complexes to release Cdc20 (Kim *et al.*, 2018). This allows APC/C to become activated and degrade Cyclin B and securin, causing the cell to enter anaphase.

MCC is constantly assembled and disassembled during prometaphase, however a single unattached kinetochore is sufficient to delay anaphase for the whole cell (Rieder *et al.*, 1994). Therefore the MCC produced at unattached kinetochores must be amplified in some way to exceed the rate of turnover and generate enough complexes to inhibit all APC/C. This is achieved by deubiquitinating enzymes that antagonise APC/C-mediated MCC subunit ubiquitination to stabilise the proteins. In this way, USP44 and USP9X restrain Cdc20 ubiquitination and degradation, and therefore MCC turnover, to amplify MCC and strengthen SAC signalling (Stegmeier *et al.*, 2007; Skowyra *et al.*, 2018). This allows efficient inhibition of all APC/C in the presence of an single unattached kinetochore to delay anaphase onset.

1.6.5 SAC silencing upon biorientation

As previously described, SAC activation at kinetochores requires extensive protein phosphorylation, mostly mediated by Mps1, but also Plk1, Aurora B and Bub1 (Saurin, 2018). Consequently in order to silence the SAC upon achieving the correct kinetochore-microtubule attachment state, phosphorylation must be reversed by phosphatase activity. This inhibits the further recruitment of checkpoint proteins to the kinetochore, and stops the production of further MCC. The main phosphatases involved in SAC silencing are PP1-Knl1 and PP2A-B56 (Rosenberg, Cross and Funabiki, 2011; Espert *et al.*, 2014; Nijenhuis *et al.*, 2014).

PP1 binds to KNL1 through the SILK/RSVF motif, and from here it aids SAC silencing by dephosphorylating MPS1-activated KNL1-MELT motifs and Aurora B substrates (Liu *et al.*, 2010; Rosenberg, Cross and Funabiki, 2011). MELT dephosphorylation causes removal of checkpoint proteins Bub3, Bub1 and BubR1 from the kinetochore, and antagonises Aurora B's microtubule destabilising activity to allow formation of stable K-fibres. PP1 is also recruited to kinetochores via the spindle-and-kinetochore-associated (Ska) complex (Sivakumar *et al.*, 2016). Ska is essential for normal chromosome congression, and is progressively loaded to congressing kinetochores to prevent detachment (Auckland *et al.*, 2017). This progressive loading of Ska may promote the maturation of K-fibres via Ska-PP1 dependant checkpoint silencing.

PP2A-B56 recruitment is essential for the generation of stable K-fibres at correctly attached kinetochores (Foley, Maldonado and Kapoor, 2011). It opposes Aurora B and Plk1-mediated phosphorylation of kinetochore substrates, such as the Ndc80 complex, to promote chromosome-spindle interactions. PP2A-B56 is recruited via BubR1 and its phosphatase activity is therefore dependent on SAC activation (Suijkerbuijk *et al.*, 2012; Espert *et al.*, 2014). PP2A-B56 recruitment to the kinetochore prevents Aurora B from inhibiting PP1 recruitment, allowing PP1 to be recruited, MELT motifs to be dephosphorylated and checkpoint proteins, including BubR1, to be removed (Nijenhuis *et al.*, 2014). Therefore PP2A-B56 activity causes its own removal from the kinetochore through a negative feedback

loop with PP1-Knl1. SAC signalling at the kinetochore is therefore a tight balance between phosphorylation (activation) and dephosphorylation (silencing). If the balance tips towards dephosphorylation then checkpoint silencing will prevail, MCC production will cease and the cell will exit mitosis following activation of APC/C^{Cdc20}.

1.7 Domain architecture and functions of Bub1

The focus of this thesis is the conserved checkpoint protein Bub1 and its role in SAC activation in human cells. Since its discovery in the initial *Saccharomyces cerevisiae* checkpoint gene screens, Budding Uninhibited by Benzimidazoles 1 (Bub1) has been characterised as an essential checkpoint protein (Hoyt, Totis and Roberts, 1991; Roberts, Farr and Hoyt, 1994; Taylor and McKeon, 1997). Bub1 is a serine-threonine kinase that is recruited to unattached kinetochores during prophase and prometaphase, and removed at anaphase. Bub1 is strongly associated with unattached kinetochores generated by nocodazole treatment (Taylor and McKeon, 1997). Nocodazole is a synthetic tubulin-binding agent which disrupts microtubule polymerisation. This causes all kinetochores to become unattached from the mitotic spindle and blocks cells in mitosis (Vasquez *et al.*, 1997)

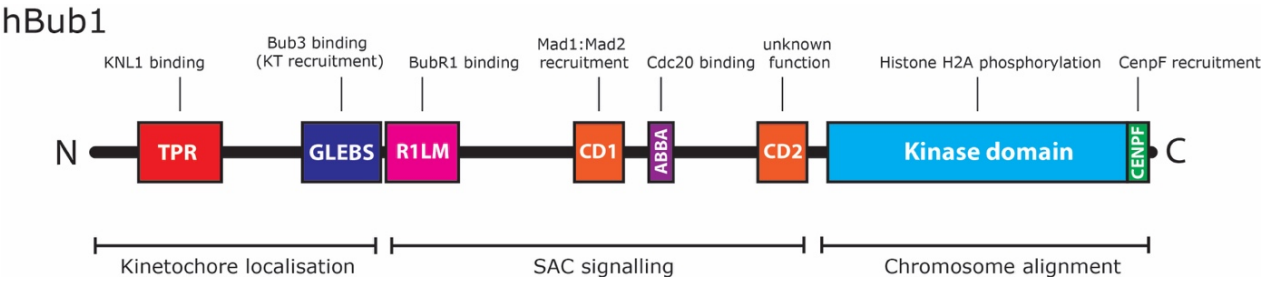

Figure 7: Organisation of Bub1 domains. The TPR domain binds KNL1 and aids Bub1 kinetochore recruitment, but is not essential. The GLEBS domain binds Bub3 and recruits Bub1 to the kinetochore. The R1LM recruits BubR1 and CD1 recruits Mad1:Mad2 following Mps1 phosphorylation. The ABBA motif binds Cdc20. The CD2 domain is highly conserved however its function is unknown. The C-terminus kinase domain phosphorylates histone H2A and the 'tail' region recruits CenpF.

The 1085 amino acid protein can be divided into three main sections, each with different functions (Figure 7). The N-terminal 300 amino acids of Bub1 are required for its kinetochore localisation. This region includes three tetratricopeptide repeats (TPRs) and the Gle2p-binding sequence (GLEBs) domain that facilitate binding of KNL1 and Bub3 respectively (Taylor and McKeon, 1997; Taylor, Ha and McKeon, 1998; Larsen *et al.*, 2007; Krenn *et al.*, 2012). The central region is necessary for SAC function, mainly through the conserved CD1 domain that recruits Mad1:Mad2 complexes (Klebig, Korinth and Meraldi, 2009) and ABBA motif that recruits Cdc20 (Di Fiore *et al.*, 2015). It also contains the R1LM BubR1 recruitment domain (Zhang *et al.*, 2015). The C-terminus consists of the kinase domain, implicated in chromosome biorientation and error correction, but not checkpoint activity (Klebig, Korinth and Meraldi, 2009; Baron *et al.*, 2016), and the CenpF recruitment site at the 'tail' region (Raaijmakers *et al.*, 2018).

1.7.1 Bub1 in human SAC signalling

Bub1 is recruited to the kinetochore through the interaction with KNL1-Bub3 via its GLEBS domain (Taylor, Ha and McKeon, 1998; Krenn *et al.*, 2012; Ricke *et al.*, 2012). The TPR domain, which is N terminal to the GLEBS domain, has also been implicated in Bub1 kinetochore recruitment (Figure 7). This region interacts directly with KNL1 but was shown to be non-essential for the kinetochore recruitment of Bub1 in HeLa cells (Krenn *et al.*, 2012). Kinetochore localisation of Bub1 is required for its SAC activity, as a Bub3-binding mutant was not able to rescue SAC-dependant mitotic arrest in Bub1Δ/Δ MEFs (Perera and Taylor, 2009).

Bub1 is one of the core checkpoint proteins implicated in SAC activation and MCC formation. In order to carry out this function, Bub1 directly recruits Mad1:Mad2 complexes to the kinetochore through a conserved region that spans amino acids 458 – 476, named the CD1 domain (Klebig, Korinth and Meraldi,

2009). In budding yeast, Mps1 phosphorylation is sufficient for Mad1 binding at the CD1 region (London and Biggins, 2014). In human cells this region is primed for activation by CDK1 phosphorylation at S459, before Mps1 phosphorylation at T461 (Ji *et al.*, 2017). Both phosphorylation steps are required for the optimal interaction with Mad1 in HeLa cells.

Bub1 also recruits the checkpoint protein BubR1 to the kinetochore through a region between residues 266 – 311 (Zhang *et al.*, 2015), however there has been debate as to whether a second binding site for BubR1 exists in the kinetochore (G. Zhang *et al.*, 2016). Bub1-dependant recruitment of BubR1 allows fine tuning of SAC activity and promotes the formation of stable kinetochore-microtubule attachments. This is mediated through BubR1-dependant recruitment of PP2A-B56 to the kinetochore (Suijkerbuijk *et al.*, 2012). Here, PP2A-B56 counters Aurora B phosphorylation and promotes SAC silencing through a negative feedback loop which promotes its own removal from kinetochores (Nijenhuis *et al.*, 2014). Bub1-dependant recruitment of BubR1 may also promote its incorporation into MCC. Consistent with this, Bub1 and BubR1 both contain an ABBA motifs which are implicated in Cdc20 recruitment to kinetochores and required for full SAC strength (Di Fiore *et al.*, 2015).

Bub1 recruits polo-like kinase 1 (Plk1) to the kinetochore through a serine – phospho-threonine – proline motif (STP) motif at residue T609 that, when phosphorylated by Cdk1, is able to bind the polo-box motif of Plk1 (Qi, Tang and Yu, 2006). Plk1 reinforces checkpoint activation through phosphorylation of Mps1 and KNL1 MELT motifs (Ikeda and Tanaka, 2017). The Bub1-Plk1 complex phosphorylates Cdc20, but this is dispensable for MCC formation. Instead it acts in parallel to MCC formation to directly inhibit APC/C^{Cdc20}. This has been proposed as a catalytic role for Bub1 in SAC signalling, and could explain why seemingly small amounts of Bub1 are able to arrest cells in mitosis, as discussed in section 1.7.3 (Jia, Li and Yu, 2016).

Alongside the recruitment of checkpoint proteins Mad1:Mad2, Cdc20 and BubR1, Bub1 acts as a scaffold protein for the recruitment of kinetochore proteins CenpF

and CenpE (Johnson *et al.*, 2004). CenpF is a large protein expressed during G2 and known to localise to the nuclear envelope prior to its recruitment to kinetochores (Feng, Huang and Yen, 2006; Bolhy *et al.*, 2011). Its role during mitosis is unclear, but it has been recently proposed to act as a negative regulator of dynein stripping from kinetochores (Auckland and McAinsh, 2019). CenpE is a plus-end directed microtubule motor protein involved in chromosome congression (Yao *et al.*, 2000). Bub1 has been shown to directly recruit with CenpF, while it indirectly recruits CenpE via BubR1 kinetochore recruitment (Ciossani *et al.*, 2018). Bub1 is proposed to be stringently required for the recruitment of CenpF, and this interaction was shown to be mediated by the final 21 amino acids of Bub1, following the C-terminus kinase domain (Raaijmakers *et al.*, 2018). Bub1 kinase activity is not required for this interaction.

1.7.2 Bub1 in chromosome biorientation

Early evidence suggested the Bub1 kinase domain was required for SAC function as a budding yeast Bub1 kinase mutant (*bub1-K733R*) failed to rescue the benomyl sensitivity exhibited by a Bub1 null strain (Roberts, Farr and Hoyt, 1994). However, this mutation was later shown to destabilise Bub1 protein, effectively rendering the mutant a Bub1-null (Warren *et al.*, 2002). A truncation mutant lacking the kinase domain was shown to be checkpoint proficient, and the kinase domain was shown to be involved in recruitment of Shugoshin-1 (Sgo1) (Fernius and Hardwick, 2007). This was later shown to be via Bub1-dependant phosphorylation of histone H2A, conserved in yeast (serine 121) and human cells (threonine 120 – H2A-pT120) (Kawashima *et al.*, 2010). Sgo1 has been shown to have multiple roles at the centromere, mostly through the associated recruitment of PP2A-B56 (Liu, Rankin and Yu, 2013). Shown in HeLa cells, Sgo1-PP2A protects sister chromatid cohesion via dephosphorylation of sororin to antagonise the cohesin-degrading protein WAPL. Sgo1 has been shown to play a crucial role in chromosome biorientation in budding yeast, as depletion of Sgo1 causes an increase in lagging chromosomes after microtubule drug washout (Indjeian, Stern and Murray, 2005). This lead to Sgo1 being proposed as the key centromere tension sensor that co-

ordinates microtubule binding with SAC silencing and the dissolution of sister chromatid cohesion.

The contribution of Bub1-dependant Sgo1 recruitment to chromosome biorientation in human cells remains unclear. Sgo1 was shown to be recruited to heterochromatin prior to mitosis during G2 via the H2K9me3-HP1 pathway, a process which is Bub1-independent (Perera and Taylor, 2009). Sgo1 then becomes more diffuse throughout the nucleus before the onset of mitosis where it is targeted back to centromeres in a manner dependant on Bub1 kinase activity. It is suggested that the G2 recruitment of Sgo1 sets up sister chromatid cohesion, and the Bub1-dependant mitotic recruitment is dispensable for this process.

It was more recently reported that cohesin and H2A-pT120, a target of Bub1 kinase, specify two distinct pools of Sgo1-PP2A at inner centromeres and kinetochores respectively in HeLa cells (Liu, Jia and Yu, 2013). Sgo1 spreads to chromosome arms in the absence of H2A-pT120 but importantly Bub1 is not required for the ability of Sgo1 to bind to cohesin, confirming that Bub1 is not essential for cohesion protection through Sgo1. In the same study Sgo1 was shown to redistribute in response to tension from inner centromeres where it interacts with cohesin, to kinetochores where it overlaps with the H2A-pT120 signal. Authors propose that the redistribution of Sgo1 from the centromere to the kinetochore allows unprotected centromeric cohesin to be efficiently cleaved upon checkpoint satisfaction. In this way, Bub1 may contribute to co-ordinated sister chromatid separation by providing a checkpoint-dependant binding site for Sgo1 following its removal from centromeres under tension.

Bub1-mediated phosphorylation of H2A-T120 has been implicated in directly controlling the localisation and activity of Aurora B kinase at the centromere in yeast (Yamagishi *et al.*, 2010) and mice (Ricke *et al.*, 2012). Loss of Bub1 kinase activity was shown to cause chromosome misalignment and aneuploidy in MEFs. However, a later report proposed that Aurora B is recruited to centromeres via Sgo1, indirectly of Bub1 kinase activity (Meppelink *et al.*, 2015). In both the absence and inhibition of Bub1, Aurora B is redistributed from centromeres to

chromosome arms (Ricke *et al.*, 2012; Baron *et al.*, 2016). However, Aurora B can be separately recruited to the centromere through Haspin-mediated phosphorylation of H3T3, via interactions with the CPC component Survivin (Kelly *et al.*, 2010). Therefore both phosphorylated H3 and H2A are thought to be necessary to create a high affinity binding site to concentrate Aurora B at the centromere (Baron *et al.*, 2016).

Furthermore, Sgo1 has been shown to fine tune Aurora B activity in RPE1 cells by mediating both its centromere recruitment, and the recruitment of its antagonist PP2A-B56 (Meppelink *et al.*, 2015). Removal of Sgo1 results in a reduction in Aurora B recruitment, however the kinase becomes hyperactivated due to the associated loss of PP2A-B56. This result suggests that Bub1-dependant recruitment of Sgo1 is not required for error correction, at least in RPE1 cells, as Aurora B is functional in its absence. Therefore the contribution of Bub1 kinase activity and Sgo1 to functional error correction is unclear.

1.7.3 Is Bub1 essential for SAC signalling in human cells? - A review of previous findings

While the role of Bub1 in SAC signalling is well established, the relative contribution of Bub1 to mammalian checkpoint signalling has been the subject of debate since its identification. Initial work on the murine homolog of Bub1 showed that it localised to the kinetochores or unaligned chromosomes, and diminished following biorientation (Taylor and McKeon, 1997). Tetracycline-induced expression of a dominant-negative N-terminus mutant of murine Bub1 (amino acids 1-331) in HeLa cells disrupted checkpoint-dependent arrest in response to nocodazole. Cells expressing this mutant were able to delay anaphase onset in response to unattached kinetochores generated by nocodazole, but they less efficient at sustaining a long term mitotic arrest. Authors concluded that Bub1 functions to maintain mitotic arrest in response to spindle damage and monitors kinetochore-microtubule attachment states in prometaphase.

In the following years, RNA interference (RNAi) became widely used for studying the functions and hierarchy of checkpoint proteins. First described in 1998 by Fire and Mello, who later went on to win the 2006 Nobel Prize for their discovery, RNAi was successfully used in *C. elegans* to manipulate gene expression (Fire *et al.*, 1998). This initial method used double stranded RNA (dsRNA), but this was not successful for mediating gene knockdown in human cells. Instead, short 21-nucleotide small interfering RNAs (siRNAs) are necessary to deplete the target mRNA (Elbashir *et al.*, 2001). Briefly, single stranded siRNA oligos are incorporated into the RNA-induced silencing complex (RISC), which can scan and bind the target mRNA sequence via complementary via Watson-Crick base pairing. This induces mRNA cleavage and the cut mRNA is degraded by the cell, thus silencing translation and gene expression. One limitation of this method is that it does not have 100% efficiency, and can therefore leave residual amounts of protein that may be functional in the cell. These variations can be due to siRNA oligo design, cell type or transfection efficiency, which can all manifest in varying depletion levels of the target protein.

siRNA was first used to unpick the hierarchy of kinetochore proteins that are recruited by Bub1 to kinetochores in a later study from the Taylor Lab (Johnson *et al.*, 2004). Bub1 was shown to be recruited to kinetochores in early prophase, following Aurora B recruitment where it acts as a key scaffold for further checkpoint protein recruitment. Bub1 localisation then triggers sequential recruitment of BubR1, CenpE and finally Mad2. Bub1 was also shown to recruit CenpF in early prophase, which contributes to the recruitment of CenpE during prometaphase. However, when the DLD-1 (colorectal adenocarcinoma) cells used in this study were transfected with Bub1 RNAi to deplete Bub1 to ~98% of wild type levels, cells displayed a robust mitotic arrest in response to nocodazole and did not show the SAC maintenance defect seen in earlier studies using HeLa cells (Taylor and McKeon, 1997). Authors were unsure whether to attribute this

surprising result to insufficient repression of Bub1 by siRNA, or the possibility that a second, Bub1-independent pathway was sufficient to maintain mitotic arrest.

A study published at a similar time from the Yu Lab implicated Bub1 in the regulation of centromeric cohesion rather than checkpoint signalling (Tang *et al.*, 2004). Bub1 was depleted in HeLa cells using siRNA but authors conversely found that cells accumulated in mitosis, suggesting SAC-dependant arrest, but no checkpoint failure. They attributed this to weakened centromeric cohesion, due to loss of Sgo1, which leads to premature sister-chromatid separation before the SAC can be satisfied. This leads to separated chromatids that can no longer achieve biorientation, which constitutively activate the SAC causing an increased mitotic index. The true contribution of Bub1 to human SAC signalling was now under question.

A study published a year later from the Sorger lab reported achieving ~99.5% depletion of Bub1 in HeLa cells using siRNA (Meraldi and Sorger, 2005). In contrast to the two earlier studies, these Bub1-depleted cells were unable to arrest in response to nocodazole, and showed mitotic exit comparable to untreated cells and Mad2 depletion. Authors concluded that Bub1was essential for SAC signalling in human cells, consistent with yeast that are known to only possess one linear pathway for SAC signalling. They further showed that Bub1 was required for chromosome congression and KT-MT attachment. Crucially, authors attributed the inconsistencies with the two previous studies on Bub1 SAC function to incomplete Bub1 depletion (Johnson *et al.*, 2004; Tang *et al.*, 2004). They stated that very low levels of kinetochore bound Bub1 (2-5% of wild type) is sufficient to sustain the SAC functions of Bub1, but leads to accumulation of misoriented chromatids due to Bub1's other role in congression. They proposed that incomplete depletion of Bub1 leads to a misleading situation where Bub1 is depleted to levels where congression is impaired but the checkpoint is functional, leading to cell cycle arrest. Importantly, at this time the RZZ complex was gaining traction as a key player in SAC signalling of higher organisms (Buffin *et al.*, 2005;

Karess, 2005). The RZZ complex has no obvious homologs in amongst yeast proteins, suggesting the metazoan SAC mechanism is more elaborate. Whether Bub1 was essential for SAC signalling or not become a question of upmost importance to the field, as it has large ramifications for role of RZZ.

To further clarify the role of Bub1 in SAC signalling, a genetic approach was required. The Taylor lab generated a mouse line in which *BUB1* could be disrupted by administering tamoxifen to activate *LoxP* sites integrated between exons 7 and 8 (Perera *et al.*, 2007). This approach bypassed the embryonic lethality known to be associated with Bu1 loss and did not rely on RNAi penetrance. Heterozygous mice were generated to harbour one Bub1-null allele and one Bub1 Cre-*LoxP* allele, which can be transduced with Cre to make $BUB1^{\Delta/\Delta}$ mouse embryonic fibroblasts (MEFs) which have 100% Bub1 depletion efficiency. These cells could not arrest in the presence of monastrol and this defect was rescued by expression of a Myc-tagged Bub1 transgene. However, supplementary data showed these $BUB1^{\Delta/\Delta}$ MEFs could delay mitotic exit by ~1 hour in response to taxol and nocodazole. Nevertheless, authors concluded that Bub1 was essential for preventing mitotic exit in the presence of unattached kinetochores. However, these data could be interpreted to suggest that initial SAC activation can be supported in the absence of Bub1, at least in the presence of nocodazole and taxol, suggesting that Bub1 is not essential for SAC signalling in metazoan cells.

The precise functions of Bub1 were further investigated in a later study from the Meraldi lab using an RNAi complementation system in both HeLa-Flp-In and hTERT-RPE1-Flp-In cells (Klebig, Korinth and Meraldi, 2009). They identified the region between amino acids 458 – 476 as being essential for Bub1 SAC function, and named this the CD1 domain. They again concluded that Bub1 is essential for SAC signalling in human cells when depleted by RNAi in HeLa and RPE1 cells, as these cells did not accumulate in mitosis when treated with nocodazole. However, these experiments were judged by mitotic index, where the percentage of 'rounded up' mitotic cells was calculated within a population

following nocodazole treatment. The main limitation of this type of experiment is that it cannot distinguish between cells which have slipped through mitosis or cells which have arrested in G2 and never progressed to mitosis.

Overall, the combination of these data points to an essential role for Bub1 in human checkpoint signalling. However, the limitations of RNAi studies cannot be overlooked and a clean genetic approach is needed to further clarify the contribution of Bub1 to SAC signalling in human cells. Furthermore, data from BUB1-disrupted MEFs arrested in taxol or nocodazole suggests that Bub1 is not essential for SAC activation in higher organisms (Perera *et al.*, 2007). Therefore the true contribution of Bub1 to SAC signalling in human cells remains unclear, and the RZZ complex could offer an alternative SAC activation pathway.

1.8 The two pathway model of human checkpoint signalling

As previously described, metazoan cells possess a set of conserved kinetochore proteins that do not have homologs in yeast. These proteins make up the Rod-Zwilch-ZW10 complex (RZZ), which interacts with the dynein adaptor protein Spindly (Mosalaganti *et al.*, 2017). Recruitment of the RZZ complex involves an interaction with Zwint1, which forms a stable complex with KNL1 as shown in HeLa cells (Wang *et al.*, 2004; Varma *et al.*, 2013). The RZZ complex has been implicated in the recruitment of Mad1:Mad2 complexes to kinetochores in human cells (Buffin *et al.*, 2005; Kops *et al.*, 2005). Interestingly, Spindly has been shown to directly bind Mad1 in *C. elegans*, although an interaction has not been confirmed in human cells (Yamamoto *et al.*, 2008). It has therefore been of great interest to the field to determine whether the RZZ and KNL1-Bub1-Bub3 (KBB) pathways provide separate receptors of Mad1:Mad2, or form one linear pathway of checkpoint activation.

Previous work in our laboratory has shown that when KNL1 is depleted using siRNA in hTERT-RPE1 cells, the checkpoint can still be activated in response to

nocodazole, although long-term mitotic arrest is perturbed (Silió, McAinsh and Millar, 2015). The rationale behind this experiment was that removal of KNL1 will cause subsequent removal of Bub1 and loss of the canonical Bub1-dependant pathway of Mad1:Mad2 recruitment (KBB pathway) (Klebig, Korinth and Meraldi, 2009; London and Biggins, 2014). Therefore, checkpoint signalling in the absence of KNL1 is suggested to operate through a separable Bub1-independent pathway mediated by RZZ complex, which is known to contribute to Mad1:Mad2 recruitment (Karess, 2005; Kops *et al.*, 2005; Varma *et al.*, 2013).

Interestingly, KNL1-depleted RPE1 cells were observed to erroneously progress through unperturbed mitosis before completing chromosome congression to the metaphase plate, but were capable of delaying anaphase in response to a single unattached kinetochore generated by low dose nocodazole treatment. The interpretation of this data was that uncongressed chromosomes depleted of KNL1 that are not able to delay anaphase onset are not properly bi-oriented but, critically, are bound to spindle microtubules in some manner. This suggests that KNL1, and therefore Bub1, is required to activate the SAC at mis-aligned kinetochores that have already bound spindle microtubules but are not fully biorientated. These are termed immature attachments. Unattached kinetochores appear to be capable of activating the SAC independently of KNL1 and Bub1.

These data resulted in the two pathway model: the RZZ pathway recruits a Bub1-independant pool of Mad1:Mad2 to kinetochores that is removed by dynein-mediated stripping via Spindly upon microtubule binding (Figure 8). The KBB pathway then keeps the checkpoint switched on until kinetochore-microtubule attachments become fully matured and biorientated, through Mad1:Mad2 binding to Bub1. It is important to note here that we do not yet understand what constitutes the mature attachments that the KBB pathway appears to respond to. The conclusion from this model is that the RZZ pathway can independently activate the checkpoint in response to unattached kinetochores in a manner separable from the KBB pathway. However, this study is limited by the use of siRNA as KNL1 depletion will not be totally efficient and a few molecules may

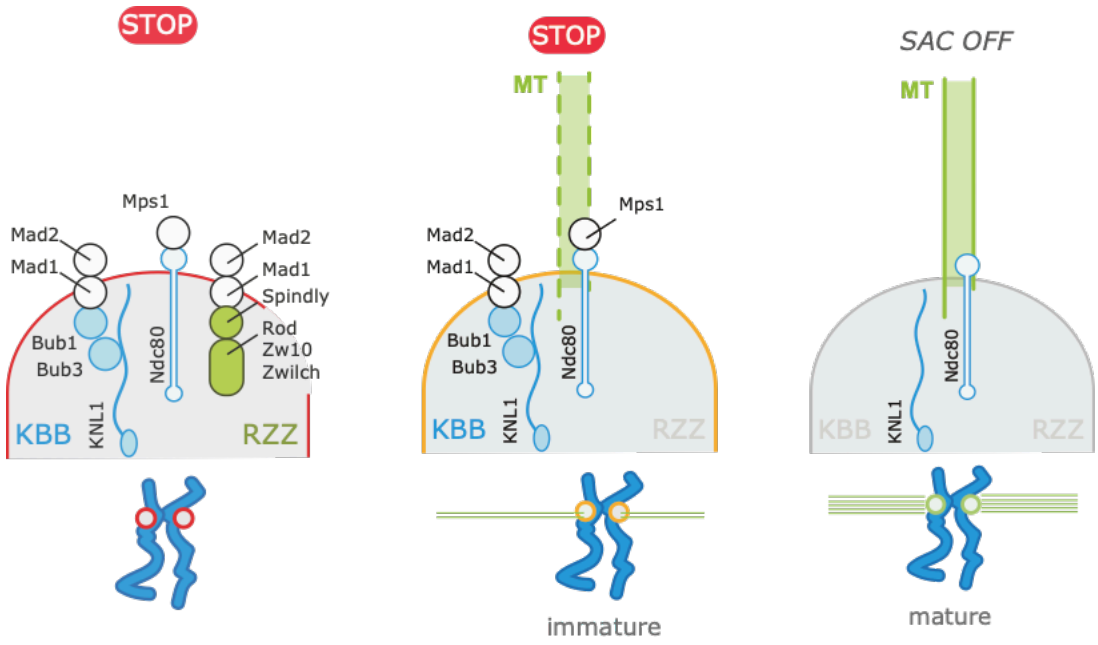

Figure 8: Two pathway model of SAC signalling. At unattached kinetochores, Mad1 and Mad2 are recruited by both the KNL1-Bub1-Bub3 (KBB) and Rod-Zwilch-ZW10 (RZZ) pathways. At immaturely attached kinetochores, RZZ/Mad1:Mad2 is stripped from the kinetochore along the bound microtubule by spindly and dynein. The KBB/Mad1:Mad2 pathway activity is maintained at immaturely attached kinetochores. Once the attachment has matured, the KBB pathway is silenced. It is unknown what constitutes a mature attachment. Figure adapted from Silió, McAinsh and Millar, 2015.

remain at kinetochores. These few KNL1 molecules could, in theory, support Bub1-mediated SAC signalling as previous studies concluded that Bub1 depletion below 98% is required to cause SAC failure (Meraldi and Sorger, 2005). Furthermore, depletion of KNL1 may cause partial unloading of RZZ from the kinetochore due to the KNL1-Zwint1 recruitment pathway (Varma *et al.*, 2013).

There has also been debate in the field as to whether Bub1 contributes to RZZ recruitment at kinetochores. Experiments using siRNA in HeLa cells showed that ZW10, an RZZ complex subunit, can be recruited to kinetochores in the absence of Zwint-1, suggesting a second binding site (Zhang *et al.*, 2015). ZW10 recruitment was shown to be facilitated by a truncated form of KNL1 which contains MELT motifs but not the Zwint-1 binding site in the C-terminus of KNL1. Further experiments found that the CD1 region of Bub1 contributed to the recruitment of ZW10. A separate study obtained similar results in HeLa cells following Bub1 depletion, also measuring ZW10 kinetochore recruitment (Caldas

et al., 2015). The authors found that ZW10 was reduced by 80% following Bub1 siRNA in prometaphase cells. However, ZW10 was fully retained when Bub1 depleted cells were treated with nocodazole, and Rod siRNA had no effect on Bub1, suggesting that the RZZ complex can bind to kinetochores in a Bub1-independent manner. However, these results could also suggest that the removal of the RZZ complex via dynein-mediated stripping is increased in the absence of Bub1, leading to a reduction in the presence of microtubules.

1.9 Recent advances in human checkpoint signalling

Recent evidence, including the data presented in this thesis, has provided further insight into the mechanisms of checkpoint signalling in human cells. However, the contribution of Bub1 still remains controversial. Apparent override of Bub1 knockout using CRISPR-Cas9 has caused further uncertainty regarding whether Bub1 is essential for SAC signalling in human cells (Currie *et al.*, 2018; Raaijmakers *et al.*, 2018; Rodriguez-Rodriguez *et al.*, 2018; Meraldi, 2019; Zhang *et al.*, 2019). This debate forms the basis of this thesis and will be discussed thoroughly in Chapters 3 and 4.

1.10 Aim of thesis

The exact mechanism of checkpoint signalling in higher organisms remains elusive. There is debate as to whether signalling is conserved from yeast to human, or whether a second, separable pathway has evolved in mammalian cells. At the heart of this debate is the contribution of Bub1. Is it essential, as in yeast, or can a second pathway contribute to checkpoint activation, making it non-essential? This project aims to answer this question using CRISPR-Cas9 technology to disrupt the BUB1 gene in hTERT-RPE1 cells. Once generated, this cell line can be used to investigate the contribution of Bub1 to checkpoint signalling and error correction.

Presented in this thesis is data further supporting the two pathway model of checkpoint signalling, showing that Bub1 is not essential for checkpoint activation in response to unattached kinetochores in human cells. I will address unforeseen issues concerning CRISPR-Cas9 adaption, and further show that, although Bub1 is not essential at unattached kinetochores, it is required for SAC activation at immaturely attached kinetochores. I will also present preliminary evidence that suggests a premitotic role for Bub1.

Chapter 2: Materials and Methods

2.1 Cell biology methods

2.1.1 Cell culture and drug treatments

Immortalised (hTERT) diploid human retinal pigment epithelial (RPE1; ATCC® CRL-4000™) cells (female) were grown in Sigma Dulbecco's Modified Eagle Media (DMEM) F12-HAM + 10% fetal bovine serum + 1% Penstrep + 2mM L-Glutamine. All cell cultures were maintained at 37°C with 5% CO_2 in a humidified incubator. For drug treatment conditions, see Table 1.

Drug	Use	Conditions	Reference
Nocodazole (SIGMA)	Depolymerise microtubules	330 nM, 16 hr	(Vasquez *et al.*, 1997)
Nocodazole	Nocodazole washout, biochemistry	3.3 μM, 2 hr	(Vasquez *et al.*, 1997)
Nocodazole	Induce polar chromosomes	5 nM or 20 nM, 2 hr	(Dick and Gerlich, 2013; Silió, McAinsh and Millar, 2015)
Reversine (SIGMA)	Inhibit Mps1	1 μM, 2 hr	(Santaguida *et al.*, 2010)
Monastrol (SIGMA)	Inhibit Eg5, monastrol arrest	100 μM, 2 hr	(Kapoor *et al.*, 2000)
BAY-320	Inhibit Bub1 kinase activity	3 μM 16 hr	(Baron *et al.*, 2016)

Table 1: Drug treatments

2.1.2 siRNA treatments

siRNA oligonucleotides (53nM) were transfected at ~60 % cell confluency using oligofectamine (Invitrogen) according to manufacturer's guidelines. Media was changed 24 hr later and experiments performed 48 hr after transfection. Briefly, two tubes were prepared, tube 1 containing 150 µl optiMEM (Gibco) and 4.5 µl siRNA duplex, tube 2 containing 36 µl optiMEM and 9.5 ml oligofectamine (volumes per 35 mm well). These were incubated separately at room temperature for 8 min, after which tube 2 was added to tube 1, mixed by flicking and incubated for a further 25 min at room temperature. The final mixture (200 µl) was added to cells dropwise in a 35 mm well containing 1.5 ml fresh DMEM. After 24 hr incubation, either the media was replaced with 2 ml fresh or cells were split into fluorodishes (World Precision Instruments or Thermo Fisher) for live cell imaging 24 hr later. For siRNA oligo sequences, see Table 2.

Target	Sequence (5' – 3') (+tt)	Supplier	Reference
Lamin A (control)	GGACCUGGAGGUCUGCUGU	Sigma	N/A
Bub1	CCCAUUUGCCAGCUCAAGC	Sigma	(Jia, Li and Yu, 2016)
CenpF	AAGAGAAGACCCCAAGUCAUC	Sigma	(Holt *et al.*, 2005)

Table 2: siRNA oligo sequences

2.1.3 Quantitative immunofluorescence

For quantitative immunofluorescence (IF), cells were seeded on coverslips previously washed with 70% ethanol and PBS. Cells were fixed at room temperature in PTEM-F (20 mM PIPES, 10 mM EGTA, 1 mM $MgCl_2$, 0.2% Triton X-100 and 4% formaldehyde) for 10 min, then permeabilised with 0.1%

Antibody	Target/Uniprot ID	Identifier	Supplier	Dilution
Bub1 (Ms)	BUB1 aa 1-130 (043683)	ab54893	Abcam	1/500
Bub1 CD1 (Rb)	BUB1 aa 336–489	-	Meraldi Lab	1/4000
BubR1	BUB1B (060566)	ab4637	Abcam	1/200
KNL1	KNL1 (Q8NG31)	ab70537	Abcam	1/500
Rod	KNTC1 (P50748)	ab56745	Abcam	1/50
Mad2 (Rb)	MAD2L2 (Q9UI95)	poly19246	Biolegend	1/500
Mad2 (Ms)	MAD2L2 (Q9UI95)	107-276-3	Santa Cruz	1/1000
CenpE	Centromere protein E (Q02224)	-	Meraldi Lab	1/1500
Zwilch	Zwilch (Q9H900)	-	Musacchio Lab	1/1000
CenpF	Centromere protein F (P49454)	ab90	Abcam	1/200
ZW10	ZW10 (O43264)	ab21582	Abcam	1/200
Spindly	Spindly (Q96EA4)	A301-354A	Bethyl Laboratories Inc.	1/200
α-Tubulin	Tubulin alpha 4A chain (P68366)	T6074	Sigma Aldrich	1/1000
CenpC	Centromere protein C (Q03188)	PD030	MBL	1/2000
CREST	Centromere proteins	15-234-0001	Antibodies Inc.	1/200
Sgo1	Shugoshin 1 (Q5FBB7)	ab58023	Abcam	1/200
Hec1 pSer55	Phosphorylated serine 55, a target of Aurora B (014777)	15359041	Invitrogen	1/300
Tpr	TPR, nucleoporin (P12270)	Ab84516	Abcam	1/500

Table 3: Primary antibodies for immunofluorescence

Triton X-100 PBS for 5 min, washed three times with PBS and blocked with 3% BSA PBS for 60 min. Cells were then incubated with primary antibodies at the appropriate dilution in blocking solution for 2 hours washed three times with PBS and incubated with secondary antibodies for 1 hr at room temperature in the dark. For primary antibodies, see Table 3. Secondary antibodies were Alexa Fluor conjugated antibodies (Invitrogen) used at 1/500 for 1 hour. A final three PBS washes were performed, and slides were mounted using Vectasheild with DAPI (Vector Laboratories). Three-dimensional image stacks were acquired (1x1 binning) in 0.2 μm steps using a 100× oil NA 1.4 objective on an Olympus Deltavision Elite microscope (Applied Precision, LLC) equipped with a DAPI-fluorescein isothiocyanate-Rhod/TR–CY5 filter set (Chroma) and a Coolsnap HQ2 camera.

2.1.4 Live cell imaging

For live cell imaging, cells were seeded into either a fluorodish (WPI) or Lab-Tek 2 or 8 chamber slide (Thermo Fisher). RPE1 cells were incubated with 0.5 μM Sir-DNA (Spirochrome) for ~60 min to visualise chromosomes. This treatment does not alter mitotic progression compared to previous work with Histone2B-RFP (not shown). Image stacks (7 x 2 μm optical sections; 1x1 binning) were acquired every 3 min for either a 12 hr or 3 hr period with a 40x oil-immersion 1.3 NA objective using an Olympus DeltaVision Elite microscope (Applied Precision, LLC) equipped with a CoolSNAP HQ2 camera (Roper Scientific). Images were acquired at 10% neutral density using Cy5 filter and an exposure time of 0.08s. A stage-top incubator maintained cells at 37°C and 5% CO2 with further stabilisation from a microscope enclosure (Weather station; PrecisionControl) held at 37°C. Image sequences were inspected and analysed by hand using SoftWorx (Applied Precision, LLC). For nocodazole or monastrol arrest treatments and reversine experiments, drugs were added at the stated concentrations 2 hr prior to imaging. For nocodazole or monastrol washout experiments, 3.3 μM nocodazole or 100 μM monastrol and 0.5 μM Sir-DNA dye was added to cells 2 hr prior to imaging. After

incubation, media was removed, and cells were gently washed 3 times with warm media then reincubated with fresh media containing SiR-DNA. Cells were imaged for a 3 hr period, with the time from washout to start of movie being noted. For long term mitotic arrest experiments, cells were imaged for 40 hr with images taken every 10 min. Data was plotted using excel or MATLAB.

2.1.5 CRISPR-Cas9 genome editing

Small guide RNAs (sgRNAs) targeting exon 2 of Bub1 (Table 4) were designed using http://crispr.mit.edu and cloned into an *S. pyogenes* Cas9 and GFP plasmid, pspCas9(BB)-2A-GFP (Addgene PX458) using the BbsI restriction enzyme as previously described (Ran *et al.*, 2013). Plasmids were sequenced with the U6 forward promoter to check for correct insertion of sgRNAs. For transfection, RPE1 cells were grown in a 10 cm dish to 60% confluency. Cells were then transfected with 4 μg of prepared plasmid in 1.5 mL optiMEM, using Fugene HD at a ratio of 1:5. The mixture was added dropwise to cells in 12 mL fresh media. Cells were grown for 24 hr, when media was replaced with fresh DMEM. After a further 24 hr, cells were prepared for FACS sorting by trypsinisation, centrifugation. Cells were then filtered to remove clumps and debris, and held in starving media (DMEM, 1% FBS, 1% PenStrep and 2nM L-glutamine). A pool of GFP positive cells was isolated by FACS sorting (BD Influx FACS cell sorter), and

Guide sequence (5' – 3')	Use	Supplier
CACCGTACAAGGGCAATGACCCTCTTG	Bub1 CRISPR (forward)	Sigma
AAACAGAGGGTCATTGCCCTTGTAC	Bub1 CRISPR (reverse)	Sigma

Table 4: CRISPR guide sequences

single clones were generated by dilution and plating of 500 cells into a 15 cm dish. Cells were allowed to expand for 2-3 weeks until single colonies were visible by eye. These were then selected using cloning discs (Sigma) and trypsin to be expanded in a 12 well dish. For Bub1 knockout, clones were screened by immunofluorescence (see section 2.1.3 Quantitative immunofluorescence) using a mouse anti-Bub1 antibody (ab54893, Abcam).

2.2 Molecular biology methods

2.2.1 PCR

Genomic DNA for all samples was obtained from cell pellets using the DNeasy Blood and Tissue Kit (Qiagen). For all PCR reactions, the reaction mix consisted of 100 ng genomic DNA, 1 μM each specific primer, 200 μM dNTPs, 10 μl 5X Q5 reaction buffer and 1 μl of Q5 polymerase enzyme. For DNA amplification, the following protocol was used for all reactions, with annealing time adjusted for specific primer sets: [1] Initial denaturation at 98°C for 10 sec, [2] denaturation for 98°C for 10 sec, [3] annealing at primer specific temperature for 20 sec, [4] extension at 72°C for 30 s, [5] final extension at 72°C for 10 min. Steps [2-4] were repeated for 34 cycles. Reactions were performed in a thermocycler. PCR products were separated on a 1% agarose gel, and the correct sized bands were excised and purified using Monarch® DNA Gel Extraction Kit, eluted into ddH_20. Primer sequences can be found in Table 5.

2.2.2 Bacterial transformation

For the transformation step, the appropriate amount of PCR reaction product was added to the appropriate amount of dH5α cells on ice. For CRISPR sgRNA cloning, 11 μl product was added to 100 μl dH5α cells. Cells were incubated for 5 min on ice, then heat shocked at 42°C for 1 m 30 s and returned to ice for 5 min.

dH5α cells were gently resuspended in 100 µl of liquid broth (LB), and spread onto agar plates containing the appropriate antibiotic selection under a flame and incubated for >16 hr. For sgRNA cloning, cells were selected using ampicillin. Colonies were picked under a flame and amplified in 5 ml LB containing the appropriate selective antibiotic for ~16 hr at 37°C with shaking. Plasmid DNA was purified using a mini-prep kit (Qiagen).

Primer name	Sequence 5' – 3'	Use	Annealing temp	Supplier
Gateway Bub1 exon 2 1kB FW	GGGGACAAGTTTGTACAAA AAAGCAGGCTTCAGCTGGG ACTTATGGAAAAACA	Bub1$^{1-23}$ allele PCR sequencing	72°C	Sigma
Gateway Bub1 exon 2 1kB RV	GGGGACCACTTTGTACAAG AAAGCTGGGTCCTATGACT GGTTGCTGGTAGAGAGA	Bub1$^{1-23}$ allele PCR sequencing	72°C	Sigma
M13F (-20)	GTAAAACGACGGCCAGT	GATC sequencing	N/A	Sigma
U6 (Forward)	GACTATCATATGCTTACCGT	CRISPR plasmid sequencing	N/A	Sigma

Table 5: PCR and sequencing primer sequences

2.2.3 Sequencing

All plasmids were confirmed by sequencing (GATC). Plasmid DNA was sent at 80-100 ng/µl and primers were sent at 5 pmol/µl.

2.2.4 CRISPR-Cas9 allele sequencing

The Bub1$^{1-23}$ cell line was verified by PCR-cloning and DNA sequencing. Gateway PCR primers were designed (see table 5) to amplify a 1 kB region from genomic DNA, containing the Cas9 target region, using the PCR protocol described in section 2.2.1. PCR products were recombined into the pDONR-221 vector using the Gateway cloning BP reaction (Thermo Fisher Scientific). Briefly, in a total reaction volume of 15µL, 50ng of amplified DNA, 195ng of pDONR221 and 3 µl of BP Clonase™ II enzyme mix (5X) were added to the appropriate volume of TE buffer. The reaction was incubated at 25°C overnight then terminated by adding 2 µl proteinase K solution and incubated at 37°C for 10 min. 1 µl of this reaction was transformed into 50 µl dH5α cells as described in section 2.3.2. The transformation reaction was spread onto agar plates with kanamycin antibiotic selection, except for positive control DNA which required tetracycline selection. Colonies were then amplified in 5 ml LB containing kanamycin and prepared using a mini-prep kit (Qiagen). Plasmids were sent for sequencing with the M13F primer (Table 5).

2.2.5 RNA extraction and RT-PCR

For RNA extractions cells were grown in a 15cm dish and harvested. RNA was extracted using RNAeasy mini kit (Qiagen). The following mix was prepared to anneal the RNA; 50ng random hexamers, 0.8µM dNTP mix, 2.5µg template RNA and DEPC-treated water, and incubated at 65°C for 5 min, then incubated on ice for 1 min. SuperScript IV First-Strand Synthesis System (Invitrogen) was used for the RT-PCR reaction. Briefly, the following RT reaction mix was prepared; 2.5xSSIV buffer, 13mM DTT, 4 units ribonuclease inhibitor (Invitrogen) and 2 units SuperScript IV reverse transcriptase. This mix was centrifuged, added to the previously prepared annealed RNA, and incubated at 50°C for 10 mins. The reaction was inactivated by incubating at 80°C for 10 mins, then 1 unit of *E. coli* RNase H was added to the mix and incubated at 37°C for 20 mins to remove RNA. The PCR reaction was prepared using this cDNA. Bub1 primers are listed

in Table 6.

RT- PCR Primers	Sequence (5' – 3')	Supplier
Bub1 exon 1 (forward)	ACCCCGGAAAATGTCCTTCA	Sigma
Bub1 exon 8 (reverse)	AAATTCTGATTCCCCACGAATAAGC	Sigma
Bub1 exon 4 (forward)	GGAATTCAAAACCAGGCTGAAC	Sigma
Bub1 exon 4 (reverse)	GTCACTGTTGTACTCAGCAAAT	Sigma
Bub1 exon 20 (forward)	GTTCTAAGCTGGTCTATGTCCAT	Sigma
Bub1 exon 22 (reverse)	CACAGTCATGCACTTGCTC	Sigma

Table 6: RT-PCR primers

2.3 Biochemistry methods

2.3.1 Biochemistry

For immunoblots, cell extracts were prepared by lysing cells in NP40 buffer (1% NP40, 10 mM TrisCl pH 7.5, 150 mM NaCl, 10% glycerol) or UTB buffer (8M Urea, 50mM Tris pH7.5, 150mM β-mercaptoethanol, ddH_20) containing 1 mM PMSF, Complete mini EDTA-free Protease Inhibitor Cocktail and Phosphatase Inhibitor Tablets (Roche Applied Science). Lysate protein concentration was determined using a Bradford assay. Proteins were separated by SDS-polyacrylamide gel electrophoresis (SDS-PAGE) and gels were electroblotted onto nitrocellulose membranes and probed with the following antibodies: anti-Bub1

Antibody	Target	Identifier	Supplier	Dilution
Bub1	Aa 1-300	GTX30097	Genetex	1/500
Bub1 (SB1.3)	aa 336 - 489	N/A	Stephen Taylor	1/500
a-tubulin	TUBA1A (Q71U36)	T9026	Sigma	1/20000
BubR1	BUB1B (060566) (aa 350-400)	A300-386A	Bethyl Laboratories	1/1000
APC4	APC4 (Q9UJX5) (aa 758 – 808)	A301-176A	Bethyl Laboratories	1/500
Mad2	MAD2L2 (Q9UI95) (aa 150 to C term)	A300-301A	Bethyl Laboratories	1/500
Cdc20	Cdc20 (Q12834)	sc-8358	Santa Cruz Biotechnology	1/500
Cdc20	Cdc20 (Q12834)	sc-13162	Santa Cruz Biotechnology	1/500
APC3	APC3 (30260) (aa 145 – 343)	610455	BD Transduction Lab	1/500

Table 7: Primary antibodies for biochemistry

rabbit antibody (1:500, GeneTex GTX30097), anti-Bub1 SB1.3 sheep antibody (1:500, a kind gift from Stephen Taylor), anti-α-Tubulin mouse antibody (1:20000, Sigma T9026), anti- BubR1 rabbit antibody (1:1000, Bethyl Laboratories A300-386A), anti-APC4 rabbit antibody (1:500, Bethyl Laboratories A301-176A), anti-Mad2 rabbit antibody (1:500, Bethyl Laboratories A300-301A), anti-Cdc20 rabbit antibody (1:500, Santa Cruz Biotechnology sc-8358), anti-APC3 mouse antibody (1:500, BD Transduction Lab 610455), anti-Cyclin B mouse antibody (1:1000, BD Transduction Lab 610220) and anti- hSecurin mouse antibody (1:500, Santa Cruz sc-56207). Proteins were visualized using the enhanced chemiluminescence (ECL) detection system according to the manufacturer's instructions (GE Healthcare).

For immunoprecipitation experiments, whole extracts (1 mg) were incubated with normal mouse IgG (Santa Cruz Biotechnology) for 30 min and subsequently with protein G-Sepharose beads (GE Healthcare) for 45 min at 4ºC. After centrifugation, beads were kept as pre-immune (PI) and the same extract was incubated with anti-Cdc20 or anti-APC3 mouse antibodies (Santa Cruz Biotechnology and BD Transduction Lab, respectively) for 2 hours followed by an incubation with protein G-Sepharose beads for another 45 min and the beads were kept as Immune (I). Beads were washed six times with NP40 buffer and bound proteins were solubilised by the addition of SDS-sample buffer heated at 95ºC for 5 min.

2.4 Data analysis

2.4.1 SiD analysis

Following image collection, kinetochore signal intensities were measured using a GUI-driven software package within MATLAB called SiD (spot intensity detector), which can be found at https://github.com/cmcb-warwick/SiD. This requires MATLAB version R2017a or later. Briefly, kinetochores are detected within images using a reference signal (CREST or CENP-C) by splitting the histogram of intensities, separating the spots from background. The centres of spots were calculated using a mixture model of 3D Gaussians and spots manually filtered to remove false positives and any poorly localised spot centres. Raw intensities of kinetochore components in the first channel (reference) and second channel were calculated as the mean intensity within a sphere of 300 nm radius around the kinetochore's spot centre. Intensities were then corrected for average background intensity, defined as the mean intensity of the image. Intensities were normalised to the reference signal intensity on a spot-by-spot basis.

2.4.2 Nuclear envelope quantification

Nuclear envelope intensity analysis was performed manually using SoftWorx software (Applied Precision, LLC). A 20x10 pixel box was used to record pixel intensity values at four points of the nuclear envelope, within the nucleus and the background. Average values for the three regions were calculated, then the background value was subtracted from nuclear envelope and nucleus values. Box and whisker plots were created in Excel.

2.4.3 Figure preparation and statistical analysis

Data were plotted using either SiD, Microsoft excel, R or MATLAB. Representative immunofluorescence images were prepared using Softworx (Applied Precision), with scale bars added using FIJI, or OMERO. Movie stills were prepared in OMERO or FIJI. Two-sided Mann-Whitney U-tests to compare median values were an automatic output from SiD software (MATLAB). All other statistical tests were performed using MATLAB. P values are represented as follows; * = $p < 0.05$, ** = $p < 0.01$, *** = $p < 0.001$. All figures were edited and prepared using Adobe Illustrator CS5.

Chapter 3: Bub1 is not essential for the checkpoint response to unattached kinetochores in hTERT-RPE1 cells

3.1 Introduction

As discussed in Chapter 1, the role of Bub1 in SAC signalling has been extensively debated in the literature. After its initial discovery in *Saccharomyces cerevisiae* checkpoint screens in 1991, Bub1 was characterised as an essential checkpoint protein in yeast (Hoyt, Totis and Roberts, 1991). However in 2000, the discovery of a second set of checkpoint proteins that are not conserved in yeast raised the possibility of a more elaborate SAC signalling pathway to control mitosis in metazoans (Chan *et al.*, 2000).

The Taylor Lab used RNAi to unpick the hierarchy of kinetochore proteins which are recruited by Bub1 (Johnson *et al.*, 2004). However, when the colorectal adenocarcinoma DLD-1 cells used in this study were transfected with Bub1 RNAi to deplete Bub1 to ~98% of the wild type, cells displayed a robust checkpoint in response to nocodazole. Authors were unsure whether to attribute this surprising result to insufficient repression of Bub1 by RNAi, or the possibility that a second, Bub1-independent pathway was sufficient to maintain mitotic arrest in human cells. Interestingly, 20% expression of BubR1, a protein known to be recruited by Bub1, was detectable at kinetochores in these cells depleted of Bub1.

A study published at a similar time from the Yu Lab implicated Bub1 in the regulation of centromeric cohesion rather than checkpoint signalling (Tang *et al.*, 2004). Bub1 was depleted in cervical cancer HeLa cells using RNAi but authors conversely found that cells accumulated in unperturbed mitosis due to the presence of prematurely separated sister chromatids, suggesting SAC-dependant

arrest and no checkpoint override. These two papers together provided the first evidence that Bub1 may not be essential for SAC signalling in human cells.

A later study from the Sorger lab was able to very efficiently deplete Bub1 using siRNA in HeLa cells (Meraldi and Sorger, 2005). There was a ~25 fold depletion in total Bub1 protein, and a ~150-200 fold depletion at the kinetochore, representing ~99.5% depletion of Bub1. BubR1 was easily detectable at kinetochores in the absence of Bub1 in Hela cells, consistent with the previous report in DLD-1 cells (Johnson *et al.*, 2004). In contrast to the two earlier studies these cells were unable to arrest in response to nocodazole treatment and authors concluded that Bub1 is essential for SAC signalling in human cells, consistent with yeast. Crucially, authors attributed the inconsistencies with the two previous studies on Bub1 SAC function to incomplete Bub1 depletion (Johnson *et al.*, 2004; Tang *et al.*, 2004). They stated that very low levels of kinetochore bound Bub1 (2-5% of wild type) was sufficient to sustain the SAC response, but leads to an accumulation of misoriented chromatids due to Bub1's role in chromosome alignment. This leads to a situation where Bub1 is depleted to levels where congression is impaired but the checkpoint is functional, leading to mitotic arrest.

To further clarify the role of Bub1, the Taylor lab generated a mouse line in which *BUB1* can be inactivated by administering tamoxifen to activate *LoxP* sites integrated between exons 7 and 8 (Perera *et al.*, 2007). Extracted $BUB1^{\Delta/\Delta}$ mouse embryonic fibroblasts (MEFs) failed to delay anaphase onset in the presence of monastrol and this defect was rescued by expression of a Myc-tagged Bub1 transgene, suggesting Bub1 is required for SAC dependant arrest in these cells. However, a closer look at the supplementary data provided with this publication showed that $BUB1^{\Delta/\Delta}$ MEFs could delay anaphase onset by ~1 hour in response to taxol and nocodazole. Authors concluded that Bub1 is essential to prevent anaphase onset in the presence of unattached kinetochores, however these data suggest that the SAC can be initially activated in the absence of Bub1, at least in the presence of nocodazole and taxol. Interestingly, BubR1 was not detectable at

kinetochores of $BUB1^{\Delta/\Delta}$ MEFs, in contrast to the two earlier studies using cancer cells (Johnson *et al.*, 2004; Meraldi and Sorger, 2005).

The detailed functions of Bub1 were further investigated in a later study from the Meraldi lab using an RNAi complementation system in both HeLa-Flp-In and hTERT-RPE1-Flp-In cells (Klebig, Korinth and Meraldi, 2009). Various Bub1 truncation mutants failed to arrest in nocodazole following Bub1 RNAi complementation experiments as judged by mitotic index in HeLa and RPE1 cells. Authors also saw 20% of BubR1 retained at kinetochores in HeLa cells after Bub1 depletion and 10% in hTERT-RPE1 cells. Authors concluded that Bub1 is required for SAC signalling in human cells.

At the same time, the Rod-Zwilch-ZW10 (RZZ) complex was being implicated in SAC signalling. Work in *Drosophila* larval neuroblasts from the Karess Lab in 2005 showed that fluorescently tagged Mad2 and Rod are closely associated in early mitosis, localise together to the corona, and are removed from kinetochores together via 'stripping' along the spindle microtubules (Buffin *et al.*, 2005). ZW10, a subunit of the RZZ complex, was shown to bind Zwint-1 (an outer kinetochore component that binds KNL1) and contribute to Mad1:Mad2 recruitment to unattached kinetochores of HeLa cells (Kops *et al.*, 2005; Varma *et al.*, 2013). These discoveries raised the possibility that there may be a second pathway for SAC signalling in higher organisms that was not conserved in yeast. Later work using RNAi directly proposed that RZZ and the KNL1-Bub1-Bub3 (KBB) pathway could provide two separable pathways for Mad recruitment and SAC signalling in human cells (Caldas *et al.*, 2015; Silió, McAinsh and Millar, 2015). Now the unanswered question in the field was: does RZZ contribute to SAC signalling in a Bub1-independent manner, or through one linear pathway? The contribution of Bub1 to SAC signalling was now highly relevant and controversial.

The variable nature of RNAi effectiveness, due to oligo design and transfection efficiency between cell lines could account for the different phenotypes reported

in response to Bub1 loss. Residual amounts of Bub1 (>2%) could, in principle, support SAC signalling, explaining why some Bub1 depleted human cells are able to delay in response to spindle poisons (Johnson *et al.*, 2004; Tang *et al.*, 2004), and others are not (Meraldi and Sorger, 2005; Klebig, Korinth and Meraldi, 2009). A further issue of RNAi is that it has unpredictable off target effects, the most common of which is Mad2 due to high sequence similarity to the *MAD2* 3-UTR (Sigollit *et al.*, 2012). The best way to overcome the limitations of previous studies would be to silence Bub1 at the endogenous locus using gene editing.

To reinvestigate the contribution of Bub1 to human checkpoint signalling, we used the CRISPR-Cas9 gene editing system to target the *BUB1* gene in hTERT-RPE1 cells with the aim of generating a Bub1 'knock-out' cell line. CRISPR-Cas9 is a targeted nuclease that can be applied to anywhere in the genome using a custom 20 nucleotide sequence within its guide RNA. Here it can perform a double-strand DNA break, which is preferentially repaired by the error prone non-homologous end joining (NHEJ) pathway. This leads to the creation of insertion-or-deletion (INDEL) mutations, which result in frame shifts and premature stop codons within the endogenous sequence causing the gene to be silenced.

The aim of this chapter is to directly test the two pathway model of checkpoint activation, where KBB and RZZ are proposed to form separable pathways that recruit Mad1:Mad2 complexes to kinetochores and delay anaphase onset (Silió, McAinsh and Millar, 2015). It is proposed that the RZZ-dependant pool of Mad1:Mad2 is removed along kinetochore microtubules through the process of dynein-mediated 'stripping' via Spindly following microtubule capture (Gassmann *et al.*, 2010). The KBB pathway then retains a second pool of Mad1:Mad2 at immaturely attached kinetochores to allow further stabilisation of attachments. A direct prediction of this model is that cells are able to activate the SAC in response to unattached kinetochores in the absence of Bub1, as the RZZ complex will be present at the kinetochore to facilitate Mad1:Mad2 recruitment. Following the successful application of CRISPR-Cas9 technology to create a Bub1 'knock-out'

cell line, various experiments were performed to test this model and investigate the role of Bub1 in spindle assembly checkpoint signalling.

3.2 hTERT-RPE1 Bub1 knockout cell line generation

The use of the targeted nuclease, CRISPR-Cas9, has revolutionised gene editing by allowing the creation of precise, targeted changes in a more reliable and efficient manner than previous methods. Briefly, the RNA-guided Cas9 nuclease from the microbial clustered regularly interspaced short palindromic repeats (CRISPR) adaptive immune system facilitates genome engineering at any specific locus in the human genome via a 20-nt targeting sequence within its guide RNA. The target sequence must always be associated with a 5' -NGG protospacer adjacent motif (PAM) in the genomic DNA. The nuclease induces a double stand break at the target region, which can then be repaired by either error-prone non-homologous end joining (NHEJ), or high fidelity homologous directed repair (HDR). NHEJ leaves scars in the form of INDEL mutations, which can be harnessed to mediate gene knockouts. INDELs occurring within the coding region of a gene may lead to frameshift mutations and premature stop codons (Ran *et al.*, 2013). The presence of a premature stop codon activates the nonsense mediated decay (NMD) pathway to degrade mutated mRNA and subsequently inhibit translation of the protein (Losson and Lacroute, 1979; Hentze and Kulozik, 1999).

Off target effects must be considered when using the CRISPR-Cas9 system, as improper guide RNA design can cause Cas9 to bind and cut DNA at regions other than the prospective target. Guide RNA sequences should be checked for specificity using NCBI basic local alignment search tool (BLAST) before use. Any guide sequences which display homology with coding regions of DNA must be discarded. For efficient gene knockout, the N-terminus should be targeted as close to the start ATG as possible to limit the amount of coding sequence produced before a stop codon is reached. It is likely that the truncated polypeptide would be unstable and therefore degraded shortly after synthesis via the NMD pathway,

however this should not be assumed and it is wise to induce a stop codon as early as the genomic sequence allows.

Two versions of Cas9 can be used with the CRISPR system. The wild type *s. pyogenes* Cas9 is known to make a blunt cut between the 17th and 18th bases in the target sequence, causing a double strand break (Cong *et al.*, 2013). Mutating one of the two catalytic residues in Cas9 converts it into a DNA nicking enzyme, known as Cas9-nickase, which makes single strand breaks or 'nicks' (Jinek *et al.*, 2012; Cong *et al.*, 2013). The wild type Cas9 is preferred for generation of 'knock-out' cell lines as the DNA double strand break is preferentially repaired by the error prone NHEJ pathway, producing INDEL mutations and premature stop codons in the genomic sequence. For precise and accurate DNA repair, and the incorporation of repair templates to generate 'knock-in' cell lines, the nickase-Cas9 is superior (Ran *et al.*, 2013).

To overcome the limitations of siRNA experiments and fully remove Bub1 protein from cells, the CRISPR-Cas9 system was used to generate Bub1 'knockout' clones in hTERT immortalised human retinal pigment epithelial cells (hTERT-RPE1, ATCC® CRL-4000™). We selected hTERT-RPE1 cells as they are an immortalised, non-transformed diploid human cell line. We chose not to use HeLa cells as they display high CIN and genomic instability which could complicate results. It is also harder to perform gene editing in HeLa cells as there may be multiple alleles due to their abnormal karyotype.

The wild type Cas9 from *S. pyogenes* was used to induce a double strand break at the cut site in the *BUB1* gene. Briefly, small guide (sg) RNAs were designed targeting exon 2, with the aim of generating INDEL mutations and premature stop codons in both alleles to silence the gene product. Exon 1 could not be targeted due to its short coding region and lack of PAM sites. First, a plasmid expressing an sgRNA targeting *BUB1* exon 2 and GFP-Cas9 was transfected into RPE1 cells and a GFP-positive population was separated using fluorescence-activated cell

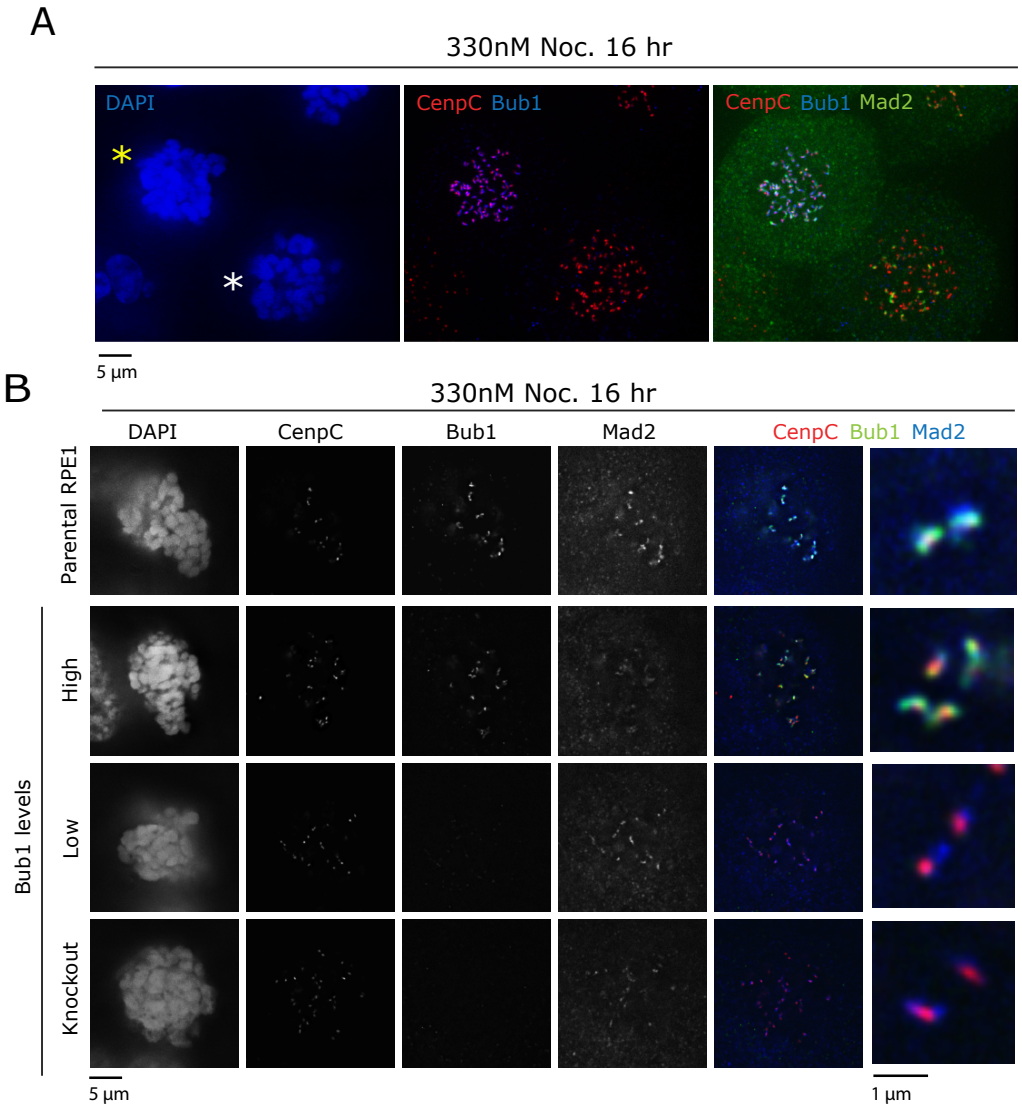

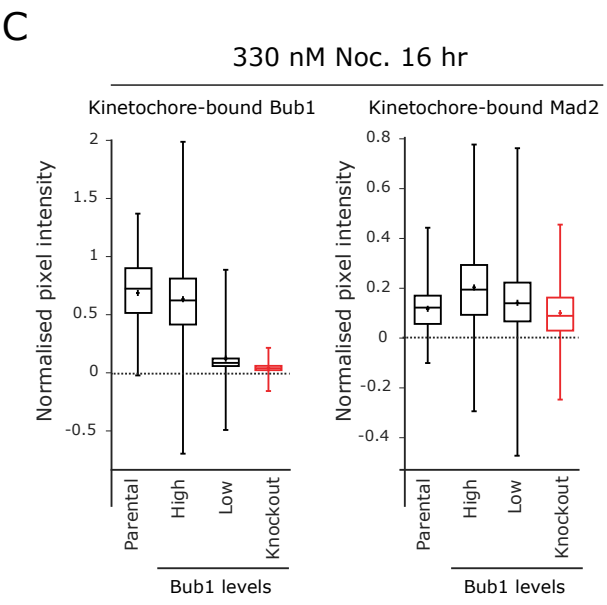

Figure 9: Analysis of mosaic population (clone 67) from sgBUB1 transfected hTERT-RPE1 cells. A) Single field of view showing nocodazole arrested cells with Bub1 present (yellow star) and Bub1 absent (white star) from kinetochores. Cells were also stained with anti-Mad2 antibodies (green) which is present in both cells. B) For quantification cells from the mosaic population were separated out into three groups based on kinetochore-bound Bub1 levels: High (0.15 to 1.2), Low (0.06 to 0.14) and knockout (below 0.06 – undetectable). All signals were normalised to CenpC intensity. Bub1 was visualised using a anti-Bub1 antibody targeting its N-terminus. Anti-Mad2 antibodies were used to detect Mad2 in the same cells. C) Kinetochore-bound Bub1 and Mad2 signal was plotted, showing that Mad2 is invariant to Bub1 level.

sorting (FACS). Next, multiple single clones were isolated through dilution and plating.

Analysis of a clonal line (clone 67) using quantitative immunofluorescence with an anti Bub1 antibody recognising the N-terminal region of the protein (amino acids 1-130) showed a mixture of cells with varying levels of Bub1. A subset of these cells had no Bub1 signal detectable at kinetochores (Figure 9A, white star). To test if these cells had a functional SAC, cells were treated with 330 nM nocodazole, which depolymerises microtubules. This creates an artificial situation in which all kinetochores are unattached and signalling maximally to the checkpoint. Cells were then fixed and stained with anti-Bub1 and anti-Mad2 antibodies. Images were processed for intensity analysis using a semi-automated MATLAB code named SiD, as described in methods section 2.4.1. Briefly, kinetochores are detected using a reference signal (CenpC or CREST), Spots were manually filtered to remove false positives, and the intensity of the second 'test' channel was calculated as the mean intensity within a sphere of 300 nm radius around the kinetochore's spot centre. Intensities were normalised to the reference signal intensity on a spot-by-spot basis. Analysed cells were separated into three groups based on kinetochore-bound Bub1 intensity for analysis; 'high' (0.15 to 1.2), 'low' (0.06 to 0.14) and 'knockout' (> 0.06 – undetectable). Bub1 signal was visible by eye in the high and low expressing populations, but was not visible at kinetochores in the 'knockout' population (Figure 9B). This analysis showed that kinetochores with undetectable Bub1 ('knockout') could still recruit Mad2, albeit at slightly lower levels than cells with high levels of Bub1 (Figure 9B, C).

The main limitation of this experiment is the mosaic nature of the population. We therefore carried out another round of clonal selection from the same pool of FACS sorted cells (Figure 10A). From this a second, homogeneous, clonal line was isolated (clone 13) which had no detectable Bub1 at kinetochores in prometaphase cells using the same anti Bub1 antibody (Figure 10B,C) Quantification showed the average Bub1 intensity to be 1.4% to kinetochores compared to parental cells. This

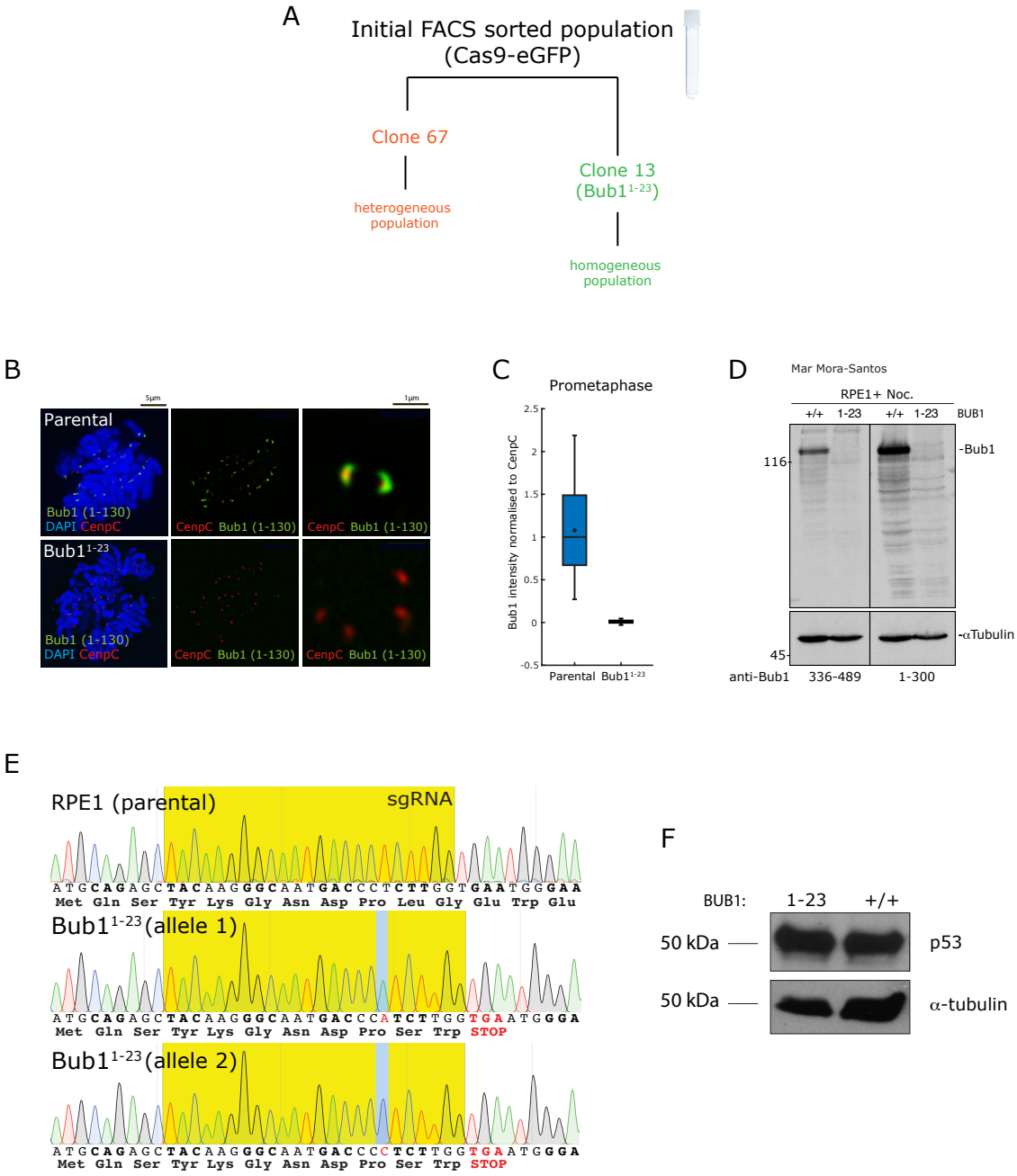

Figure 10: Validation of Bub1$^{1-23}$ clonal hTERT-RPE1 line. A) Schematic to show origin of *BUB*1 targeted single clones. B) Representative images of prometaphase parental and Bub1$^{1-23}$ cells stained with DAPI, CenpC or Bub1 (aa 1-130) antibodies. C) Quantification of kinetochore-bound Bub1, normalised to CenpC. Data from 2 independent experiments. D) Full immunoblots of whole cell lysates from parental or Bub1$^{1-23}$ cells treated with 3.3μM nocodazole, using antibodies against aa 336-489 (left) or aa 1-300 (right). a-tubulin was used as loading control. Blots were done by Mar Mora-Santos. E) Genome sequencing of Bub1$^{1-23}$ clone showing a frameshift mutation in both BUB1 alleles due to a single base pair insertion. The frameshift induces stop codons in both alleles as indicated. F) Immunoblot of whole cell lysates from parental and Bub1$^{1-23}$ cells using antibodies against p53 and a-tubulin as loading control.

clonal population was consistent with cells in the 'knockout' population of the mosaic clone 67.

As we had already established that cells with undetectable Bub1 can recruit Mad2 and arrest in nocodazole, cells were treated for 3.3 μM nocodazole for 16 hr and harvested by mitotic shake off for immunoblotting (Figure 10D). Pellets were lysed using NP40 extract to keep the proteins in their native, properly folded state. Clone 13 was examined for Bub1 protein by immunoblotting using two antibodies; one targeting the first 300 amino acids (Figure 10D, right panel) and one targeting a region between amino acids 336-489 (Figure 10D, left panel). Amino acids 336-489 includes the CD1 domain, which is the binding site for Mad1/Mad2 (Klebig, Korinth and Meraldi, 2009; London and Biggins, 2014). This antibody was used to determine the presence of any truncated forms of Bub1, which could potentially support checkpoint signalling. A truncated protein could, in principle, be undetected by the N-terminal targeting antibody used for immunofluorescence. However, Clone 13 showed no detectable protein with both antibodies confirming no truncated forms of Bub1 were present.

To confirm that Clone 13 was a homozygous knockout cell line, we wanted to separate the PCR products from each allele for genome sequencing. PCR primers were designed to amplify the region of genomic DNA surrounding the cut site, and the PCR products were separated by cloning into vectors (see methods section 2.2.4 for details). Sanger sequencing of the cloned PCR products revealed a single base pair insertion on each allele (+A or +C), which resulted in a frame shift mutation. This frame shift induced premature stop codons in both alleles after amino acid 23 (Figure 10E). This CRISPR mutant clonal line was therefore named $Bub1^{1-23}$, as the first 23 amino acids could potentially be expressed. The region between amino acid 1 and 23 is a truncation of the TPR domain implicated in binding to KNL1, but this region is not sufficient for kinetochore recruitment (Krenn *et al.*, 2012).

It has been reported that CRISPR-Cas9 genome editing can induce a p53-dependant DNA damage response, and this can lead to clonal selection against cells with a functional p53 pathway (Haapaniemi *et al.*, 2018). The p53 pathway is essential for correct cell cycle regulation, therefore we wanted to check p53 expression the Bub1$^{1-23}$ clonal line. Asynchronous cells were harvested and lysed in NP40 lysis buffer, and p53 expression was checked by immunoblotting. p53 was shown to be expressed at the same levels in Bub1$^{1-23}$ cells as in parental cells (Figure 10F).

To conclude this section, we isolated a homozygous clonal line with biallelic single base pair insertions following a Cas9 mediated double strand break, which may allow expression of only the first 23 amino acids of Bub1. This cell line is equivalent to the 'knockout' population of cells seen in the mosaic clone 67 where kinetochore-bound Bub1 intensity is below 0.06 (normalised to CenpC). Bub1 intensity in Bub1$^{1-23}$ cells was calculated to be 0.05 (data not shown), and no Bub1 signal was visible by eye at kinetochores. There is no detectable Bub1 protein in the Bub1$^{1-23}$ cell line as confirmed by immunoblotting.

3.3 Analysis of kinetochore proteins in the absence of Bub1

After concluding that the Bub1$^{1-23}$ cell line was a homozygous truncation mutant of Bub1, we wanted to investigate the binding of other kinetochore proteins in this cell line. This was done by quantitative immunofluorescence in prometaphase cells using SiD automated analysis in either early prometaphase or during nocodazole treatment (Figure 11A). Firstly we checked levels of BubR1 in the Bub1$^{1-23}$ cell line as Bub1 is reported to contribute to its kinetochore localisation, although the extent of Bub1's role in this is unclear (Johnson *et al.*, 2004; Perera *et al.*, 2007; Klebig, Korinth and Meraldi, 2009). Interestingly, BubR1 was undetectable at kinetochores in early prometaphase Bub1$^{1-23}$ RPE1 cells (Figure 11B,C). This is inconsistent with studies where ~30% of BubR1 remains at kinetochores following efficient Bub1 RNAi in DLD-1 or HeLa cells (Johnson *et*

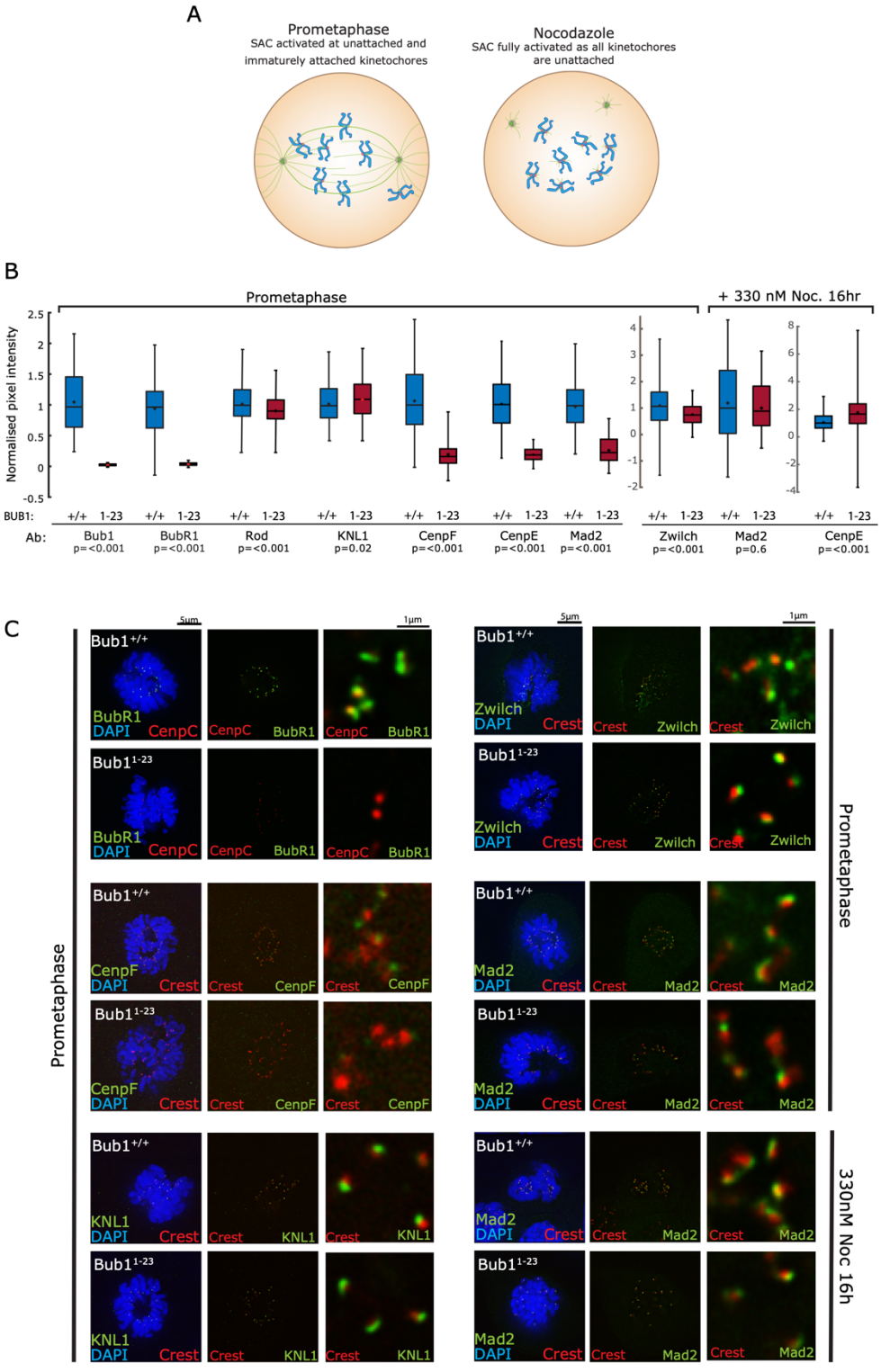

Figure 11: Analysis of kinetochore proteins in Bub1$^{1-23}$ cells. A) Schematic to illustrate SAC signalling during prometaphase and nocodazole treatment. B) Quantification of kinetochore-bound Bub1, BubR1, CenpF, KNL1, Rod, Cenp E, Zwilch and Mad2 signals normalised to Crest or CenpC intensity (data normalised to respective Bub1+/+ median value); p values from a two-sided Mann-Whitney U test; data from >1 independent experiments, >700 kinetochores C) Representative images from analysis in A).

al., 2004; Vleugel *et al.*, 2015; Zhang *et al.*, 2015) and ~10% in RPE cells (Klebig, Korinth and Meraldi, 2009) but consistent with studies using the murine homolog of Bub1 (Perera *et al.*, 2007). These findings could be due to cell line differences or RNAi penetrance. Either way, the lack of kinetochore-bound BubR1 was further evidence that the Bub1$^{1-23}$ cell line does not express functional Bub1 protein.

We next wanted to check the kinetochore recruitment of the RZZ complex components during prometaphase. The RZZ complex has been proposed to recruit Mad1:Mad2 complexes to kinetochores independently of Bub1, and we wanted to check whether it had been upregulated in Bub1$^{1-23}$ cells as an adaption to Bub1 knockout. Bub1 has also been proposed to play a role in stabilising RZZ at kinetochores in HeLa cells (Caldas *et al.*, 2015; Zhang *et al.*, 2015). However, kinetochore levels of Rod and Zwilch, two subunits of the RZZ complex, were at similar levels in the Bub1$^{1-23}$ cell line as in control cells (Figure 11B,C). This allowed us to conclude that the cell line had not adapted in response to loss of Bub1 by upregulating SAC signalling through the RZZ pathway, and unlike in HeLa cells loss of Bub1 does not interfere with the recruitment of the RZZ complex.

KNL1 acts as the platform for SAC signalling in the outer kinetochore. Bub3-Bub1 are recruited to the MELT motifs in KNL1 following phosphorylation by Mps1 to activate the KBB pathway of SAC signalling. We therefore wanted to check that KNL1 was not affected by Bub1 loss as a control for kinetochore structure during prometaphase. This was confirmed by immunofluorescence, showing that kinetochore-bound KNL1 was at the same levels in parental and Bub1$^{1-23}$ cells (Figure 11B,C). This suggests that outer kinetochore assembly does not change in the absence of Bub1.

On the other hand, Bub1 is implicated in establishment of the corona through recruitment of CenpF and CenpE to the kinetochore (Johnson *et al.*, 2004; Ciossani *et al.*, 2018). Therefore, we wanted to examine kinetochore-bound CenpF and

CenpE in the absence of Bub1 during prometaphase. CenpF is a large protein (~360 kDa) which contains two microtubule binding domains (Feng, Huang and Yen, 2006). CenpE (kinesin 7) is a plus-end directed motor protein implicated in chromosome congression (Kapoor *et al.*, 2006). We found that CenpF was reduced by ~80% in prometaphase cells, consistent with the previous study (Figure 11B,C) (Johnson *et al.*, 2004). However this result is inconsistent with a more recent study which suggests that Bub1 is stringently required for CenpF localisation to the kinetochore in HeLa cells (Ciossani *et al.*, 2018). Another recent study shows that CenpF is recruited by the C-terminal tail of Bub1 in a kinase independent manner in HAP1 cells (Raaijmakers *et al.*, 2018). Our results suggest that the C-terminus of Bub1 may not be the only binding site for CenpF in the kinetochore of RPE1 cells as ~20% remains kinetochore-bound in Bub1$^{1-23}$ cells.

CenpE was also reduced by ~70%, in prometaphase Bub1$^{1-23}$ cells (Figure 11B), but surprisingly levels increased and became comparable with parental cells upon treatment with 330 nM nocodazole (Figure 11B, far right panel). CenpF levels did not recover in nocodazole (data not shown). Further work in our laboratory has provided an explanation for this result. It has been shown in HeLa cells that CenpE is removed from the kinetochore via stripping mediated by the minus end directed motor protein Dynein. This process is though to be negatively regulated by CenpF. As microtubules are removed in nocodazole, CenpE can no longer be transported away from the kinetochore by dynein, and it instead accumulates (Auckland and McAinsh, 2019 BioRXiv). These results suggest that dynein-mediated stripping, a process also implicated in checkpoint silencing, is active in the absence of Bub1, as CenpE stripping appears to be overactive in prometaphase.

Alongside investigating kinetochore components in Bub1$^{1-23}$ cells, we wanted to investigate the function of the Bub1 kinase domain. This would allow us to see if there was an residual Bub1 activity present in Bub1$^{1-23}$ cells. Therefore we wanted

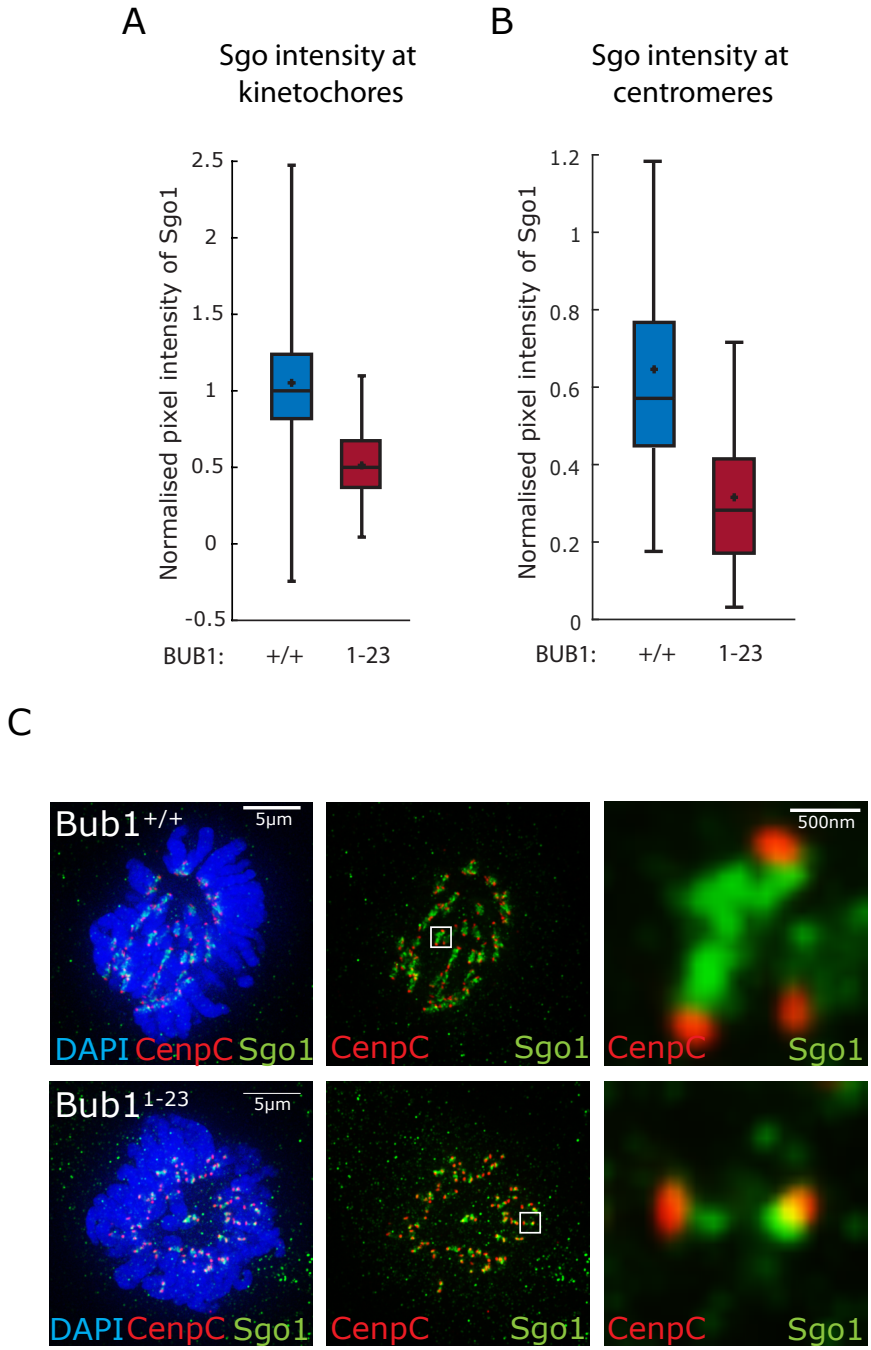

Figure 12: Sgo1 localisation is affected in Bub1$^{1-23}$ cells. A) Quantification of Sgo1 levels at kinetochores in parental and Bub1$^{1-23}$ prometaphase cells. Sgo1 intensity is normalised to the respective CenpC value. Data from two independent experiments, > 700 kinetochores. B) Quantification of Sgo1 levels at centromeres in parental and Bub1$^{1-23}$ prometaphase cells. Sgo1 intensity is normalised to the respective CenpC value. Representative data from one experiment; two independent repeats. > 100 kinetochores. C) Representative images from analysis in A) and B).

to further confirm the absence of Bub1 by investigating levels of Shugoshin 1 (Sgo1). Sgo1 is recruited to phosphorylated Histone H2A at threonine 120 (T120), an established target of Bub1 kinase activity (Kawashima *et al.*, 2010). We measured Sgo1 intensity in early prometaphase cells and found it to be reduced by ~50% in Bub1$^{1-23}$ cells at the kinetochore (Figure 12A) and the centromere (Figure 12B). It is unclear in the literature as to whether histone H2A-T120 phosphorylation is essential for Sgo1 localisation in human cells. A study from the Yu laboratory reported that cohesin and histone H2A-T120 specify two distinct pools of Sgo1 at inner centromeres and kinetochores respectively (Liu, Jia and Yu, 2013). The expression pattern seen in Bub1$^{1-23}$ cells was not consistent with this report, as we see loss at both the centromere and the kinetochore, while Bub1 is thought to specify the kinetochore pool (Figure 12C). However, these experiments were done in HeLa cells so we reasoned that differences could be due to cell line and experimental variation, and attributed to the 50% remaining Sgo1 to recruitment via cohesin. In conclusion, Sgo1 recruitment was disrupted in Bub1$^{1-23}$ cells consistent with loss of Bub1 kinase activity and endogenous removal of Bub1.

Finally, we wanted to test the ability of kinetochores to bind Mad2 in the absence of Bub1. Mad2 is recruited to kinetochores to allow formation of MCC, which sequesters the APC/C co-activator Cdc20 and delays anaphase onset. We measured Mad2 levels in prometaphase cells and cells treated with 330 nM nocodazole to remove the mitotic spindle and stimulate a full checkpoint response. Steady state levels of kinetochore-bound Mad2 were lower in prometaphase Bub1$^{1-23}$ cells than the parental, however when cells were treated with 330nM nocodazole Mad2 levels became comparable (Figure 11B,C). Interestingly, this mimics the result of CenpE recovery in nocodazole, suggesting that the two proteins may be removed from the kinetochore through the same pathway. These results show that in a unperturbed mitosis less Mad2 is recruited to kinetochores, due to loss of the Mad1:Mad2 binding site on Bub1, but Bub1$^{1-23}$ cells can generate a full checkpoint response when all kinetochores are unattached in nocodazole, presumably through the RZZ pathway.

In conclusion, investigation of kinetochore components in the Bub1$^{1-23}$ cell line shows that BubR1 is not recruited in the absence of Bub1. We also show that CenpF and CenpE are reduced at Bub1-null kinetochores in prometaphase, while CenpE recovers in nocodazole. Kinetochore components KNL1, Rod and Zwilch are unaffected by loss of Bub1, confirming that kinetochore assembly is not affected and the RZZ pathway is not upregulated. Sgo1 is reduced at centromeres and kinetochores, consistent with loss of Bub1 kinase activity. Finally, we show that Mad2 levels are decreased in prometaphase on loss of Bub1, but treatment with 330 nM for 16 hr to leave all kinetochores unattached allows recruitment of Mad2 that is comparable with parental cells. These results suggest that cells lacking Bub1 are able to signal to the SAC and delay anaphase in response to unattached kinetochores.

3.4 Bub1 is not essential for the checkpoint response in RPE1 cells

Having rigorously validated the Bub1$^{1-23}$ clonal line, we concluded it appeared to be a bona fide 'knockout' in which no functional Bub1 is expressed. We next wanted to assess the effect of Bub1 gene editing on chromosome congression and anaphase onset in individual cells using live cell imaging. Chromosomes were visualised using SiR-DNA dye, which does not alter mitotic progression compared to previous work with histone H2B-RFP (data not shown) and cells were imaged for 12 hours. Analysis of live cell movies showed that Bub1$^{1-23}$ cells were able to complete congression to the metaphase plate as efficiently as parental cells (Figure 13A), and enter anaphase after a 3 minute delay in metaphase (Figure 13B). There was a 3 minute extension in the timing of NEB to anaphase in Bub1$^{1-23}$ cells compared to the parental, arising from the delay in metaphase (27 min versus 24 min, median values) (Figure 13C). These results suggested the checkpoint is functional in unperturbed mitosis, as when Mad1 is removed cells accelerate

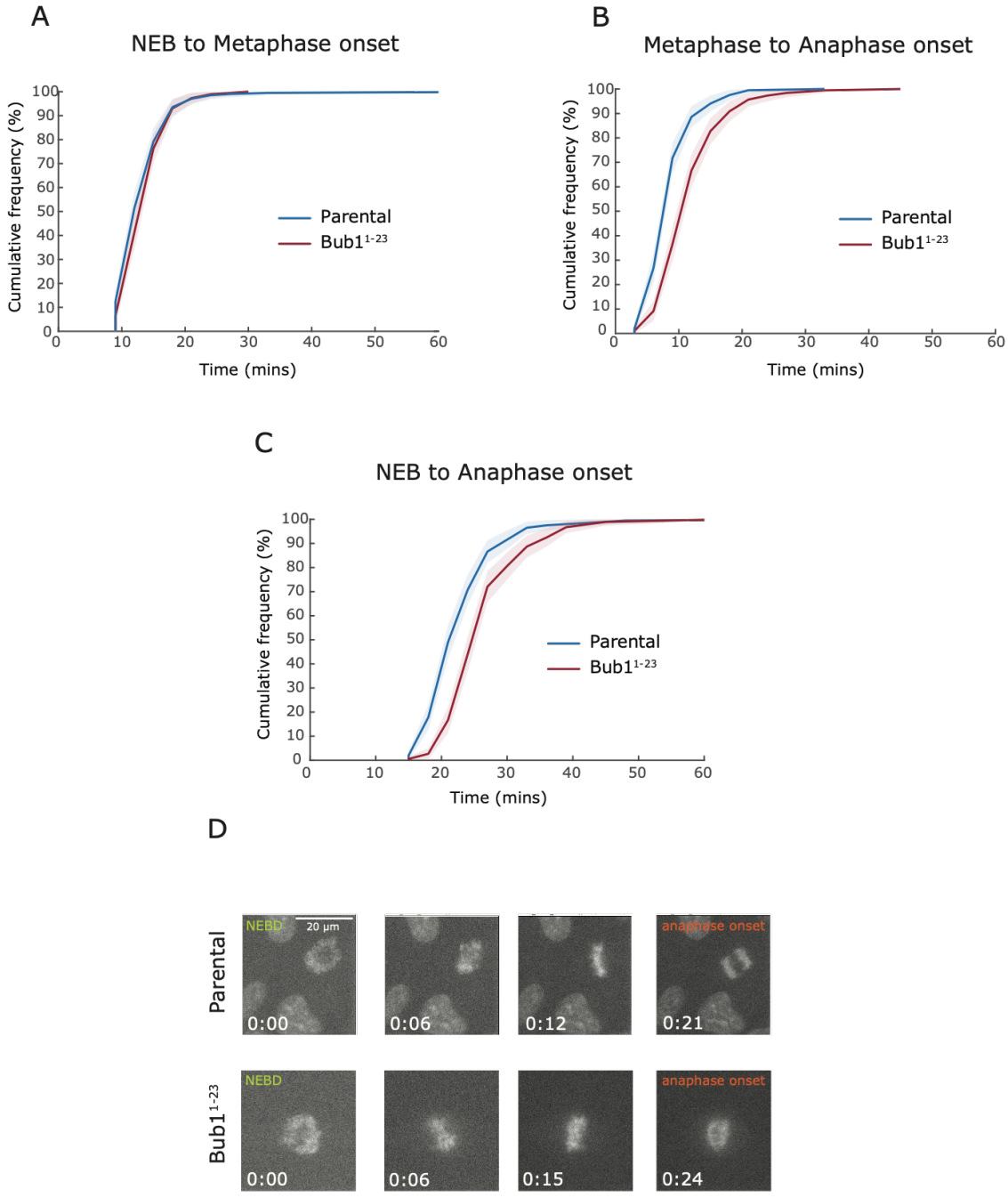

Figure 13: Bub1$^{1-23}$ cells progress normally through unperturbed mitosis. A) Time spent in mitosis from NEB to metaphase onset from 12 hour live cell imaging of parental and Bub1$^{1-23}$ cells treated with SiR-DNA. N = 186 for parental and 186 for Bub1$^{1-23}$ cells. B) Time spent in mitosis from metaphase to anaphase from the same data set. C) Time spent in mitosis from NEB to anaphase from the same data set. D) Representative stills from live cell imaging of parental and Bub1$^{1-23}$cells treated with SiR-DNA. Time in hour:min.

through anaphase in 12 min (Meraldi, Draviam and Sorger, 2004). This acceleration phenotype has been attributed to loss of interphase MCC generation at the nuclear pore (Rodriguez-Bravo *et al.*, 2014). As Bub1$^{1-23}$ cells completed NEB to anaphase in a median of 27 mins this suggests that Bub1 is not required for nuclear pore-associated MCC generation. However, Bub1$^{1-23}$ cells produced more mis-segregation errors during unperturbed mitosis than parental cells (8.5% versus 0%, data not shown). These errors consisted of mostly anaphase bridges with a few cells performing a tripolar mitosis and one cell displaying a lagging chromosome. Anaphase bridges generally arise from errors which occur during DNA replication in S phase. Recently the Bub1-Bub3 complex has been implicated in telomere DNA replication, which could explain this result (Li *et al.*, 2018). As only one Bub1$^{1-23}$ cell displayed a lagging chromosome (out of 186 cells) we concluded that loss of Bub1 could have a very subtle effect on chromosome segregation. However, this result was surprising as loss of Bub1 is reported to cause major chromosome congression defects and segregation errors in HeLa and HAP1 cells (Tang *et al.*, 2004; Meraldi and Sorger, 2005; Klebig, Korinth and Meraldi, 2009; Raaijmakers *et al.*, 2018), which were not seen in Bub1$^{1-23}$ cells. This may be due to the ability of RPE1 cells to rapidly attach and biorientate kinetochores following NEBD (Sikirzhytski *et al.*, 2018)

As we had already found that steady state levels of Mad2 were equivalent in parental and Bub1$^{1-23}$ cells in response to nocodazole treatment (Figure 11B), we wanted to further investigate SAC strength in the absence of Bub1. To directly test whether Bub1 is required for mitotic arrest in response to unattached kinetochores, parental and Bub1$^{1-23}$ cells were filmed for 36 hours in the presence of 330nM nocodazole and the duration of mitotic arrest was measured. Bub1$^{1-23}$ cells were able to delay anaphase onset for 995 min (16 hours) in response to 330 nM nocodazole, suggesting that the SAC is active (Figure 14A). However, Bub1$^{1-23}$ cells were not able to maintain mitotic arrest for as long as parental cells (995 min versus 1660 min over a 36 hr min imaging period) (Figure 14A, B). This

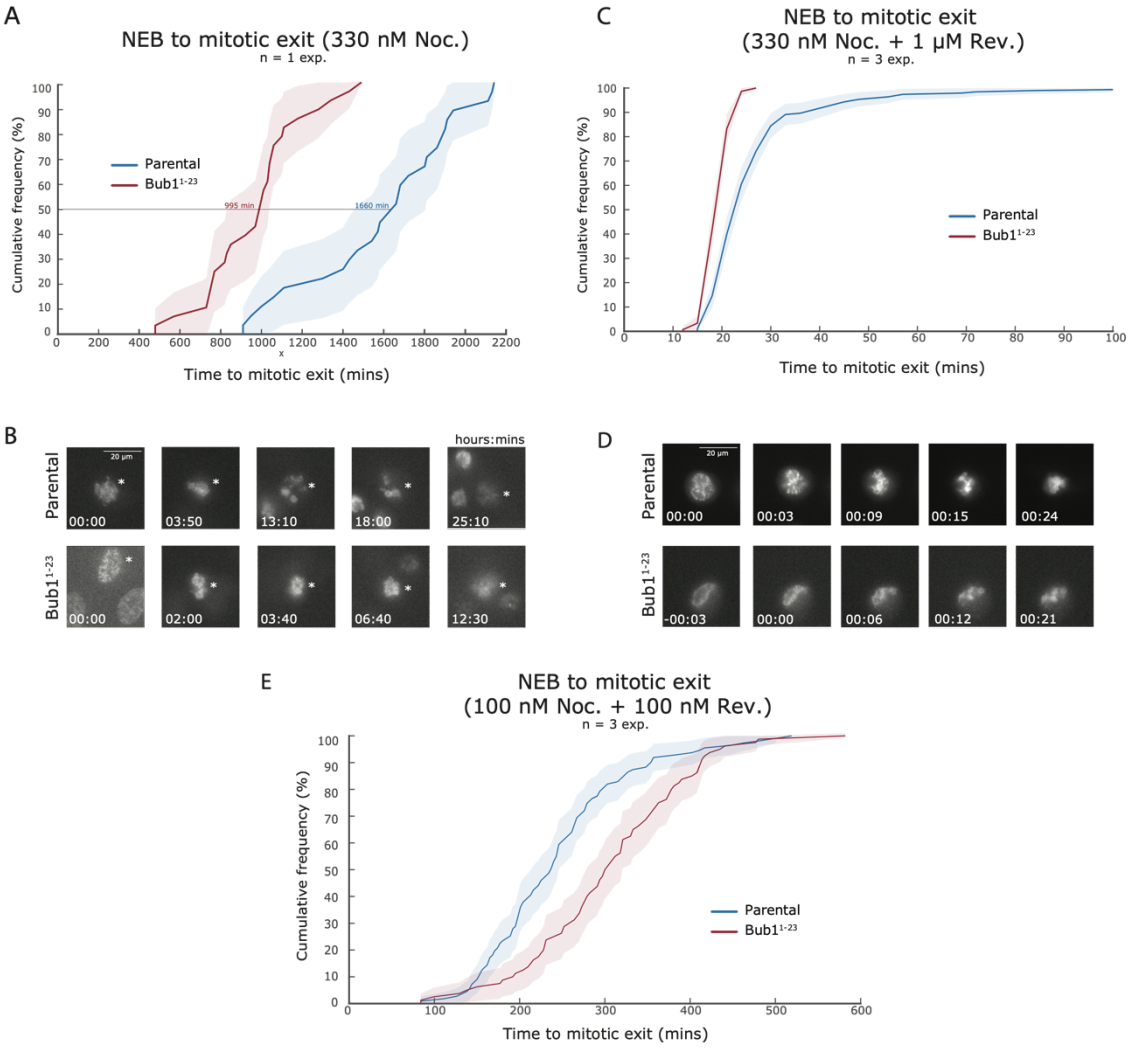

Figure 14: Bub1 contributes to, but is not required for mitotic arrest. A) Time spent in mitosis from NEBD to mitotic exit from 36 hour live cell imaging of parental and Bub1$^{1\text{-}23}$ cells in 300 nM nocodazole (n = 27 cells for parental and 28 for Bub1$^{1\text{-}23}$ cells). Data from one experiment. Shaded regions represent 95% confidence intervals. B) Representative stills from live cell imaging of parental and Bub1$^{1\text{-}23}$ cells analysed in A). Time in hour:min. Star identifies cell of interest. C) Time spent in mitosis from NEBD to mitotic exit from 12 hour live cell imaging of parental and Bub1$^{1\text{-}23}$ cells treated with 330 nM nocodazole and 1 μM reversine (n = 193 for parental and 148 for Bub1$^{1\text{-}23}$ cells). Data from three independent experiments; Shaded regions represent 95% confidence intervals. D) Representative stills from live cell imaging of parental and Bub1$^{1\text{-}23}$ cells analysed in C). Time in hour:min. E) Time spent in mitosis from NEBD to mitotic exit from 12 hour live cell imaging of parental and Bub1$^{1\text{-}23}$ cells treated with 100 nM nocodazole and 100 nM reversine (n = 111 for parental and 80 for Bub1$^{1\text{-}23}$ cells). Data from 3 independent experiments; shaded region represents 95% confidence interval.

reduction in mitotic arrest suggests that Bub1 contributes to long term maintenance of checkpoint signalling, rather than the initial activation.

Bub1 is known to play a role in SAC activation by recruiting Mad1:Mad2 complexes to kinetochores via its CD1 domain in an Mps1 dependant manner (London and Biggins, 2014). We therefore wanted to uncover the contribution of Bub1 to SAC signalling in RPE1 cells, as the phenotype of Bub1$^{1-23}$ cells is minor. To do this, parental and Bub1$^{1-23}$ cells were treated with 330 nM nocodazole and 1μM reversine. Reversine is a small molecule inhibitor of Mps1 kinase (Santaguida *et al.*, 2010). Reversine treatment dampens SAC activation by reducing KNL1-MELT motif phosphorylation and will cause any checkpoint defects in Bub1$^{1-23}$ cells to be exaggerated. This allows us to see the contribution of Bub1 to SAC signalling when compared to parental cells which are expressing Bub1 in a unperturbed manner. As the reversine treatment does not totally inhibit Mps1, we would expect to see some remnants of checkpoint activity in parental cells, which are able to recruit Bub1 to the kinetochores and activate the SAC, but not in Bub1$^{1-23}$ cells. Analysis of live cell movies showed an acceleration in mitotic exit when Mps1 inhibition was combined with loss of Bub1 (21 min in Bub1$^{1-23}$ cells versus 24 min in parental cells) (Figure 14C, D). Importantly, we did see parental cells that were able to arrest for up to ~100 mins, while Bub1$^{1-23}$ cells were never able to arrest for longer than 24 mins. This reveals a role for Bub1 in checkpoint activation when SAC signalling is severely compromised, although this role appears minor. It is important to note that Mps1 was recently shown to be required for stimulating RZZ-Spindly oligomerisation by releasing Spindly autoinhibition (Sacristan *et al.*, 2018). This interaction then drives kinetochore expansion. Therefore, inhibition of Mps1 by reversine may also affect SAC signalling through the RZZ pathway.

During optimisation of the above experiment, different dose combinations of nocodazole and reversine were used on parental and Bub1$^{1-23}$ cells. Surprisingly, when cells were treated with lower doses of nocodazole and reversine (100 nM for

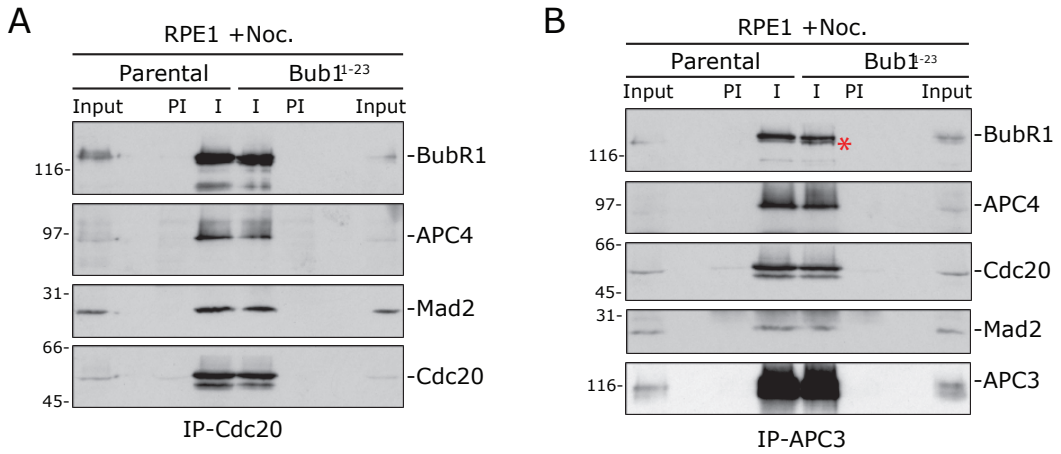

Figure 15: MCC and APC/C^{MCC} is formed in Bub1$^{1-23}$ cells . A) Parental or Bub1$^{1-23}$ cells were treated with 3.3 μM nocodazole and whole cell extracts were immunoprecipitated with mouse anti-Cdc20 (Immune; I) or normal mouse igG (Preimmune; PI) antibodies, and complexes were analysed by immunoblotting with indicated antibodies. B) Same as A) except cell extracts with immunoprecipitated with anti-APC3 (Immune; I) antibodies. Both experiments were done by Mar Mora-Santos.

both), Bub1$^{1-23}$ cells delayed mitotic exit for 73 min longer than parental cells (Figure 14E). This most likely represents a silencing defect in Bub1$^{1-23}$ cells rather than stronger SAC signalling, as we have shown that SAC maintenance is perturbed in Bub1$^{1-23}$ cells (Figure 13A). PP2A-B56 is a key phosphatase required for removal of Mps1-mediated phosphorylation of KNL1-MELT motifs, and is recruited to the kinetochores via the KARD domain on BubR1 (Espert *et al.*, 2014). As described earlier, BubR1 is undetectable at kinetochores in Bub1$^{1-23}$ cells and it is therefore assumed that the subsequent pool of PP2A-B56 is not present (Figure 11B). The slight SAC defect caused by low dose reversine causes loss of BubR1-PP2A-B56 mediated silencing to have a larger effect than loss of Bub1-mediated SAC activation. The checkpoint therefore remains activated for longer as the balance now tips towards phosphorylation rather than dephosphorylation and silencing is perturbed. This also supports the finding that RZZ can efficiently activate the SAC in the absence of Bub1 (Figure 14A). However, it should be noted that this delay could also arise from the presence of defective attachments in the absence of Bub1, leading to prolonged signalling. We have not further dissected the cause of the delay here, but it could be done by fixing cells and examining for Mad2 foci at unattached kinetochores.

Finally, we wanted to test whether MCC is efficiently assembled in the Bub1$^{1-23}$ cells, and subsequently that this MCC can bind to the APC/C to cause its inhibition. To do this, parental or Bub1$^{1-23}$ were arrested in nocodazole and harvested by mitotic shake off. Whole cell lysates were immunoprecipitated against either Cdc20 or APC3 to check for MCC binding to APC/C and vice versa. We found that BubR1, APC4 and Mad2 were able to bind Cdc20 to form MCC and bind APC/C as efficiently in Bub$^{1-23}$ cells as the parental cell line in the presence of nocodazole (Figure 15A). We also found that MCC subunits were able to bind APC3 to the same extent in parental and Bub1$^{1-23}$ cells, suggesting that the APC/C is efficiently inhibited in the absence of Bub1 (Figure 15B). This provides further evidence that Bub1 is not required for the formation of MCC or APC/C^{MCC}, and therefore SAC signalling, in response to unattached kinetochores.

The incorporation of BubR1 in MCC generated in Bub1$^{1-23}$ cells suggests that Bub1 is required for the localisation of BubR1 to kinetochores but not for its inclusion into MCC, and BubR1 does not need to cycle through kinetochores before MCC is formed. However, BubR1 phosphorylation status is altered in Bub1$^{1-23}$ cells (Figure 14B, red asterisk). BubR1 is hyperphosphorylated in mitosis by PLK1, resulting in the characteristic double-band pattern (Elowe *et al.*, 2007). In Bub1$^{1-23}$ cells there is more protein present in the lower band, suggesting BubR1 phosphorylation reduces when it is not recruited to the kinetochore via Bub1. It is unsure what effect this could have on MCC stability.

In conclusion, live cell imaging experiments show that the loss of Bub1 has no effect on unperturbed mitosis in Bub1$^{1-23}$ cells, however these cells display a long-term SAC maintenance defect when all kinetochores are unattached. Bub1 does contribute to SAC activity but its role is only uncovered upon partial Mps1 inhibition, suggesting the contribution is small. Finally, we have shown that cells are capable of generating MCC and inhibiting APC/C in the absence of Bub1.

Taken together these data suggest that Bub1 is not required to generate a mitotic arrest in hTERT-RPE1 cells.

3.5 Conclusions

In this chapter we have presented data supporting the two pathway model of spindle assembly checkpoint signalling through examining the contribution of Bub1. hTERT-RPE1 cells with homozygous frameshift mutations in the *BUB1* locus were generated which theoretically allow only expression of the first 23 amino acids of Bub1 (Bub1$^{1-23}$). These cells displayed no detectable Bub1 protein by western blot with multiple antibodies. BubR1, a checkpoint protein recruited by Bub1, was undetectable at kinetochores. CenpF, also known to be recruited by Bub1, was reduced by ~70% at kinetochores consistent with previous literature. Sgo1, recruited downstream of Bub1 kinase activity, was reduced at both kinetochores and centromeres by ~50%, also consistent with previous literature. Importantly, steady-state Mad2 levels were reduced at kinetochores in prometaphase Bub1$^{1-23}$ cells, but was fully recruited in response to unattached kinetochores generated by nocodazole treatment, suggesting that cells lacking Bub1 can still activate the SAC.

Bub1$^{1-23}$ cells progressed normally through unperturbed mitosis, and were able to delay mitotic exit in response to unattached kinetochores generated by nocodazole treatment. However, long term mitotic arrest was compromised in the absence of Bub1 suggesting that Bub1 plays a role in long term SAC maintenance. Treatment with reversine shows that Bub1 makes a small contribution to checkpoint activation when Mps1 activity is compromised. Finally, we have shown that MCC is produced and the APC/C is inhibited in the absence of Bub1, and that BubR1 kinetochore localisation is not required for its incorporation into MCC.

We conclude that Bub1 is not essential for the recruitment of Mad2 to unattached kinetochores, and subsequently the generation of MCC and inhibition of APC/C

to delay anaphase onset. Therefore, Bub1 is not essential for SAC signalling, and a second pathway is able to effectively activate the checkpoint in its absence. During peer review of this work, a paper from the Medema group was published showing consistent results upon knockout of Bub1 in HAP1 cells (Raaijmakers *et al.*, 2018).

Chapter 4: Functional analysis of 'zombie' Bub1

4.1 Introduction

Shortly after publication of the work presented in Chapter 3, a collaborative study from the Jallepalli and Cheeseman laboratories reported evidence for Bub1 re-expression following successful disruption of the gene with CRISPR-Cas9 (Figure 16) (Rodriguez-Rodriguez *et al.*, 2018). Single clones isolated following BUB1 disruption with AdenoCas9 (AdCas9) showed partial (3-30%) recovery of Bub1 expression, kinetochore localisation and H2A phosphorylation to confirm kinase activity. These experiments were performed using antibodies targeting Bub1's N-terminus (ab54893 - the same antibody as used in Chapter 3) or T120 phosphorylated histone H2A. RT-PCR and sequencing performed on 5 clones showed transcripts that skipped part or all of exon 4 which was targeted in this study. This exon skipping and subsequent re-expression of Bub1 was attributed to nonsense-associated alternative splicing (NAS). Normally, insertion of premature stop codons (PSCs) activates nonsense-mediated decay (NMD), a surveillance pathway that eliminates truncated mRNA transcripts (Losson and Lacroute, 1979; Hentze and Kulozik, 1999). However, premature stop codons can also trigger NAS, an obscure pathway in which splicing rules are relaxed to bypass the PSC and restore expression in the correct reading frame termed 'exon skipping' (Wang *et al.*, 2002). This altered splicing allowed truncated forms of Bub1 to be expressed in this study that, importantly, used hTERT-RPE1 cells in which p53 had been previously knocked out using CRISPR-Cas9. It is unsure what effect loss of p53 would have on CRISPR-mediated gene editing. These truncated forms of Bub1 were shown to be functional as multiple clones exhibited partial or complete recovery of mitotic arrest when exposed to nocodazole, which correlated with levels of Bub1 re-expression. Interestingly, two clones expressed no in-frame transcripts and authors described these as being the most SAC defective. However, a closer look at the data showed that these two clones arrested in 660 nM

nocodazole for a median of ~400 minutes or 6.6 hours, which suggests the SAC is still functional in these clones although long term maintenance is perturbed.

At a similar time, the Nilsson lab requested use of our Bub1$^{1-23}$ cell line, along with the HAP1 Bub1 knockout cell line (Raaijmakers *et al.*, 2018), to conduct further analysis. They had independently generated a HeLa Bub1 'knock-out' cell line, using the same sgRNA as our study, in which Bub1 was undetectable at the N-terminus and via western blotting (Figure 16). However, a very faint kinetochore signal was detectable in this HeLa cell line using a phospho-specific Bub1 antibody. Mass spectrometry analysis, following enrichment by immunoprecipitation with Bub3 or BubR1 (binding partners of Bub1), revealed Bub1 peptides present in the HeLa 'knockout' cell line. Upon treatment of this cell line with Bub1 RNAi, the phospho-specific Bub1 signal disappeared from kinetochores and peptides were no longer detected using mass spectrometry. Importantly, mitotic arrest was further reduced in response to 100 nM nocodazole when these HeLa cells were treated with Bub1 RNAi to remove the residual protein (Zhang *et al.*, 2019). The Nilsson laboratory tested for any residual Bub1 expression in our RPE1 and the HAP1 cell lines to see if they had suffered the same fate.

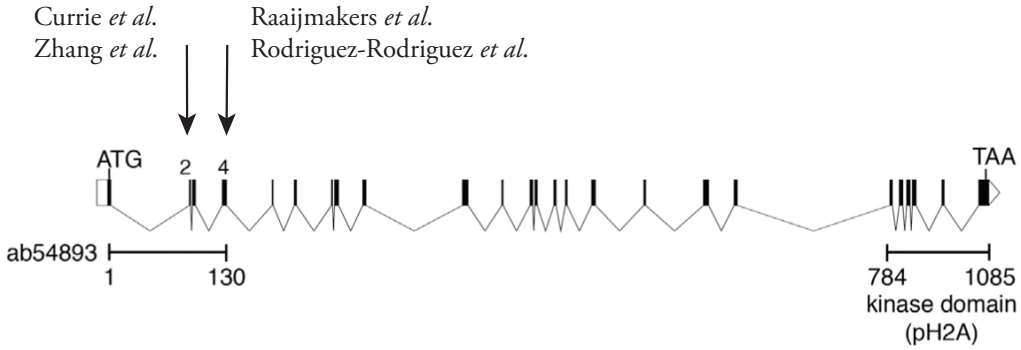

Figure 16: Schematic showing CRISPR-Cas9 sgRNA target exons used in various publications targeting BUB1 (adapted from Rodriquez-Rodriquez *et al*, 2018).

Cell line	Time arrested in 100nM Noc. (mins)					Average decrease in arrest (mins)
	Control	siBub1#1	siBub1#2	siBub1#3	siBub1#4	
HeLa	620	220	155	400	295	353
RPE1	505	140	90	280	305	292
HAP1	485	265	285	330	300	190

Table 8: Summary of mitotic arrest duration of HeLa, RPE1 and HAP1 Bub1 'knockout' cell lines treated with Bub1 RNAi to deplete any residual Bub1 expression. Bub1 RNAi treatment reduces the duration of mitotic arrest, supporting the observation that Bub1 knockout cells express some residual Bub1 protein that contributes to checkpoint signalling.

The Nilsson lab found that both our RPE1 and the HAP1 Bub1 'knockout' cell lines expressed residual Bub1 protein which was detectable by mass spectrometry, same as the HeLa cell line. Residual Bub1 expression was estimated to be 4%, 8% and 2.5% in HeLa, RPE1 and HAP1 Bub1 targeted cell lines respectively (Zhang *et al.*, 2019). Treatment of all three cell lines with 4 different Bub1 RNAi oligos further decreased the duration of mitotic arrest in nocodazole by 278 min or 4.6 hours on average, compared to cells treated with control RNAi (Table 8). They reported our Bub1$^{1\text{-}23}$ RPE1 cells exiting mitosis after ~90 mins arrest upon Bub1 RNAi treatment using one of the oligos, which suggests that residual Bub1 is supporting SAC signalling in a sub-stoichiometric manner. It may be that not all oligos had the same effect on residual Bub1 depletion causing variation, and no data was presented to show depletion levels in these experiments. Importantly, 90 mins is still three times the length of unperturbed mitosis in RPE1 cells (24 min), as shown in Chapter 3. The Bub1 'knock-out' HeLa clonal line was therefore treated with Bub1 RNAi (oligo from Klebig, Korinth and Meraldi, 2009) for all further experiments to remove any residual Bub1 protein in the Nilsson publication (Zhang *et al.*, 2019).

The Nilsson laboratory publication was highlighted in an EMBO 'News and Views' article from Patrick Meraldi, titled 'Bub1 – the zombie protein that CRISPR cannot kill' (Meraldi, 2019). This article brought together the four recent publications concerning the role of Bub1 in the SAC (Currie *et al.*, 2018; Raaijmakers *et al.*, 2018; Rodriguez-Rodriguez *et al.*, 2018; Zhang *et al.*, 2019), and suggested that Bub1 must be very efficiently depleted to cause a strong SAC defect. Meraldi proposed that the best strategy for absolute Bub1 removal would be deletion of a large segment of the gene. As a nod to the title of this article, the residual Bub1 expressed in our Bub1$^{1\text{-}23}$ cells is referred to as 'zombie' Bub1 in this chapter.

The aim of this chapter was to investigate the existence and function of 'zombie' Bub1 protein in our hTERT-RPE1 Bub1$^{1\text{-}23}$ cell line. We were surprised by the discovery of residual Bub1 expression in our cell line as found by the Nilsson laboratory so wanted to repeat these experiments in our own hands. Following verification of this residual Bub1 expression, we set out to repeat key experiments detailed in Chapter 3 to further test the two pathway model of SAC activation and elucidate the true function of Bub1 in SAC signalling.

4.2 Residual 'zombie' Bub1 is expressed following *BUB1* disruption

The collaborative study from the Cheeseman and Jallepalli laboratories reported that upon targeting Bub1 with CRISPR-Cas9 in p53$^{-/-}$ hTERT-RPE1 cells, Bub1 expression was regained to varying extents (Rodriguez-Rodriguez *et al.*, 2018). These cells displayed exon skipping in the Bub1 mRNA which was attributed to nonsense-associated alternative splicing (NAS). We therefore wanted to test for the presence of exon skipping in our Bub1$^{1\text{-}23}$ cell line, which could explain the residual re-expression as discovered by the Nilsson laboratory using mass spectrometry (Zhang *et al.*, 2019).

To do this, we performed RT-PCR on mRNA isolated from Bub1$^{1\text{-}23}$ cells. NAS, the mechanism attributed to exon skipping, increases levels of alternatively spliced

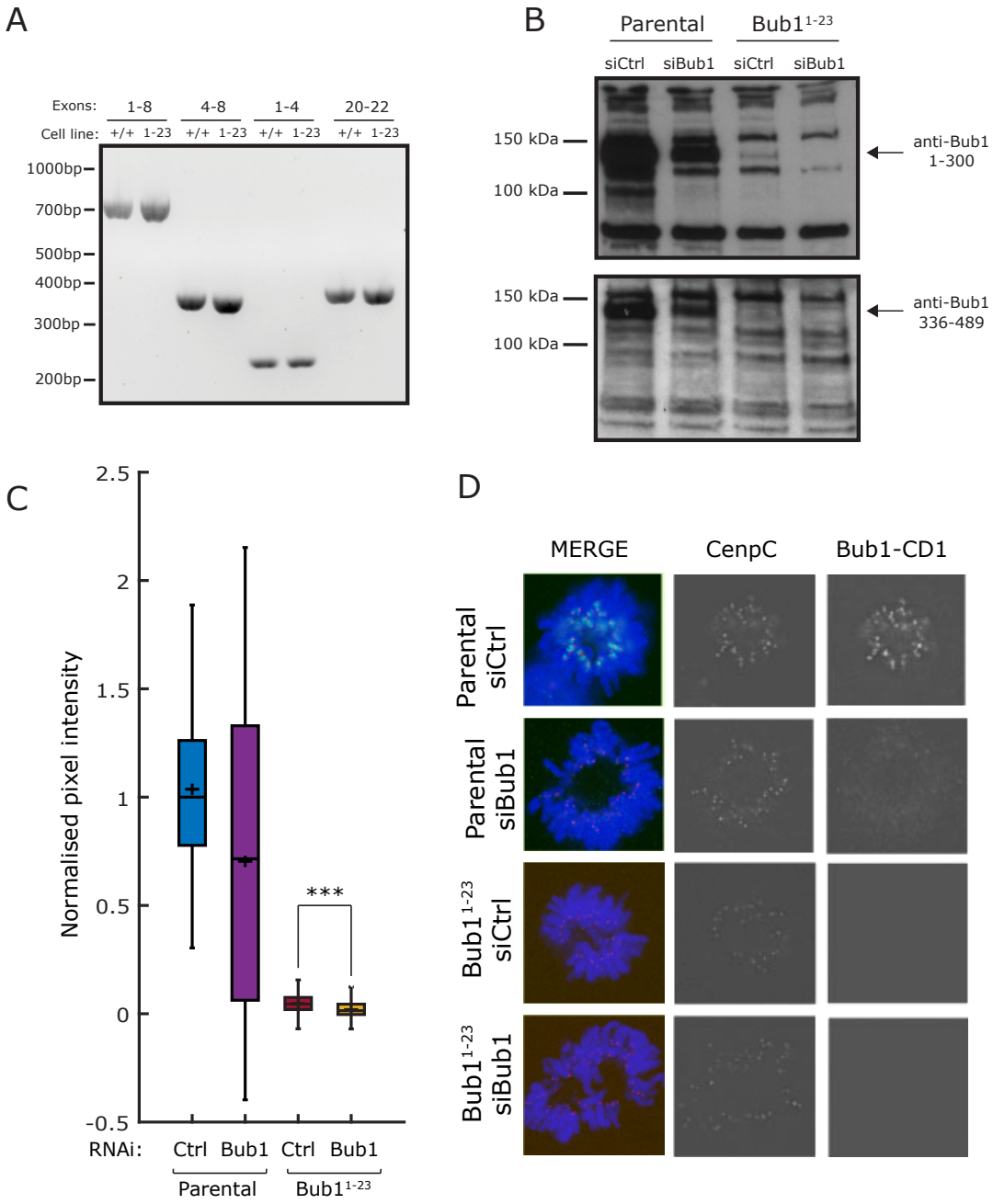

Figure 17: Identification of 'zombie' Bub1 in Bub1$^{1-23}$ cells. A) Reverse transcription PCR performed on genomic DNA from parental and Bub1$^{1-23}$ cells. Experiment done by Paula Esquivias. B) Immunoblots from whole cell lysates, prepared in urea buffer, from parental and Bub1$^{1-23}$ cells treated with control or Bub1 RNAi. Cells were treated with 330 nM nocodazole, and blotted using antibodies against Bub1 aa 1-300 (top) and aa 336-489 (bottom). Experiment done by Paula Esquivias. C) Quantification of kinetochore bound Bub1, using antibodies against the Bub1 CD1 region normalised to CenpC. Parental ana Bub1$^{1-23}$ cells were treated with control or Bub1 RNAi and imaged in prometaphase. P value from a two-sided Mann Whitney U test. Data from one experiment, >700 kinetochores per condition. D) Representative images from analysis in C).

transcripts that have skipped the mutated exon containing the PSC, so these would be identified as shortened Bub1 mRNA transcripts if present. mRNA extracted from parental and Bub1$^{1-23}$ cells was converted to complementary DNA (cDNA) using a reverse transcriptase, and multiple regions of Bub1 were amplified by PCR using different PCR primers. PCR products were then separated using agarose gel electrophoresis to check for any size differences between the parental and Bub1$^{1-23}$ cell lines (Figure 20.1A). No evidence of whole exon skipping was seen in the Bub1$^{1-23}$ cell line, as there were no large band shifts. However, we cannot rule out the possibility that smaller sections of mRNA were skipped, although this is unlikely.

Next, we investigated whether we could detect 'zombie' Bub1 at the protein level using immunoblotting. Cell extracts were prepared using a denaturing lysis buffer (UTB), which breaks down the chromatin and unfolds proteins, to make sure all epitopes would be accessible to our antibodies. The same two antibodies were used as previously shown in Chapter 3, targeting the N-terminus and CD1 region of Bub1 respectively. Interestingly, when Bub1$^{1-23}$ cell extracts were prepared using the denaturing buffer, 'zombie' Bub1 now became visible upon overexposure of the membranes using the antibody which recognised amino acids 1-300 (Figure 17B, top blot). This may suggest the truncated 'zombie' Bub1 protein is folded differently, which disrupted antibody epitope accessibility and rendered it undetectable previously using native extract. This residual expression would also have not been detected in previous blots as long overexposure was necessary to see this residual band, as apparent in the density of the band in the parental control sample (lane 1). Importantly, when Bub1$^{1-23}$ cells were treated with Bub1 RNAi (oligo c from Jia *et al,* 2016, used for the whole of this chapter), this residual band disappeared (lane 4, top blot) suggesting it is not a non-specific band. This blot provides some evidence for the existence of 'zombie' Bub1 in Bub1$^{1-23}$ cells. However, when an antibody targeting amino acids 336 – 489 (Figure 17B, lower blot) was used to try and detect 'zombie' Bub1 there was no clear evidence. Therefore 'zombie' Bub1 is hard to detect in Bub1$^{1-23}$ cells, suggesting it is a very unstable protein.

Following immunoblotting for 'zombie' Bub1 protein in our Bub1$^{1-23}$ cell line, we wanted to see if it was present at kinetochores in prometaphase cells. To do this we used a second Bub1-CD1 antibody obtained from the Meraldi lab that recognises the region between amino acids 336-489 (Klebig, Korinth and Meraldi, 2009). The CD1 region contains the site for Mad2 recruitment to Bub1, following phosphorylation by Cdk1 and Mps1 (Ji *et al.*, 2017). Immunostaining using this Bub1-CD1 antibody in prometaphase Bub1$^{1-23}$ cells showed a faint kinetochore signal following automated analysis, which was barely detectable by eye above background levels (Figure 17C, D). This staining pattern was not seen with the Bub1 N-terminus antibody used in Chapter 3, which was undetectable by eye and automated analysis. Importantly this residual signal was no longer detectable once Bub1$^{1-23}$ cells were treated with Bub1 RNAi (Figure 17C, D). We conclude that 'zombie' Bub1 can be recruited to kinetochores in the Bub1$^{1-23}$ cell line, but is either a highly unstable protein or unstably bound to kinetochores due to its very low kinetochore signal. Immunofluorescence experiments performed in Chapter 3 used an antibody recognising amino acids 1 to 130, which contains the Cas9 cut site. This region is likely mutated or truncated in 'zombie' Bub1, which could explain why no signal was detected in the Bub1$^{1-23}$ cell line using this antibody. Puzzlingly, BubR1 was also undetectable at kinetochores in Bub1$^{1-23}$ cells, which is indicative of total Bub1 removal. The BubR1 antibody may be less sensitive than the Bub1-CD1 antibody, or the BubR1 epitope may be less accessible when bound to 'zombie' Bub1. There is also the possibility that 'zombie' Bub1 may not facilitate recruitment of BubR1 to kinetochores in Bub1$^{1-23}$ cells. However this hypothesis is unlikely given that the Bub3 binding site, essential for Bub1 kinetochore localisation (Taylor, Ha and McKeon, 1998), is before the BubR1 binding site suggesting this region of Bub1 is intact and functional as 'zombie' Bub1 can be seen at kinetochores.

Finally, we wanted to see if Bub1 RNAi treatment in Bub1$^{1-23}$ cells had any further effects on Sgo1 localisation. Sgo1 is recruited to centromeres via phosphorylated H2A-T120, a well-established target of Bub1 kinase activity (Kawashima *et al.*, 2010). The contribution of Bub1 to Sgo1 localisation is unclear in the literature, as

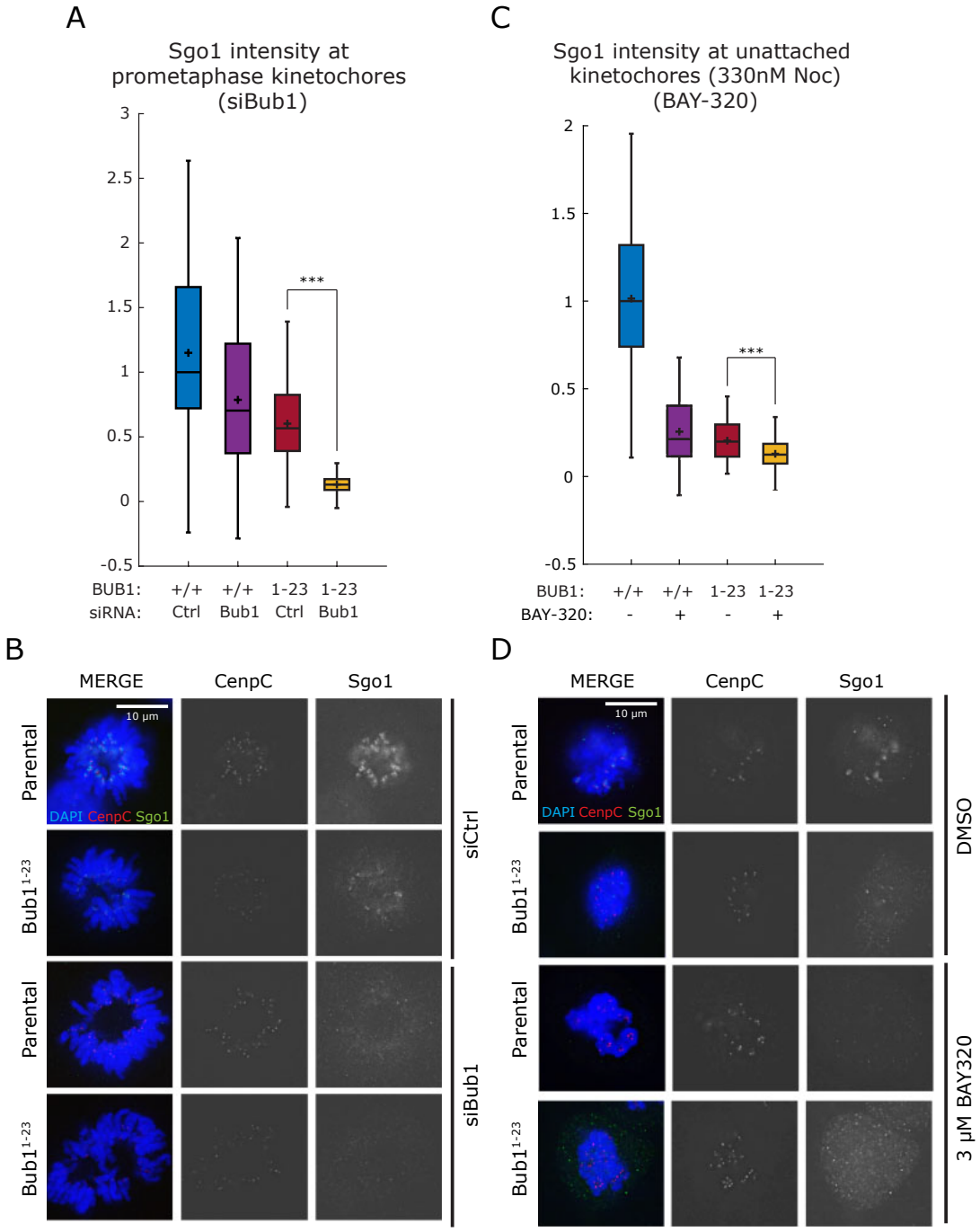

Figure 18: Analysis of 'zombie' Bub1 kinase activity in Bub1$^{1-23}$ cells. A) Quantification of Sgo1 intensity at kinetochores in parental and Bub1$^{1-23}$ cells treated with control or Bub1 RNAi. Cells were imaged in prometaphase and Sgo1 levels were normalised to CenpC. All conditions were normalised to the median value of parental control cells. Data from one representative experiment, >700 kinetochores. Experiment was repeated three times. P value from a Mann Whitney U test. B) Representative images from analysis in A). C) Quantification of Sgo1 intensity at kinetochores in parental and Bub1$^{1-23}$ cells treated with 330 nM nocodazole plus DMSO or 3 μM BAY-320. Sgo1 levels were normalised to CenpC. All conditions were normalised to the median value of parental DMSO treated cells. Data from 1 experiment, >500 kinetochores. P value from a Mann Whitney U test. D) Representative images from analysis in C).

it is suggested that cohesin and H2A-pT120 specify two separate pools of Sgo1(Liu, Jia and Yu, 2013). As shown in Chapter 3, Sgo1 was reduced by 50% in Bub1$^{1-23}$ cells, and we reasoned this remaining Sgo1 was recruited via cohesin. However, now we wondered if this was mediated by 'zombie' Bub1. To test for residual Bub1 kinase activity, Bub1$^{1-23}$ and parental cells were treated with control and Bub1 siRNA and levels of Sgo1 were measured in prometaphase cells. Surprisingly, when 'zombie' Bub1 was depleted in Bub1$^{1-23}$ cells by Bub1 RNAi, Sgo1 recruitment at kinetochores was abolished confirming that 'zombie' Bub1 kinase activity was contributing to its localisation (Figure 18A,B). To control for off target effects of the Bub1 RNAi oligo, we repeated the experiment in the presence of nocodazole and BAY-320, a small molecule inhibitor of Bub1 kinase activity (Baron *et al.*, 2016). We again saw the same decrease in Sgo1 localisation to kinetochores upon treatment of Bub1$^{1-23}$ cells with BAY-320 (Figure 18C, D). These results show that the kinase domain of 'zombie' Bub1 is functional in Bub1$^{1-23}$ cells, and Bub1-mediated phosphorylation of histone H2A is necessary for Sgo1 recruitment to kinetochores/centromeres.

To conclude this section, we have confirmed the existence of 'zombie' Bub1 in our Bub1$^{1-23}$ cell line. This form of Bub1 is expressed at very low levels following BUB1 disruption, but does not experience the consequences of exon skipping. We have shown that it can be recruited to kinetochores, confirming that the Bub1 protein is functional from at least the GLEBS domain (Bub3 binding/kinetochore localisation) onwards. It also has kinase activity which is capably of recruiting 50% of the Sgo1 seen in parental cells. Importantly, once Bub1$^{1-23}$ cells are treated with Bub1 RNAi, Sgo1 recruitment is abolished in RPE1 cells.

4.3 'Zombie' Bub1 contributes to maintenance of long term mitotic arrest

As described in Chapter 3, Bub1$^{1-23}$ cells show a shortened mitotic arrest compared to parental cells when treated with 330 nM nocodazole (Figure 14).

Bub1$^{1-23}$ cells were able to support mitotic arrest for 16.5 hr, while parental cells arrested for 27 hr. However, these cells were expressing the undetected 'zombie' Bub, which we have now established to be present at kinetochores in Bub1$^{1-23}$ cells. Therefore we decided to repeat this experiment and treat Bub1$^{1-23}$ cells with a different siBub1 oligo to deplete 'zombie' Bub1 and assess the effects in our mitotic arrest assay using 330 nM nocodazole. Depletion of 'zombie' Bub1 in Bub1$^{1-23}$ cells reduced the duration of long term mitotic arrest to a median of 420 min or 7 hours (yellow line), compared to 1030 min or 17.1 hours for Bub1$^{1-23}$ cells treated with control RNAi (red line) (Figure 19A, B). This is a decrease of 610 min or 10.1 hours following removal of the very poorly expressed 'zombie' Bub1.

To test if the presence of microtubules is important for SAC signalling upon loss of Bub1, we decided to perform the same mitotic arrest experiment using 100 μM monastrol. Monastrol is a small molecule inhibitor of kinesin-5 (Eg5), a motor protein that organises microtubules to form the mitotic spindle, and induces persistent monopolar spindles (Kapoor *et al.*, 2000). Monastrol causes enrichment of sister kinetochores that are syntelically attached to microtubules originating from the same spindle pole. These kinetochores become monotelically attached and subsequently activate the SAC through the activity of Aurora B, causing mitotic arrest (Kapoor *et al.*, 2000; Hauf *et al.*, 2003). Bub1$^{1-23}$ cells treated with Bub1 RNAi were able to arrest in 100 μM monastrol for a median of 530 min or 8.8 hours, while Bub1$^{1-23}$ cells arrested for a median of 1035 mins or 17.2 hours (Figure 19C, D). Bub1$^{1-23}$ cells treated with control RNAi behaved exactly the same in 330 nM nocodazole and 100 μM monastrol (1030 min vs 1035 min respectively), while Bub1$^{1-23}$ cells depleted of 'zombie' Bub1 arrested for 110 min longer in monastrol than nocodazole (530 min vs 420 min respectively). This modest increase in mitotic arrest duration in the presence of monastrol could suggest that the presence of the mitotic spindle has a small positive effect on MCC formation and APC/C inhibition.

To conclude, SAC dependant arrest in Bub1$^{1-23}$ cells depleted of 'zombie' Bub1 is dramatically reduced compared to Bub1$^{1-23}$ cells that express this poorly expressed, truncated form of Bub1. However, Bub1$^{1-23}$ cells depleted of 'zombie' Bub1 are

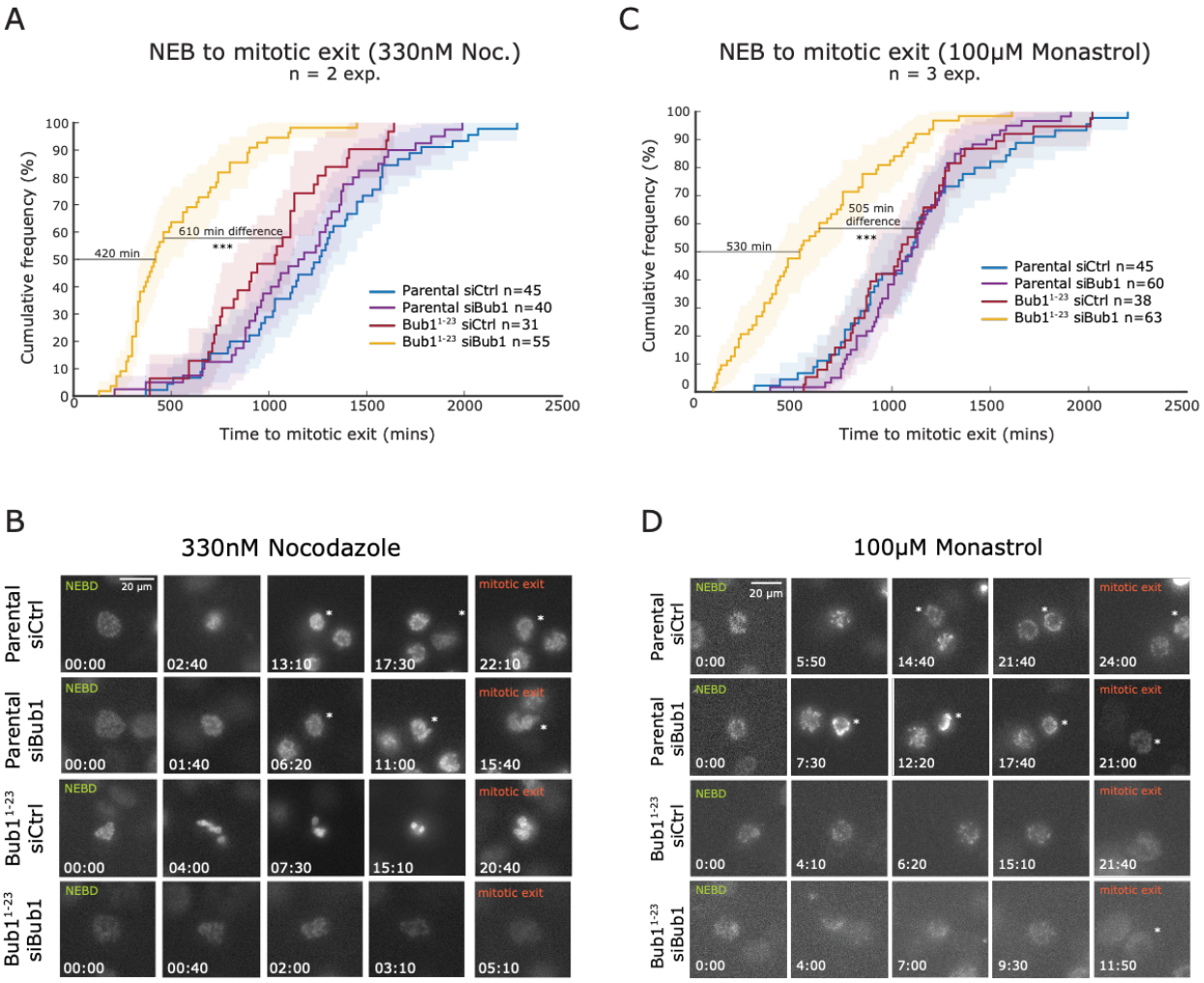

Figure 19: 'Zombie' Bub1 contributes to SAC activity in Bub1$^{1-23}$ cells. A) Time spent in mitosis from NEBD to mitotic exit of parental and Bub1$^{1-23}$ cells treated with control or Bub1 RNAi. Cells were arrested in 330 nM nocodazole and SiR-DNA (to visualise DNA), and filmed for 40 hr. Data from 2 independent experiments, shaded area represents 95% confidence interval. P value from a Wilcoxon rank sum test comparing Bub1$^{1-23}$ siCtrl and parental siCtrl treated cells. B) Movie stills from live cell imaging of parental and Bub1$^{1-23}$ cells analysed in A). Time in hours:mins. Star denotes cell of interest. C) Same analysis as in A) except cells were treated with 100 μM monastrol. Data from 3 independent experiments. D) Movie stills from live cell imaging of parental and Bub11-23 cells analysed in C). Time in hours:mins. Star denotes cell of interest.

able to arrest for over 6 hours in response to unattached kinetochores created by both nocodazole and monastrol. This is consistent with results from the Nilsson laboratory in that 'zombie' Bub1 contributes to SAC signalling, but the magnitude of the contribution appears to be less in our hands. It should be noted at this point that in the Nilsson laboratory publication, cells were subject to two RNAi treatments and synchronisation with thymidine (S-phase arrest) over 48 hours prior to nocodazole arrest experiments (Zhang *et al.*, 2019). In our experiments cells are not synchronised and received one RNAi treatment.

4.4 Unattached kinetochores can load Mad2 and delay anaphase onset in the absence of 'zombie' Bub1

As reported above, depletion of 'zombie' Bub1 further reduced the duration of mitotic arrest in response to unattached kinetochores generated by nocodazole and monastrol (Figure 19A, C). This suggests that kinetochores are capable of recruiting Mad2 and producing MCC in the total absence of Bub1. To directly test this, we arrested parental or Bub1$^{1\text{-}23}$ cells treated with control or Bub1 RNAi in 330 nM nocodazole overnight for 16 hr and performed immunostaining using Mad2 antibodies. It is worth noting here that a different antibody recognising Mad2 was used than in Chapter 3, as the previous antibody was no longer produced to the same quality. However the antibody used in this chapter (sc-65492) produced high quality staining comparable with the previous antibody (poly19246). Mad2 was easily visible at kinetochores in all treatments, and analysis showed that kinetochore-Mad2 was comparable in Bub1$^{1\text{-}23}$ cells with and without 'zombie' Bub1 depletion (Figure 20A, B). This suggests that Bub1 is not required for recruitment of Mad2 at unattached kinetochores, consistent with previous results.

One prediction of the two pathway model of SAC signalling is that a single unattached kinetochore in an otherwise normal bipolar spindle is able to recruit Mad2 in the absence of Bub1. It has been shown that a single chromosome

detached from the mitotic spindle either by laser microsurgery or treatment with low dose nocodazole causes a delay in anaphase (Dick and Gerlich, 2013).

Therefore, to directly test whether Mad2 can bind to unattached kinetochores in the presence of kinetochores already bound to spindle microtubules, we treated cells with low dose nocodazole. 5nM nocodazole treatment gives rise to a few polar, monotelic chromosomes in RPE1 cells, which were shown to recruit Mad2 and delay mitosis following RNAi depletion of KNL1 (Silió, McAinsh and Millar, 2015). The assumption is that polar chromosomes have a higher probability of being unattached compared to kinetochores within the spindle body. To perform this experiment, parental or Bub1$^{1\text{-}23}$ cells treated with control or Bub1 RNAi were treated with 5nM nocodazole for 2 hours then fixed and immunostained using anti-CenpC, tubulin and Mad2 antibodies. This treatment induced polar chromosomes, although they were rare. All cells, including Bub1$^{1\text{-}23}$ cells depleted of 'zombie' Bub1, were able to load Mad2 to the kinetochores of polar chromosomes, confirming that Bub1 is not required for the recruitment of Mad2 to unattached kinetochores (Figure 20C, D). Although present, Mad2 at the kinetochores of polar chromosomes in cells fully depleted of Bub1 appeared reduced compared to the other treatments, and this was confirmed by quantification (Figure 20C). Interestingly, in each kinetochore pair one kinetochore always had more Mad2 bound than the other. This may represent the attached vs unattached kinetochore at the pole.

Following confirmation that a single unattached kinetochore could recruit Mad2 in the absence of 'zombie' Bub1, we wanted to see if this was capable of delaying anaphase onset. As 5 nM nocodazole rarely produced polar chromosomes as seen on fixed slides, we used a dose of 20 nM for the live cell imaging experiment toincrease the frequency of polar chromosomes and collect data more easily. We treated parental and Bub1$^{1\text{-}23}$ cells with control or Bub1 RNAi, and then treated with 20 nM nocodazole and SiR-DNA (to visualise chromosomes) for 2 hours before imaging. We saw polar chromosomes induced in all conditions, although these were not very frequent. Nevertheless, we separated data into cells which did and did not display polar chromosomes and compared mitotic timing from NEB

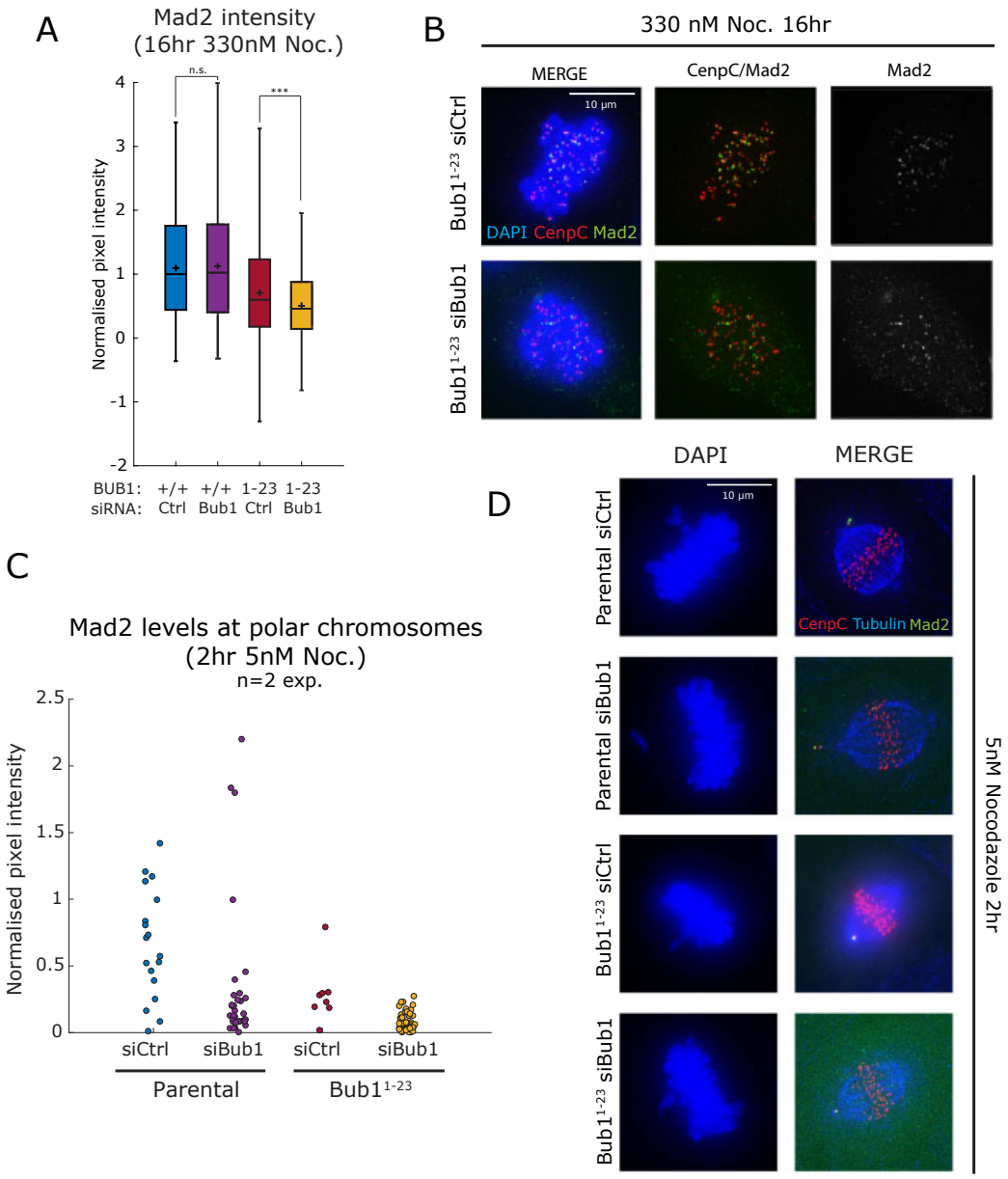

Figure 20: 'Zombie' Bub1 is not required for Mad2 recruitment to unattached kinetochores. A) Quantification of kinetochore bound Mad2 in parental and Bub1$^{1-23}$ cells treated with control or Bub1 RNAi and arrested in 330 nM nocodazole for 16 hr. Mad2 intensity was normalised to respective CenpC intensity, and all conditions are normalised to the median value of the parental control. Data from one experiment, >600 kinetochores. P values from a Mann U Whitney test. B) Representative images from the analysis in A). C). Quantification of kinetochore-bound Mad at polar chromosomes in parental and Bub1$^{1-23}$ cells treated with control or Bub1 RNA, induced by treatment with 5nM nocodazole. Polar chromosomes were identified by their presence at spindle poles, away from the metaphase plate. Mad2 intensity was normalised to respective CenpC intensity following subtraction of background signal. Data pooled from two independent experiments. D) Representative images from analysis in C).

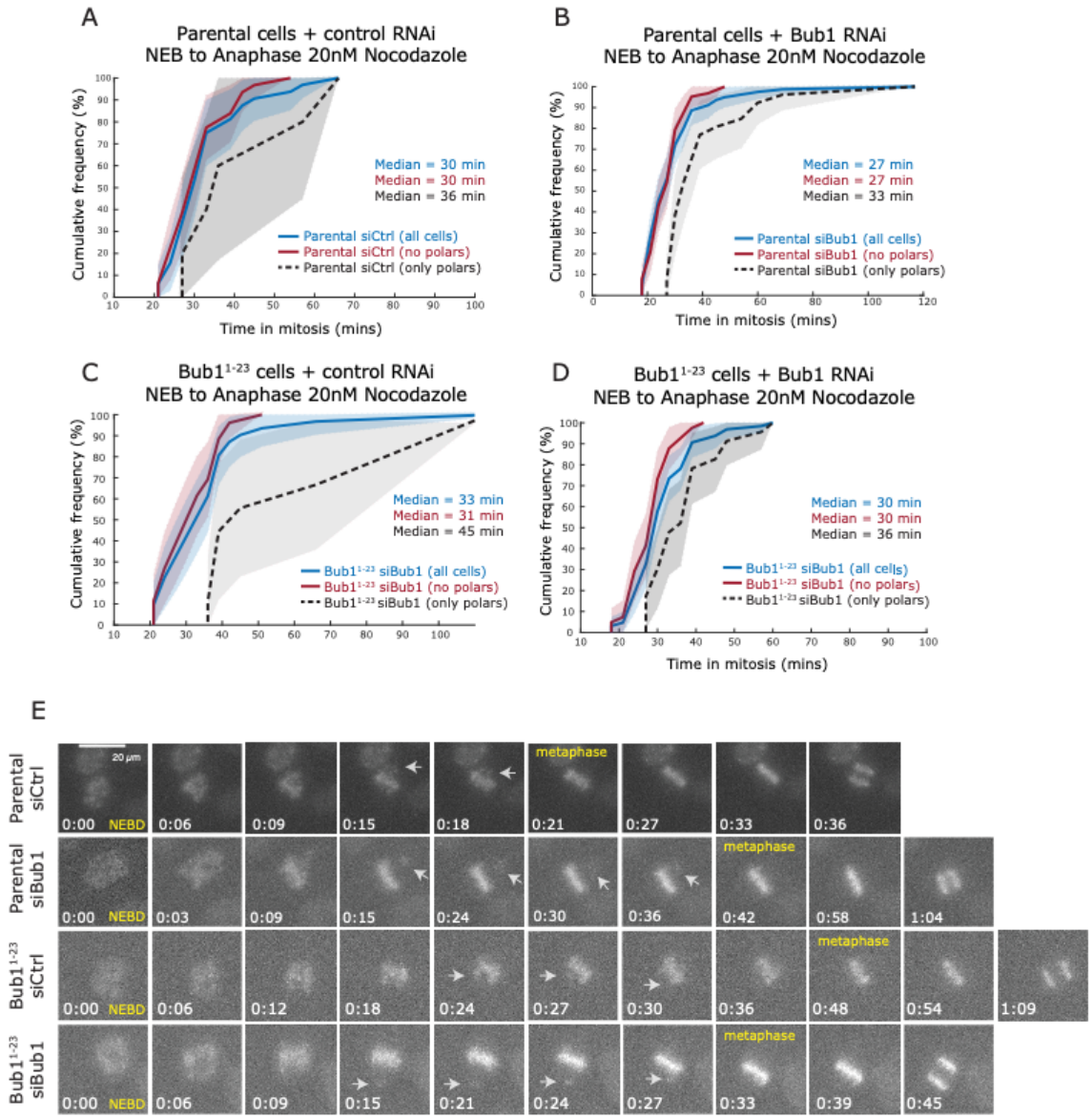

Figure 21: RPE1 cells depleted of Bub1 are able to delay anaphase onset in response to a single unattached kinetochore. A) Quantification of total time in mitosis (NEBD to anaphase) of parental RPE1 cells transfected with control RNAi treated with 20nM nocodazole. Mitotic timing of all cells (blue line n=32) are compared to subpopulations of cells with polar chromosomes (black dashed line n=5) and without polar chromosomes (red line n=26). Data from 3 independant experiments. B) Same as A) except parental cells treated with Bub1 RNAi. Mitotic timing of all cells (blue line n=79) are compared to subpopulations of cells with polar chromosomes (black dashed line n=19) and without polar chromosomes (red line n=63). Data from 5 independant experiments. Same as A) except Bub1$^{1-23}$ cells treated with control RNAi. Mitotic timing of all cells (blue line n=31) are compared to subpopulations of cells with polar chromosomes (black dashed line n=9) and without polar chromosomes (red line n=26). Data from 2 independant experiments. D) Same as A) except Bub1$^{1-23}$ cells treated with Bub1 RNAi. Mitotic timing of all cells (blue line n=64) are compared to subpopulations of cells with polar chromosomes (black dashed line n=23) and without polar chromosomes (red line n=41). Data from 4 independant experiments. E) Representative movie stills from analysis in A-D showing examples of cells delaying anaphase in response to polar chromosomes. Time in hours:mins.

to anaphase onset. For all conditions, cells with visible polar chromosomes delayed anaphase onset compared to cells which did not possess polar chromosomes (Figure 21 A-D). Crucially, we saw clear examples of Bub1$^{1-23}$ cells displaying polar chromosomes that remained in mitosis until this chromosome became aligned and congressed to the metaphase plate (Figure 21 D). The cells then underwent a co-ordinated anaphase. Furthermore, Bub1$^{1-23}$ + Bub1 RNAi cells displaying polar chromosomes delayed anaphase onset for a median of 6 mins longer than cells which did not possess polar chromosomes, consistent with parental cells and Bub1$^{1-23}$ cells treated with control RNAi. This shows that the SAC can be activated at a single unattached kinetochore in the absence of Bub1, and is sufficient to delay anaphase onset. This also suggests that Aurora-B mediated error correction is functional in cells fully depleted of Bub1, as polar chromosomes were biorientated in a similar fashion to control cells.

Taken together, these results show that Bub1 is not required for the recruitment of Mad2 to unattached kinetochores in RPE1 cells, consistent with the conclusions drawn in Chapter 3. A single unattached kinetochore that cannot recruit Bub1 in an otherwise normal mitotic spindle can recruit Mad2 and, crucially, this single unattached kinetochore is sufficient to delay anaphase onset for the whole cell. These data, collected in the absence of 'zombie' Bub1 and therefore very efficient depletion of Bub1, support the two pathway model of checkpoint activation at unattached kinetochores.

4.5 Loss of Bub1 causes increased syntelic attachments after nocodazole washout

Bub1 is reported to have a dual role in both SAC signalling and chromosome alignment. The latter is mediated through recruitment of Shugoshin 1 (Sgo1) to the centromere via the phosphorylation of histone H2A at T120, the target of Bub1 kinase activity (Fernius and Hardwick, 2007; Kawashima *et al.*, 2010). As well as contributing to sister chromatid cohesion, Sgo1 is implicated in the recruitment of Aurora B, the master kinase regulating error correction from the CPC

(Meppelink *et al.*, 2015). However, in a separate study, Bub1 phosphorylation of H2A-T120 was implicated in directly controlling localisation and activity of Aurora B at the centromere (Ricke, Jeganathan and van Deursen, 2011).

From experiments using 20 nM nocodazole to induce polar chromosomes, we had observed successful congression and alignment of chromosomes occurring in Bub1$^{1-23}$ cells in both the presence and absence of 'zombie' Bub1 suggesting error correction was unperturbed. We therefore wanted to test the efficiency of error correction in Bub1$^{1-23}$ cells using a functional assay. To do this, we released Bub1$^{1-23}$ cells from a 2 hour 3.3 μM nocodazole arrest and filmed mitotic progression. Parental cells entered anaphase in a median of 48 mins, while Bub1$^{1-23}$ cells took a median of 54 mins (Figure 22A). The cumulative frequency curve for Bub1$^{1-23}$ cells is shifted to the right compared to parental cells, meaning the population is delayed before entering anaphase. However, all cells completed chromosome congression successfully to the metaphase plate and entered a coordinated anaphase. Surprisingly, Bub1$^{1-23}$ cells had less anaphase errors than the parental cells. This was confirmed when comparing lagging chromosomes and total segregation errors (including anaphase bridges) between the two cell lines (Figure 22B). Bub1$^{1-23}$ cells had 55% less lagging chromosomes than parental cells, and 63% less total errors than parental cells in the nocodazole washout assay.

These experiments were performed in the presence of 'zombie' Bub1, so we repeated the nocodazole washout following Bub1 RNAi treatment in parental and Bub1$^{1-23}$ cells. We have already shown that depletion of 'zombie' Bub1 by RNAi in Bub1$^{1-23}$ cells reduced Sgo1 to undetectable levels at centromeres (Figure 18). We found no additive effects on the timing of anaphase onset following nocodazole washout after depletion of 'zombie' Bub1 in Bub1$^{1-23}$ cells (Figure 22C). However segregation errors increased to 25%, comparable with parental cells (Figure 22D). These errors consisted of mainly lagging chromosomes, with a few cells progressing to anaphase with uncongressed chromosomes suggesting SAC override. Taken together these results suggest that disrupting Sgo1 centromere localisation, resulting from loss of Bub1-mediated H2A-T120

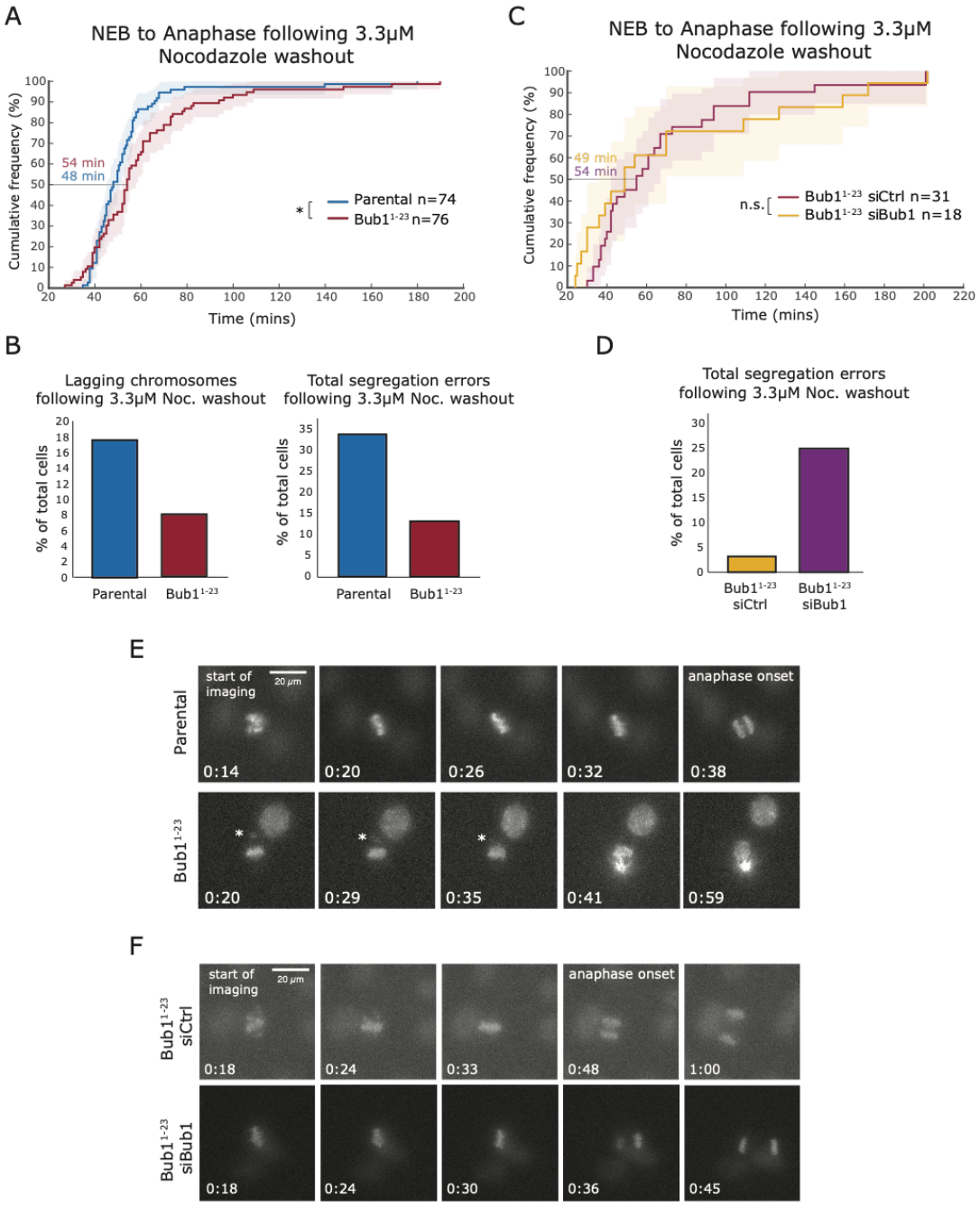

Figure 22: Bub1 contributes to recovery from nocodazole arrest. A) Quantification of mitotic progression (NEB to Anaphase) following 3.3μM nocodazole washout in parental and Bub1$^{1\text{-}23}$ cells. P value from a Wilcoxon rank sum test. Data from 5 independent experiments. B) Quantification of mitotic errors following 3.3μM nocodazole washout; lagging chromosomes (left) and total segregation errors (right). C) Same experiment as A) except Bub1$^{1\text{-}23}$ cells were treated with control of Bub1 RNAi. P value from a Wilcoxon rank sum test. Data from 4 independent experiments. D) Same as B), except Bub1$^{1\text{-}23}$cells are treated with control or Bub1 RNAi. E) Movie stills from live cell imaging used for the analysis in A). Chromosomes are visualised using SiR-DNA. Star denotes slow congressing chromosomes. F) Movie stills from live cell imaging used for the analysis in C). Chromosomes are visualised using SiR-DNA.

phosphorylation, to undetectable levels has no further effect on error correction in RPE1 cells.

Occasionally, in Bub1$^{1-23}$ cells, a few chromosomes persisted away from the metaphase plate, before successfully congressing and segregating with the rest of the chromosomes (Figure 18E). These were reminiscent of the polar chromosomes induced by 20 nM nocodazole. Therefore we wanted to investigate the attachment status of these kinetochores to see if they were indeed polar. To do so we performed the same nocodazole washout experiment followed by a fixed time course (Figure 23A). Cells were immunostained for spindle microtubules, DNA and kinetochores using antibodies and DAPI (Figure 23B). First we quantified the formation of bipolar spindles following nocodazole washout, and found that both cell lines were able to assemble bipolar spindles correctly (Figure 23C). During analysis of spindle assembly, we indeed saw there was a notable increase in polar chromosomes in Bub1$^{1-23}$ cells. We therefore quantified the percentage of cells which displayed polar chromosomes on bipolar spindles at various time point after nocodazole washout. Polar chromosomes were defined as those behind the spindle pole (Figure 23B, dotted line). We found that parental and Bub1$^{1-23}$ cells showed the same amount of cells with polar chromosomes 20 min after washout, but these polar chromosomes persisted longer in Bub1$^{1-23}$ cells (30 min) before eventually being resolved (40 min). As these analyses were performed on fixed samples the frequency of polar chromosomes is likely overestimated, however they were readily observed in Bub1$^{1-23}$ cells. We reasoned that these polar chromosomes represent syntelic or monotelic attachments, and we can identify clear examples of this (Figure 19B, zoom box). This suggests chromosomes are more likely to become polar, and therefore syntelically attached in the absence of Bub1. We note here that polar chromosomes were more commonly induced using 20 nM in Bub1$^{1-23}$ cells (~ 30%) than parental cells (~20%) (data not shown), which supports the idea that when Bub1 is depleted, chromosomes may be more likely to become polar. We do not suggest that polar chromosomes have trouble being corrected, as polar chromosomes induced using 20 nM nocodazole in parental and Bub1$^{1-23}$ cells were corrected in a similar time

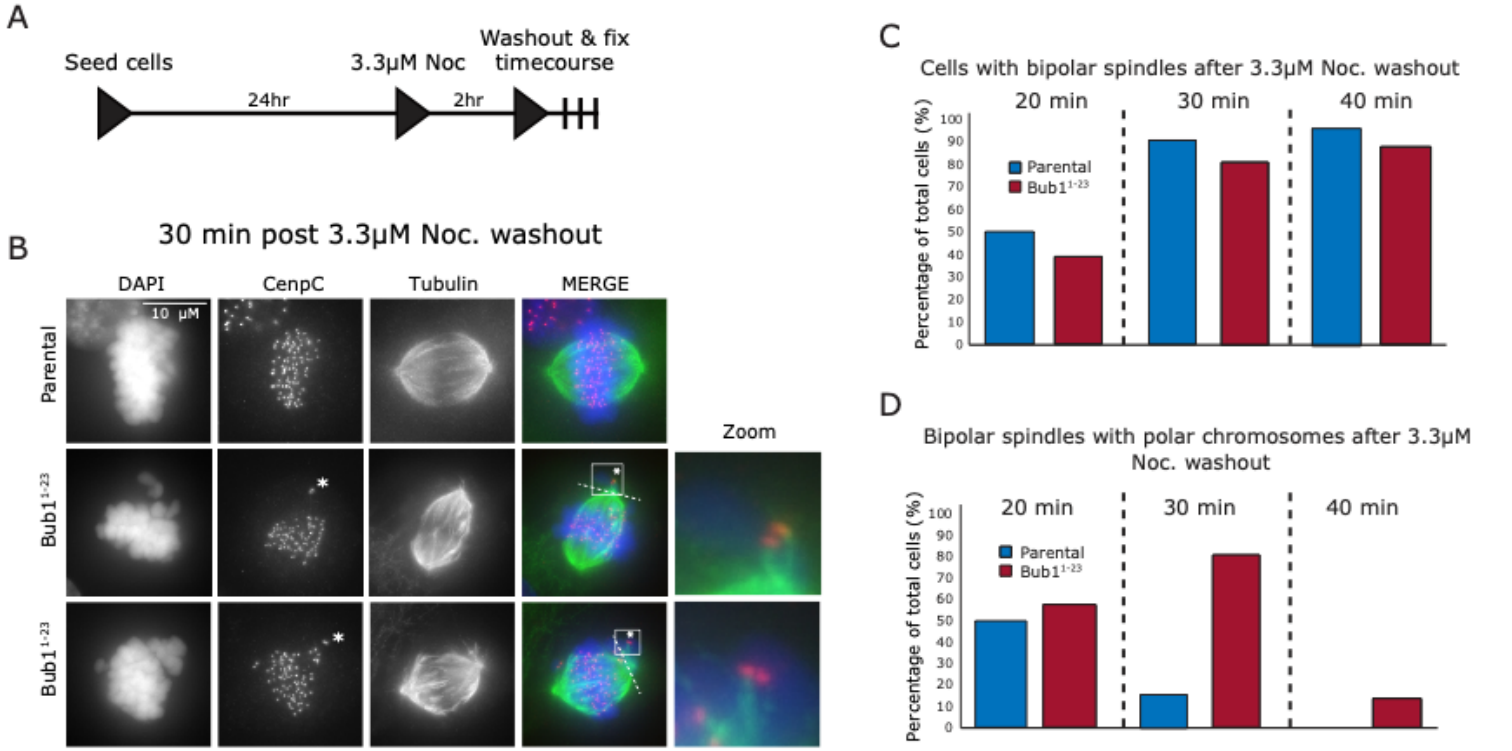

Figure 23: Bub1 contributes to efficient chromosome biorientation following nocodazole washout. A) Protocol used for fixed time course following 3.3μM nocodazole washout. B) Representative images of parental and Bub1$^{1\text{-}23}$ cells fixed 30 mins after 3.3 μM nocodazole washout. Stars denote polar chromosomes, which are identified as being behind the spindle pole (dashed line). Zoom box shows clear syntelic attachment of a polar chromosome in a Bub1$^{1\text{-}23}$ cell. C) Quantification of the percentage of parental and Bub1$^{1\text{-}23}$ cells with bipolar spindles at 10 minute time intervals following 3.3 μM nocodazole washout. Data pooled from two independent experiments. D) Quantification of the percentage of parental and Bub1$^{1\text{-}23}$ cells with bipolar spindles (in C) which have polar chromosomes at 10 minute time intervals following 3.3 μM nocodazole washout. Data pooled from two independent experiments.

scale, however more data is needed to make solid conclusions on this. We propose that increased syntelic attachments formed in Bub1$^{1-23}$ cells following nocodazole washout cause a delay in anaphase onset while they are being corrected, and that the process of error correction itself is functional. The increased proportion of syntelically attached polar chromosomes could represent a problem with the formation of initial kinetochore-microtubule attachments in the absence of Bub1. If this was true then in the presence of BAY-320, a Bub1 kinase inhibitor, instead of Bub1 siRNA we would expect no increase in syntelic attachments, assuming that the kinase activity is not playing a role in this mechanism, and would also see no problems with error correction. In other words, there would be no phenotype. However, BAY-320 is not completely potent and there is always the possibility of residual Bub1 kinase activity that is sufficient for its functionality. This also assumes that Bub1 kinase activity does not contribute to SAC signalling (Klebig, Korinth and Meraldi, 2009; Baron *et al.*, 2016), which has been the subject of controversy (Tang *et al.*, 2004b).

To conclude, we observed a delay in anaphase onset following nocodazole washout in Bub$^{11-23}$ cells, which was not worsened by depletion of 'zombie' Bub1. Fixed time course immunostaining showed that Bub1$^{1-23}$ cells generate more polar chromosomes following nocodazole washout, which persist away from the metaphase plate but are eventually aligned. As described earlier, cells depleted of Bub1 (and 'zombie' Bub1) are able to activate the SAC in response to polar chromosomes, so we expect this causes the delay seen in anaphase onset following nocodazole washout. Surprisingly this seems to lead to a decrease in chromosome segregation errors in Bub1$^{1-23}$ cells following nocodazole washout. We propose this is due to the increased time period in which merotelic attachments can be corrected. The mechanism by which chromosomes are more likely to become polar in the absence of Bub1 is unclear at this time, but is likely due to a reduction in CenpE, shown in Figure 11, as CenpE is known to play an essential role in congression of monoorientated chromosomes from the spindle pole to the spindle equator (Kapoor *et al.*, 2006). It could also be due to an unknown role of Sgo1 or Bub1 in generating initial kinetochore-microtubule interactions.

4.6 Conclusions

Unexpectedly, when the Bub1 locus is targeted via gene editing an unstable, poorly expressed and likely truncated form of Bub1 remains in Bub1$^{1-23}$ cells at almost undetectable levels. This residual pool of Bub1 was termed 'zombie' Bub1 (Meraldi, 2019), and in this chapter we have shown that this near undetectable form of Bub1 contributes to checkpoint signalling in Bub1$^{1-23}$ cells. 'Zombie' Bub1 is recruited to kinetochores at very low levels, suggesting it is highly unstable. It is only detectable using an antibody recognising amino acids 336 – 489, and not with an antibody recognising amino acids 1 – 130, suggesting the N terminus is either truncated or mutated. 'Zombie' Bub1 was shown to be capable of recruiting 50% of Sgo1 to centromeres compared to parental cells, confirming that it has functional kinase activity.

When 'zombie' Bub1 is depleted from Bub1$^{1-23}$ cells using Bub1 RNAi, the arrest in nocodazole is reduced by 10 hrs and in monastrol is reduced by 8.4 hrs compared to control Bub1$^{1-23}$ cells. These data suggest that Bub1 is functioning substoichiometrically to maintain checkpoint signalling, as this very small amount of Bub1 had a surprisingly large contribution to SAC maintenance. At this stage it is unknown which property of Bub1 is allowing this functionality, as the kinase activity has been shown not to contribute to checkpoint signalling (Klebig, Korinth and Meraldi, 2009; Baron *et al.*, 2016). This point will be further discussed in Chapter 6. However, crucially, Bub1$^{1-23}$ cells depleted of 'zombie' Bub1 arrested for a median of over 6 hours in both nocodazole and monastrol. This confirms the conclusions drawn in Chapter 3, and provides even further evidence to support the two pathway model of checkpoint signalling in RPE1 cells.

We have shown that while Bub1 is required for the long-term maintenance of checkpoint signalling, it is dispensable for initial checkpoint activation as seen by the recruitment of Mad2 at unattached kinetochores in nocodazole. Cells fully depleted of Bub1 were able to recruit Mad2 and delay anaphase onset in response to a single unattached kinetochore generated by treatment with 5nM or 20nM

nocodazole. This confirms that recruitment of Mad2, and subsequently MCC generation and APC/C inhibition from unattached kinetochores is possible in the absence of Bub1. We have also presented data to suggest that Bub1 is not required for error correction in RPE1 cells, but instead it may play a role in polar chromosome congression potentially mediated by CenpE recruitment.

While siRNA depletion of 'zombie' Bub1 has been useful to further dissect the role of Bub1 in the SAC using Bub1$^{1-23}$ cells, a total null cell line is necessary. This will be challenging in hTERT-RPE1 cells as two alleles must be successfully targeted in a single cell. During completion of this work, we received a personal correspondence from the Medema lab who have been able to make a HAP1 Bub1 total null cell line. These cells are haploid, therefore only one allele needs to be targeted. Two guides were used to cut in exon 1 and exon 24 respectively, and the excised BUB1 gene was confirmed to not be reintegrated elsewhere in the genome. Analysis of two independent clones showed mitotic arrest in nocodazole was unaffected in the total absence of Bub1, as parental cells and two independent clones arrested for a median of 600 mins. Importantly, both independent clones became SAC deficient upon treatment of 250 nM reversine, while the parental cells could arrest for a median of 400 mins. This suggests that SAC signalling is further weakened once Mps1 has been sensitised in Bub1-null clones, but the SAC can function at full efficiency in response to unattached kinetochores. These data further support our data and the conclusion that Bub1 is not strictly required for spindle assembly checkpoint activation in response to unattached kinetochores in human cells. The contribution of Bub1 to SAC signalling at immaturely attached kinetochores remains unclear, and will be investigated in Chapter 5.

Chapter 5: Preliminary evidence for a premitotic role of Bub1

5.1 Introduction

Unattached kinetochores scaffold the production of mitotic checkpoint complex (MCC) during mitosis through the activity of the spindle assembly checkpoint (SAC). Diffusible MCC inhibits all APC/C^{Cdc20} complexes and delays anaphase onset. This mechanism allows the cell to remain in mitosis until all kinetochores reach biorientation and the SAC is satisfied. At this point, the inhibition of APC/C^{Cdc20} is released to allow securin and cyclin B1 degradation causing subsequent sister chromatid segregation and mitotic exit.

The APC/C is a master cell cycle regulator which is expressed throughout interphase and mitosis. In order for cells to complete the cell cycle successfully, it is essential that APC/C activity is tightly controlled. The APC/C must remain inhibited during interphase to allow accumulation of mitotic cyclins that signal for the cell to divide following DNA replication. Insufficient inhibition of the APC/C during S and G2 phases causes a G2 block where cells do not reach mitosis, caused by insufficient accumulation of cyclins A and B1 (Di Fiore and Pines, 2007; Hein and Nilsson, 2016). One mechanism by which APC/C inhibition during interphase is achieved is through Early Mitotic Inhibitor 1 Emi1. Emi1 is as an APC/C inhibitor that accumulates prior to mitotic entry and is destroyed during prophase independently of APC/C activity (Reimann *et al.*, 2001). Emi1 was shown to be required for inhibition of APC/C^{Cdh1} during S and G2 phases to stabilise mitotic cyclins and promote mitotic entry (Di Fiore and Pines, 2007). This represents a SAC-independent mechanism by which APC/C^{Cdh1} is inhibited prior to mitosis. Furthermore, Cdc20 expressed during interphase is phosphorylated by cyclin A2 – Cdk2 to negatively regulate the interaction of interphase Cdc20 with the APC/C during S/G2 phases, when cyclin A expression is high. This mechanism of interphase APC/C inhibition also allows for mitotic cyclin stabilisation to promote mitotic entry (Hein and Nilsson, 2016). Therefore, established mechanisms exist

by which the APC/C can be inhibited during interphase independently of the spindle checkpoint (Figure 24). Following the appropriate accumulation of cyclins, cells exit G2 and enter M-phase.

Briefly, there are two co-activators that interact with mitotic APC/C; Cdc20, which is necessary for the metaphase/anaphase transition, and Cdh1, which interacts with APC/C during late mitosis and G1 (Kramer *et al.*, 2000). Cdh1 can only interact with APC/C once Cdk1 activity has dropped, restricting its activity to after mitotic exit (Peters, 1998; Kramer *et al.*, 2000). However, Cdc20 can interact with the APC/C once it becomes phosphorylated by Cdk1 as the cell enters mitosis (Kramer *et al.*, 2000; Qiao *et al.*, 2016). Cdc20 is sequestered within MCC during

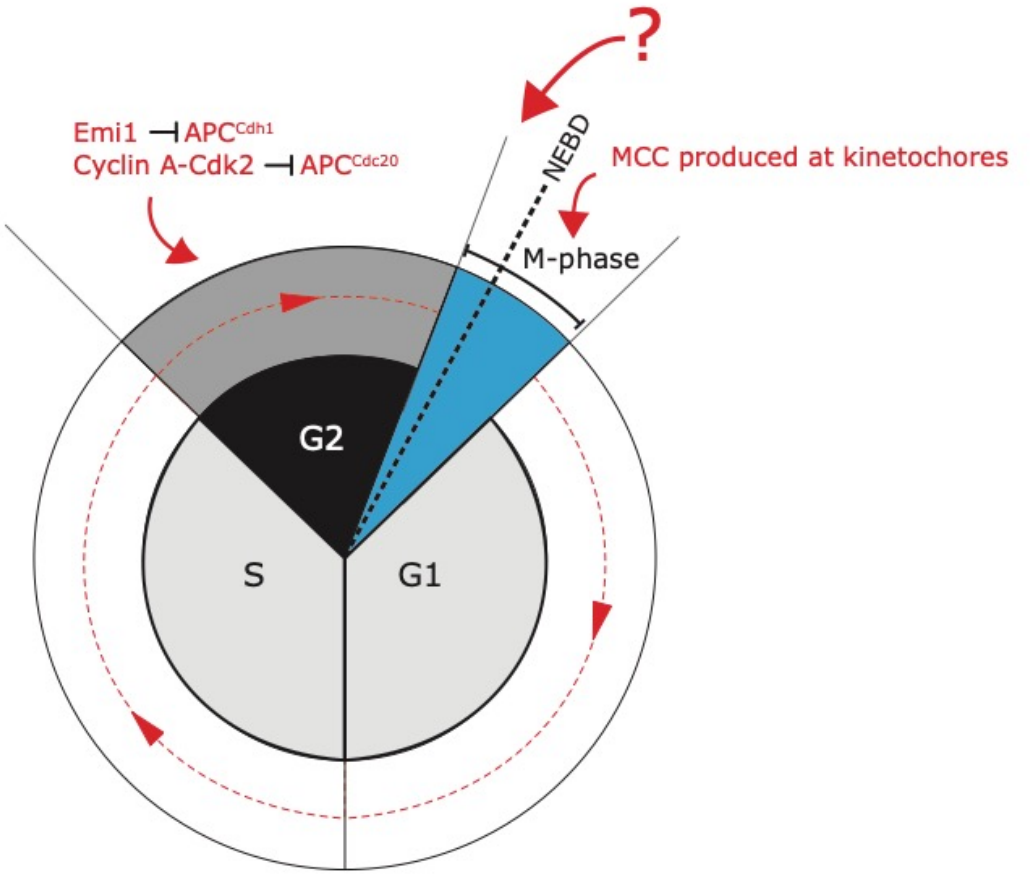

Figure 24: Mechanisms of APC/C inhibition during G2 and M phase. APC is inhibited during G2 via the actions of Emi1 and CyclinA-Cdk2. Emi1 inhibits APC/C^{Cdh1} and CyclinA-Cdk2 phosphorylates Cdc20 to inhibit its binding to APC/C. Emi1 is phosphorylated during prophase but CyclinA-Cdk2 only inhibit Cdc20 during S and G2. Cdc20 is then sequestered in MCC produced at unattached kinetochores following NEBD in mitosis. However, the mechanisms of Cdc20 inhibition during the G2/M transition prior to NEBD are unclear.

mitosis by the activity of the spindle assembly checkpoint (SAC) at unattached kinetochores to prevent premature anaphase onset (Dawson, Roth and Artavanis-Tsakonas, 1995; Sudakin, Chan and Yen, 2001). However, SAC signalling at kinetochores only occurs in prometaphase following nuclear envelope breakdown. Cdc20 must therefore be inhibited during prophase and very early prometaphase, independent to kinetochore-mediated SAC signalling, to efficiently inhibit APC/C until its activation is required. The precise mode of APC/C^{Cdc20} inhibition during early mitosis is a subject of debate in the field.

Interestingly, Mad1:Mad2 complexes localise to nuclear pores on the nuclear envelope of cells during interphase. This localisation is conserved in yeast and higher organisms (Scott *et al.*, 2005; Lee *et al.*, 2008; Lince-Faria *et al.*, 2009). Mad1:Mad2 are known to bind the nuclear pore complex (NPC) via the nuclear pore component Translocated Promoter Region (Tpr) (Lee *et al.*, 2008). Disrupting this interaction reduces the levels of Mad1 at the nuclear envelope and subsequently at kinetochores during early prometaphase. It has been suggested that the localisation of Mad1:Mad2 to the nuclear envelope is necessary to prime the Mad1:Mad2 complex for mitotic SAC signalling from kinetochores before mitotic entry. Recent reports have suggested that Mad1:Mad2 is localised at the NPC simply to ensure its rapid recruitment to kinetochores upon NEBD, mediated by CyclinB1-Cdk1 and Mps1 (Jackman *et al.*, 2019; Osswald *et al.*, 2019).

However, an alternative mode has been proposed in which nuclear pores act as a separate scaffold for MCC production prior to mitotic entry (Rodriguez-Bravo *et al.*, 2014). In this model, the recruitment of Mad1:Mad2 complexes to NPCs allows assembly of interphase MCC as a premitotic inhibitory signal to inhibit APC/C^{Cdc20} and further stabilise cyclin B1 before mitotic entry. This pathway requires the localisation of Mad1:Mad2 complexes to NPCs via Tpr. Authors propose that the production of interphase MCC defines the minimum length of mitosis, and when disrupted hTERT-RPE1 cells were seen to accelerate anaphase onset in ~12 mins with increased lagging chromosomes following NEBD. This was attributed to insufficient inhibition of APC/C during early mitosis, which

prevented the correction of merotelic errors due to a lack of time before anaphase onset. The phenotype was rescued by a transgene of Mad1 tethered to the nuclear pore via an interaction with Nup-153, suggesting that NPC localisation is required for the production of interphase MCC, but not the specific interaction with Tpr.

A recent paper, published after the initial submission of this thesis, also proposed that Mad1:Mad2 complexes inhibit APC/C activity in G2 to allow accumulation of cyclin B and subsequent mitotic entry through a different mechanism (Lara-Gonzalez *et al.*, 2019). They propose that Mad2:Cdc20 complexes are formed during interphase, which acts alongside CDK phosphorylation of Cdc20 to reduce its affinity for APC/C inhibits its activity. This data does not support the idea that interphase MCC is needed to inhibit the APC/C^{Cdc20} prior to the G2/M transition, as depletion of BubR1 did not reduce levels of cyclin B prior to NEBD in U2OS cells.

In summary, the mechanisms by which APC/C^{Cdc20} is inhibited before NEBD and the contribution this makes to mitotic checkpoint signalling remain unclear. It is debated as to whether the localisation of Mad1:Mad2 complexes to the nuclear envelope is required for APC/C inhibition through catalysis of interphase MCC, or whether this is simply a way to ensure the timely recruitment of Mad1:Mad2 to unattached kinetochores following NEBD. Furthermore, interphase-specific mechanisms of APC/C inhibition have been identified, such as Emi1 and Cyclin A-Cdk2, so the importance of Mad1:Mad2 complexes at the nuclear pore during interphase is uncertain.

The aim of this chapter was to further investigate the role of Bub1 during mitosis. In Chapter 4 we established that Bub1 is not required for the SAC response to unattached kinetochores, but if the two pathway model is correct then Bub1 would be required to sense immature attachments and delay anaphase onset until these can be stabilised (Silió, McAinsh and Millar, 2015). These types of attachments are present during prometaphase, therefore we decided to investigate the contribution of Bub1 to SAC signalling and mitotic exit in an unperturbed mitosis.

These experiments led us to investigate a potential role for Bub1 in APC/C inhibition prior to NEBD.

5.2 Bub1 is required for Mad2 recruitment in prometaphase

We had previously established that Bub1 is not required to recruit Mad2 to unattached kinetochores and delay anaphase onset, as described in Chapter 4. Next, we wanted to test whether Mad2 was recruited to immaturely-attached (or not-unattached) kinetochores in the absence of Bub1 in otherwise unperturbed cells. These attachments occur during prometaphase in hTERT-RPE1 cells as most kinetochores are rapidly attached to spindle microtubules and biorientated (Sikirzhytski *et al.*, 2018). As described in Chapter 3, Mad2 levels were reduced by ~80% in prometaphase Bub1$^{1-23}$ cells compared to parental cells. This could be considered a surprisingly result, as the two-pathway model implies that cells depleted of Bub1 should not be able to respond to immature attachments after the

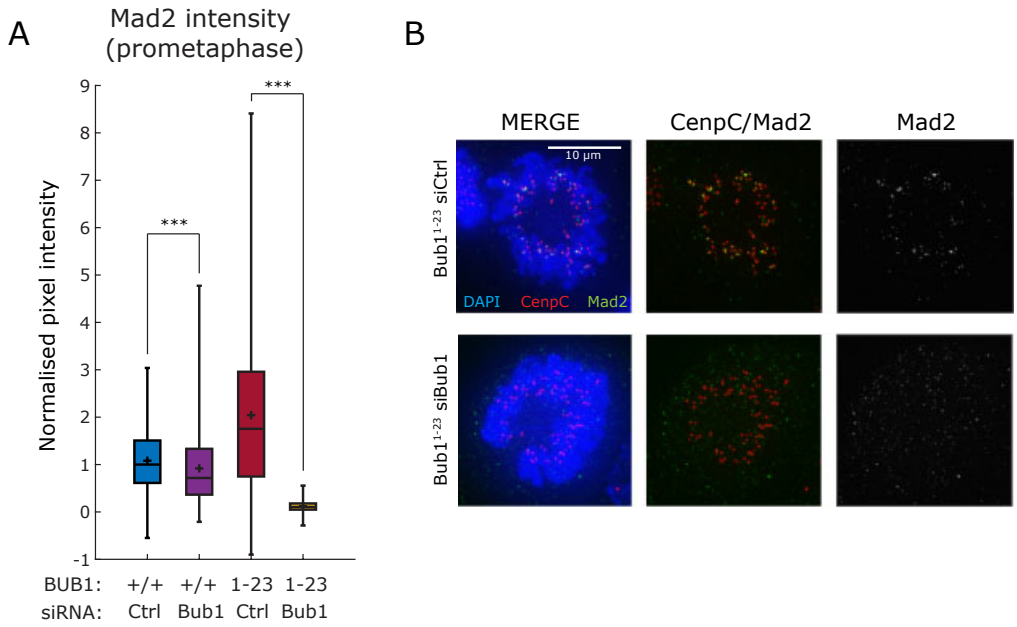

Figure 25: 'Zombie' Bub1 is required for Mad2 recruitment to kinetochores in prometaphase. A) Quantification of kinetochore bound Mad2 in parental and Bub1$^{1-23}$ cells treated with control or Bub1 siRNA and imaged in prometaphase. Mad2 intensity was normalised to respective CenpC intensity, and all conditions are normalised to the median value of the parental control. P value from a Mann Whitney U test. Data from one experiment, >600 kinetochores. B) Representative images from the analysis in A).

RZZ/Mad1:Mad2 complex is stripped following initial microtubule capture. We therefore wanted to test Mad2 recruitment during prometaphase in the absence of 'zombie' Bub1.

To do this, parental and Bub1$^{1-23}$ cells were treated with control or Bub1 RNAi and stained with anti-Mad2 antibodies. By selecting cells fixed during early prometaphase we found that, upon the removal of 'zombie' Bub1 in Bub1$^{1-23}$ cells, Mad2 was recruited kinetochores in early prometaphase cells to 10% of the levels in parental cells treated with control RNAi (Figure 25A,B). This reduction in Mad2 recruitment was not due to a kinetochore structure that does not allow binding of Mad2, as it was recruited efficiently to unattached kinetochores in the presence of nocodazole (Chapter 4). Importantly Mad2 was detectable at prometaphase kinetochores in Bub1$^{1-23}$ cells treated with a control siRNA (Figure 25A), suggesting that 'zombie' Bub1 is functional at kinetochores in early prometaphase Bub1$^{1-23}$ cells and responsible for recruiting a residual amount of Mad2.

5.3 Bub1 depletion causes an acceleration in unperturbed mitosis

As Mad2 loading was perturbed at immaturely-attached, early prometaphase kinetochores in Bub1$^{1-23}$ cells in the absence of 'zombie' Bub1, we wanted to see if this had an effect on mitotic progression. To do this we transfected a control and Bub1 siRNA into parental and Bub1$^{1-23}$ cells, then performed live cell imaging to observe unperturbed mitosis using SiR-DNA. The majority of Bub1$^{1-23}$ cells depleted of 'zombie' Bub1 completed NEB to anaphase in ~24 mins with no defects, comparable with control cells. However, 33% of cells were observed to enter anaphase very rapidly (18 mins or less), some cells in as fast as 12 mins (Figure 26A). Furthermore, 20% of cells performed anaphase before congressing all chromosomes to the metaphase plate, with no delay in mitotic timing. (Figure 26B, C). A third of these cells with uncongressed chromosomes displayed lagging chromosomes at anaphase, suggesting that the SAC had been switched off prematurely before the correct attachment state could be reached. These

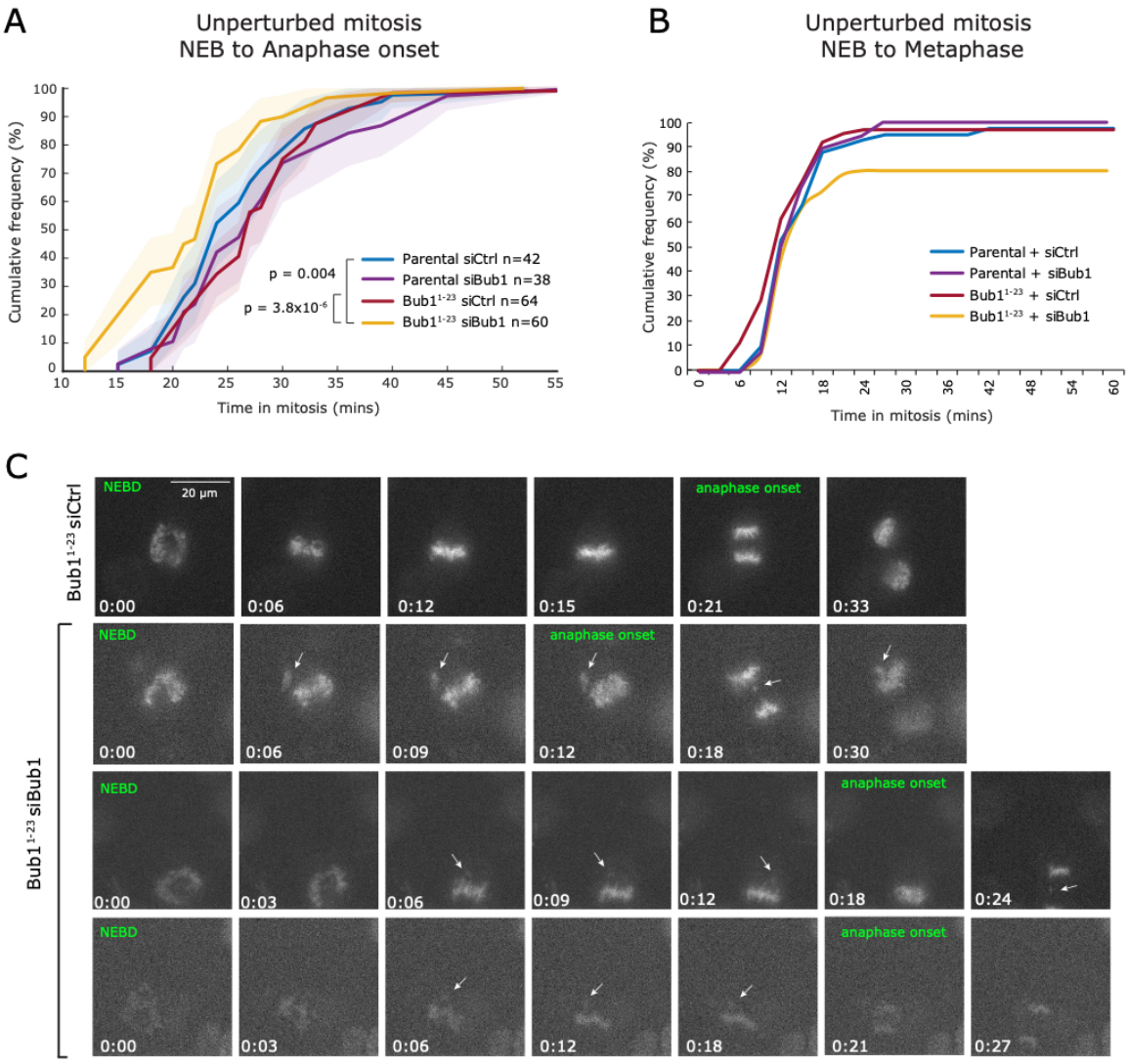

Figure 26: Bub1 depletion causes acceleration in unperturbed mitosis. A) Time spent in mitosis from NEBD to anaphase of parental and Bub1$^{1\text{-}23}$ cells treated with control or Bub1 RNAi. Cells were treated with SiR-DNA (to visualise DNA), and filmed for 12 hr. Data pooled from 3 independent experiments, shaded area represents 95% confidence interval. P values from a Wilcoxon rank sum test comparing Bub1$^{1\text{-}23}$ siBub1 and parental siCtrl treated cells, and Bub1$^{1\text{-}23}$ siBub1 and Bub1$^{1\text{-}23}$ siCtrl treated cells. B) Same as A), except data shows time spent in mitosis from NEBD to alignment on the metaphase plate. C) Movie stills from live cell imaging used for the analysis in A) and B). Arrow points to uncongressed chromosomes. Time in hours:mins.

observations point to SAC failure rather than an alignment defect, as the majority of Bub1$^{1-23}$ + siBub1 cells successfully congressed all chromosomes to the metaphase plate before entering anaphase in ~24 mins. This acceleration phenotype is reminiscent of that reported in HeLa cells following Mad2 or BubR1 RNAi, where cells are observed to accelerate through anaphase in ~12 mins with increased segregation errors (Meraldi, Draviam and Sorger, 2004). Moreover, it was also observed when the NPC pool of Mad1 was disrupted in hTERT-RPE1 cells (Rodriguez-Bravo *et al.*, 2014).

5.4 Bub1 contributes to Mad2 localisation at the nuclear envelope

We wanted to further investigate the acceleration phenotype seen in Bub1$^{1-23}$ cells following depletion of 'zombie' Bub1. As this phenotype is consistent with that seen following disruption of the NPC pool of Mad1:Mad2 in interphase hTERT-RPE1 cells, we wanted to see whether Mad2 recruitment to the NPC was affected

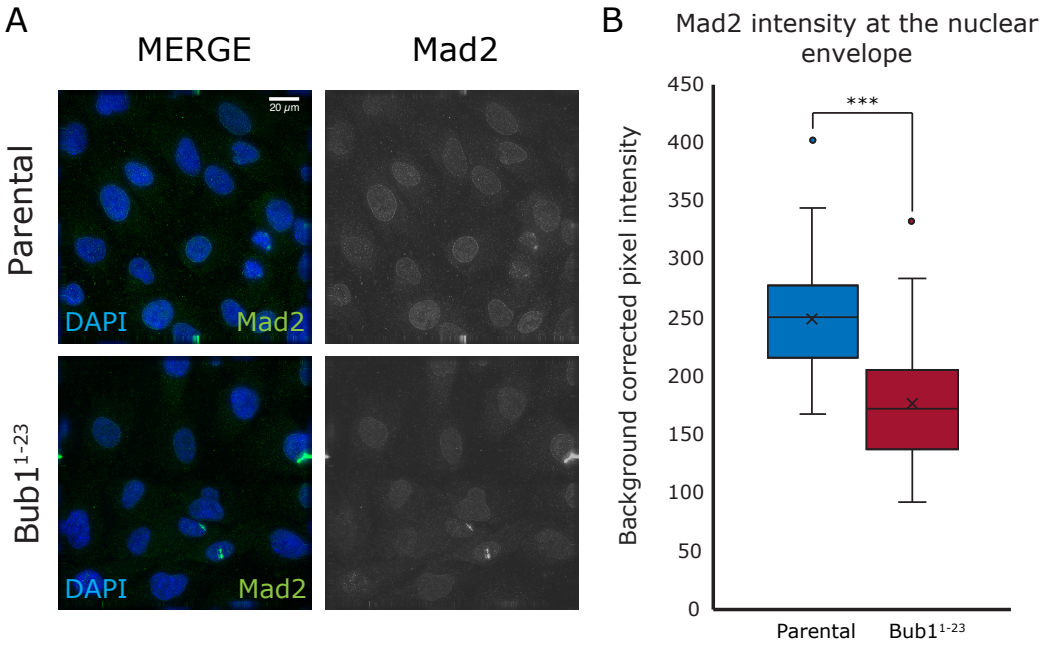

Figure 27: Bub1 depletion causes a reduction in Mad2 at the nuclear envelope. A) Representative images from parental and Bub1$^{1-23}$ cells in interphase stained with DAPI and anti-Mad2 antibodies. B) Analysis of background corrected Mad2 intensity at the nuclear envelope in parental and Bub1$^{1-23}$ cells, Data from one experiment, n = 50 cells. P value from a Mann Whitney U test.

in the absence of Bub1 (Rodriguez-Bravo *et al.*, 2014). To do this, we fixed and immunostained parental and Bub1$^{1-23}$ cells with Mad2 antibodies and DAPI. Mad2 was seen localising to the nuclear envelope in parental interphase cells, however, in Bub1$^{1-23}$ cells the nuclear envelope staining of Mad2 was decreased by around 30% (Figure 27 A, B). It is important to note here that the Mad2 foci visible are an artefact of antibodies accumulating inside a furrow that runs through the nucleus. This was seen to occur in all cells in all conditions (data not shown). Bub1$^{1-23}$ cells do not accelerate through unperturbed mitosis, so this decrease is not enough to cause any phenotype. Unfortunately, the antibody used to visualise Mad2 at NPCs is no longer available from the commercial supplier. Therefore at this time we cannot test the effects of depleting 'zombie' Bub1 on Mad2 NPC localisation, although we suspect the effect would be more penetrant. However this result does suggest that Mad1:Mad2 recruitment to the NPC is perturbed in the absence of Bub1. This could explain the acceleration phenotype observed during live cell imaging of Bub1$^{1-23}$ cells depleted of 'zombie' Bub1.

5.5 Bub1 depletion causes loss of Tpr from the nuclear envelope

Tpr is a nucleoporin which localises at the nucleoplasmic side of the nuclear pore, within the nuclear basket of the pore complex. Tpr is known to directly bind Mad1 and Mad2 for their recruitment to NPCs (Lee *et al.*, 2008). Tpr has been implicated in interphase APC/C inhibition, as deletion of the Tpr-binding region on Mad1 causes cells to accelerate through unperturbed mitosis (Rodriguez-Bravo *et al.*, 2014). This acceleration phenotype was attributed to defects in interphase MCC assembly, which caused insufficient APC/C inhibition leading to premature anaphase onset. Therefore we decided to further investigate the reduction of Mad2 staining at the nuclear envelope in Bub1$^{1-23}$ cells by testing levels of Tpr in the absence of Bub1.

To do this, we treated parental or Bub1$^{1-23}$ cells with control or Bub1 RNAi, then fixed and immunostained using anti-Tpr antibodies and DAPI (Figure 28A).

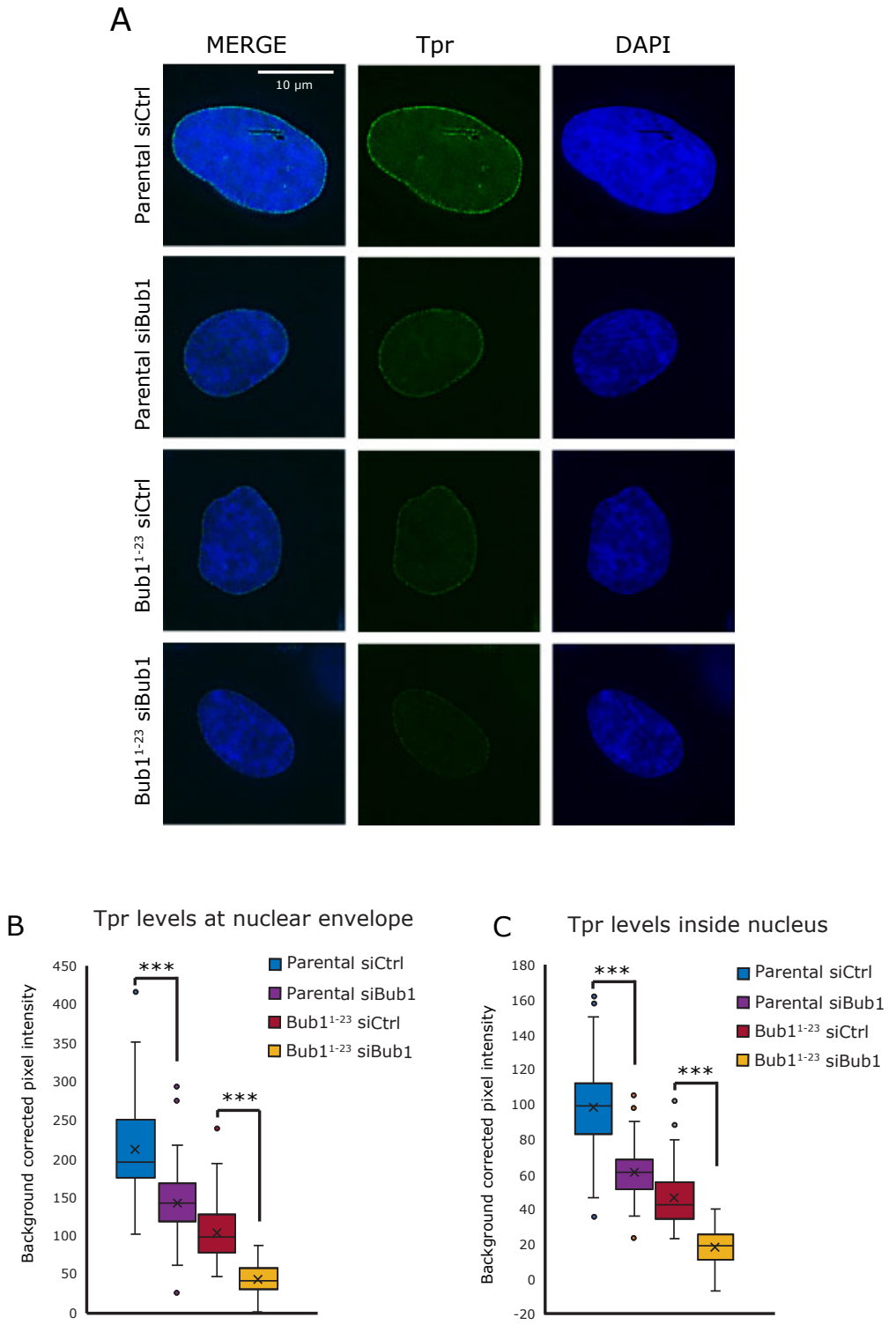

Figure 28: Bub1 depletion affects Tpr levels at nuclear pores. A) Representative images from parental and Bub1$^{1-23}$ cells in interphase treated with either control or Bub1 RNAi, stained with DAPI and anti-Tpr antibodies. B) Analysis of Tpr levels at the nuclear envelope in parental and Bub1$^{1-23}$ cells treated with control or Bub1 RNAi. Data pooled from two independent experiments, n = 20 cells. P value from a Mann Whitney U test. C) Analysis of TPR levels in the nucleus in parental and Bub1$^{1-23}$ cells treated with control or Bub1 RNAi. Data pooled from two independent experiments, n = 20 cells. P value from a Mann Whitney U test.

Interphase cells were imaged and pixel intensities at the nuclear envelope were analysed manually. To our surprise, we found that Tpr was lost from the nuclear envelope in a clear Bub1-dependant manner (Figure 28B). Tpr was reduced to 20% of control levels at the nuclear envelope in Bub1$^{1-23}$ cells treated with siBub1. We then quantified Tpr levels inside the nucleus and found that Tpr was also decreased here to 19% of control levels in Bub1$^{1-23}$ cells treated with siBub1 (Figure 28C). This effect of Bub1 loss on Tpr was not due to adaption of cells to CRISPR targeting of Bub1 or off-target effects, as Tpr was reduced in parental cells treated with Bub1 RNAi by 25%.

We have therefore found that Bub1 appears to exert an influence on Tpr levels at the nuclear envelope in cells during interphase. From these data we may extrapolate that Mad2 is further reduced at the nuclear envelope in Bub1$^{1-23}$ cells depleted of 'zombie' Bub1 as Tpr levels in these cells were lower than Bub1$^{1-23}$ cells treated with control RNAi. This result also suggests that 'zombie' Bub1 is also present and functional during interphase, and may contribute to the localisation of Tpr.

5.6 CenpF also contributes to Tpr localisation at the nuclear envelope

CenpF, a binding partner of Bub1 during mitosis, is known to accumulate in the nucleus during interphase with levels peaking at G2. CenpF then becomes targeted to the nuclear envelope at the G2/M transition before binding to unattached kinetochores following NEBD (Bolhy *et al.*, 2011). Here CenpF is thought to contribute to the tethering of centrosomes to the nuclear envelope during prophase, facilitated by its interaction with dynein. As CenpF is a known binding partner of Bub1 that localises to the nuclear envelope, we therefore wanted to test whether CenpF depletion had any effect on Tpr levels at the nuclear envelope during interphase.

To do this, we depleted CenpF using siRNA in RPE1 cells. We first confirmed that the CenpF RNAi was effective by treating cells with control

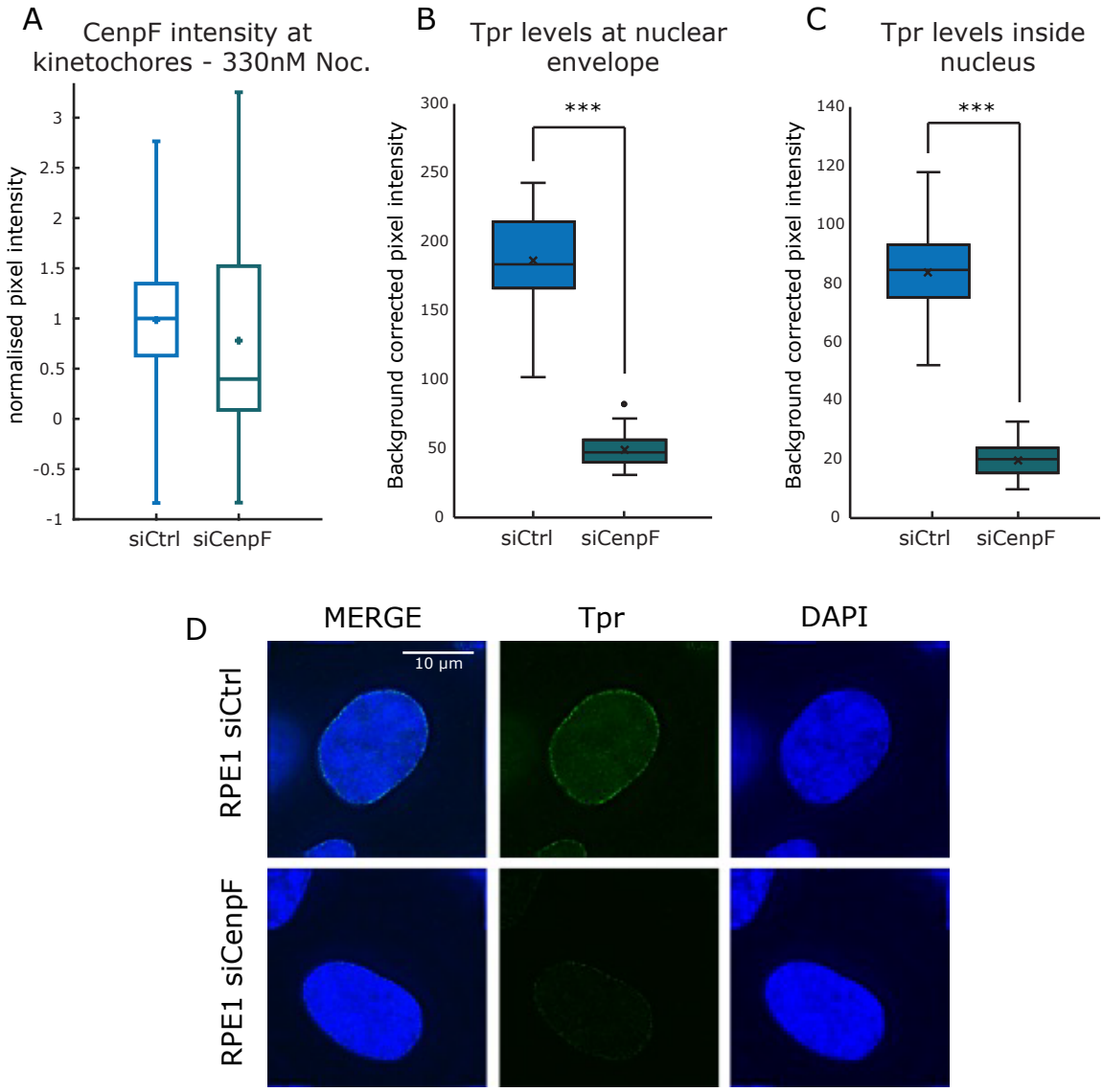

Figure 29: CenpF depletion affects Tpr at nuclear pores. A) Analysis of CenpF intensity at kinetochores in RPE1 cells treated with control or CenpF RNAi and 330nM nocodazole to confirm that the siRNA was working. Data from one experiment, n > 600 kinetochores. B) Analysis of TPR levels at the nuclear envelope in parental cells treated with control or CenpF RNAi. Data from one experiment, n = 10 cells. P value from a Mann Whitney U test. C) Analysis of TPR levels in the nucleus in parental cells treated with control or CenpF RNAi. Data from one independent experiments, n = 10 cells. P value from a Mann Whitney U test. D) Representative images from parental cells in interphase treated with either control or CenpF RNAi, stained with DAPI and anti-Tpr antibodies.

and CenpF oligos, and arresting in 330 nM nocodazole for 16hr to enrich CenpF kinetochore recruitment. We then measured CenpF intensity at kinetochores, normalised to the respective values of CenpC. CenpF RNAi was effective in 60% of these cells, as seen by a decrease in CenpF staining, however 40% remained unaffected (Figure 29A). We did not check in our cells whether depleting CenpF affected levels of Bub1, however is reported that CenpF siRNA has no effect on Bub1 in DLD1 cells (Johnson *et al.*, 2004).

Nevertheless, we performed a separate experiment to measure Tpr levels in interphase RPE1 cells depleted of CenpF. Surprisingly we found that Tpr was reduced to 25% of control levels at the nuclear envelope and 23% inside the nucleus following CenpF depletion (Figure 29B,C,D). This was comparable with the Tpr levels seen in Bub1$^{1-23}$ cells treated with siBub1 (Figure 28B.C), which is surprising as the CenpF RNAi was only 60% effective. We also did not select for late G2 cells, where CenpF is known to accumulate at the nuclear envelope. This may suggest that CenpF plays a more important role than Bub1 in Tpr regulation, and any perturbations to CenpF function during the cell cycle result in loss of Tpr at the nuclear pore.

5.7 Bub1 is expressed in interphase hTERT-RPE1 cells

The loss of Tpr and Mad2 from the nuclear envelope of interphase cells, along with the acceleration phenotype of unperturbed mitosis, suggests a premitotic role for Bub1. Bub1 has been shown to be expressed during interphase of *Xenopus* egg extract, where it is in a complex with Bub3 (Sharp-Baker and Chen, 2001). We wanted to confirm expression of interphase Bub1 in our hTERT-RPE1 cell lines. To do this, we fixed and stained parental and Bub1$^{1-23}$ cells with an antibody against the N terminus of Bub1. We could detect a weak signal in interphase parental cells using this antibody that seemed to be both nuclear and cytoplasmic,

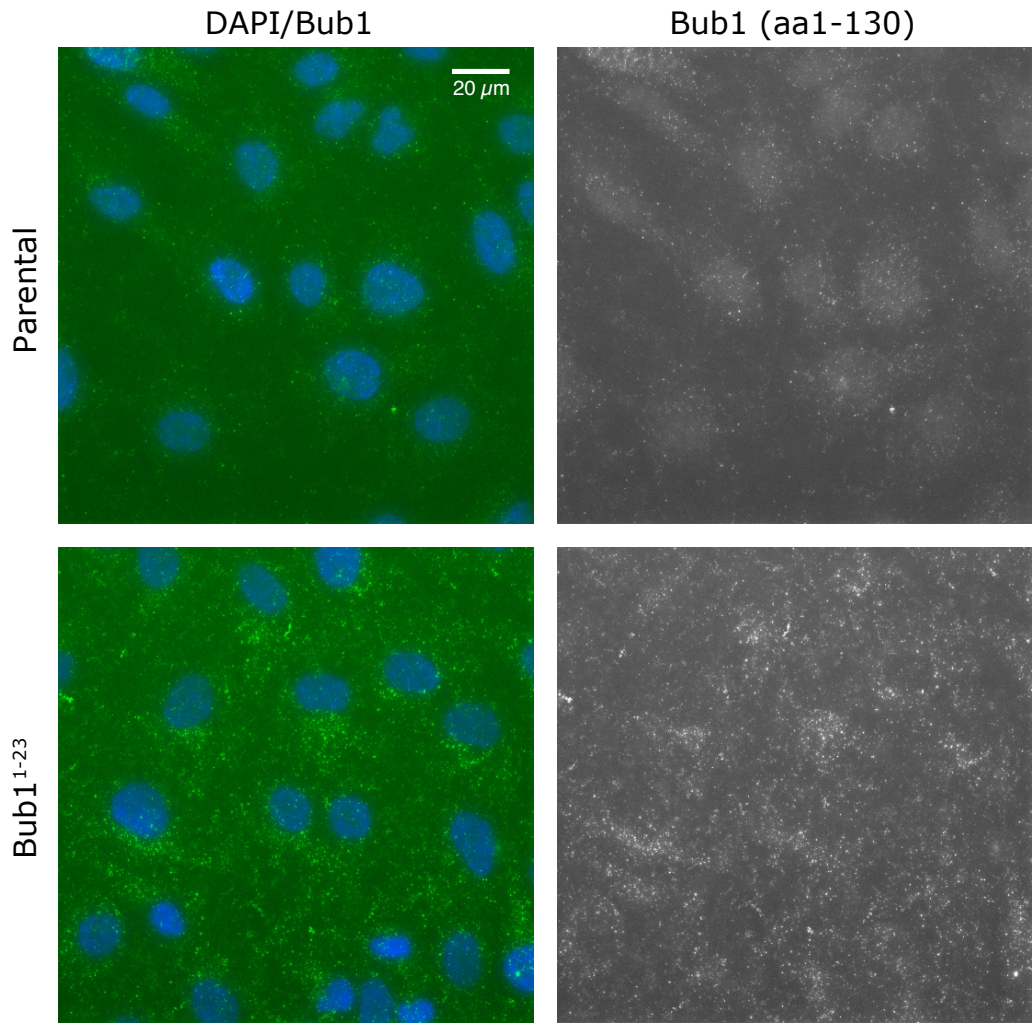

Figure 30: Bub1 is expressed in the nucleus and cytoplasm of interphase RPE1 cells. A) Representative images of fixed parental and Bub1$^{1-23}$ cells stained with DAPI to visualise nuclei and a Bub1 antibody recognising aa 1-130. Bub1 is no longer detectable in interphase Bub1$^{1-23}$ cells.

but did not show localisation to the nuclear envelope, however we did not select for cells in specific stages of the cell cycle (Figure 6). This staining was not present in Bub1$^{1-23}$ cells. We therefore suggest that Bub1 is expressed during interphase in hTERT-RPE1 cells.

5.8 Conclusions

In this chapter, we have presented preliminary evidence to show that, while not essential for SAC activation at unattached kinetochores, Bub1 plays an important

role in unperturbed mitosis. We suggest this is at least partially through a novel, premitotic role of Bub1. We have shown that that when Bub1$^{1-23}$ cells were treated with Bub1 RNAi to remove the residual pool of 'zombie' Bub1, cells could accelerate through unperturbed mitosis in as fast as 12 mins. We also observed cells that recruited no visible Mad2 to prematurely attached kinetochores in Bub1$^{1-23}$ cells depleted of 'zombie' Bub1. These results prompted us to consider the possibility that Bub1 could play a role in interphase APC/C inhibition, as cells are reported to accelerate through mitosis in ~12 mins when this pathway is perturbed (Meraldi, Draviam and Sorger, 2004; Rodriguez-Bravo *et al.*, 2014).

Consistent with a role for Bub1 during interphase, we observed a decrease in Mad2 at the nuclear envelope in Bub1$^{1-23}$ cells. Unexpectedly, we further observed a strong correlation between the levels of Tpr, the nucleoporin to which Mad1:Mad2 complexes bind at the NPC, and Bub1. Furthermore, we found that upon CenpF depletion, Tpr was again significantly reduced at the nuclear envelope. We do not know whether the number of nuclear pores is affected in the absence of Bub1 or CenpF, or whether this is a specific effect on Tpr only. However, depletion of Tpr using RNAi did not cause nuclear pore disassembly in a previous study, therefore Tpr itself is not required for NPC assembly in RPE1 cells (Rodriguez-Bravo *et al.*, 2014). This result, combined with our data, suggests that Bub1 and CenpF could directly regulate Tpr itself, rather than nuclear pore assembly, however this needs to be properly investigated. This novel effect on Tpr appears to be important for accurate mitosis, as cells were seen to accelerate from NEBD to anaphase with uncongressed and lagging chromosomes when this regulation was perturbed by depleting Bub1.

Further work is needed to firstly confirm, then elucidate a mechanism for Tpr regulation by Bub1 and CenpF and establish whether any other mitotic or nuclear pore proteins are involved. We cannot draw conclusions as to whether Bub1 plays a role in the catalysis of interphase MCC, or simply contributes to localisation of Mad1:Mad2 complexes to the nuclear envelope to allow their rapid recruitment to unattached kinetochores. It could also be that Bub1 itself is shuttled through the

nuclear pore, and this has a specific function. However, this finding may improve understanding of the mechanisms by which the APC/C is inhibited during interphase. Either way, this is a new role for Bub1 that has not been described previously.

Chapter 6: Discussion

6.1 Summary of findings

Overall in this thesis we have further defined the role of Bub1 during mitosis in human diploid cells. This has been a topic of debate in the literature over many years and the data presented here has helped to provide clarity, at least for the situation in RPE1 cells. We originally aimed to use CRISPR-Cas9 to produce a gene edited 'knockout' hTERT-RPE1 cell line, which silences Bub1 expression at the endogenous locus. This approach would overcome the limitations of siRNA studies where a few Bub1 molecules may remain and support SAC signalling, making interpretation of data difficult. We were able to make and verify this cell line, however further work from the Nilsson laboratory using mass spectrometry identified residual Bub1 peptides, concluding it was not a true knockout. We then addressed this major caveat by repeating key experiments in the presence of Bub1 siRNA to deplete any residual Bub1 and made three major findings: (1) Bub1 is not essential for the SAC response at unattached kinetochores, (2) Bub1 is required for correct mitotic timing in unperturbed mitosis and (3) Bub1 has a undefined premitotic role affecting the nuclear envelope which contributes to SAC signalling. Taken together these findings provide further evidence that SAC signalling can function independently through the KNL1-Bub1-Bub3 (KBB) and Rod-Zwilch-ZW10 (RZZ) pathways at unattached kinetochores in human cells. We suggest the same is true for all higher organisms in which the RZZ complex is conserved. This is in contrast to yeast, in which RZZ is not conserved and Bub1 is essential for SAC signalling. We also propose a new role for Bub1 during interphase.

It is important, however, to note a number of caveats to this work. Firstly, the use of CRISPR-Cas9 is not as straight-forward as previously thought, and while the cell line described in this thesis was validated to the gold standard of the time, residual Bub1 expression was able to go undetected by our methods. We would agree that the new gold standard for screening knockout cell lines should be to

perform mass spectrometry to identify any residual peptides of the targeted protein. However, it is difficult to prove a negative result even using these methods. Secondly, the use of siRNA in a CRISPR cell line to further deplete the protein is not ideal as we cannot be completely sure that all peptides are removed, although from results obtained in this study it appears that Bub1 is depleted below a functional level in Bub1$^{1-23}$ cells when treated with Bub1 siRNA, discussed in section 6.3. We also cannot be sure that off target effects are not occurring as a result of the siRNA, despite careful selection of oligo sequences. Rescue experiments should be performed to control for this, however overexpression of Bub1 is known to cause mitotic defects due to Aurora B kinase hyperactivation (Ricke, Jeganathan and van Deursen, 2011). Therefore levels of Bub1 would have to be tightly controlled, and it would be preferable to perform an endogenous rescue however this would mean a second round of CRISPR targeting.

6.2 Bub1 CRISPR targeted clones regain 'zombie' Bub1 protein expression

We wanted to investigate how the residual 'zombie' Bub1 protein had become re-expressed to avoid this happening in the future. A collaborative publication from the Jallepalli and Cheeseman labs found that *BUB1* disruption is often overcome by nonsense-associated alternative splicing (NAS), which results in exon skipping leading to truncated transcripts as seen in RT-PCR. However, when we tested for the presence of truncated transcripts, they were not seen in Bub1$^{1-23}$ cells (Figure 17A). We therefore decided to run the mutated Bub1$^{1-23}$ sequence through a translate tool (https://web.expasy.org/translate/) to search for any open reading frames which could allow reinitiation of translation. Surprisingly, we found an cryptic open reading frame (ORF) which allows in-frame expression of Bub1 following the single base pair insertion in exon 2 resulting from CRISPR-Cas9 targeting (Figure 31). This sequence lacks the first 5 amino acids of Bub1, then

Figure 31: Cryptic open reading frame initiated in Bub1$^{1-23}$ cells. Translate tool analysis showed presence of a cryptic open reading frame induced by the Cas9-induced single base pair insertion in Bub1$^{1-23}$ cells. This open reading frame does not express the first 5 amino acids of Bub1, then expressed 17 mutant amino acids before being shifted into the correct reading frame by the single base insertion.

expresses 17 mutant amino acids before being frame shifted into the correct reading frame by the singe base pair insertion. This ORF leads to expression of a N-terminus mutant of Bub1, explaining why it was undetectable with the antibody recognising amino acids 1-130, that otherwise retains all functions. The N-terminus region of Bub1 contains TPR repeats, which are implicated in KNL1-binding (Krenn *et al.*, 2012). However, this region is not essential for kinetochore localisation of Bub1 as this is mediated through the Bub3-binding domain (Taylor, Ha and McKeon, 1998; Krenn *et al.*, 2012). This mutant form of Bub1 will therefore be recruited to kinetochores, which was confirmed in Chapter 4 using an antibody recognising amino acids 336-489 (Figure 17C, D). We conclude that the insertion of a single base pair allowed reinitiation of translation from a cryptic start site within the N-terminus of Bub1, allowing amino acids 23 -1085 to be expressed at very low levels. The most puzzling factor here is that BubR1 was not seen to localise to kinetochores in Bub1$^{1-23}$ cells, whereas this hypothesis implies

that it should be recruited at low levels. It is possible that the antibody epitope on BubR1 is masked when binding to 'zombie' Bub1, which would allow it to go undetected.

The phenomenon of induced cryptic start codons is termed nonsense mutation-dependant reinitiation of translation. A recent publication investigating N-terminus mutants of p53 found that reinitiation can stabilise transcripts that contain premature stop codons, allowing them to evade the nonsense mediated decay pathway (Cohen *et al.*, 2019). This phenomenon was observed in HEK293T and HCT116 cell lines, and now hTERT-RPE1 cells in this study, suggesting it is a prevalent mechanism which can overcome CRISPR-Cas9 targeting. This must be taken into account when generating future knockout cell lines by targeting CRISPR-Cas9 at the N-terminus.

6.3 Bub1 is depleted to below functional levels in this study

As previously discussed, the Nilsson laboratory identified residual Bub1 expression in three Bub1 'knockout' RPE, HAP1 and HeLa cell lines which contributed to SAC signalling (Zhang *et al.*, 2019). To address this, they used Bub1 siRNA in the Bub1 'knockout' cell lines to deplete the residual 'zombie' Bub1. Nevertheless authors stated they could not rule out the possibility that undetectable amounts of Bub1 remained in Bub1 CRISPR + siRNA cell lines, and this could be responsible for the reduced but still apparent delay in mitotic exit seen in Bub1 CRISPR + siRNA cells when treated with nocodazole. However, this is unlikely seeing as the delay was abolished when Rod was depleted by siRNA, suggesting it is solely dependent on the RZZ pathway. We make the assumption here that RZZ is capable of producing MCC in the absence of Bub1 – this is yet to be shown.

While it could be formally possible that an even smaller amount of Bub1 protein remains in Bub1$^{1\text{-}23}$ cells following Bub1 siRNA, we argue that, even if present, it

is reduced below the threshold required for KBB mediated SAC signalling in the majority of cells because we see a penetrant defect in these cells undergoing unperturbed mitosis (Figure 26). Some Bub1$^{1-23}$ cells accelerated through an unperturbed mitosis following Bub siRNA treatment, which means not enough MCC is being produced to sufficiently inhibit the APC/C and delay anaphase onset. Not all Bub1$^{1-23}$ cells displayed the acceleration phenotype, but this could be due to the stochastic nature of unperturbed mitosis rather than Bub1 levels. Some cells depleted of Bub1 may enter prometaphase with an unattached kinetochore, and we have shown that this is sufficient to produce enough MCC to delay anaphase onset in the absence of Bub1 (Figure 20, Figure 21). We argue that if Bub1 is not expressed at sufficient levels to support SAC signalling in unperturbed mitosis, it is unlikely to support signalling in the presence of nocodazole, and SAC activation here must be due to a Bub1-independant pathway. There is variation in the duration of Bub1$^{1-23}$ + Bub1 siRNA cells arresting in nocodazole which could be due to variation in depletion levels of 'zombie' Bub1, however the fastest cell exits mitosis in 130 mins or 2.1 hours, which is still a 5-fold delay compared to unperturbed mitosis. We therefore conclude that the delay seen in the presence of nocodazole in Bub1$^{1-23}$ cells is likely a result of signalling through the RZZ pathway of SAC activation. We assume that this arrest would be abolished if RZZ components were depleted simultaneously, but have not tested this ourselves. However this has been confirmed by the Nilsson lab (Zhang *et al.*, 2019). The acceleration phenotype seen in unperturbed mitosis further suggests that Bub1 is required to either produce MCC at immaturely attached kinetochores, or is involved in the production of premitotic MCC which defines the minimum length of mitosis. These possibilities are discussed in section 6.8 and 6.9. The disproportionate contribution of 'zombie' Bub1 to SAC signalling suggests Bub1 is functioning stoichiometrically, the possibility of which will be discussed in more detail during section 6.5.

6.4 Bub1 is not essential for the SAC response at unattached kinetochores in human cells

As presented in Chapter 3, we first generated a hTERT-RPE1 clonal cell line in which the *BUB1* gene was 'knocked out' using CRISPR-Cas9. Original data obtained using this cell line to investigate SAC signalling was consistent with a separate, parallel study from the Medema Lab using HAP1 cells (Raaijmakers *et al.*, 2018). In that study, Bub1 was identified as being synthetic lethal upon loss of the checkpoint, suggesting it is more important for regulating chromosome alignment and only plays a minor role in the SAC. Loss of Bub1 had no effect on nocodazole arrest in HAP1 cells, completely in line with our data in RPE1 cells. However, these Δ*BUB1* HAP1 cells had major chromosome alignment defects in unperturbed mitosis. Δ*BUB1* HeLa cells also showed similar alignment defects in unperturbed mitosis, which resulted in extended an extended period of NEB to metaphase for both cell lines (Raaijmakers *et al.*, 2018; Zhang *et al.*, 2019). In contrast, we did not see such alignment defects in Bub1$^{1\text{-}23}$ cells, even when Bub1 was further depleted by siRNA (Figure 13, Figure 26). This could represent a difference in Bub1 function between diploid and aneuploid cell lines, where aneuploid cell lines may be more reliant on the Bub1 – pH2A-T120 – Sgo1 axis for Aurora B mediated error correction.

To address the caveat of residual 'zombie' Bub1 being expressed in Bub1$^{1\text{-}23}$ cells, we repeated the key experiments reported in Currie *et al.*, 2018 to test SAC activity in the presence of Bub1 siRNA. Work from the Nilsson lab showed that 'zombie' Bub1 contributed to SAC signalling in Bub1$^{1\text{-}23}$ cells as mitotic arrest in 100 nM nocodazole was reduced upon treatment with Bub1 siRNA (Zhang *et al.*, 2019). We found that Bub1$^{1\text{-}23}$ cells depleted of 'zombie' Bub1 could arrest in 330 nM nocodazole for a median of 420 mins or 7 hours, which is a reduction of 10 hours when compared to Bub1$^{1\text{-}23}$ cells treated with control siRNA, but still a 16-fold increase in the length of mitosis compared to unperturbed cells (Figure 19). Furthermore, Mad2 was recruited to these kinetochores, confirming that the SAC

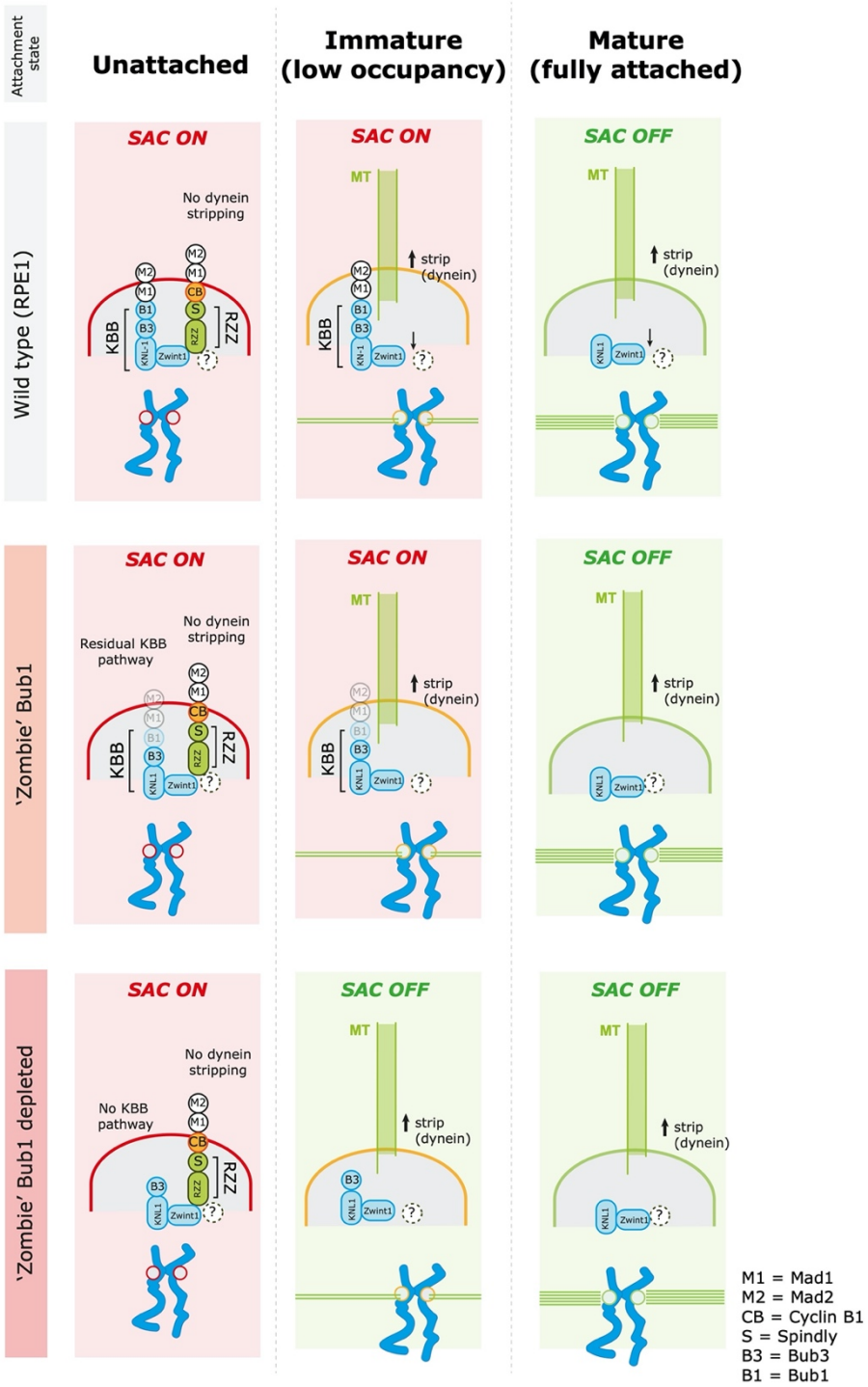

Figure 32: Model for SAC signalling at human kinetochores through the KBB and RZZ pathways. Wild type cells load Mad1:Mad2 complexes to unattached kinetochores through both the KBB and RZZ pathways. When a microtubule binds, Mad1:Mad2 bound through the RZZ pathway is stripped away along the microtubule via dynein (immature attachment). When the attachment matures, the KBB pathway stops signalling and the SAC is switched off. 'Zombie' Bub1 reduces the amount of Mad1:Mad2 loaded to the KBB arm, and the SAC is still functional at immaturely attached and unattached kinetochores. When 'zombie' Bub1 is depleted, the kinetochore can no longer recognise immature attachments and the SAC is prematurely silenced, however can still be activated at unattached kinetochores through RZZ. Figure adapted from Silió *et al*, 2015.

was activated in the absence of Bub1 (Figure 20). We have also expanded on the data presented in Zhang *et al*, 2019 by showing that Bub1$^{1-23}$ cells depleted of 'zombie' Bub1 can recruit Mad2 to a single unattached kinetochore and this is sufficient to delay anaphase onset (Figure 21). The effect of 'zombie' Bub1 depletion was not as dramatic as the Nilsson paper suggests, where they saw Bub1$^{1-23}$ cells exiting mitosis in as little as 90 mins when Bub1 siRNA was used. Crucially, 90 mins still represents a three-fold increase in the duration of unperturbed mitosis (24 mins) which shows the SAC has been activated to delay mitotic exit. Interestingly, the siRNA oligo used for this experiment has a predicted off target of Spindly, the dynein adaptor that binds the RZZ complex, with 68% coverage and 100% identity (data not shown). It is also important to note that the Nilsson experiments were done in the presence of 100 nM nocodazole. Microtubules are still present at this dosage, although a mitotic spindle cannot form (Images in Silió, McAinsh and Millar, 2015). This situation may sensitise SAC signalling if these microtubules bind kinetochores as dynein-dependant stripping along microtubules is thought to facilitate RZZ:Mad1:Mad2 removal. Another important difference is that in the Nilsson laboratory publication, Bub1$^{1-23}$ RPE1 cells were subject to two siRNA treatments and synchronisation with thymidine (S-phase arrest) over a period of 48 hours, with the second siRNA and thymidine block performed 24 hours before filming (Zhang *et al*., 2019). Authors suggested this protocol was necessary to obtain full depletion of 'zombie' Bub1. However in our experiments cells were not synchronised and received one siRNA treatment, and 'zombie' Bub1 depletion was efficient. In our hands, hTERT-RPE1 cells are sensitive to transfections and we worry that cells could become unhappy following the Nilsson lab double siRNA and synchronisation protocol. This difference in protocols could contribute to the varying results seen between this thesis and the Nilsson laboratory data, if Nilsson's cells were indeed unhappy.

Overall, we conclude that Bub1 is not essential for the SAC response at unattached kinetochores in human diploid cells, where SAC signalling can be activated by the RZZ complex. A model for this is described in Figure 32.

6.5 A catalytic role for Bub1 in MCC production?

The phenomenon of very small amounts of Bub1 supporting SAC signalling in a substoichiometric manner is perhaps not surprising given that previous siRNA studies have shown Bub1 can function at very low levels. It was reported that 99.5% depletion of Bub1 (compared to wild type levels) was necessary to abolish SAC signalling in HeLa cells (Meraldi and Sorger, 2005), while 98% depletion preserved SAC activity (Johnson *et al.*, 2004). Mass spectrometry analysis allowed the Nilsson lab to estimate that Bub1 is expressed at 8% of wild type levels in $Bub1^{1\text{-}23}$ cells, however our western blot analysis suggests it may be less than this. Either way, the SAC response produced is disproportionate to the amount of Bub1 present in the cell and suggests a catalytic role. It is important to note here that Bub1 kinase activity is not thought to contribute to SAC signalling in a large body of literature (Sharp-Baker and Chen, 2001; Klebig, Korinth and Meraldi, 2009; Baron *et al.*, 2016; Raaijmakers *et al.*, 2018).

A catalytic role for Bub1 has been suggested previously in the literature. Bub1 is shown to recruit Plk1 to the kinetochore, which scaffolds Plk1-mediated phosphorylation of Cdc20 (Jia, Li and Yu, 2016). Bub1-Plk1 was shown to phosphorylate multiple sites on Cdc20 to directly inactivate APC/C^{Cdc20} in vitro, increasing the stabilisation of cyclin B1. This mechanism could act in parallel to MCC-mediated inhibition of APC/C. This potential catalytic role for Bub1 doesn't rely on its kinase activity as Bub1-Plk1 function is not Bub1-kinase dependant. We have shown indirect evidence for reduced Plk1 at kinetochores in $Bub1^{1\text{-}23}$ cells, as seen in the decreased BubR1 upshifted band present in MCC from $Bub1^{1\text{-}23}$ cells described in Chapter 3 (Figure). This upshift is thought to be due to phosphorylation by Plk1 (Elowe *et al.*, 2007). It is possible that 'zombie' Bub1 allows partial recruitment of Plk1, which phosphorylates a pool of Cdc20 to inhibit APC/C directly, and this is abolished once Bub1 is further depleted. However, the contribution of the Bub1-Plk1 pathway to APC/C inhibition and SAC signalling in human cells is unclear. 'Zombie' Bub1 plays a clear role in long term

maintenance of SAC signalling rather than the initial activation and authors investigating the role of Bub1-Plk1 at the kinetochore do not present any live cell imaging data showing the effect of disrupting this interaction on long term mitotic arrest. However they do propose that Bub1-Plk1 is required to inactive any free Cdc20 that is present during mitotic arrest (Jia, Li and Yu, 2016). This activity of Bub1-Plk1 could contribute to towards long term SAC maintenance.

A relevant study from the Musacchio lab aimed to reconstitute a near-complete SAC signalling system using purified components and monitor the formation of MCC in real time using Förster resonance energy transfer (FRET) sensors (Faesen *et al.*, 2017). They used this system to probe activators of MCC formation following Mad1-C-Mad2 assembly by examining the contribution of Bub1-Bub3 and Mps1 kinase. The combination of Mad1-C-Mad2, Bub1-Bub3 and Mps1 allowed the MCC formation reaction to mimic that reported to exist in cells. Removal of Mps1 resulted in a strong reduction in the rate of MCC formation, while removing Bub1-Bub3 had a large but less substantial effect. The addition of reversine (Mps1 kinase inhibitor) had substantial negative consequences for MCC formation while addition of BAY-320 (Bub1 kinase inhibitor) had a much milder effect. This suggests that Bub1 kinase activity makes a relatively small contribution to the catalytic activation of MCC. This result is consistent with our data, where it seems that Bub1 is not required for the initial formation of MCC but is needed for long term maintenance. In this extreme situation where high amounts of MCC are needed to be produced for a long period of time, the loss of Bub1 kinase activity may be enough to tip that balance towards SAC failure. Authors concluded that the contribution of Bub1 to MCC assembly appears to require interactions with Cdc20, and Bub1 kinase can mildly promote this interaction. This is mediated by the ABBA motifs on Bub1, which are known to bind Cdc20 (Di Fiore *et al.*, 2015). Bub1 is also known to phosphorylate Cdc20 itself, and this could enhance its affinity to other MCC components (Tang *et al.*, 2004). This could represent the mechanism by which Bub1 catalytic activity that promotes MCC formation.

Bub1 could be acting catalytically simply through its role as a scaffold protein to bring together the components to generate APC/C^{MCC}; C-Mad2, Bub3, BubR1 and Cdc20. It possesses sites which have been shown to recruit each of these proteins, as discussed in Chapter 1. Interestingly, one study implicated the checkpoint machinery in recruiting separate APC/C subunits to kinetochores in order to place them into close proximity with MCC and improve the efficiency of signalling (Acquaviva *et al.*, 2004). A dominant-negative mutant of Bub1 (amino acids 1-331), which was described as checkpoint defective, prevented kinetochore localisation of APC3, APC1 and APC10 in HeLa cells, suggesting that Bub1 or the KBB pathway may be implicated in APC/C recruitment to kinetochores as well as MCC generation. It is unknown whether this is a direct or indirect role of Bub1, but could represent a catalytic mechanism in the generation of APC/C^{MCC} by bringing them together at kinetochores. This may be supported by 'zombie' Bub1 and could greatly increase checkpoint activity if true.

6.6 The KBB and RZZ pathways are capable of separately activating the SAC at unattached kinetochores, but both are required for long term maintenance

The mitotic arrest of 420 mins in 330 nM nocodazole seen when 'zombie' Bub1 was depleted in Bub1$^{1-23}$ cells (Figure 19) is totally consistent with data shown in the report from the Jallepalli and Cheeseman labs. In that publication, two hTERT-RPE1 clones generated using inducible Cas9 and showing no in-frame BUB1 mRNA transcripts arrested for a median of ~400 min in the presence of 660 nM nocodazole (Rodriguez-Rodriguez *et al.*, 2018). The combination of these two results, obtained from independent labs, suggests that this represents the true contribution of Bub1 to SAC signalling at unattached kinetochores in RPE1 diploid, non-cancer cells. We assume the ~400 min delay in mitotic exit is a function of the RZZ pathway, as proposed in the two pathway model (Silió, McAinsh and Millar, 2015). The combination of these data suggest that Bub1 is

required for long term SAC maintenance and inhibition of APC/C, rather than the initial SAC activation step in the presence of unattached kinetochores.

The hypothesis that Bub1 is required for SAC maintenance is further supported by experiments in BUB1Δ/Δ mouse embryonic fibroblasts (MEFs) (Perera *et al.*, 2007). These cells were not able to delay mitotic exit in response to 100 μM monastrol, but data presented in the supplement showed they can arrest for ~1 hour longer than unperturbed cells in response to both 660 nM nocodazole and 10 μM taxol. This ~1 hour delay before mitotic exit suggests that APC/C^{Cdc20} is being initially inhibited by the activity of the SAC following NEBD, but this inhibition cannot be supported long term. It is unclear why cells do not behave in the same way in the presence of monastrol.

Consistently, experiments from the Nilsson laboratory showed that the ~100 minute nocodazole arrest in Bub1 CRISPR + siRNA treated HeLa cells is further shortened to 35 mins upon simultaneous depletion of Rod by siRNA, which represents total SAC failure (Zhang *et al.*, 2019). Rod is a major component of the RZZ complex, and removal this protein will likely result in dissolution of the complex and therefore the RZZ pathway of Mad1:Mad2 recruitment. This result strongly suggests that RZZ and KBB are capable of separable SAC activation, and inhibition of both pathways simultaneously is necessary for complete SAC failure following NEBD.

We propose that both the RZZ and the KBB pathways are capable of independently activating the SAC at unattached kinetochores in human cells, but both pathways are required for efficient long term SAC maintenance. Consistent with this, ΔROD HAP1 cells delay mitotic exit in response to 830 nM nocodazole for ~180 min, suggesting they can support initial SAC activation but not long term maintenance (Raaijmakers *et al.*, 2018). Interestingly, ΔROD HAP1 cells were more defective in SAC maintenance than ΔBUB1 HAP1 cells, which arrested for ~350 mins suggesting that the RZZ pathway may play a larger role in human SAC

signalling than the KBB pathway (Raaijmakers *et al.*, 2018). However, of course, these ΔBUB1 HAP1 cells were shown to express residual Bub1 which makes interpretation of these results problematic (Zhang *et al.*, 2019). Nevertheless, a full *BUB1* gene deletion created in HAP1 cells has further proved that Bub1 is dispensable for SAC signalling, with ΔBUB1 cells arresting for ~600 mins in nocodazole comparable with control cells (Medema Lab, personal correspondence). Furthermore, independent Rod, Zwilch and ZW10 HeLa clonal knockout cell lines all delayed mitotic exit in response to 660 nm nocodazole for ~250 mins, while RPE1 *BUB1*-disrupted clones expressing no in frame transcripts of Bub1 arrested for ~400 mins (Rodriguez-Rodriguez *et al.*, 2018). This result again suggests that the RZZ pathway may play a larger role in human SAC signalling than the KBB pathway, but both are necessary for long term maintenance.

6.7 Recent evidence for a second Mad1:Mad2 binding site in human kinetochores

Two recently published bioRXiv preprints have uncovered surprising new roles for Cyclin B1 in SAC signalling. In one study, Cyclin B1 was shown to bind to Mad1 at the nuclear pore complex (NPC) to coordinate NPC disassembly with kinetochore assembly (Jackman *et al.*, 2019, bioRXiv). The cyclin B1 interaction is proposed to be necessary for the correct release of Mad1 from Tpr at the nuclear pore, allowing it to be recruited onto unattached kinetochores to generate a robust SAC signal in early mitosis. This step may be important for initial SAC activation. The second study proposes a role for cyclin B1 in Mad1 kinetochore recruitment (Allan *et al.*, 2019, bioRXiv). Cyclin B1 binds to the N-terminus of Mad1 and recruits it to the corona, where its localisation becomes resistant to Mps1 activity upon corona extension as it is spatially removed from the outer kinetochore. Mad1 is ~66nm long, and the C-terminus is proposed to extend from the corona into the outer kinetochore and bind Bub1. Here Mad1 is phosphorylated by Mps1 to

bind and activate Mad2 and form MCC. This study provides a key insight into how SAC signalling is facilitated by the Bub1-independant pathway, however the binding site for cyclin B1 at the corona is unknown. The combination of these papers suggests that Cyclin B1 could be crucial for SAC activation by releasing Mad1:Mad2 from NPCs and recruiting it to the corona, where it can extend into the outer kinetochore interact with Bub1. These new papers, combined with the data presented in this thesis, provide compelling evidence that the checkpoint can be activated in a Bub1-independent manner from the corona (Figure 32). The synergy of the KBB and RZZ:Cyclin B1 pathways remains unclear, but these data suggests they may co-ordinate to ensure timely activation of the APC/C.

A paper from the laboratory of Francis Barr suggests that Mad1 itself recruits Cyclin B – CDK1 to unattached kinetochores at the onset of NEBD (Alfonso-Pérez *et al.*, 2019). They also suggest that Cyclin B-CDK1 recruitment to unattached kinetochores is necessary for efficient phosphorylation of CDK1 targets, including Bub1 S459, which is required for the recruitment of Mad1 to Bub1 in human cells (Ji *et al.*, 2017). This suggests that Cyclin B acts very upstream in SAC signalling. However, whether Cyclin B brings Mad1 to unattached kinetochores, or vice versa, remains a question in the field. Nevertheless, there is now mounting evidence to suggest that the complex could be assembled at the NPC and recruited to unattached kinetochores.

6.8 Bub1 may be required to activate the SAC at immaturely attached kinetochores

The second pathway for Mad1:Mad2 recruitment at kinetochores is proposed to be via the RZZ complex at the corona, and this pool is thought to be removed from kinetochores via dynein-mediated stripping along spindle microtubules towards spindle poles (Buffin *et al.*, 2005; Kops *et al.*, 2005; Gassmann *et al.*, 2010; Silió, McAinsh and Millar, 2015). We have shown that that, in an unperturbed

mitosis, some cells depleted of Bub1 progress to anaphase prematurely with uncongressed chromosomes (Figure 26). We wondered if this could be due to untimely silencing of the checkpoint in the absence of Bub1, causing premature anaphase onset before metaphase alignment. A recent report has provided evidence that the RZZ and KBB pathways silence at differing microtubule occupancy levels on kinetochores (Etemad *et al.*, 2019). At 50% maximum microtubule occupancy, Mad1:Mad2 and RZZ pathway members were barely detectable, however Bub1, BubR1 and pMELTs were clearly visible at kinetochores suggesting that dynein stripping occurs prior to MELT dephosphorylation and SAC silencing. It would make sense, therefore, that when the KBB pathway is lost, SAC activation dependant on the RZZ pathway could be silenced faster in the presence of microtubules causing premature anaphase onset.

Further to this, recent work from our laboratory has proposed a role for CenpF in modulating dynein motor activity at kinetochores through recruitment of the dynein regulators Nde/Nde1/Lis1 (Auckland and McAinsh, 2019, bioRXiv). In the absence of CenpF, Cenp-E (a cargo of dynein) was prematurely stripped from kinetochores along microtubules suggesting dynein over-activation. Bub1 is reported to be stringently required for the recruitment of CenpF to the kinetochore, and we have shown that it is reduced by 80% in Bub1$^{1\text{-}23}$ cells (Ciossani *et al.*, 2018; Raaijmakers *et al.*, 2018). Strikingly, Mad2 and CenpE showed similar staining patterns in Bub1$^{1\text{-}23}$ cells suggesting both proteins are prematurely stripped from kinetochores in the absence of Bub1 (Figure 11). These data may allude to an indirect role of Bub1 in control of dynein-mediated stripping via recruitment of CenpF to kinetochores. In the absence of Bub1, CenpF is reduced at the kinetochore presumably along with the regulatory proteins Nde1/Ndel1/Lis1, which may cause over-activation of dynein. This could lead to premature and/or overactive stripping of the RZZ:Mad1:Mad2 complex by dynein at kinetochores with low microtubule occupancy. As the KBB pathway is defective in the absence of Bub1, low occupancy kinetochores are no longer recognised causing premature checkpoint silencing and anaphase onset. The combination of

premature silencing at low occupancy kinetochores, and potential overactivation of dynein-mediated stripping to remove Mad1:Mad2 could potentially explain why cells fully depleted of Bub1 accelerate through an unperturbed mitosis.

6.9 A novel, premitotic role for Bub1 is required for correct mitotic timing

During analysis of unperturbed mitosis in Bub1$^{1\text{-}23}$ cells treated with Bub1 siRNA, we were surprised to see cells progressing to anaphase in as fast as 12 mins (Figure 26). This phenotype is reminiscent of that seen following loss of a premitotic inhibitory signal generated at the nuclear envelope (NE), which defines the minimum length of mitosis (Rodriguez-Bravo *et al.*, 2014). In this model, Mad1:Mad2 complexes are tethered at the nuclear pore complex (NPC) by the nucleoporin Tpr, and this localisation scaffolds the production of interphase MCC to inhibit APC/C prior to mitotic entry and define the minimum length of mitosis.

However a contrasting model suggests that phosphorylation of Bub1 at S459/T461 is required as an attachment independent 'timer' for mitosis in HeLa cells (Qian *et al.*, 2017). These residues are phosphorylated by Cdk1 and Mps1 respectively to fully recruit Mad2 to the Cd1 domain (Ji *et al.*, 2017). Interestingly, when both these residues were mutated HeLa cells progressed through unperturbed mitosis in ~15 mins. Authors also showed that in Mad1-ΔNP2 HCT-116 cells, where Mad1 cannot bind to the nuclear pore, siBub1 treatment further accelerated unperturbed mitosis from ~ 27 mins to ~ 15 mins, suggesting Bub1 acts in parallel to the NPC-dependant pathway. It is of note that all cells in this study were synchronised using RO3305, a Cdk1 inhibitor, prior to experiments which could potentially produce artefacts in Cdk1 phosphorylation substrates downstream. Authors did not describe any effects of Bub1 depletion on the nuclear envelope pool of Mad2.

From our data we do not have evidence to suggest that Bub1 acts as a 'timer' via Cdk1 and Mps1 phosphorylation of the CD1 domain during early mitosis, but rather propose that Bub1 controls mitotic timing through a premitotic pathway that contributes to Mad1:Mad2 loading to the nuclear envelope during interphase. We found that Mad2 was reduced at the NE in Bub1$^{1-23}$ cells, suggesting that the acceleration in unperturbed mitosis could originate from either a reduction in interphase MCC generated at the nuclear pore, or perturbed migration of Mad1:Mad2 complexes from the NPC to kinetochores (Figure 27). Consistent with this, we saw a reduction in Mad2 at kinetochores in Bub1$^{1-23}$ cells depleted of Bub1 during early prometaphase (Figure 25). Additional investigation found that localisation of Tpr, the nucleoporin that constitutes the binding site for Mad1:Mad2 at the NE, was reduced in a Bub1-dependant manner (Figure 28). These unexpected data suggest that Bub1 contributes to Mad1:Mad2 loading at the NPC via regulation of Tpr, and therefore premitotic SAC signalling at nuclear pores (Figure 33).

Bub1 was implicated in normal mitotic timing in one of the first papers describing its function (Taylor and McKeon, 1997). Authors found when cells were synchronised at the G1/S boundary, HeLa cells expressing a stably transfected dominant-negative truncation mutant of Bub1 returned to the next G1 phase approximately 25 minutes faster than control cells as seen by flow cytometry. However, a later study depleting Bub1 with siRNA in HeLa cells saw no acceleration in mitosis by use of live cell imaging, and concluded that Bub1 is not required for correct mitotic timing (Meraldi, Draviam and Sorger, 2004). The recently published HeLa and HAP1 CRISPR cell lines depleted of Bub1 show chromosome alignment defects, which most likely result in unattached kinetochores and SAC activation via the RZZ pathway. This causes a delay in prometaphase during unperturbed mitosis, which would mask any defects resulting from loss of Bub1 in interphase (Raaijmakers *et al.*, 2018; Zhang *et al.*, 2019). Acceleration was also not observed upon Bub1 inactivation in MEFs using the Cre-LoxP system where cells proceeded through mitosis with normal timing (Perera *et al.*, 2007). However, these cells displayed increased polar chromosomes

on inactivation of Bub1, which would mask any effects on interphase MCC. hTERT-RPE1 cells could be the ideal cell line in which to observe Bub1's premitotic function as they appear to not rely on the Bub1 – pH2A-T120 – Sgo1 axis for error correction and alignment. This was shown in Chapter 4 where Bub1$^{1-23}$ cells experience only a short delay following nocodazole washout before correctly aligning chromosomes (Figure 22). This situation may allow defects in interphase MCC production to 'spill over' into mitosis, where they would otherwise be masked by Bub1 independent-MCC production at unattached kinetochores.

A function for Bub1 upstream of nuclear pores is not obvious. CenpF, known to be recruited to kinetochores via Bub1, becomes recruited to the nuclear envelope during the G2/M transition. Here it is implicated in bipolar spindle assembly, through interactions with Nup133 and Nde1/Ndel1 (Bolhy *et al.*, 2011). Nup133 is thought to be required for anchoring of the dynein/dynactin complex to the NE during prophase, which maintains centrosome association with the NE at mitotic entry. It could be possible that a Bub1-CenpF interaction may play a role in premitotic checkpoint signalling in interphase cells, and we have shown some preliminary evidence to support this hypothesis. Tpr was dramatically reduced to 20% of control levels at the nuclear envelope in response to CenpF depletion using siRNA (Figure 29). CenpF and Bub1 have not been shown to interact during interphase, but Bub1 foci are reported become visible at the G2/M transition as CenpF is recruited to the nuclear envelope, therefore they are both expressed at this stage of the cell cycle (Hussein and Taylor, 2002). We have also shown that Bub1 is detectable during interphase in RPE1 cells (Figure 30). Puzzlingly, CenpF is known to bind the cytoplasmic side of the nuclear envelope, where it interacts with dynein and Nup133, while Tpr and Mad1:Mad2 complexes are known to reside on the nucleoplasmic side (Lee *et al.*, 2008; Bolhy *et al.*, 2011; Berto *et al.*, 2018). Therefore, how depletion of CenpF leads to loss of Tpr is unclear as they are spatially separated, unless depletion of CenpF leads to NPC disassembly. It may be possible that depletion of CenpF or Bub1 could interfere with signalling in G2, however cells enter mitosis in the absence of both CenpF and Bub1

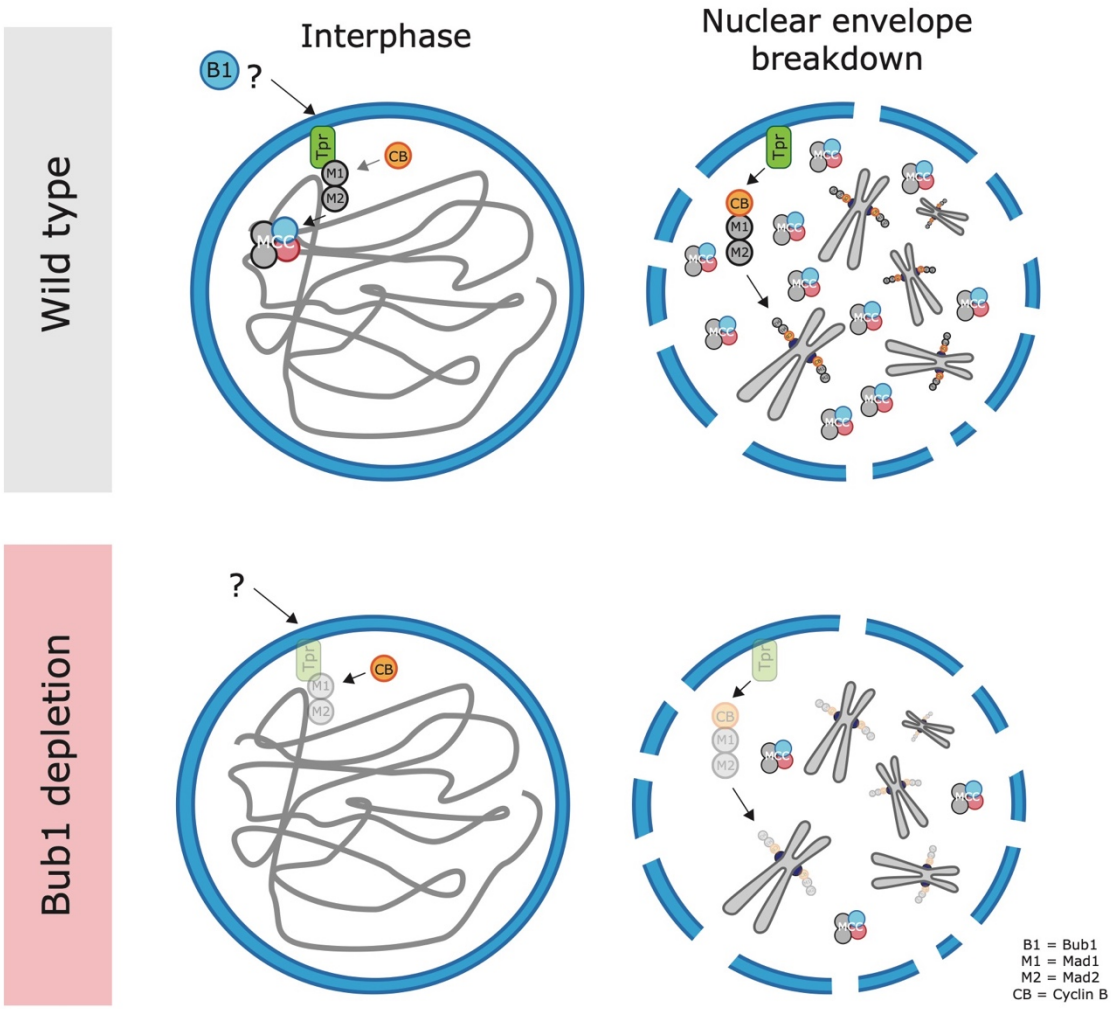

Figure 33: Potential model for the premitotic role of Bub1. In wild type cells, Bub1 regulates the level of Tpr at the nuclear envelope through an unknown function. This allows recruitment of Mad1:Mad2 complexes and creation of interphase MCC generation. Upon NEBD, Cyclin B binds Mad1:Mad2 and the complex migrates to kinetochores. Levels of MCC are high due to interphase generation. Upon depletion of Bub1, levels of Tpr and Mad1:Mad2 are reduced at the nuclear envelope, and interphase MCC generation is low. Upon NEBD, less Mad1:Mad2 is recruited to kinetochores and levels of MCC are low, causing cells to accelerate to anaphase due to insufficient APC/C inhibition during early mitosis.

suggesting they are not blocked in G2 and complete this stage of the cell cycle successfully. There may also be problems with re-establishment of the nuclear envelope following mitotic exit in the absence of Bub1 or CenpF, which could affect levels of Tpr and nuclear envelope structure, but we do not have evidence for this.

A further search of the literature for NPC components highlighted Rae1, a nucleoporin component of the outer NPC implicated in mRNA export from the nucleus. Rae1 shares extensive sequence homology with Bub3 in yeast and higher eukaryotes (Wang *et al.*, 2001). Interestingly, human Rae1 has been shown to bind human Bub1 via a GLEBs domain, and the two proteins accumulate together at kinetochores of prometaphase HeLa cells (Wang *et al.*, 2001). A later study proposed a role for Rae1 in the SAC (Babu *et al.*, 2003). Authors generated Rae1 heterozygous MEFs, which could not sustain a mitotic arrest in response to nocodazole treatment as judged by p-H3 staining. Interestingly, similar results were seen in $Bub3^{+/-}$ MEFs, but overexpression of Rae1 was able to rescue the arrest in nocodazole. These results suggests that the role of Rae1 and Bub3 in SAC activation overlap. Interestingly, Rae1 has been proposed to form a complex with Nup98 to inhibit APC/C^{Cdh1} during early mitosis and prevent premature securin degradation, however heterozygous mice showed no acceleration in anaphase onset (Jeganathan, Malureanu and Van Deursen, 2005). It is important to note that these mice express small amounts of both Rae1 and Nup98. Rae1 has also been shown to bind microtubules and form a complex with NuMA-Nup98-Dynein during mitosis (Wong, Blobel and Coutavas, 2006) and siRNA depletion of Rae1 causes spindle defects and loss of bipolarity (Blower *et al.*, 2005; Wong, Blobel and Coutavas, 2006). Most relevantly, overexpression of Rae1 has been shown to stabilise cyclin B1 in *Drosophila melanogaster* (Jahanshahi *et al.*, 2016). A role for Rae1 in premitotic human checkpoint signalling has not been described, but it is certainly an interesting candidate, being the only NPC component known to bind Bub1 as of yet.

There is also the possibility that Bub1 itself is shuttled in and out of the nucleus through the NPC during interphase, as it possesses a nuclear localisation sequence. This mean that Bub1 moves through the nuclear basket and therefore nearby the Mad1:Mad2 complexes tethered here on each pass. This could potentially provide a platform for the generation of Mad2:Cdc20 complexes that have been shown to inhibit APC/C^{Cdc20} during G2 (Lara-Gonzalez *et al.*, 2019). This hypothesis could be tested by inhibiting nuclear transport by addition of a drug, of which many are

available (Kosyna and Depping, 2018). However, a mitotic phenotype following nuclear transport inhibition does not directly implicate Bub1 as thousands of molecules are transported in and out of the nucleus. It would be interesting to endogenously tag Bub1 with a fluorescent marker and firstly see if it is present at the nuclear envelope during interphase. Nuclear transport could then be inhibited and if Bub1 is transported through the NPC it would accumulate in the cytoplasm. This could provide preliminary evidence to start unpicking a mechanism for the role of Bub1 during interphase.

6.10 Conclusions and future directions

Overall, in this thesis we have further clarified the role of Bub1 in human spindle assembly checkpoint signalling. We have generated a hTERT-RPE1 cell line where the *BUB1* locus was disrupted using CRISPR-Cas9 to insert a single base pair in each allele and deplete Bub1 to undetectable levels by standard techniques. This cell line was named Bub1$^{1\text{-}23}$. Unfortunately, we later found that this cell line expressed residual 'zombie' Bub1 protein, which contributed to SAC signalling. We have addressed this major caveat by depleting 'zombie' Bub1 from Bub1$^{1\text{-}23}$ cells using siRNA to further reduce Bub1 to undetectable levels as measured by western blot and immunofluorescence. Using this combination of CRISPR targeting and siRNA we have been able to further prove that Bub1 is not essential for SAC activation at unattached kinetochores in hTERT-RPE1 cells. We assume that SAC signalling in the absence of Bub1 is a function of the Rod-Zwilch-ZW10 (RZZ) complex. We have also shown data to suggest that Bub1 has a novel premitotic role in SAC signalling upstream of nuclear pores and we now can now further examine this. Further work will aim to elucidate the role of Bub1 in the generation of this premitotic inhibitory signal, by exploring the idea that Bub1 itself could be shuttled in and out of the nucleus during interphase via nuclear transport. Using an endogenously tagged Bub1 cell line (to be generated), we could investigate first the presence of Bub1 nuclear transport, and then if the evidence

is positive, we could start to investigate the kinetics. This would then open up the opportunity to manipulate this transport by mutating the Bub1 nuclear localisation sequence, and seeing if this has a similar effect on mitotic timing as reported in this thesis. Secondly, it would be interesting to see whether Bub1 plays an indirect role in dynein-mediated stripping through the recruitment of CenpF to the kinetochore. To do this we would use a stripping assay recently established in our lab to see if depletion of Bub1 increases the rate of stripping, by investigating the levels of CenpE (a known dynein cargo) at kinetochores (Auckland and McAinsh, 2019 BioRXiv).

Chapter 7: Bibliography

Acquaviva, C., Herzog, F., Kraft, C., & Pines, J. (2004). The anaphase promoting complex/cyclosome is recruited to centromeres by the spindle assembly checkpoint. *Nature Cell Biology*, *6*(9), 892–898. https://doi.org/10.1038/ncb1167

Adams, R. R., Carmena, M., & Earnshaw, W. C. (2001). Chromosomal passengers and the (aurora) ABCs of mitosis. *Trends in Cell Biology*, *11*(2), 49–54. https://doi.org/10.1016/S0962-8924(00)01880-8

Akiyoshi, B., Nelson, C. R., Ranish, J. A., & Biggins, S. (2009). Analysis of Ipl1-mediated phosphorylation of the Ndc80 kinetochore protein in Saccharomyces cerevisiae. *Genetics*, *183*(4), 1591–1595. https://doi.org/10.1534/genetics.109.109041

Alfieri, C., Chang, L., Zhang, Z., Yang, J., Maslen, S., Skehel, M., & Barford, D. (2016). Molecular basis of APC/C regulation by the spindle assembly checkpoint. *Nature*, *536*(7617), 431–436. https://doi.org/10.1038/nature19083

Alfieri, C., Zhang, S., & Barford, D. (2017). Visualizing the complex functions and mechanisms of the anaphase promoting complex/cyclosome (APC/C). *Open Biology*, *7*(11). https://doi.org/10.1098/rsob.170204

Alfonso-Pérez, T., Hayward, D., Holder, J., Gruneberg, U., & Barr, F. A. (2019). MAD1-dependent recruitment of CDK1-CCNB1 to kinetochores promotes spindle checkpoint signaling. *Journal of Cell Biology*, *218*(4), 1108–1117. https://doi.org/10.1083/jcb.201808015

Allan, L. A., Reis, M., Liu, Y., Huis, P., Kops, G. J. P. L., Musacchio, A., & Saurin, A. T. (2019). Cyclin B1 scaffolds MAD1 at the corona to activate the spindle assembly checkpoint. *BioRxiv*, 1–19.

Alushin, G. M., Musinipally, V., Matson, D., Tooley, J., Todd Stukenberg, P., & Nogales, E. (2012). Multimodal microtubule binding by the Ndc80 kinetochore complex. *Nature Structural and Molecular Biology*, *19*(11), 1161–1167. https://doi.org/10.1038/nsmb.2411

Auckland, P., Clarke, N. I., Royle, S. J., & McAinsh, A. D. (2017). Congressing kinetochores progressively load Ska complexes to prevent force-dependent detachment. *Journal of Cell Biology*, *216*(6), 1623–1639. https://doi.org/10.1083/jcb.201607096

Auckland, P., & McAinsh, A. D. (2019). CENP-F controls force generation and the dynein-dependent stripping of CENP-E at kinetochores. *BioRxiv*.

Babu, J. R., Jeganathan, K. B., Baker, D. J., Wu, X., Kang-Decker, N., & Van Deursen, J. M. (2003). Rae1 is an essential mitotic checkpoint regulator that cooperates with Bub3 to prevent chromosome missegregation. *Journal of Cell Biology*, *160*(3), 341–353. https://doi.org/10.1083/jcb.200211048

Bakhoum, S. F., Ngo, B., Laughney, A. M., Cavallo, J. A., Murphy, C. J., Ly, P., … Cantley, L. C. (2018). Chromosomal instability drives metastasis through a cytosolic DNA response. *Nature*, *553*(7689), 467–472. https://doi.org/10.1038/nature25432

Baron, A. P., von Schubert, C., Cubizolles, F., Siemeister, G., Hitchcock, M., Mengel, A., … Nigg, E. A. (2016). Probing the catalytic functions of Bub1 kinase using the small molecule inhibitors BAY-320 and BAY-524. *ELife*, *5*(FEBRUARY2016), 1–26. https://doi.org/10.7554/eLife.12187

Berto, A., Yu, J., Morchoisne-Bolhy, S., Bertipaglia, C., Vallee, R., Dumont, J., … Doye, V. (2018). Disentangling the molecular determinants for Cenp-F localization to nuclear pores and kinetochores. *EMBO Reports*, *19*(5), e44742. https://doi.org/10.15252/embr.201744742

Blower, M. D., Nachury, M., Heald, R., & Weis, K. (2005). A Rae1-containing ribonucleoprotein complex is required for mitotic spindle assembly. *Cell*, *121*(2), 223–234. https://doi.org/10.1016/j.cell.2005.02.016

Bolhy, S., Bouhlel, I., Dultz, E., Nayak, T., Zuccolo, M., Gatti, X., … Doye, V. (2011). A Nup133-dependent NPC-anchored network tethers centrosomes to the nuclear envelope in prophase. *Journal of Cell Biology*, *192*(5), 855–871. https://doi.org/10.1083/jcb.201007118

Buffin, E., Lefebvre, C., Huang, J., Gagou, M. E., & Karess, R. E. (2005). Recruitment of Mad2 to the kinetochore requires the Rod/Zw10 complex. *Current Biology*, *15*(9), 856–861. https://doi.org/10.1016/j.cub.2005.03.052

Cairo, L. V., Ptak, C., & Wozniak, R. W. (2013). Mitosis-Specific Regulation of Nuclear Transport by the Spindle Assembly Checkpoint Protein Mad1p. *Molecular Cell*, *49*(1), 109–120. https://doi.org/10.1016/j.molcel.2012.10.017

Caldas, G. V., Lynch, T. R., Anderson, R., Afreen, S., Varma, D., & De Luca, J. G. (2015). The RZZ complex requires the N-terminus of KNL1 to mediate optimal Mad1 kinetochore localization in human cells. *Open Biology*, *5*(11). https://doi.org/10.1098/rsob.150160

Campbell, C. S., & Desai, A. (2013). Tension sensing by Aurora B kinase is independent of survivin-based centromere localization. *Nature*, *497*(7447), 118–121. https://doi.org/10.1038/nature12057

Campbell, M. S., Chan, G. K. T., & Yen, T. J. (2001). Mitotic checkpoint proteins HsMAD1 and HsMAD2 are associated with nuclear pore complexes in interphase. *Journal of Cell Science*, *114*(5), 953–963.

Chan, G. K. T., Jablonski, S. A., Starr, D. A., Goldberg, M. L., & Yen, T. J. (2000). Human Zw10 and ROD are mitotic checkpoint proteins that bind to kinetochores. *Nature Cell Biology*, *2*(12), 944–947. https://doi.org/10.1038/35046598

Cheeseman, I. M., Chappie, J. S., Wilson-Kubalek, E. M., & Desai, A. (2006). The Conserved KMN Network Constitutes the Core Microtubule-Binding Site of the Kinetochore. *Cell*, *127*(5), 983–997. https://doi.org/10.1016/j.cell.2006.09.039

Cheeseman, I. M., & Desai, A. (2008). Molecular architecture of the kinetochore-microtubule interface. *Nature Reviews Molecular Cell Biology*, *9*(1), 33–46. https://doi.org/10.1038/nrm2310

Ciossani, G., Overlack, K., Huis in 't Veld, P. J., Koerner, C., Wohlgemuth, S., Maffini, S., & Musacchio, A. (2018). The kinetochore proteins CENP-E and CENP-F directly and specifically interact with distinct BUB mitotic checkpoint Ser/Thr kinases. *Journal of Biological Chemistry*, *293*(26), 10084–10101. https://doi.org/10.1074/jbc.ra118.003154

Clarke, P. R., & Zhang, C. (2008). Spatial and temporal coordination of mitosis by Ran GTPase. *Nature Reviews Molecular Cell Biology*, *9*(6), 464–477. https://doi.org/10.1038/nrm2410

Cohen, S., Kramarski, L., Levi, S., Deshe, N., Ben David, O., & Arbely, E. (2019). Nonsense mutation-dependent reinitiation of translation in mammalian cells. *Nucleic Acids Research*, 1–9. https://doi.org/10.1093/nar/gkz319

Combes, G., Barysz, H., Garand, C., Gama Braga, L., Alharbi, I., Thebault, P., … Elowe, S. (2018). Mps1 Phosphorylates Its N-Terminal Extension to Relieve Autoinhibition and Activate the Spindle Assembly Checkpoint. *Current Biology*, *28*(6), 872-883.e5. https://doi.org/10.1016/j.cub.2018.02.002

Comings, D. E., & Okada, T. A. (1971). Fine structure of kinetochore in Indian muntjac. *Experimental Cell Research*, *67*(1), 97–110. https://doi.org/10.1016/0014-4827(71)90625-2

Cong, L., Ran, F. A., Cox, D., Lin, S., Barretto, R., Habib, N., … Zhang, F. (2013). *Multiplex genome engineering using CRISPR/Cas9 systems*. (February), 819–824.

Cooke, C. A., Schaar, B., Yen, T. J., & Earnshaw, W. C. (1997). Localization of CENP-E in the fibrous corona and outer plate of mammalian kinetochores from prometaphase through anaphase. *Chromosoma*, *106*(7), 446–455. https://doi.org/10.1007/s004120050266

Currie, C. E., Mora-Santos, M. D., Smith, C., McAinsh, A. D., & Millar, J. B. (2018). Bub1 is not essential for the checkpoint response to unattached kinetochores in diploid human cells. *BioRXiv*, *28*(17), 278820. https://doi.org/10.1101/278820

Davenport, J., Harris, L. D., & Goorha, R. (2006). Spindle checkpoint function requires Mad2-dependent Cdc20 binding to the Mad3 homology domain of BubR1. *Experimental Cell Research*, *312*(10), 1831–1842. https://doi.org/10.1016/j.yexcr.2006.02.018

Dawson, I. A., Roth, S., & Artavanis-Tsakonas, S. (1995). *The Drosophila cell cycle gene fizzy is required for normal degradation of Cyclins A and B during mitosis and has homology to the CDC20 gene of Saccharomyces cerevisiae*. *129*(3), 725–737.

De Antoni, A., Pearson, C. G., Cimini, D., Canman, J. C., Sala, V., Nezi, L., … Musacchio, A. (2005). The Mad1/Mad2 Complex as a Template for Mad2 Activation in the Spindle Assembly Checkpoint. *Current Biology*, *15*, 214–225. https://doi.org/10.1016/j

Dej, K. J., & Orr-Weaver, T. L. (2000). Separation anxiety at the centromere. *Trends in Cell Biology*, *10*(9), 392–399. https://doi.org/10.1016/S0962-8924(00)01821-3

Di Fiore, B., Davey, N., Hagting, A., Izawa, D., Mansfeld, J., Gibson, T., & Pines, J. (2015). The ABBA Motif binds APC/C activators and is shared by APC/C substrates and regulators. *Developmental Cell*, *32*(3), 358–372. https://doi.org/10.1016/j.devcel.2015.01.003

Di Fiore, B., & Pines, J. (2007). Emi1 is needed to couple DNA replication with mitosis but does not regulate activation of the mitotic APC/C. *Journal of Cell Biology*, *177*(3), 425–437. https://doi.org/10.1083/jcb.200611166

Dick, A. E., & Gerlich, D. W. (2013). Kinetic framework of spindle assembly checkpoint signalling. *Nature Cell Biology*, *15*(11), 1370–1377. https://doi.org/10.1038/ncb2842

Downing, K. H., & Nogales, E. (1998). Tubulin and microtubule structure. *Current Opinion in Cell Biology*, *10*(1), 16–22. https://doi.org/10.1016/S0955-0674(98)80082-3

Elbashir, S. M., Harborth, J., Lendeckel, W., Yalcin, A., Weber, K., & Tuschl, T. (2001). Duplexes of 21-nucleotide RNAs mediate RNA interference in cultured mammalian cells. *Nature*, *411*(6836), 494–498. https://doi.org/10.1038/35078107

Elowe, S., Hümmer, S., Uldschmid, A., Li, X., & Nigg, E. a. (2007a). on BubR1 regulates the stability of kinetochore – microtubule interactions. *Genes & Development*, *21*(17), 2205–2219. https://doi.org/10.1101/gad.436007.2004

Elowe, S., Hümmer, S., Uldschmid, A., Li, X., & Nigg, E. a. (2007b). Tension sensitive Plk1 phosphorylation on BubR1 regulates the stability of kinetochore – microtubule interactions. *Genes & Development*, *21*(17), 2205–2219. https://doi.org/10.1101/gad.436007.2004

Espert, A., Uluocak, P., Bastos, R. N., Mangat, D., Graab, P., & Gruneberg, U. (2014). PP2A-B56 opposes Mps1 phosphorylation of Knl1 and thereby promotes spindle assembly checkpoint silencing. *Journal of Cell Biology*, *206*(7), 833–842. https://doi.org/10.1083/jcb.201406109

Etemad, B., Vertesy, A., Kuijt, T. E. F., Sacristan, C., Van Oudenaarden, A., & Kops, G. J. P. L. (2019). Spindle checkpoint silencing at kinetochores with submaximal microtubule occupancy. *Journal of Cell Science*, *132*(12). https://doi.org/10.1242/jcs.231589

Faesen, A. C., Thanasoula, M., Maffini, S., Breit, C., Müller, F., Van Gerwen, S., … Musacchio, A. (2017). Basis of catalytic assembly of the mitotic checkpoint complex. *Nature*, *542*(7642), 498–502. https://doi.org/10.1038/nature21384

Fang, G. (2002). Checkpoint Protein BubR1 acts Synergistically with Mad2 to Inhibit Anaphase-promoting Complex. *Molecular Biology of the Cell*, *13*(April), 755–766. https://doi.org/10.1091/mbc.01

Fenech, M. (2000). The in vitro micronucleus technique. *Mutation Research - Fundamental and Molecular Mechanisms of Mutagenesis*, *455*(1–2), 81–95. https://doi.org/10.1016/S0027-5107(00)00065-8

Feng, J., Huang, H., & Yen, T. J. (2006). CENP-F is a novel microtubule-binding protein that is essential for kinetochore attachments and affects the duration of the mitotic checkpoint delay. *Chromosoma*, *115*(4), 320–329. https://doi.org/10.1007/s00412-006-0049-5

Fernius, J., & Hardwick, K. G. (2007). Bub1 kinase targets Sgo1 to ensure efficient chromosome biorientation in budding yeast mitosis. *PLoS Genetics*, *3*(11), 2312–2325. https://doi.org/10.1371/journal.pgen.0030213

Fire, A., Xu, S., Montogomery, M., Kostas, S., Driver, S., & Mello, C. (1998). Potent and specific genetic interference by double-stranded RNA in Caenorhabditis elegans. *Nature*, *391*(February), 806–811.

Foley, E. A., Maldonado, M., & Kapoor, T. M. (2011). Formation of stable attachments between kinetochores and microtubules depends on the B56-PP2A phosphatase. *Nature Cell Biology*, *13*(10), 1265–1271. https://doi.org/10.1038/ncb2327

Funk, L. C., Zasadil, L. M., & Weaver, B. A. (2016). Living in CIN: Mitotic Infidelity and Its Consequences for Tumor Promotion and Suppression. *Developmental Cell*, *39*(6), 638–652. https://doi.org/10.1016/j.devcel.2016.10.023

Gama, J. B., Pereira, C., Simões, P. A., Celestino, R., Reis, R. M., Barbosa, D. J., … Cheerambathur, D. K. (2017). *Molecular mechanism of dynein recruitment to kinetochores by the Rod – Zw10 – Zwilch complex and Spindly*. *216*(4). https://doi.org/10.1083/jcb.201610108

Gassmann, R., Holland, A. J., Varma, D., Wan, X., Filiz, C., Oegema, K., … Desai, A. (2010). Removal of Spindly from microtubule-attached kinetochores controls spindle checkpoint signalling in human cells. *Genes & Development*, *24*, 957–971. https://doi.org/10.1101/gad.1886810

Green, R. A., Paluch, E., & Oegema, K. (2012). Cytokinesis in Animal Cells. *Annu. Rev. Cell. Dev. Biol.*, *28*, 29–58. https://doi.org/10.1016/S0074-7696(08)60059-5

Griffis, E. R., Stuurman, N., & Vale, R. D. (2007). Spindly, a novel protein essential for silencing the spindle assembly checkpoint, recruits dynein to the kinetochore. *Journal of Cell Biology*, *177*(6), 1005–1015. https://doi.org/10.1083/jcb.200702062

Güttinger, S., Laurell, E., & Kutay, U. (2009). Orchestrating nuclear envelope disassembly and reassembly during mitosis. *Nature Reviews Molecular Cell Biology*, *10*(3), 178–191. https://doi.org/10.1038/nrm2641

Haapaniemi, E., Botla, S., Persson, J., Schmierer, B., & Taipale, J. (2018). CRISPR–Cas9 genome editing induces a p53-mediated DNA damage response. *Nature Medicine*, 1. https://doi.org/10.1038/s41591-018-0049-z

Hahn, W. C., Counter, C. M., Lundberg, A. S., Beijersbergen, R. L., Brooks, M. W., & Weinberg, R. A. (1999). Creation of human tumour cells with defined genetic elements. *Nature*, *400*(July), 464–468.

Hauf, S., Cole, R. W., LaTerra, S., Zimmer, C., Schnapp, G., Walter, R., … Peters, J. M. (2003). The small molecule Hesperadin reveals a role for Aurora B in correcting kinetochore-microtubule attachment and in maintaining the spindle assembly checkpoint. *Journal of Cell Biology*, *161*(2), 281–294. https://doi.org/10.1083/jcb.200208092

Hein, J. B., & Nilsson, J. (2016). Interphase APC/C-Cdc20 inhibition by cyclin A2-Cdk2 ensures efficient mitotic entry. *Nature Communications*, *7*, 1–10. https://doi.org/10.1038/ncomms10975

Hentze, M. W., & Kulozik, A. E. (1999). A perfect message: RNA surveillance and nonsense-mediated decay. *Cell*, *96*(3), 307–310. https://doi.org/10.1016/S0092-8674(00)80542-5

Hershko, A. (1999). Mechanisms and regulation of the degradation of cyclin B. *Philosophical Transactions of the Royal Society B: Biological Sciences*, *354*, 1571–1576.

Holt, S. V., Vergnolle, A. S., Hussein, D., Wozniak, M. J., Allan, V. J., & Taylor, S. S. (2005). Silencing Cenp-F weakens centromeric cohesion, prevents chromosome alignment and activates the spindle checkpoint. *Journal of Cell Science*, *118*(20), 4889–4900. https://doi.org/10.1242/jcs.02614

Howell, B. J., McEwen, B. F., Canman, J. C., Hoffman, D. B., Farrar, E. M., Rieder, C. L., & Salmon, E. D. (2001). Cytoplasmic dynein/dynactin drives kinetochore protein transport to the spindle poles and has a role in mitotic spindle checkpoint inactivation. *Journal of Cell Biology*, *155*(7), 1159–1172. https://doi.org/10.1083/jcb.200105093

Hoyt, M. A., Totis, L., & Roberts, B. T. (1991). S. cerevisiae genes required for cell cycle arrest in response to loss of microtubule function. *Cell*, *66*(3), 507–517. https://doi.org/10.1016/0092-8674(81)90014-3

Hughes, A. F., & Swann, M. M. (1947). Anaphase Movements in the Living Cell. *Journal of Experimental Biology*, *24*(45).

Hussein, D., & Taylor, S. S. (2002). Farnesylation of Cenp-F is required for G2/M progression and degradation after mitosis. *Journal of Cell Science*, *115*(17), 3403–3414.

Hwang, L. H., Lau, L. F., Smith, D. L., Mistrot, C. A., Hardwick, K. G., Hwang, E. S., … Murray, A. W. (1998). Budding yeast Cdc20: A target of the spindle checkpoint. *Science*, *279*(5353), 1041–1044. https://doi.org/10.1126/science.279.5353.1041

Ikeda, M., & Tanaka, K. (2017). Plk1 bound to Bub1 contributes to spindle assembly checkpoint

activity during mitosis. *Scientific Reports*, *7*(1), 1–15. https://doi.org/10.1038/s41598-017-09114-3

Indjeian, V. B., Stern, B. M., & Murray, A. W. (2005). The centromeric protein Sgo1 is required to sense lack of tension on mitotic chromosomes. *Science*, *307*(5706), 130–133. https://doi.org/10.1126/science.1101366

Iouk, T., Kerscher, O., Scott, R. J., Basrai, M. A., & Wozniak, R. W. (2002). The yeast nuclear pore complex functionally interacts with components of the spindle assembly checkpoint. *Journal of Cell Biology*, *159*(5), 807–819. https://doi.org/10.1083/jcb.200205068

Jackman, M., Marcozzi, C., Pardo, M., Yu, L., Tyson, A. L., Jyoti, S., & Pines, J. (2019). Cyclin B1-Cdk1 binding to MAD1 links to nuclear pore disassembly to chromosomal stability. *BioRxiv*.

Jahanshahi, M., Hsiao, K., Jenny, A., & Pfleger, C. M. (2016). The Hippo Pathway Targets Rae1 to Regulate Mitosis and Organ Size and to Feed Back to Regulate Upstream Components Merlin, Hippo, and Warts. *PLoS Genetics*, *12*(8), 1–47. https://doi.org/10.1371/journal.pgen.1006198

Jeganathan, K. B., Baker, D. J., & Van Deursen, J. M. (2006). Securin associates with APCCdh1 in prometaphase but its destruction is delayed by Rae1 and Nup98 until the metaphase/anaphase transition. *Cell Cycle*, *5*(4), 366–370. https://doi.org/10.4161/cc.5.4.2483

Jeganathan, K. B., Malureanu, L., & Van Deursen, J. M. (2005). The Rae1-Nup98 complex prevents aneuploidy by inhibiting securin degradation. *Nature*, *438*(7070), 1036–1039. https://doi.org/10.1038/nature04221

Ji, Z., Gao, H., Jia, L., Li, B., & Yu, H. (2017). A sequential multi-target Mps1 phosphorylation cascade promotes spindle checkpoint signaling. *ELife*, 1–23. https://doi.org/10.7554/eLife.22513

Jia, L., Li, B., & Yu, H. (2016). The Bub1-Plk1 kinase complex promotes spindle checkpoint signalling through Cdc20 phosphorylation. *Nature Communications*, *7*, 10818. https://doi.org/10.1038/ncomms10818

Jinek, M., Chylinski, K., Fonfara, I., Hauer, M., Doudna, J. A., & Charpentier, E. (2012). A Programmable Dual-RNA–Guided DNA Endonuclease in Apaptive Bacterial Immunity. *Science*, *337*(August), 816–822.

Johnson, V. L., Scott, M., Holt, S. V., Hussein, D., & Taylor, S. S. (2004). Bub1 is required for kinetochore localization of BubR1, Cenp-E, Cenp-F and Mad2, and chromosome congression. *Journal of Cell Science*, *117*(8), 1577–1589. https://doi.org/10.1242/jcs.01006

Kang, J., Chen, Y., Zhao, Y., & Yu, H. (2007). Autophosphorylation-dependent activation of human Mps1 is required for the spindle checkpoint. *Proceedings of the National Academy of Sciences*, *104*(51), 20232–20237. https://doi.org/10.1073/pnas.0710519105

Kapoor, T M, Lampson, M. A., Hergert, P., Cameron, L., Cimini, D., Salmon, E. D., … Khodjakov, A. (2006). *Chromosomes can congress to the metaphase plate before biorientation*. *311*(January), 388–391.

Kapoor, Tarun M., Mayer, T. U., Coughlin, M. L., & Mitchison, T. J. (2000). Probing spindle assembly mechanisms with monastrol, a small molecule inhibitor of the mitotic kinesin, Eg5. *Journal of Cell Biology*, *150*(5), 975–988. https://doi.org/10.1083/jcb.150.5.975

Karess, R. (2005). Rod-Zw10-Zwilch: A key player in the spindle checkpoint. *Trends in Cell Biology*, *15*(7), 386–392. https://doi.org/10.1016/j.tcb.2005.05.003

Kawashima, S., Yamagishi, Y., Ishiguro, K., & Watanabe, Y. (2010). Phosphorylation of H2A by Bub1 Prevents Chromosomal Instability Through Localizing Shugoshin. *Science*, *372*(172), 172–177. https://doi.org/10.1126/science.1180189

Kelly, A. E., Ghenoiu, C., Xue, J. Z., Zierhut, C., Kimura, H., & Funabiki, H. (2010). Survivin reads phosphorylated Histone H3 Threonine 3 to activate the mitotic kinase Aurora B. *Science*, *330*(October), 235–239. https://doi.org/10.2307/j.ctv9zcj2n.53

Khodjakov, A., Copenagle, L., Gordon, M. B., Compton, D. A., & Kapoor, T. M. (2003). Minus-end capture of preformed kinetochore fibers contributes to spindle morphogenesis. *Journal of Cell Biology*, *160*(5), 671–683. https://doi.org/10.1083/jcb.200208143

Kim, D. H., Han, J. S., Ly, P., Ye, Q., McMahon, M. A., Myung, K., … Cleveland, D. W. (2018). TRIP13 and APC15 drive mitotic exit by turnover of interphase- and unattached kinetochore-produced MCC. *Nature Communications*, *9*(1). https://doi.org/10.1038/s41467-018-06774-1

Kim, S. H., Lin, D. P., Matsumoto, S., Kitazono, A., & Matsumoto, T. (1998). Fission yeast Slp1: An effector of the Mad2-dependent spindle checkpoint. *Science*, *279*(5353), 1045–1047. https://doi.org/10.1126/science.279.5353.1045

Kirschner, M., & Mitchison, T. (1986). Beyond self-assembly: From microtubules to morphogenesis. *Cell*, *45*(3), 329–342. https://doi.org/10.1016/0092-8674(86)90318-1

Klebig, C., Korinth, D., & Meraldi, P. (2009). Bub1 regulates chromosome segregation in a kinetochore-independent manner. *Journal of Cell Biology*, *185*(5), 841–858. https://doi.org/10.1083/jcb.200902128

Kops, G. J P L, Kim, Y., Weaver, B. A. A., Mao, Y., McLeod, I., Yates, J. R., … Cleveland, D. W. (2005). ZW10 links mitotic checkpoint signaling to the structural kinetochore. *Journal of Cell Biology*, *169*(1), 49–60. https://doi.org/10.1083/jcb.200411118

Kops, Geert J.P.L., Kim, Y., Weaver, B. A. A., Mao, Y., McLeod, I., Yates, J. R., … Cleveland, D. W. (2005). ZW10 links mitotic checkpoint signaling to the structural kinetochore. *Journal of Cell Biology*, *169*(1), 49–60. https://doi.org/10.1083/jcb.200411118

Kops, Geert J P L, Weaver, B. A. A., & Cleveland, D. W. (2005). On the road to cancer: Aneuploidy and the mitotic checkpoint. *Nature Reviews Cancer*, *5*(10), 773–785. https://doi.org/10.1038/nrc1714

Koshland, D. E., Mitchison, T. J., & Kirschner, M. W. (1988). Polewards chromosome movement driven by microtubule depolymerization in vitro. *Nature*, *331*(6156), 499–504. https://doi.org/10.1038/331499a0

Kosyna, F., & Depping, R. (2018). Controlling the Gatekeeper: Therapeutic Targeting of Nuclear Transport. *Cells*, *7*(11), 221. https://doi.org/10.3390/cells7110221

Kramer, E. R., Scheuringer, N., Podtelejnikov, A. V., Mann, M., & Peters, J. M. (2000). Mitotic regulation of the APC activator proteins CDC20 and CDH1. *Molecular Biology of the Cell*, *11*(5), 1555–1569. https://doi.org/10.1091/mbc.11.5.1555

Krenn, V., Wehenkel, A., Li, X., Santaguida, S., & Musacchio, A. (2012). Structural analysis reveals features of the spindle checkpoint kinase Bub1-kinetochore subunit Knl1 interaction.

Journal of Cell Biology, *196*(4), 451–467. https://doi.org/10.1083/jcb.201110013

Lampson, M., & Grishchuk, E. (2017). Mechanisms to Avoid and Correct Erroneous Kinetochore-Microtubule Attachments. *Biology*, *6*(1), 1. https://doi.org/10.3390/biology6010001

Lara-Gonzalez, P., Moyle, M. W., Budrewicz, J., Mendoza-Lopez, J., Oegema, K., & Desai, A. (2019). The G2-to-M Transition Is Ensured by a Dual Mechanism that Protects Cyclin B from Degradation by Cdc20-Activated APC/C. *Developmental Cell*, *51*(3), 313-325.e10. https://doi.org/10.1016/j.devcel.2019.09.005

Larsen, N. A., Al-bassam, J., Wei, R. R., & Harrison, S. C. (2007). *Structural analysis of Bub3 interactions in the mitotic spindle checkpoint*. *104*(4), 1201–1206.

Lee, S. H., Sterling, H., Burlingame, A., & McCormick, F. (2008). Tpr directly binds to Mad1 and Mad2 and is important for the Mad1-Mad2-mediated mitotic spindle checkpoint. *Genes and Development*, *22*(21), 2926–2931. https://doi.org/10.1101/gad.1677208

Li, F., Kim, H., Ji, Z., Zhang, T., Chen, B., Ge, Y., … Songyang, Z. (2018). The BUB3-BUB1 Complex Promotes Telomere DNA Replication. *Molecular Cell*, *70*(3), 395-407.e4. https://doi.org/10.1016/j.molcel.2018.03.032

Li, Rong, & Murray, A. W. (1991). *Feedback control of mitosis in budding yeast*. *66*(Figure 1).

Li, Ruhong, Yerganian, G., Duesberg, P., Kraemer, A., Willer, A., Rausch, C., & Hehlmann, R. (1997). Aneuploidy correlated 100% with chemical transformation of Chinese hamster cells. *Proceedings of the National Academy of Sciences of the United States of America*, *94*(26), 14506–14511. https://doi.org/10.1073/pnas.94.26.14506

Li, Y., & Benezra, R. (1996). Identification of a human mitotic checkpoint gene: hsMAD2. *Science*, *274*(5285), 246–248. https://doi.org/10.1126/science.274.5285.246

Lince-Faria, M., Maffini, S., Orr, B., Ding, Y., Florindo, C., Sunkel, C. E., … Maiato, H. (2009). Spatiotemporal control of mitosis by the conserved spindle matrix protein megator. *Journal of Cell Biology*, *184*(5), 647–657. https://doi.org/10.1083/jcb.200811012

Liu, D., Vader, G., Vromans, M. J. M., Lampson, M. A., & Lens, S. M. A. (2009). Sensing Chromosome Bi-Orientation by Spatial Separation of Aurora B Kinase from Kinetochore Substrates. *Science*, *323*(March), 1350–1353. https://doi.org/10.1126/science.1167000

Liu, D., Vleugel, M., Backer, C. B., Hori, T., Fukagawa, T., Cheeseman, I. M., & Lampson, M. A. (2010). Regulated targeting of protein phosphatase 1 to the outer kinetochore by KNL1 opposes Aurora B kinase. *Journal of Cell Biology*, *188*(6), 809–820. https://doi.org/10.1083/jcb.201001006

Liu, H., Jia, L., & Yu, H. (2013). Phospho-H2A and cohesin specify distinct tension-regulated sgo1 pools at kinetochores and inner centromeres. *Current Biology*, *23*(19), 1927–1933. https://doi.org/10.1016/j.cub.2013.07.078

Liu, H., Rankin, S., & Yu, H. (2013). Phosphorylation-enabled binding of SGO1-PP2A to cohesin protects sororin and centromeric cohesion during mitosis. *Nature Cell Biology*, *15*(1), 40–49. https://doi.org/10.1038/ncb2637

London, N., & Biggins, S. (2014). Mad1 kinetochore recruitment by Mps1-mediated phosphorylation of Bub1 signals the spindle checkpoint. *Genes and Development*, *28*(2), 140–152. https://doi.org/10.1101/gad.233700.113

London, N., Ceto, S., Ranish, J. A., & Biggins, S. (2012). Phosphoregulation of Spc105 by Mps1 and PP1 regulates Bub1 localization to kinetochores. *Current Biology*, *22*(10), 900–906. https://doi.org/10.1016/j.cub.2012.03.052

Losson, R., & Lacroute, F. (1979). Interference of nonsense mutations with eukaryotic messenger. *Proc. Natl. Acad. Sci. USA*, *76*(10), 5134–5137.

Luo, X., Tang, Z., Rizo, J., & Yu, H. (2002). The Mad2 spindle checkpoint protein undergoes similar major conformational changes upon binding to either Mad1 or Cdc20. *Molecular Cell*, *9*(1), 59–71. https://doi.org/10.1016/S1097-2765(01)00435-X

Magidson, V., Paul, R., Yang, N., Ault, J. G., O'Connell, C. B., Tikhonenko, I., … Khodjakov, A. (2015). Adaptive changes in the kinetochore architecture facilitate proper spindle assembly. *Nature Cell Biology*, *17*(9), 1134–1144. https://doi.org/10.1038/ncb3223

Maiato, H., DeLuca, J., Salmon, E. D., & Earnshaw, W. C. (2004). The dynamic kinetochore-microtubule interface. *Journal of Cell Science*, *117*(Pt 23), 5461–5477. https://doi.org/10.1242/jcs.01536

Makino, S., & Nakanishi, Y. H. (1955). A quantitative study on anaphase movement of chromosomes in living grasshopper spermatocytes. *Chromosoma*, *7*, 439–450.

Mansfeld, J., Collin, P., Collins, M. O., Choudhary, J. S., & Pines, J. (2011). APC15 drives the turnover of MCC-CDC20 to make the spindle assembly checkpoint responsive to kinetochore attachment. *Nature Cell Biology*, *13*(10), 1234–1243. https://doi.org/10.1038/ncb2347

McEwen, B. F., Heagle, A. B., Cassels, G. O., Buttle, K. F., & Rieder, C. L. (1997). Kinetochore fiber maturation in PtK 1 cells and its implications for the mechanisms of chromosome congression and anaphase onset. *Journal of Cell Biology*, *137*(7), 1567–1580. https://doi.org/10.1083/jcb.137.7.1567

Mcintosh, J. R. (2016). Mitosis. *Cold Spring Harb Perspect Biol*, (8), a023218.

Meppelink, A., Kabeche, L., Vromans, M. J. M., Compton, D. A., & Lens, S. M. A. (2015). Shugoshin-1 Balances Aurora B Kinase Activity via PP2A to Promote Chromosome Bi-orientation. *Cell Reports*, *11*(4), 508–515. https://doi.org/10.1016/j.celrep.2015.03.052

Meraldi, P, & Sorger, P. K. (2005). A dual role for Bub1 in the spindle checkpoint and chromosome congression. *Embo J*, *24*(8), 1621–1633. https://doi.org/10.1038/sj.emboj.7600641

Meraldi, Patrick. (2019). *Bub 1 - the zombie protein that CRISPR cannot kill. e101912*.

Meraldi, Patrick, Draviam, V. M., & Sorger, P. K. (2004). Timing and checkpoints in the regulation of mitotic progression. *Developmental Cell*, *7*(1), 45–60. https://doi.org/10.1016/j.devcel.2004.06.006

Mitchison, T., & Kirschner, M. (1984). Dynamic instability of microtubule growth. *Nature*, *312*(5991), 237–242. Retrieved from http://www.bioku.net/wp-content/uploads/2011/10/Mitchison1984bNature.pdf

Mora-Santos, M. M., Hervas-Aguilar, A., Sewart, K., Lancaster, T. C., Meadows, J. C., & Millar, J. B. A. (2016). Bub3-Bub1 Binding to Spc7 / KNL1 Toggles the Spindle Checkpoint Switch by Licensing the Interaction of Bub1 with Mad1-Mad2. *Current Biology*, *1*, 1–9. https://doi.org/10.1016/j.cub.2016.07.040

Morin, V., Lorca, T., Morin, N., Prieto, S., Abrieu, A., Melines, S., … Hem, S. (2012). CDK-Dependent Potentiation of MPS1 Kinase Activity Is Essential to the Mitotic Checkpoint. *Current Biology*, *22*(4), 289–295. https://doi.org/10.1016/j.cub.2011.12.048

Mosalaganti, S., Keller, J., Altenfeld, A., Winzker, M., Rombaut, P., Saur, M., … Musacchio, A. (2017). Structure of the RZZ complex and molecular basis of its interaction with Spindly. *The Journal of Cell Biology*, *216*(4), jcb.201611060. https://doi.org/10.1083/jcb.201611060

Musacchio, A., & Salmon, E. D. (2007). The spindle-assembly checkpoint in space and time. *Nature Reviews. Molecular Cell Biology*, *8*(5), 379–393. https://doi.org/10.1038/nrm2163

Nijenhuis, W., Vallardi, G., Teixeira, A., Kops, G. J. P. L., & Saurin, A. T. (2014). *Negative feedback at kinetochores underlies a responsive spindle checkpoint signal*. *16*(12). https://doi.org/10.1038/ncb3065

Osswald, M., Cunha-silva, S., Goemann, J., Barbosa, J., & Luis, M. (2019). *Mps1 releases Mad1 from nuclear pores to ensure a robust mitotic checkpoint and accurate chromosome segregation*.

Palmer, D. K., O'Day, K., Wener, M. H., Andrews, B. S., & Margolis, R. L. (1987). A 17-kD centromere protein (CENP-A) copurifies with nucleosome core particles and with histones. *Journal of Cell Biology*, *104*(4), 805–815. https://doi.org/10.1083/jcb.104.4.805

Perera, D., & Taylor, S. S. (2009). Sgo1 establishes the centromeric cohesion protection mechanism in G2 before subsequent Bub1-dependent recruitment in mitosis. *Journal of Cell Science*, *123*(5), 653–659. https://doi.org/10.1242/jcs.059501

Perera, David, Tilston, V., Hopwood, J. A., Barchi, M., Boot-Handford, R. P., & Taylor, S. S. (2007). Bub1 Maintains Centromeric Cohesion by Activation of the Spindle Checkpoint. *Developmental Cell*, *13*(4), 566–579. https://doi.org/10.1016/j.devcel.2007.08.008

Peters, J. M. (1998). SCF and APC: The yin and yang of cell cycle regulated proteolysis. *Current Opinion in Cell Biology*, *10*(6), 759–768. https://doi.org/10.1016/S0955-0674(98)80119-1

Petrovic, A., Keller, J., Liu, Y., Overlack, K., John, J., Dimitrova, Y. N., … Musacchio, A. (2016). Structure of the MIS12 Complex and Molecular Basis of Its Interaction with CENP-C at Human Kinetochores. *Cell*, *167*(4), 1028-1040.e15. https://doi.org/10.1016/j.cell.2016.10.005

Pines, J. (2011). Cubism and the cell cycle: The many faces of the APC/C. *Nature Reviews Molecular Cell Biology*, *12*(7), 427–438. https://doi.org/10.1038/nrm3132

Qi, W., Tang, Z., & Yu, H. (2006). Phosphorylation- and Polo-Box–dependent Binding of Plk1 to Bub1 Is Required for the Kinetochore Localization of Plk1. *Molecular Biology of the Cell*, *17*(August), 3705–3716. https://doi.org/10.1091/mbc.E06

Qian, J., García-Gimeno, M. A., Beullens, M., Manzione, M. G., Van der Hoeven, G., Igual, J. C., … Bollen, M. (2017). An Attachment-Independent Biochemical Timer of the Spindle Assembly Checkpoint. *Molecular Cell*, *68*(4), 715-730.e5. https://doi.org/10.1016/j.molcel.2017.10.011

Qiao, R., Weissmann, F., Yamaguchi, M., Brown, N. G., VanderLinden, R., Imre, R., … Peters, J.-M. (2016). Mechanism of APC/C CDC20 activation by mitotic phosphorylation . *Proceedings of the National Academy of Sciences*, *113*(19), E2570–E2578. https://doi.org/10.1073/pnas.1604929113

Raaijmakers, J. A., Van Heesbeen, R. G. H. P., Blomen, V. A., Janssen, L. M. E., Van Diemen,

F., Brummelkamp, T. R., & Correspondence, R. H. M. (2018). *BUB1 Is Essential for the Viability of Human Cells in which the Spindle Assembly Checkpoint Is Compromised*. 1424–1438. https://doi.org/10.1016/j.celrep.2018.01.034

Ran, F. A., Hsu, P. P. D., Wright, J., Agarwala, V., Scott, D. a, & Zhang, F. (2013). Genome engineering using the CRISPR-Cas9 system. *Nature Protocols*, *8*(11), 2281–2308. https://doi.org/10.1038/nprot.2013.143

Rattner, J. B. (1987). The organization of the mammalian kinetochore: a scanning electron microscope study. *Chromosoma*, *95*(3), 175–181. https://doi.org/10.1007/BF00330348

Rattner, J. B., Rao, A., Fritzler, M. J., Valencia, D. W., & Yen, T. J. (1993). CENP-F is a ca 400 kDa kinetochore protein that exhibits a cell-cycle dependent localization. *Cell Motility and the Cytoskeleton*, *26*(3), 214–226. https://doi.org/10.1002/cm.970260305

Reimann, J. D. R., Freed, E., Hsu, J. Y., Kramer, E. R., Peters, J. M., & Jackson, P. K. (2001). Emi1 is a mitotic regulator that interacts with Cdc20 and inhibits the anaphase promoting complex. *Cell*, *105*(5), 645–655. https://doi.org/10.1016/S0092-8674(01)00361-0

Ricke, R. M., Jeganathan, K. B., Malureanu, L., Harrison, A. M., & Deursen, J. M. Van. (2012). *Bub1 kinase activity drives error correction and mitotic checkpoint control but not tumor suppression. 199*(6), 931–949. https://doi.org/10.1083/jcb.201205115

Ricke, R. M., Jeganathan, K. B., & van Deursen, J. M. (2011). Bub1 overexpression induces aneuploidy and tumor formation through Aurora B kinase hyperactivation. *Journal of Cell Biology*, *193*(6), 1049–1064. https://doi.org/10.1083/jcb.201012035

Rieder, C L, & Salmon, E. D. (1998). The vertebrate cell kinetochore and its roles during mitosis. *Trends in Cell Biology*, *8*(8), 310–318. https://doi.org/10.1016/j.physbeh.2017.03.040

Rieder, Conly L., Schultz, A., Cole, R., & Sluder, G. (1994). Anaphase onset in vertebrate somatic cells is controlled by a checkpoint that monitors sister kinetochore attachment to the spindle. *Journal of Cell Biology*, *127*(5), 1301–1310. https://doi.org/10.1083/jcb.127.5.1301

Ris, H., & Witt, P. L. (1981). Structure of the mammalian kinetochore. *Chromosoma*, *82*(2), 153–170. https://doi.org/10.1007/BF00286101

Roberts, B. T., Farr, K. A., & Hoyt, M. A. (1994). The Saccharomyces cerevisiae checkpoint gene BUB1 encodes a novel protein kinase. *Molecular and Cellular Biology*, *14*(12), 8282–8291. https://doi.org/10.1128/mcb.14.12.8282

Rodriguez-Bravo, V., Maciejowski, J., Corona, J., Buch, H. K., Collin, P., Kanemaki, M. T., … Jallepalli, P. V. (2014). Nuclear pores protect genome integrity by assembling a premitotic and Mad1-dependent anaphase inhibitor. *Cell*, *156*(5), 1017–1031. https://doi.org/10.1016/j.cell.2014.01.010

Rodriguez-Rodriguez, J.-A., Lewis, C., Mckinley, K. L., Khodjakov, A., Cheeseman, I. M., Jallepalli, P. V, … Corona, J. (2018). Distinct Roles of RZZ and Bub1-KNL1 in Mitotic Checkpoint Signaling and Kinetochore Expansion. *Current Biology*, 1–8. https://doi.org/10.1016/j.cub.2018.10.006

Rosenberg, J. S., Cross, F. R., & Funabiki, H. (2011). KNL1/Spc105 recruits PP1 to silence the spindle assembly checkpoint. *Current Biology*, *21*(11), 942–947. https://doi.org/10.1016/j.cub.2011.04.011

Sacristan, C., Ahmad, M. U. D., Keller, J., Fermie, J., Groenewold, V., Tromer, E., … Kops, G.

J. (2018). Dynamic kinetochore size regulation promotes microtubule capture and chromosome biorientation in mitosis. *Nature Cell Biology*, *20*(7), 800–810. https://doi.org/10.1038/s41556-018-0130-3

Sansregret, L., & Swanton, C. (2017). The role of aneuploidy in cancer evolution. *Cold Spring Harbor Perspectives in Medicine*, *7*(1), 1–18. https://doi.org/10.1101/cshperspect.a028373

Santaguida, S., Tighe, A., D'Alise, A. M., Taylor, S. S., & Musacchio, A. (2010). Dissecting the role of MPS1 in chromosome biorientation and the spindle checkpoint through the small molecule inhibitor reversine. *Journal of Cell Biology*, *190*(1), 73–87. https://doi.org/10.1083/jcb.201001036

Santaguida, S., Vernieri, C., Villa, F., Ciliberto, A., & Musacchio, A. (2011). Evidence that Aurora B is implicated in spindle checkpoint signalling independently of error correction. *EMBO Journal*, *30*(8), 1508–1519. https://doi.org/10.1038/emboj.2011.70

Saurin, A. T. (2018). *Kinase and Phosphatase Cross-Talk at the Kinetochore*. *6*(June), 1–23. https://doi.org/10.3389/fcell.2018.00062

Saurin, A. T., van der Waal, M. S., Medema, R. H., Lens, S. M. A., & Kops, G. J. P. L. (2011). Aurora B potentiates Mps1 activation to ensure rapid checkpoint establishment at the onset of mitosis. *Nat Commun*, *2*(May), 316. https://doi.org/10.1038/ncomms1319

Schvartzman, J. M., Sotillo, R., & Benezra, R. (2010). Mitotic chromosomal instability and cancer: Mouse modelling of the human disease. *Nature Reviews Cancer*, *10*(2), 102–115. https://doi.org/10.1038/nrc2781

Scott, R. J., Lusk, P., Dilworth, D. J., Aitchison, J. D., & Wozniak, R. W. (2005). Interactions between Mad1p and the nuclear transport machinery in the Yeast Saccharomyces cerevisiae. *Molecular Biology of the Cell*, *16*(September), 4362–4374. https://doi.org/10.1091/mbc.E05

Sharp-Baker, H., & Chen, R. H. (2001). Spindle checkpoint protein Bub1 is required for kinetochore localization of Mad1, Mad2, Bub3, and CENP-E, independently of its kinase activity. *Journal of Cell Biology*, *153*(6), 1239–1249. https://doi.org/10.1083/jcb.153.6.1239

Sheltzer, J. M., & Amon, A. (2011). The Aneuploidy Paradoc: costs and benefits of an incorrect karyotype. *Trends in Genetics*, *27*(11), 446–453. https://doi.org/10.1038/jid.2014.371

Shepperd, L. A., Meadows, J. C., Sochaj, A. M., Lancaster, T. C., Zou, J., Buttrick, G. J., … Millar, J. B. A. (2012). Phosphodependent recruitment of Bub1 and Bub3 to Spc7/KNL1 by Mph1 kinase maintains the spindle checkpoint. *Current Biology*, *22*(10), 891–899. https://doi.org/10.1016/j.cub.2012.03.051

Sigollit, F. D., Lyman, S., Huckins, J., Adamson, B., Chung, E., Quattrochi, B., & King, R. W. (2012). A bioinformatics method identifies prominent off-targeted transcripts in RNAi screens. *Nature Methods*, *9*(4), 363–366. https://doi.org/10.1016/j.physbeh.2017.03.040

Sikirzhytski, V., Renda, F., Tikhonenko, I., Magidson, V., McEwen, B. F., & Khodjakov, A. (2018). Microtubules assemble near most kinetochores during early prometaphase in human cells. *Journal of Cell Biology*, *217*(8), 2647–2659. https://doi.org/10.1083/jcb.201710094

Silió, V., McAinsh, A. D., & Millar, J. B. (2015). KNL1-Bubs and RZZ Provide Two Separable Pathways for Checkpoint Activation at Human Kinetochores. *Developmental Cell*, *35*(5), 600–613. https://doi.org/10.1016/j.devcel.2015.11.012

Sivakumar, S., Janczyk, P. Ł., Qu, Q., Brautigam, C. A., Stukenberg, P. T., Yu, H., & Gorbsky, G.

J. (2016). The human SKA complex drives the metaphase-anaphase cell cycle transition by recruiting protein phosphatase 1 to kinetochores. *ELife*, *5*, 1–20. https://doi.org/10.7554/elife.12902

Skowyra, A., Allan, L. A., Saurin, A. T., & Clarke, P. R. (2018). USP9X Limits Mitotic Checkpoint Complex Turnover to Strengthen the Spindle Assembly Checkpoint and Guard against Chromosomal Instability. *Cell Reports*, *23*(3), 852–865. https://doi.org/10.1016/j.celrep.2018.03.100

Stegmeier, F., Rape, M., Draviam, V. M., Nalepa, G., Sowa, M. E., Ang, X. L., … Elledge, S. J. (2007). Anaphase initiation is regulated by antagonistic ubiquitination and deubiquitination activities. *Nature*, *446*(7138), 876–881. https://doi.org/10.1038/nature05694

Stucke, V. M., Baumann, C., & Nigg, E. A. (2004). Kinetochore localization and microtubule interaction of the human spindle checkpoint kinase Mps1. *Chromosoma*, *113*(1), 1–15. https://doi.org/10.1007/s00412-004-0288-2

Sudakin, V., Chan, G. K. T., & Yen, T. J. (2001). Checkpoint inhibition of the APC/C in HeLa cells is mediated by a complex of BUBR1, BUB3, CDC20, and MAD2. *Journal of Cell Biology*, *154*(5), 925–936. https://doi.org/10.1083/jcb.200102093

Suijkerbuijk, S. J. E., Vleugel, M., Teixeira, A., & Kops, G. J. P. L. (2012). Integration of Kinase and Phosphatase Activities by BUBR1 Ensures Formation of Stable Kinetochore-Microtubule Attachments. *Developmental Cell*, *23*(4), 745–755. https://doi.org/10.1016/j.devcel.2012.09.005

Tanaka, T. U., Rachidi, N., Janke, C., Pereira, G., Galova, M., Schiebel, E., … Nasmyth, K. (2002). Evidence that the Ipl1-Sli15 (Aurora Kinase-INCENP) complex promotes chromosome bi-orientation by altering kinetochore-spindle pole connections. *Cell*, *108*(3), 317–329. https://doi.org/10.1016/S0092-8674(02)00633-5

Tang, Z., Shu, H., Oncel, D., Chen, S., & Yu, H. (2004). Phosphorylation of Cdc20 by Bub1 provides a catalytic mechanism for APC/C inhibition by the spindle checkpoint. *Molecular Cell*, *16*(3), 387–397. https://doi.org/10.1016/j.molcel.2004.09.031

Tang, Z., Sun, Y., Harley, S. E., Zou, H., & Yu, H. (2004). Human Bub1 protects centromeric sister-chromatid cohesion through Shugoshin during mitosis. *Proceedings of the National Academy of Sciences of the United States of America*, *101*(52), 18012–18017. https://doi.org/10.1073/pnas.0408600102

Taylor, S S, & McKeon, F. (1997). Kinetochore localization of murine Bub1 is required for normal mitotic timing and checkpoint response to spindle damage. *Cell*, *89*(5), 727–735. Retrieved from http://www.ncbi.nlm.nih.gov/pubmed/9182760

Taylor, Stephen S., Ha, E., & McKeon, F. (1998). The human homologue of Bub3 is required for kinetochore localization of Bub1 and a Mad3/Bub1-related protein kinase. *Journal of Cell Biology*, *142*(1), 1–11. https://doi.org/10.1083/jcb.142.1.1

Thompson, S. L., Bakhoum, S. F., & Compton, D. A. (2010). Mechanisms of Chromosomal Instability. *Current Biology*, *20*(6), R285–R295. https://doi.org/10.1016/j.cub.2010.01.034

Uhlmann, F., Wernic, D., Poupart, M.-A., Koonin, E. V, & Nasmyth, K. (2000). Cleavage of Cohesin by the CD Clan Protease Separin triggers Anaphase in Yeast. *Cell*, *103*, 375–386. Retrieved from papers2://publication/uuid/88ADE173-EC89-4C2A-B826-E6F298269010

Varma, D., & Salmon, E. D. (2012). The KMN protein network - chief conductors of the kinetochore orchestra. *Journal of Cell Science*, *125*(24), 5927–5936. https://doi.org/10.1242/jcs.093724

Varma, Dileep, Wan, X., Cheerambathur, D., Gassmann, R., Suzuki, A., Lawrimore, J., … Salmon, E. D. (2013). Spindle assembly checkpoint proteins are positioned close to core microtubule attachment sites at kinetochores. *Journal of Cell Biology*, *202*(5), 735–746. https://doi.org/10.1083/jcb.201304197

Vasquez, R. J., Howell, B., Yvon, A. M. C., Wadsworth, P., & Cassimeris, L. (1997). Nanomolar concentrations of nocodazole alter microtubule dynamic instability in vivo and in vitro. *Molecular Biology of the Cell*, *8*(6), 973–985. https://doi.org/10.1091/mbc.8.6.973

Vasudevan, A., Baruah, P. S., Smith, J. C., Wang, Z., Sayles, M. N., Andrews, P., … Sheltzer, J. M. (2019). Single chromosome gains can function as metastasis supressors and metastasis promoters. *BioRXiv*. https://doi.org/10.1017/CBO9781107415324.004

Vleugel, M., Hoek, T. A., Tromer, E., Sliedrecht, T., Groenewold, V., Omerzu, M., & Kops, G. J. (2015). Dissecting the roles of human BUB1 in the spindle assembly checkpoint. *J Cell Sci*, *128*(16), 2975–2982. https://doi.org/10.1242/jcs.169821

Wang, H., Hu, X., Ding, X., Dou, Z., Yang, Z., Shaw, A. W., … Yao, X. (2004). Human Zwint-1 specifies localization of Zeste White 10 to kinetochores and is essential for mitotic checkpoint signaling. *Journal of Biological Chemistry*, *279*(52), 54590–54598. https://doi.org/10.1074/jbc.M407588200

Wang, Jie, Yi, S., Zhou, J., Zhang, Y., & Guo, F. (2016). The NF-B subunit RelB regulates the migration and invasion abilities and the radio-sensitivity of prostate cancer cells. *International Journal of Oncology*, *49*(1), 381–392. https://doi.org/10.3892/ijo.2016.3500

Wang, Jun, Chang, Y.-F., Hamilton, J. I., & Wilkinson, M. F. (2002). Nonsense-Associated Altered Splicing: A Frame-Dependent Reponse Distinct from Nonsense-Mediated Decay. *Molecular Cell*, *10*(4), 951–957. https://doi.org/10.1016/s1097-2765(02)00635-4

Wang, X., Babu, J. R., Harden, J. M., Jablonski, S. A., Gazi, M. H., Lingle, W. L., … Van Deursen, J. M. A. (2001). The Mitotic Checkpoint Protein hBUB3 and the mRNA Export Factor hRAE1 Interact with GLE2p-binding Sequence (GLEBS)-containing Proteins. *Journal of Biological Chemistry*, *276*(28), 26559–26567. https://doi.org/10.1074/jbc.M101083200

Warren, C. D., Brady, D. M., Johnston, R. C., Hannah, J. S., Hardwick, K. G., & Spencer, F. A. (2002). Distinct Chromosome Segregation Roles for Spindle Checkpoint Proteins. *Molecular Biology of the Cell*, *13*(September), 3029–3041. https://doi.org/10.1091/mbc.E02

Weaver, Beth A., & Cleveland, D. W. (2008). The Aneuploidy Paradox in Cell Growth and Tumorigenesis. *Cancer Cell*, *14*(6), 431–433. https://doi.org/10.1016/j.ccr.2008.11.011

Weaver, Beth AA, & Cleveland, D. W. (2006). Does aneuploidy cause cancer? *Current Opinion in Cell Biology*, *18*(6), 658–667. https://doi.org/10.1016/j.ceb.2006.10.002

Williams, B. R., Prabhu, V. R., Hunter, K. E., Glazier, C. M., Whittaker, C. a, Housman, D. E., & Amon, A. (2008). Aneuploidy affects Proliferation and Spontaneous Immortalization in Mammalian Cells. *Science*, *322*, 703–710.

Wong, R. W., Blobel, G., & Coutavas, E. (2006). Rae1 interaction with NuMA is required for bipolar spindle formation. *Proceedings of the National Academy of Sciences of the United States of America*, *103*(52), 19783–19787. https://doi.org/10.1073/pnas.0609582104

Wood, K. W., Sakowicz, R., Goldstein, L. S. B., & Cleveland, D. W. (1997). CENP-E is a plus end-directed kinetochore motor required for metaphase chromosome alignment. *Cell*, *91*(3), 357–366. https://doi.org/10.1016/S0092-8674(00)80419-5

Yamagishi, Y., Honda, T., Tanno, Y., & Watanabe, Y. (2010). Two histone marks establish the inner centrometre and chromosome bio-orientation (corrected). *Science*, *330*, 239–243. https://doi.org/10.1126/science.1194498

Yamamoto, T. G., Watanabe, S., Essex, A., & Kitagawa, R. (2008). Spdl-1 functions as a kinetochore receptor for MDF-1 in Caenorhabditis elegans. *Journal of Cell Biology*, *183*(2), 187–194. https://doi.org/10.1083/jcb.200805185

Yao, X., Abrieu, A., Zheng, Y., Sullivan, K. F., & Cleveland, D. W. (2000). CENP-E forms a link between attachment of spindle microtubules to kinetochores and the mitotic checkpoint. *Nature Cell Biology*, *2*(8), 484–491. https://doi.org/10.1038/35019518

Zhang, G., Kruse, T., Boldú, C. G., Garvanska, D. H., Coscia, F., Mann, M., … Nilsson, J. (2019). Efficient mitotic checkpoint signaling depends on integrated activities of Bub 1 and the RZZ complex. *EMBO Journal*, (e100977), 1–18. https://doi.org/10.15252/embj.2018100977

Zhang, G., Lischetti, T., Hayward, D. G., & Nilsson, J. (2015). Distinct domains in Bub1 localize RZZ and BubR1 to kinetochores to regulate the checkpoint. *Nature Communications*, *6*, 7162. https://doi.org/10.1038/ncomms8162

Zhang, G., Mendez, B., Sedgwick, G., & Nilsson, J. (2016). Two functionally distinct kinetochore pools of BubR1 ensure accurate chromosome segregation . *Nature Communication*, *7*, 1–12. https://doi.org/10.1038/ncomms12256

Zhang, S., Chang, L., Alfieri, C., Zhang, Z., Yang, J., Maslen, S., … Barford, D. (2016). Molecular mechanism of APC/C activation by mitotic phosphorylation. *Nature*, *533*(7602), 260–264. https://doi.org/10.1038/nature17973

Appendix

Correspondence

Bub1 is not essential for the checkpoint response to unattached kinetochores in diploid human cells

Cerys E. Currie[1], Mar Mora-Santos[1], Chris A. Smith[1,2], Andrew D. McAinsh[1], and Jonathan B.A. Millar[1,*]

Error-free chromosome segregation during mitosis depends on a functional spindle assembly checkpoint (SAC). The SAC is a multi-component signalling system that is recruited to unattached or incorrectly attached kinetochores to catalyse the formation of a soluble inhibitor, known as the Mitotic Checkpoint Complex (MCC), which binds and inhibits the anaphase promoting complex (APC/C) [1]. We have previously proposed that two separable pathways, composed of KNL1–Bub3–Bub1 (KBB) and Rod–Zwilch–Zw10 (RZZ), recruit Mad1–Mad2 complexes to human kinetochores to activate the SAC [2]. Although Bub1 is absolutely required for checkpoint signalling in yeast (which lack RZZ), there is conflicting evidence as to whether this is the case in human cells based on siRNA studies [2–5]. Here we show that, while Bub1 is required for recruitment of BubR1, it is not strictly required for the checkpoint response to unattached kinetochores in diploid human cells.

We used CRISPR/Cas9 genome editing to target BUB1 in human diploid hTERT-RPE1 cells using small guide (sg)RNAs targeting exon 2. We initially recovered a mosaic clonal population which arrested in nocodazole and included cells in which Bub1 was undetectable at kinetochores (Figure S1A,B in Supplemental Information, published with this article online). These kinetochores could, however, still recruit Mad2 suggesting that Bub1 is dispensable for SAC activation. To confirm this, we isolated a second clonal cell line with no detectable Bub1 protein by immunoblotting and no detectable Bub1 at kinetochores by quantitative immunofluorescence, while Mad2 could still be recruited (Figures 1A–C and S1D). Genome sequencing revealed a frame shift in both BUB1 alleles that allows expression of only the first 23 amino acids of Bub1 (Figure S1C). Importantly, Rod and Zwilch, as well as KNL1, bound kinetochores to the same extent in parental and Bub1$^{-/-}$ cells (Figures 1C and S1D). By contrast, BubR1 kinetochore-binding was abolished and binding of CENP-F severely compromised (Figures 1C and S1D), as reported previously in studies using Bub1 knockdown by siRNA [6]. Importantly, steady state levels of Mad2 at pro-metaphase kinetochores were lower in Bub1$^{-/-}$ cells than in the parental control (Figures 1C and S1D) consistent with previous findings following siRNA-mediated knockdown of KNL1 or Bub1 [2].

We next used live cell imaging of chromosomes labelled with a cell permeable dye (SiR-DNA) to assess the effect of Bub1 knockout on timing of chromosome congression and anaphase onset in individual cells. Although the efficiency of chromosome congression was largely unaffected in Bub1$^{-/-}$ cells compared to control cells, the time from nuclear breakdown (NBD) to anaphase onset was extended by ~3 min (Figure 1D). To test directly whether Bub1 is required for the SAC response to unattached kinetochores we filmed control and Bub1$^{-/-}$ cells in the presence of 330 nM nocodazole and measured the time from NBD to anaphase onset. We found that addition of nocodazole delays anaphase onset in Bub1$^{-/-}$ cells (Figure S2D). Consistently, Mad2 binds unattached kinetochores (Figure 1C, far right panel) and associates with Cdc20, BubR1 and APC/C almost as efficiently in checkpoint-arrested Bub1$^{-/-}$ cells as in the parental control (Figure S2A). These results additionally imply that, firstly, Bub1 is not required for formation of either MCC or MCC–APC/C from the RZZ complex and, secondly, that recruitment of BubR1 to kinetochores is not strictly necessary for incorporation of BubR1 into MCC nor for checkpoint signalling. Notably, however, 14% of Bub1$^{-/-}$ cells (red dots) exited mitosis during the recordings compared to zero in parental cells, suggesting the checkpoint arrest is less robust (Figure 1E). A similar acceleration of mitotic exit was observed in experiments where cells were treated with nocodazole and the SAC was compromised by inhibition of Mps1 with reversine (Figure S2B). Consistently, the rate of hSecurin and Cyclin B destruction was also advanced in Bub1$^{-/-}$ cells when nocodazole-arrested cells were forced out of mitosis by addition of reversine (Figure S2C). These data indicate that Bub1 contributes to, but is not essential for, SAC signalling in RPE1 cells.

The apparent absence of a congression defect in Bub1$^{-/-}$ cells is consistent with previous work in RPE1 cells treated with Bub1 kinase inhibitors, but is perhaps surprising given the known role of Bub1 in error correction through the Histone2A–Sgo1/PP2A–Aurora B pathway [7]. We therefore generated multiple mal-orientated attachments by releasing cells from a nocodazole arrest and measured the time to completion of congression and anaphase onset. Both events were delayed in Bub1$^{-/-}$ cells compared to the control, revealing the role for Bub1 in error correction (Figure S2D). Consistently, Sgo1 binding is reduced by approximately 50% in Bub1$^{-/-}$ cells (Figure S2E), in line with previous experiments in HeLa cells [8]. Interestingly, the frequency of lagging chromosomes was unchanged in Bub1$^{-/-}$ compared to parental cells (10% vs. 19%, $p = 0.184$ Fisher's exact test) (data not shown), suggesting that, while the efficiency of error correction is reduced, Bub1$^{-/-}$ cells are still able to successfully complete chromosome bi-orientation. Moreover, Bub1$^{-/-}$ cells with uncongressed chromosomes delay in mitosis, consistent with our conclusion that the SAC can operate without Bub1. We assume that error correction is completed in Bub1$^{-/-}$ cells by a pool of Aurora-B kinase associated with centromeric DNA via phosphorylation of histone H3 on threonine 3 (H3T3) by centromere-associated Haspin kinase [9].

The data in this paper support the notion that KBB and RZZ complexes can provide two separate receptors for the Mad1–Mad2 complex at human kinetochores [2]. Moreover, they are consistent with a recent report showing that Bub1 and RZZ are not essential for the SAC response to unattached kinetochores in near-haploid human

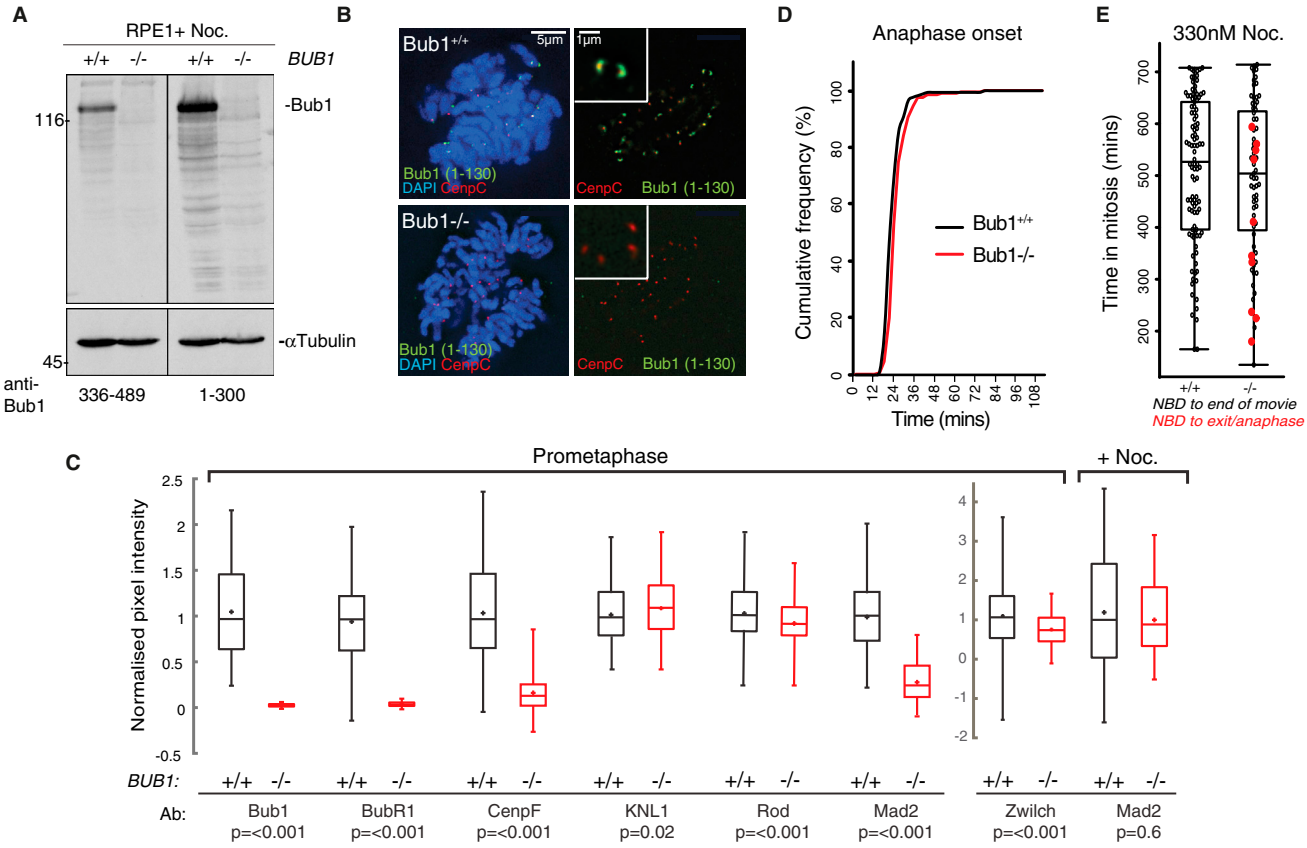

Figure 1. BUB1 is not essential for SAC activity in diploid human cells.
(A) Full immunoblots of whole-cell lysates from parental or Bub1$^{-/-}$ cells treated with 3.3 μM nocodazole using antibodies against Bub1 aa336–489 (left) or aa1–300 (right) and α-Tubulin as loading control. (B) Representative images of prometaphase parental or Bub1$^{-/-}$ cells stained with DAPI, CenpC, and Bub1 (aa1–130) antibodies. (C) Quantification of kinetochore-bound Bub1, BubR1, CenpF, KNL1, Rod, Zwilch and Mad2 signals relative to Crest or CenpC intensity (data normalised to respective Bub1$^{+/+}$ median value; p-value from a two-sided Mann-Whitney U test; data from >2 independent experiments with >500 kinetochores per dataset). Representative images in Figure S1D. (D) Time spent in mitosis (from NEB to anaphase onset/mitotic exit) from 12 hr live-cell imaging of parental or Bub1-/- cells treated with SiR-DNA (n = 218 for Bub1$^{-/-}$ and n = 183 for parental). (E) Same experiment as (D) except cells treated with 330 nM nocodazole (n = 71 for Bub1$^{-/-}$ and n = 102 for parental).

HAP1 cells [10]. It is unclear why human cells have two receptors (KBB and RZZ) for the Mad1–Mad2 complex, whereas yeast only has one (KBB). One possibility is that the KBB and RZZ pathways monitor different attachment states [2]. Furthermore, the contribution of the KBB pathway to SAC signalling and error correction may vary between cell types or state of cellular transformation [2,7]. Future work will be needed to understand the relative roles of KBB and RZZ in these different contexts.

SUPPLEMENTAL INFORMATION

Supplemental Information includes two figures, experimental procedures, author contributions and acknowledgments, and can be found with this article online at https://doi.org/10.1016/j.cub.2018.07.040.

REFERENCES

1. London, N., and Biggins, S. (2014). Signalling dynamics in the spindle checkpoint response. Nat. Rev. Mol. Cell. Biol. *15*, 736–47.
2. Silió, V., McAinsh, A.D., and Millar, J.B. (2015). KNL1-Bubs and RZZ provide two separable pathways for checkpoint activation at human kinetochores. Dev. Cell *35*, 600–613.3.
3. Klebig, C., Korinth, D., and Meraldi, P. (2009). Bub1 regulates chromosome segregation in a kinetochore-independent manner. J. Cell Biol. *185*, 841–858.
4. Jia, L., Li, B., and Yu, H. (2016). The Bub1-Plk1 kinase complex promotes spindle checkpoint signalling through Cdc20 phosphorylation. Nat. Commun. *7*, 10818.
5. Di Fiore, B., Davey, N.E., Hagting, A., Izawa, D., Mansfeld, J., Gibson, T.J., and Pines, J. (2015). The ABBA motif binds APC/C activators and is shared by APC/C substrates and regulators. Dev. Cell *32*, 358–372.
6. Johnson, V.L., Scott, M.I., Holt, S.V., Hussein, D., and Taylor, S.S. (2004). Bub1 is required for kinetochore localization of BubR1, Cenp-E, Cenp-F and Mad2, and chromosome congression. J. Cell Sci. *117*, 1577–1589.
7. Baron, A.P., von Schubert, C., Cubizolles, F., Siemeister, G., Hitchcock, M., Mengel, A., Schroder, J., Fernandez-Montalvan, A., von Nussbaum, F., Mumberg, D., *et al*. (2016). Probing the catalytic functions of Bub1 kinase using the small molecule inhibitors BAY-320 and BAY-524. eLife *5*, e12187.
8. Kitajima, T.S., Hauf, S., Ohsugi, M., Yamamoto, T., and Watanabe, Y. (2005). Human Bub1 defines the persistent cohesion site along the mitotic chromosome by affecting Shugoshin localization. Curr. Biol. *15*, 353–359.
9. Kelly, A.E., Ghenoiu, C., Xue, J.Z., Zierhut, C., Kimura, H., and Funabiki, H. (2010). Survivin reads phosphorylated histone H3 threonine 3 to activate the mitotic kinase Aurora B. Science *330*, 235–239.
10. Raaijmakers, J.A., van Heesbeen, R.G.H.P., Blomen, V.A., Janssen, L.M.E., van Diemen, F., Brummelkamp, T.R., and Medema, R.H. (2018). Bub1 is essential for the viability of human cells in which the spindle assembly checkpoint is compromised. Cell Rep. *22*, 1424–1438.

[1]Centre for Mechanochemical Cell Biology & Division of Biomedical Sciences, Warwick Medical School, University of Warwick, Gibbet Hill, Coventry, CV4 7AL, UK.
[2]Present address: Metabolic Research Laboratories and MRC Metabolic Diseases Unit, Institute of Metabolic Science, Addenbrooke's Hospital, Hills Road, Cambridge CB2 0QQ, UK.
*E-mail: J.Millar@warwick.ac.uk

Supplemental Information: Bub1 is not essential for the checkpoint response to unattached kinetochores in diploid human cells

Cerys E. Currie, Mar Mora-Santos, Chris A. Smith, Andrew D. McAinsh and Jonathan B.A. Millar

Further information and requests for resources and reagents should be directed to and will be fulfilled by the Lead Contact, Jonathan Millar (J.Millar@warwick.ac.uk)

Supplemental Experimental Procedures

Cell culture: Immortalised (hTERT) diploid human retinal pigment epithelial (RPE1; ATCC® CRL-4000™) cells (female) were grown in Sigma Dulbecco's Modified Eagle's Medium F-12 Ham + 10% fetal bovine serum + 1% Penstrep + 2mM L-Glutamine. All cell cultures were maintained at 37°C with 5% CO_2 in a humidified incubator in the Centre for Mechanochemical Cell Biology at the University of Warwick. Cell lines were free of mycoplasma contamination. Nocodazole (SIGMA) treatments were performed using the following concentrations: 330 nM (Figure 1C, 1E, S1A, S1B, and S2B) or 3.3 μM (Figure 1A, S2A, S2C and S2D) diluted in sterile DMSO. Reversine (SIGMA) treatments were performed at 1 μM (Figure S2B, S2C).

CRISPR-Cas9 editing: Small guide RNAs (sgRNAs) targeting exon 2 (Forward: 5' CACCGTACAAGGGCAATGACCCTCTTG 3'; Reverse: 5'-AAACAGAGGGTCATTGCCCTTGTAC-3') were designed using http://crispr.mit.edu, cloned into pspCas9(BB)-2A-GFP plasmid (Addgene) and transfected into hTERT-RPE1 cells using FuGENE® HD (Promega). A pool of GFP positive cells were isolated by FACS sorting, and two single clones generated by dilution and plating. Clones were screened by immunofluorescence (see below) using a mouse anti-Bub1 antibody (ab54893, Abcam). The first clone (AMC175) was a mosaic that included a population of cells in which Bub1 was undetectable at kinetochores. The Bub1$^{-/-}$ hTERT-RPE1 clonal line (AMC170) was verified by PCR-cloning and DNA sequencing. PCR primers for Gateway cloning (Thermo Fisher Scientific) were designed (Forward. primer: 5'-GGGGACAAGTTTGTACAAAAAAGCAGGCTTCAGCTGGGACTTATGGAAAAACA-3', Reverse primer: 5'-GGGGACCACTTTGTACAAGAAAGCTGGGTCCTATGACTGGTTGCTGGTAGAGAGA-3') to amplify a 1kB region from genomic DNA obtained using DNeasy Blood and Tissue Kit (Qiagen). PCR products were recombined into pDONR-221 vector using the Gateway cloning BP reaction, transformed into dH5α cells and selected using Kanamycin . Plasmids were sequenced using an M13F primer (5'-GTAAAACGACGGCCAGT-3') and data analysed using Serial Cloner 2-6-1. Two alleles were identified, both with a single base insertion after base pair 69 (either +C or +A) (Figure S1C). The ratio of Allele 1(+C) to Allele 2(+A) was 7:5. These changes result in stop codons in 23 of 25 exons limiting the possibility of exon skipping and presence of truncated protein.

Live cell imaging: RPE1 cells were incubated with 0.5 μM Sir-DNA (Spirochrome) for ~60 min to visualise chromosomes. This treatment does not alter mitotic progression compared to previous work with Histone2B-RFP (not shown). Image stacks (7 x 2 μm optical sections; 1x1 binning) were acquired every 3 min for either a 12 hr or 3 hr period with a 40x oil-immersion 1.3 NA objective using an Olympus DeltaVision Elite microscope (Applied Precision, LLC) equipped with a CoolSNAP HQ2 camera (Roper Scientific). Images were acquired at 10% neutral density using Cy5 filter and an exposure time of 0.1s. A stage-top incubator maintained cells at 37ºC and 5% CO_2 with further stabilisation from a microscope enclosure (Weather station; PrecisionControl) held at 37ºC. Image sequences were inspected and analysed by hand using SoftWorx (Applied Precision, LLC). For Nocodazole arrest and Reversine experiments, drugs were added at the stated concentrations 2 hr prior to imaging. For Nocodazole washout experiments 3.3 μM Nocodazole and Sir-DNA dye was added to cells 2 hr prior to imaging. After incubation, media was removed, and cells were gently washed 3 times with warm media then reincubated with fresh media containing SiR-DNA. Cells were imaged for a 3 hr period, with the time from washout to start of movie being noted.

Quantitative Immunofluorescence: For quantitative immunofluorescence, parental or Bub1$^{-/-}$ cells were seeded on coverslips previously washed with 70% ethanol and PBS. Cell were fixed at room temperature (RT) in PTEM-F (20 mM PIPES, 10 mM EGTA, 1 mM $MgCl_2$, 0.2% Triton X-100, and 4% formaldehyde) for 10 min, then permeabilized with 0.1% Triton X-100 PBS for 5 mins, washed three times with PBS, and blocked with 3% BSA PBS for 60 min. Cells were then incubated with primary antibodies diluted in blocking

solution for 2 hr at RT, washed three times with PBS, incubated with the secondary antibodies for 1 hr at RT and then mounted in Vectashield (Vector Laboratories). In each experiment cells were incubated with human anti-CREST (1:200, Antibodies Incorporated 15-234-0001) or guinea pig anti-CENP-C (1:2000, MBL PD030) as a reference signal and then rabbit anti-KNL1 (1:500; Abcam ab70537), mouse anti-Bub1 (1:500, Abcam ab54893), rabbit anti-Mad2 (1:500, Biolegend Poly19246 [S2,S3,S4]), mouse anti-CenpF (1:200, Abcam ab90), rabbit anti-Zwilch (1:1000, a kind gift from A. Musacchio), mouse anti-Sgo1 (1:200, Abcam ab58023), mouse anti-Rod (1:50, Abcam ab56745) or mouse anti-BubR1 (1:200, Abcam ab4637). Secondary antibodies were goat anti-rabbit/human/mouse/guinea pig conjugated to Alexa 488 or Alexa Fluor 594 or 647 (1:500; Invitrogen). DNA was visualized with DAPI (SIGMA). Three-dimensional image stacks were acquired (1x1 binning) in 0.2 μm steps using a 100× oil NA 1.4 objective on an Olympus Deltavision Elite microscope (Applied Precision, LLC) equipped with a DAPI-fluorescein isothiocyanate-Rhod/TR–CY5 filter set (Chroma) and a Coolsnap HQ2 camera. Kinetochore signal intensities were measured using a GUI-driven software package within MATLAB called SiD (spot intensity detector), which can be found at https://github.com/cmcb-warwick/SiD. This requires MATLAB version R2017a or later.

Biochemistry: For immunoblots, cell extracts were prepared by lysing cells in NP40 buffer (1% NP40, 10 mM TrisCl pH 7.5, 150 mM NaCl, 10% glycerol) containing 1 mM PMSF, Complete mini EDTA-free Protease Inhibitor Cocktail and Phosphatase Inhibitor Tablets (Roche Applied Science). Concentration was determined using a Bradford assay. Proteins were separated by SDS-polyacrylamide gel electrophoresis (SDS-PAGE) and gels were electroblotted onto nitrocellulose membranes and probed with the following antibodies: anti-Bub1 rabbit antibody (1:500, GeneTex GTX30097), anti-Bub1 SB1.3 sheep antibody (1:500, a kind gift from Stephen Taylor [S1]), anti-α-Tubulin mouse antibody (1:20000, Sigma T9026), anti-BubR1 rabbit antibody (1:1000, Bethyl Laboratories A300-386A), anti-APC4 rabbit antibody (1:500, Bethyl Laboratories A301-176A), anti-Mad2 rabbit antibody (1:500, Bethyl Laboratories A300-301A), anti-Cdc20 rabbit antibody (1:500, Santa Cruz Biotechnology sc-8358), anti-APC3 mouse antibody (1:500, BD Transduction Lab 610455), anti-CyclinB mouse antibody (1:1000, BD Transduction Lab 610220) and anti-hSecurin mouse antibody (1:500, Santa Cruz sc-56207). Proteins were visualized using the enhanced chemiluminescence (ECL) detection system according to the manufacturer's instructions (GE Healthcare). For immunoprecipitation experiments, whole extracts (1 mg) were incubated with normal mouse IgG (Santa Cruz Biotechnology) for 30 min and subsequently with protein G-Sepharose beads (GE Healthcare) for 45 min at 4ºC. After centrifugation, beads were kept as pre-immune (*PI*) and the same extract was incubated with anti-Cdc20 or anti-APC3 mouse antibodies (Santa Cruz Biotechnology and BD Transduction Lab, respectively) for 2 hours followed by an incubation with protein G-Sepharose beads for another 45 min and the beads were kept as Immune (*I*). Beads were washed six times with NP40 buffer and bound proteins were solubilised by the addition of SDS-sample buffer heated at 95ºC for 5 min.

SiD analysis: Kinetochore signal intensities were measured using a GUI-driven software package within MATLAB called SiD (spot intensity detector), which can be found at https://github.com/cmcb-warwick/SiD. This requires MATLAB version R2017a or later. Briefly, kinetochores are detected within images using a reference signal (CREST or CENP-C) by splitting the histogram of intensities, separating the spots from background. The centres of spots were calculated using a mixture model of 3D Gaussians and spots manually filtered to remove false positives and any poorly localised spot centres. Raw intensities of kinetochore components in the first channel (reference) and second channel were calculated as the mean intensity within a sphere of 300 nm radius around the kinetochore's spot centre. Intensities were then corrected for average background intensity, defined as the mean intensity of the image. Intensities were normalised to the reference signal intensity on a spot-by-spot basis.

Statistical Analysis: Statistics for Figure 1C are an automatic output from SiD software (MATLAB). P-values were calculated using a two-sided Mann Whitney U-test to compare median values. All other statistical tests were performed using MATLAB.

Author Contributions

This project was initiated by A.D.M. and J.B.M. C.E.C. conducted all experiments with the exception of biochemistry in Figure 1A, S2A and S2C, which was carried out by M.M.S.. C.A.S. wrote the code for quantification of kinetochore signals. The manuscript was written by A.D.M., J.B.M., and C.E.C..

Acknowledgements

We thank Muriel Erent for support in genome editing and Virginia Silió, John Meadows and Steve Royle for comments on the manuscript. We thank Stephen Taylor for the kind gift of Bub1 antibodies, and Andrea Musacchio for the kind gift of Zwilch antibodies. This work was supported by MRC program grant MR/K001000/1 to A.D.M. and J.B.M. C.E.C. is funded by the BBSRC Midlands Integrative Biosciences Training Partnership (MIBTP) [grant BB/M01116X/1]. A.D.M and C.A.S. were also supported by a Wellcome Trust Senior Investigator Award (grant 106151/Z/14/Z) and a Royal Society Wolfson Research Merit Award (grant WM150020).

Supplemental References

S1. Taylor, S.S., Hussein, D., Wang, Y., Elderkin, S., Morrow, C.J. (2001) Kinetochore localisation and phosphorylation of the mitotic checkpoint components Bub1 and BubR1 are differentially regulated by spindle events in human cells J. Cell Sci., *114*, 4385-4395.

S2. Klebig C., Korinth D. and Meraldi P. (2009) Bub1 regulates in a chromosome segregation in a kinetochore-independent manner, J. Cell Biol., *185*, 841-858

S3. Meraldi P. and Sorger P.K. (2005) A dual role for Bub1 in the spindle checkpoint and chromosome congression, EMBO J., *24*, 1621-1633

S4. Ballister E., Riegman M. and Lampson M.A. (2014) Recruitment of Mad2 to metaphase kinetochores is sufficient to reactivate the mitotic checkpoint, J. Cell Biol., *204*, 901-908

Supplemental Figures

There are two supplemental figures attached.

Figure S1

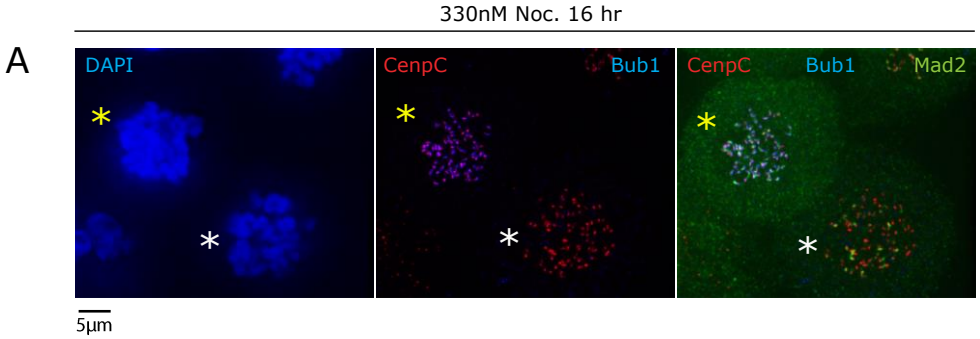

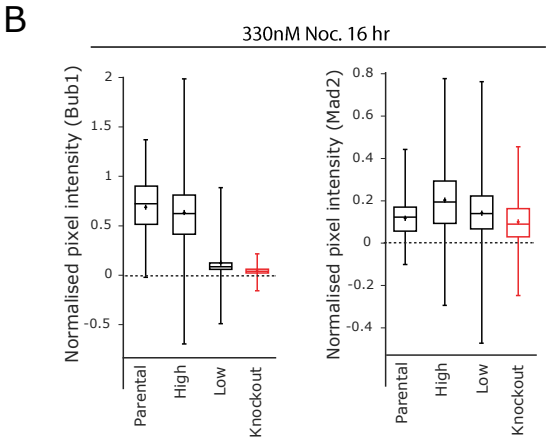

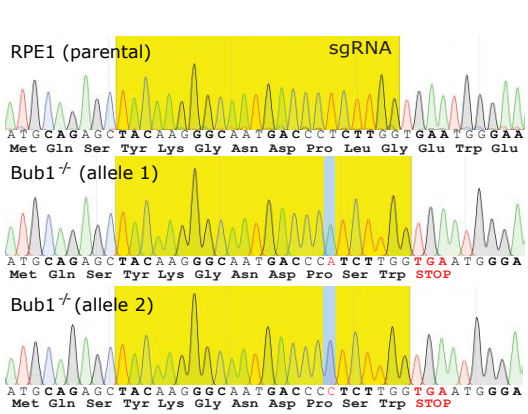

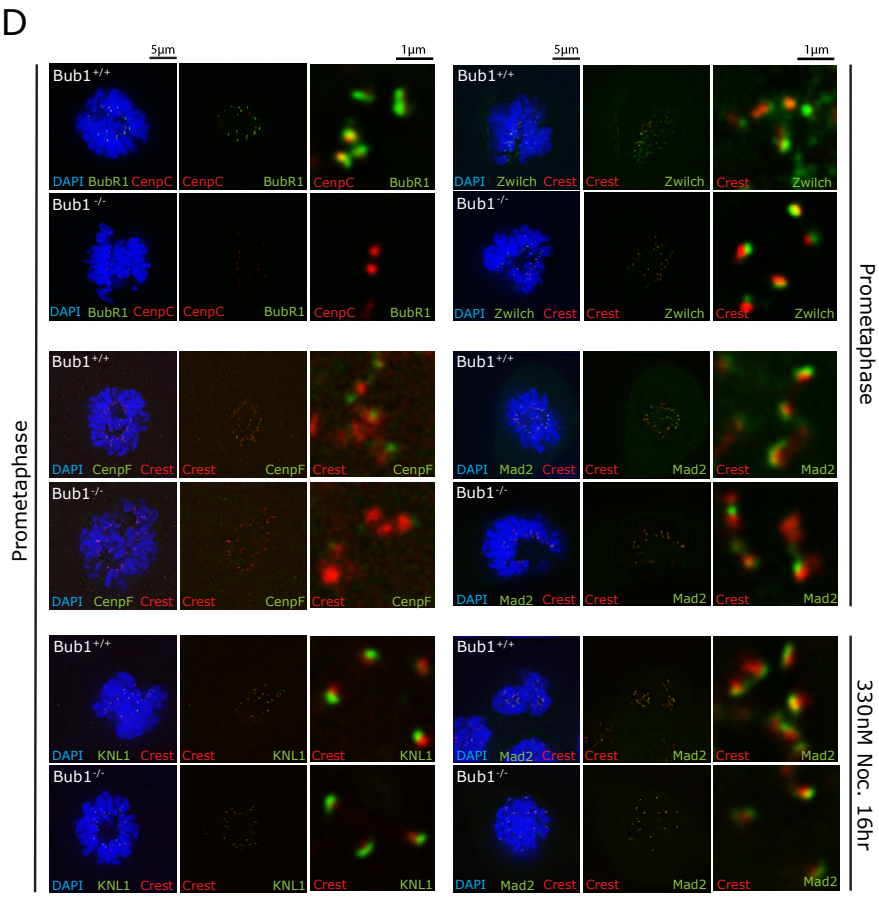

Figure S1: (A,B) Analysis of mosaic population from sgBUB1 transfected RPE1 cells. (A) Single field of view showing nocodazole-arrested cells with Bub1 present (yellow star) or absent (white star) from kinetochores. Cells were also stained with anti-Mad2 antibodies (green) which is recruited to kinetochores in both cells. (B) For quantification, cells from the mosaic population were separated into three groups based on kinetochore-bound Bub1 levels: High (0.15 to 1.2), Medium (0.06 to 0.14) and knockout (below 0.06 - undetectable; coloured red). Signals were normalised to CenpC intensity. Kinetochore-bound Mad2 signal from each population were plotted showing that recruitment is invarient to Bub1 levels. (C) Genome sequencing of Bub1$^{-/-}$ clone showing a frameshift mutation in both BUB1 alleles due to the addition of 1 base pair. The frameshift induces premature stop codons in both alleles as indicated. (D) Kinetochore protein characterisation in Bub1$^{-/-}$ cells. Representative images of prometaphase or nocodazole treated parental and Bub1$^{-/-}$ cells stained with DAPI, Crest/CenpC and BubR1, CenpF, KNL1, Zwilch and Mad2 antibodies. For quantification see Figure 1C.

Figure S2

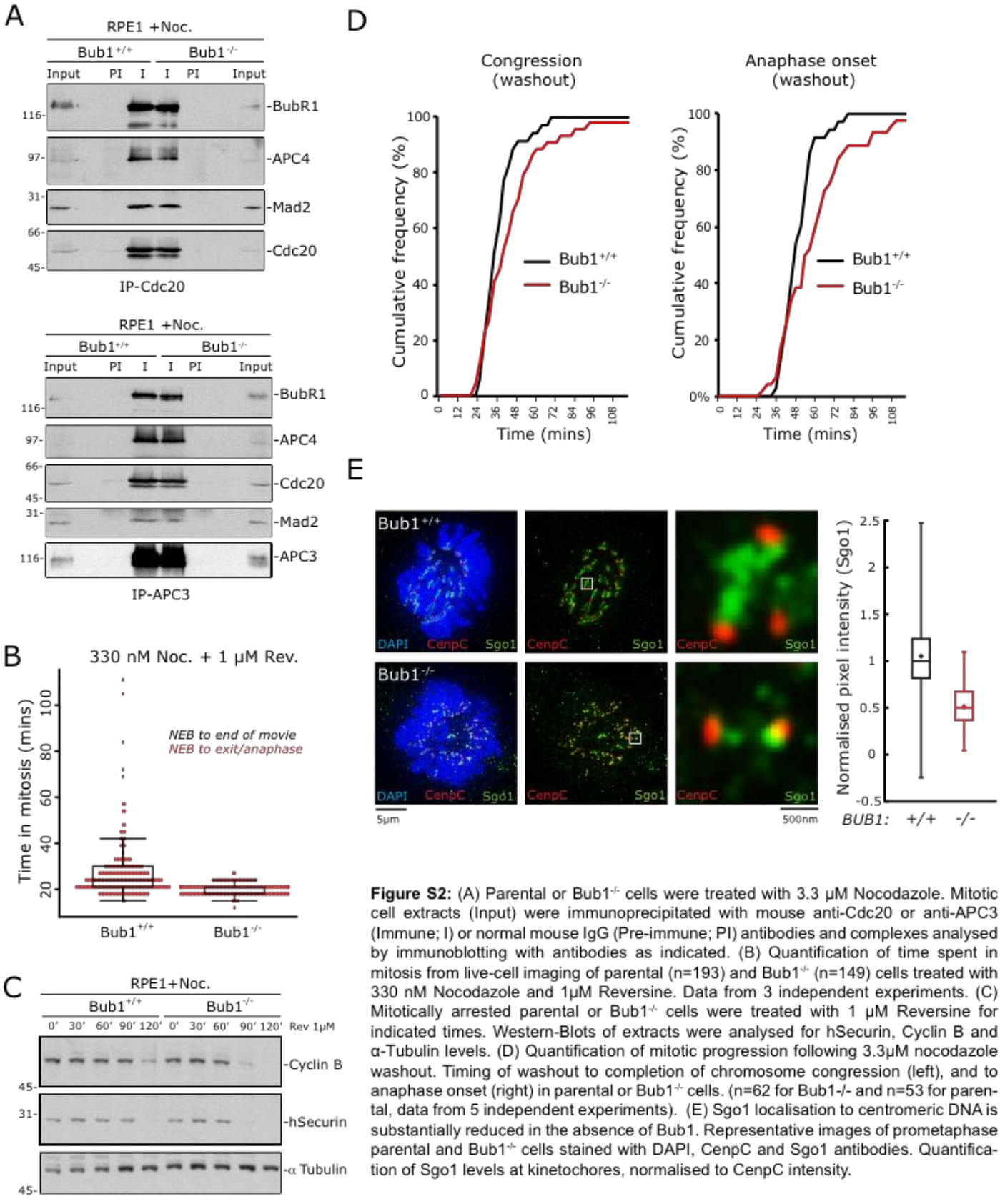

Figure S2: (A) Parental or Bub1$^{-/-}$ cells were treated with 3.3 μM Nocodazole. Mitotic cell extracts (Input) were immunoprecipitated with mouse anti-Cdc20 or anti-APC3 (Immune; I) or normal mouse IgG (Pre-immune; PI) antibodies and complexes analysed by immunoblotting with antibodies as indicated. (B) Quantification of time spent in mitosis from live-cell imaging of parental (n=193) and Bub1$^{-/-}$ (n=149) cells treated with 330 nM Nocodazole and 1μM Reversine. Data from 3 independent experiments. (C) Mitotically arrested parental or Bub1$^{-/-}$ cells were treated with 1 μM Reversine for indicated times. Western-Blots of extracts were analysed for hSecurin, Cyclin B and α-Tubulin levels. (D) Quantification of mitotic progression following 3.3μM nocodazole washout. Timing of washout to completion of chromosome congression (left), and to anaphase onset (right) in parental or Bub1$^{-/-}$ cells. (n=62 for Bub1-/- and n=53 for parental, data from 5 independent experiments). (E) Sgo1 localisation to centromeric DNA is substantially reduced in the absence of Bub1. Representative images of prometaphase parental and Bub1$^{-/-}$ cells stained with DAPI, CenpC and Sgo1 antibodies. Quantification of Sgo1 levels at kinetochores, normalised to CenpC intensity.